

This PDF was created from the British Library's microfilm copy of the original thesis. As such the images are greyscale and no colour was captured.

Due to the scanning process, an area greater than the page area is recorded and extraneous details can be captured.

This is the best available copy

D74326'87

Attention is drawn to the fact that the copyright of this thesis rests with its author.

This copy of the thesis has been supplied on condition that anyone who consults it is understood to recognise that its copyright rests with its author and that no quotation from the thesis and no information derived from it may be published without the author's prior written consent.

VI.

209

*

D 11226/87

BOOKHAM J.L.

Plates
Cdm Diagrams.

209

CITY OF LOND. Poly
(CNA A).

**PREPARATIVE AND NMR STUDIES OF
POLYPHOSPHORUS LIGANDS AND THEIR COMPLEXES**

**A Thesis submitted to the Council for National Academic
Awards in Partial Fulfilment of the Requirements for the
Degree of Doctor of Philosophy.**

by

Jonathan Leslie Bookham, B.Sc.

**Department of Chemistry
Sir John Cass Faculty of Science and Technology
City of London Polytechnic
31 Jewry Street
London EC3N 2EY**

March 1987

ABSTRACT

Preparative and N.M.R. Studies of Polyphosphorus Ligands and their Complexes

J.L. Bookham

Synthetic routes have been developed for the ready preparation of a range of novel polyphosphorus ligands containing up to seven potential donor atoms. The new ligands synthesised include $(\text{Ph}_2\text{P})_2\text{CHCH}_2\text{PPh}_2$, $(\text{Ph}_2\text{P})_2\text{C:CHPPh}_2$, $(\text{Ph}_2\text{P})_2\text{CHCH}_2\text{P(H)Ph}$, $[(\text{Ph}_2\text{P})_2\text{CHCH}_2]_2\text{PPh}$, $[(\text{Ph}_2\text{P})_2\text{CHCH}_2]\text{AsPh}$ and $[(\text{Ph}_2\text{P})_2\text{CHCH}_2]_3\text{P}$.

A large number of transition metal complexes of these ligands have been prepared and their structures determined. These are dominated by a tendency to contain five-membered chelate-rings whenever possible, but species with four-membered rings have also been prepared. Indirect routes have been devised to complexes, often embodying significant ring-strain, that are not formed by the direct reaction of the ligand with a metal substrate. In addition, the preparation and reactions of bridged bimetallic (palladium and platinum) and 'A-frame' complexes of the rigid bidentate ligand $(\text{Ph}_2\text{P})_2\text{C:CH}_2$ are reported.

In view of the analogy between the formation of an organophosphine sulphide and an organophosphine metal complex the reactions of several of the ligands with elemental sulphur have been studied. The isomeric distribution of the products can be accounted for in terms of the effective reactivity of the phosphorus atoms which depends upon conformational and configurational preferences.

The principal diagnostic tool used was high-resolution multi-element n.m.r. spectroscopy and especially ^{31}P n.m.r. Although many of the spectra were very complicated it was possible to analyse them satisfactorily with the aid of a range of sophisticated techniques including multiple-resonance and two-dimensional experiments. The ^{31}P chemical shifts and coupling constants are often found to fall into specific ranges which are diagnostic of particular structural features, and are also interpreted in terms of group and ring contributions, and coordination chemical shifts, and angular dependences of the coupling constants. In many cases spectra of other nuclei - ^1H , ^{13}C , ^{95}Mo , ^{183}W and ^{195}Pt are used to support assignment of structures, and the transition metal chemical shifts are found to follow characteristic trends.

Acknowledgements

It is a privilege and a pleasure to be able to record my appreciation of the help and encouragement I have received throughout this study from my supervisor Professor William McFarlane who suggested the initial line of work and who has been a constant source of guidance and inspiration ever since.

I would also like to thank other colleagues of mine who have been of assistance, in particular Dr. Ian Colquhoun for his helpful discussions on a range of topics and Dr. B. Wood for his help in recording some of the n.m.r. spectra.

Thanks are also due to Mr. B. Saunderson for his analytical services.

In addition I would like to thank the Inner London Education Authority for the award of a Research Assistantship

Statement of Advanced Studies

The author has attended and contributed to many national and international meetings of the Royal Society of Chemistry, in particular those associated with n.m.r. spectroscopy and various aspects of transition metal chemistry. Throughout the study constant reference was made to relevant publications such as Specialist Periodical Reports in Nuclear Magnetic Resonance, Journal of Magnetic Resonance etc., and the Dalton Transactions of the Journal of the Chemical Society, the Journal of Organometallic Chemistry and other journals were consulted regularly in order to keep abreast of the latest advances in chemistry in general.

CONTENTS

	<u>Page</u>
CHAPTER 1 INTRODUCTION	1
(1) Introduction	1
(2) Organophosphorus Ligands	2
(A) Diphosphines	2
(B) Multidentate Phosphines	6
(3) N.M.R. Spectroscopy	13
(A) ^{31}P n.m.r.	13
(i) Factors Affecting ^{31}P Chemical Shifts	13
(ii) Factors Affecting Phosphorus-Phosphorus Coupling Constants	16
(iii) Factors Affecting Metal-Phosphorus Coupling Constants	21
(B) Other Nuclei	22
CHAPTER 2 NEW POLYPHOSPHORUS LIGANDS	24
(1) Introduction	24
(2) Results and Discussion	
(A) Triphosphines and Related Species	24
(B) 1,1,2-Tris(diphenylphosphino)ethane	31
(C) Tetra- and Pentatertiary Phosphines and Related Species	46
(D) Hexatertiary Phosphines	53
(E) Heptatertiary Phosphines	57
(3) Summary	60
CHAPTER 3 OCTAHEDRAL AND SQUARE-PLANAR COMPLEXES OF 1,1,2-TRIS(DIPHENYLPHOSPHINO)ETHANE AND RELATED TRIPHOSPHINE LIGANDS	61
(1) Introduction	61
(2) Octahedral Complexes	61
(A) Introduction	61
(B) Results and Discussion	62
(i) 1,1,2-Tris(diphenylphosphino)ethane, II.	62

	<u>Page</u>
(ii) 1,1-Bis(diphenylphosphino)-2-phenyl- phosphinoethane, VI	75
(iii) 1,1,2-Tris(diphenylphosphino)ethene, X	80
(3) Square-Planar Complexes	83
(A) Introduction	83
(B) Results and Discussion	83
 CHAPTER 4 OCTAHEDRAL AND SQUARE-PLANAR TRANSITION-METAL COMPLEXES OF SOME NEW TETRA- AND PENTATERTIARY PHOSPHINE LIGANDS	 97
(1) Introduction	97
(2) Octahedral Complexes	97
(A) Introduction	97
(B) Results and Discussion	98
(3) Square-Planar Complexes	111
(A) Introduction	111
(B) Results and Discussion	111
 CHAPTER 5 1,1-BIS(DIPHENYLPHOSPHINO)ETHENE AS A BRIDGING LIGAND IN BINUCLEAR PALLADIUM AND PLATINUM COMPLEXES	 125
(1) Introduction	125
(2) Dppm as a Bridging Ligand	125
(3) Results and Discussion	127
(A) Syntheses	127
(B) Characterisation by N.M.R.	131
 CHAPTER 6 SULPHUR AND SELENIUM DERIVATIVES OF THE NEW POLYPHOSPHORUS LIGANDS	 146
(1) Introduction	146
(2) Results and Discussion	147

	<u>Page</u>
CHAPTER 7 EXPERIMENTAL	166
(1) Preparations	166
(2) Instrumentation	184
APPENDIX I	185
APPENDIX II	189
REFERENCES	192
PUBLICATIONS	200

CHAPTER 1

INTRODUCTION

1. INTRODUCTION

Since the establishment of the basis of modern coordination chemistry in the late nineteenth century, research in this and related fields has been extensive. Advances in the particular area of phosphorus-containing ligands and their transition-metal complexes have, however, only occurred within the last 30-40 years and were stimulated by discoveries that such ligands can stabilize metals in low and unusual oxidation states. More recently, work has concentrated on the synthesis of a range of exotic polyphosphorus ligands whose complexes can only now be fully characterised as a result of simultaneous advances in modern spectroscopic techniques such as n.m.r., i.r., etc.

This thesis details the development of synthetic routes to a series of new polyphosphorus ligands which are shown to demonstrate a wide range of coordinative behaviour in their transition-metal complexes, and discusses the multinuclear n.m.r. characterisation of such species. The following section reviews the syntheses and coordinative behaviour of the known polyphosphorus ligands and examines the use of n.m.r. spectroscopy to characterise these ligands and their complexes and to solve problems related to structure.

CHAPTER 1

INTRODUCTION

1. INTRODUCTION

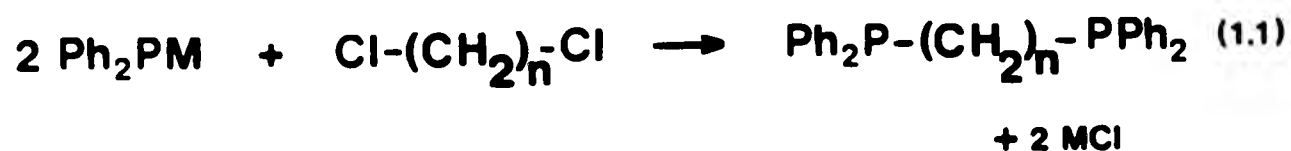
Since the establishment of the basis of modern coordination chemistry in the late nineteenth century, research in this and related fields has been extensive. Advances in the particular area of phosphorus-containing ligands and their transition-metal complexes have, however, only occurred within the last 30-40 years and were stimulated by discoveries that such ligands can stabilize metals in low and unusual oxidation states. More recently, work has concentrated on the synthesis of a range of exotic polyphosphorus ligands whose complexes can only now be fully characterised as a result of simultaneous advances in modern spectroscopic techniques such as n.m.r., i.r., etc.

This thesis details the development of synthetic routes to a series of new polyphosphorus ligands which are shown to demonstrate a wide range of coordinative behaviour in their transition-metal complexes, and discusses the multinuclear n.m.r. characterisation of such species. The following section reviews the syntheses and coordinative behaviour of the known polyphosphorus ligands and examines the use of n.m.r. spectroscopy to characterise these ligands and their complexes and to solve problems related to structure.

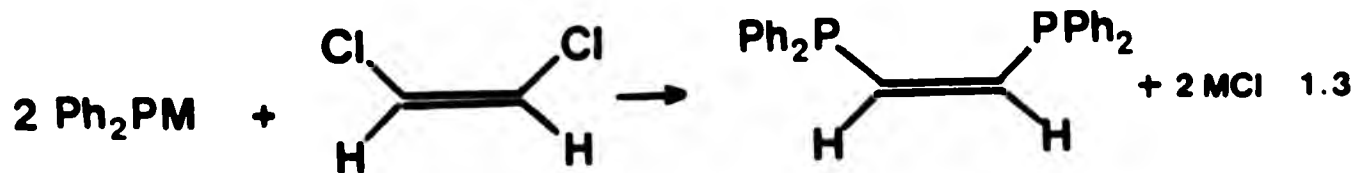
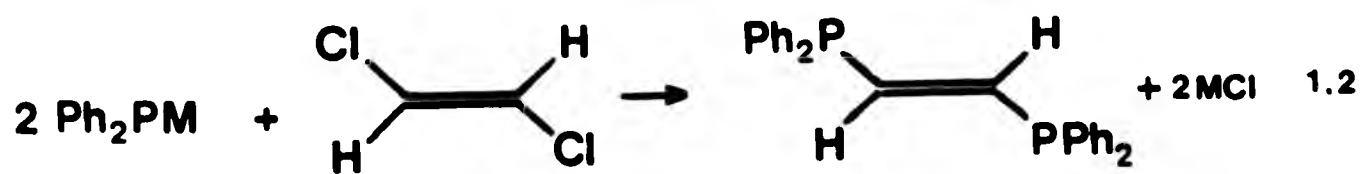
2. Organosphosphorus Ligands

(A) Diphosphines

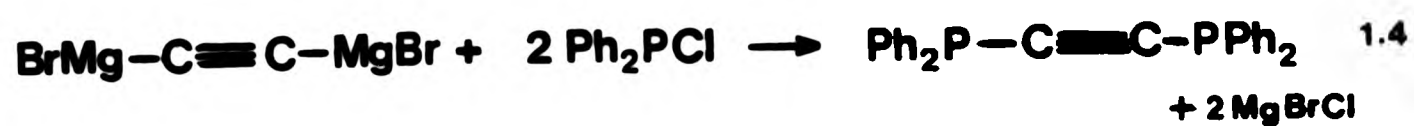
Perhaps the best documented of all polyphosphorus ligands are the ditertiary phosphine series bis(diphenylphosphino)methane (dppm), $\text{Ph}_2\text{PCH}_2\text{PPh}_2$, and its corresponding ethane and propane analogues, dppe and dppp. The preparation of these ligands employs the most widely used synthetic method for diphosphines in general, namely, the reaction between an alkali-metal phosphide and a dihaloalkane¹⁻⁴, (1.1).



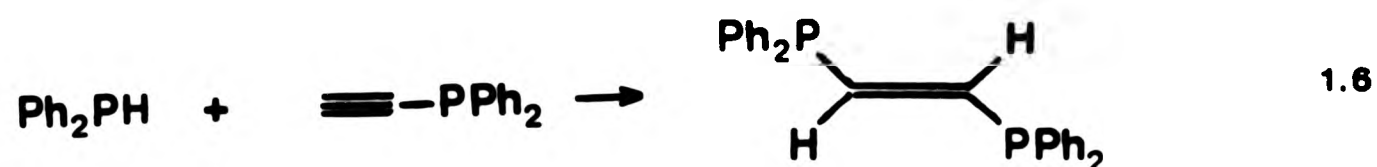
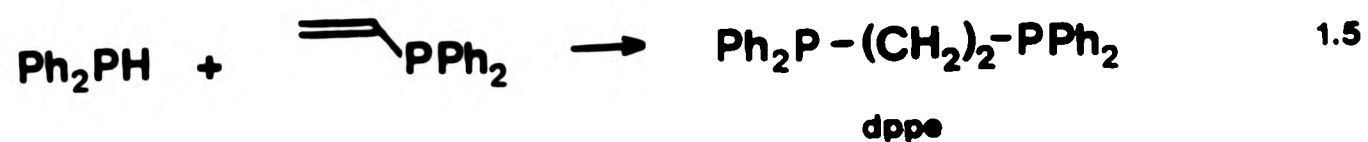
There are a few cases where this reaction is unsuitable, but in general yields are high. This reaction is also applicable to dihaloalkenes, for example, cis and trans-1,2-bis(diphenylphosphino)ethene which are obtainable from the corresponding cis and trans dihalides, the substitution being 100% regiospecific⁵ (1.2, 1.3).



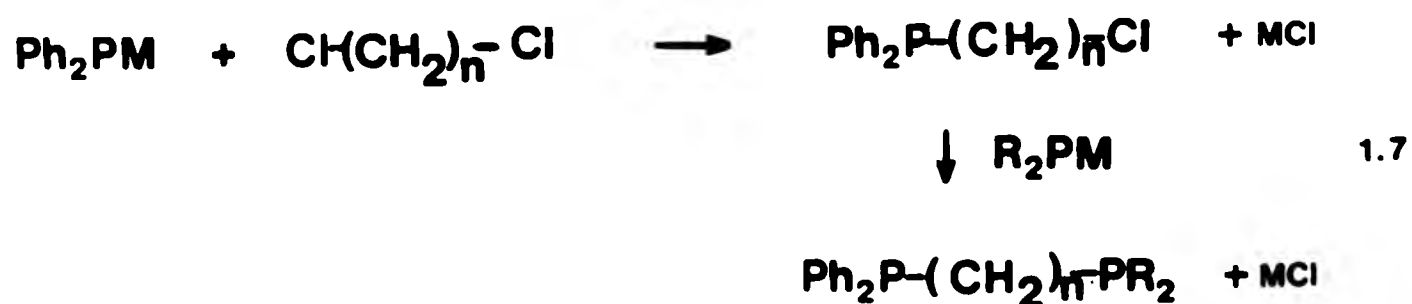
The preparation of bis(diphenylphosphino)ethyne by such methods is, however, precluded by the inaccessibility of dihaloalkynes and it is therefore best prepared in the following manner⁶. A second



method is also available for the preparation of diphosphines and utilizes base-catalysed addition of secondary phosphines to activated carbon-carbon double- or triple-bonds⁷⁻⁹. (1.5, 1.6) Furthermore,



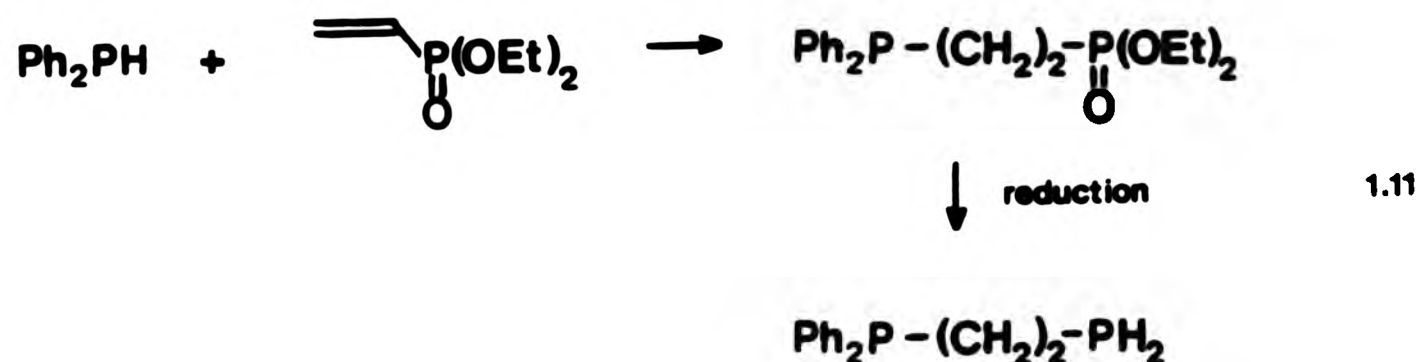
in an extension to the method of (1.1), sequential reactions between different alkali-metal phosphides and dihaloalkanes lead to the formation of asymmetric diphosphines as below¹⁰⁻¹¹.



Similarly, mixed phosphorus/arsenic analogues may be prepared by the use of alkali-metal arsenides in one of the steps¹²⁻¹⁴. Additionally, base-catalysed addition reactions may be adapted to prepare asymmetric, (1.8), and mixed donor ligands⁷ (1.9).



More recently, diphosphines containing combinations of primary, secondary and tertiary phosphine groups have been synthesised^{15,16,16a} which generally utilise addition reactions such as those below (1.10,1.11).



The coordination chemistry of diphosphine ligands is extremely wide-ranging and a wealth of research into their transition-metal complexes has been performed¹⁷⁻¹⁸. Such ligands generally coordinate in transition metal complexes in three different ways.

(i) Chelation

In forming chelate complexes a favoured ring size for a metal in an octahedral or square-planar environment is five as this is an arrangement of low strain. As a result, dppe has long been known as an excellent bidentate chelating ligand for many transition metals. The formation of a four-membered ring upon chelation of dppm, however, creates appreciable strain and consequently although its chelate chemistry is nevertheless extensive, it can and often does exhibit modes of coordination other than that of simple bidentate chelation. Similarly, although to a lesser extent, the six-membered ring structure formed by chelating dppp is not the only possibility, and here again other modes of coordination are found.

(ii) Bridging

As noted above, dppp and dppm often adopt a second type of coordination mode involving the bridging of two metals. This situation is nicely demonstrated by the series of complexes $[\text{RhCl}(\text{CO})\{\text{Ph}_2\text{P}(\text{CH}_2)_n\text{PPh}_2\}]_n$ which are bridged dimers for $n = 1$ and 3 (dppm and dppp) but a simple monomer for $n = 2$ (dppe) where chelation is preferred¹⁹. This relatively recently discovered ability of dppm and some of its analogues to bridge two metal atoms has led to considerable interest in this ligand, particularly with regard to homogeneous and heterogeneous catalysis which often invoke reactions involving two or more metal centres.

(iii) Monodentate

Perhaps the simplest of the types of coordination exhibited by such ligands is the monodentate mode. Again, because of the tendency of dppe to chelate, the monodentate forms of dppm and dppp are relatively better known, although often the chelate and corresponding monodentate

forms of transition-metal complexes can interconvert under suitable reaction conditions^{19a}.

In addition to the species exhibiting one of the three coordinative modes above, a wide variety of complexes have been reported involving combinations of these modes^{20,21} (Fig. 1.1)

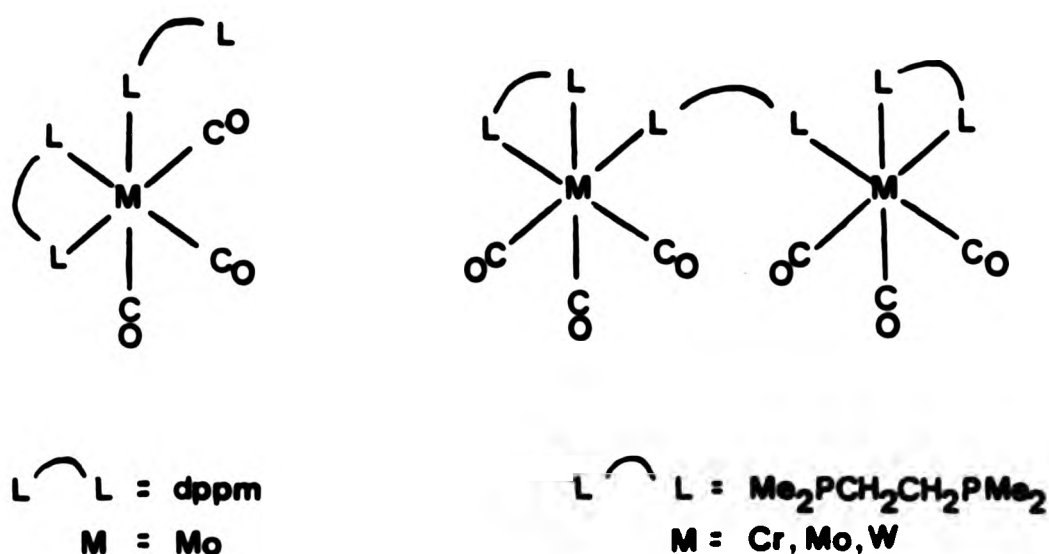
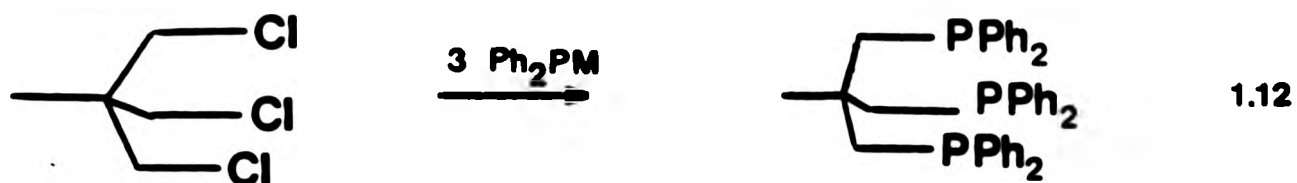


Fig 1.1

In general, whereas phenyl-substituted polyphosphines tend to be air-stable solids, the arsenic and antimony, and the alkyl-substituted analogues are often air-sensitive oily liquids, consequently making them more difficult to handle and therefore less attractive for study.

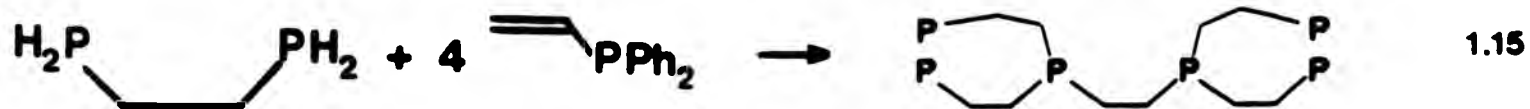
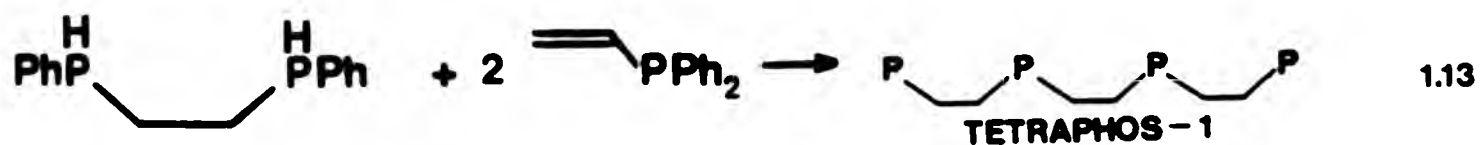
(B) Multidentate Phosphines

Continued research has in recent years led to the preparation of a large number of ligands containing three or more phosphorus atoms. The original methods for these syntheses involved replacement by phosphorus moieties of halide groups on a suitable carbon skeleton^{22,22a} (1.12), but this approach was restricted in its use because of the difficulties



of complete substitution and the inaccessibility of the starting polyhalo-alkanes.

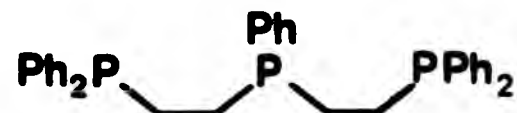
Methods devised by King²³⁻²⁵, however, utilizing base-catalysed addition reactions as previously outlined for diphosphines, have led to a variety of multidentate phosphines containing up to six phosphorus atoms. Some of the better known ligands prepared by these methods are as follows.



In discussing the coordination chemistry of triphosphine ligands it is convenient to place a particular ligand into one of two classes.

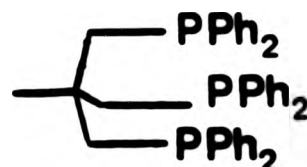
(i) Linear

e.g.



(ii) Tripodal

e.g.



Linear triphosphines can exhibit a wide variety of coordinative topologies as indicated in Fig. 1.2^{26,27} and there is a similar range of analogous modes for the tripodal ligands^{28,29}.

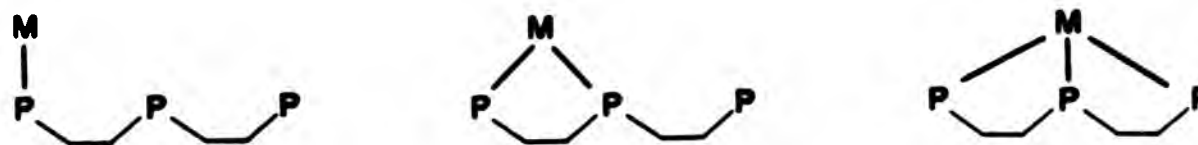
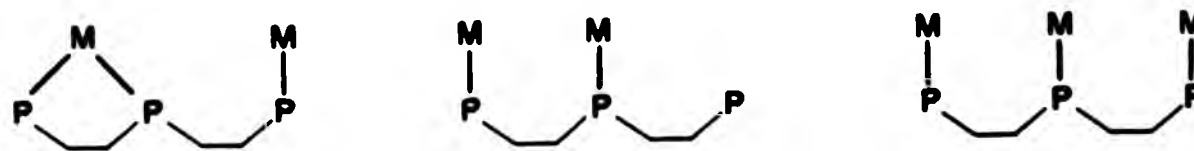


Fig 1.2



The ability of linear triphosphines to form square-planar chelate complexes such as that in Fig. 1.3 involving a planar arrangement of coordinated phosphorus atoms^{30,31} is also well known. However, for

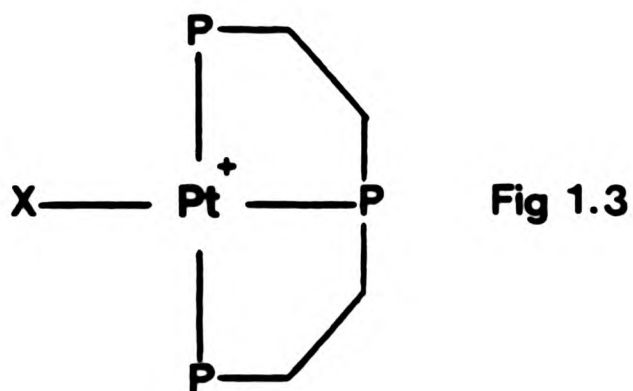


Fig 1.3

octahedral complexes the corresponding mer arrangement is not favoured since the analogous fac isomers are more stable. A study of the literature¹⁷ on such species revealed that the fac arrangement is overwhelmingly preferred for both linear and tripodal triphosphine ligands in octahedral transition-metal complexes. With regard to square-planar transition-metal complexes, the full coordination of tripodal triphosphine ligands is unlikely unless the ligand contains an extended backbone chain, and therefore partial coordination of the type shown in Fig. 1.4 is often preferred.

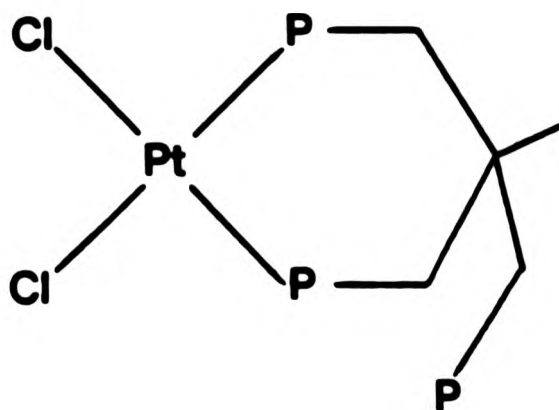
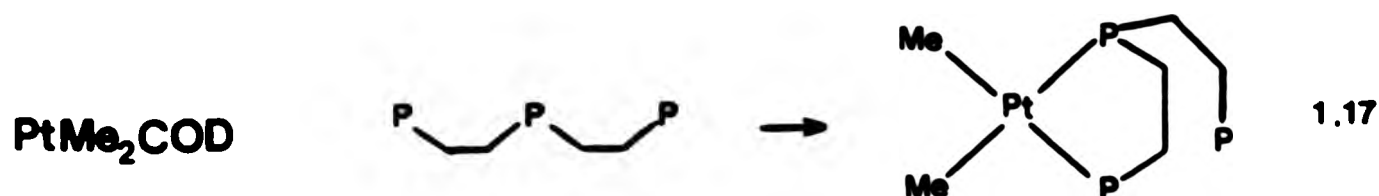
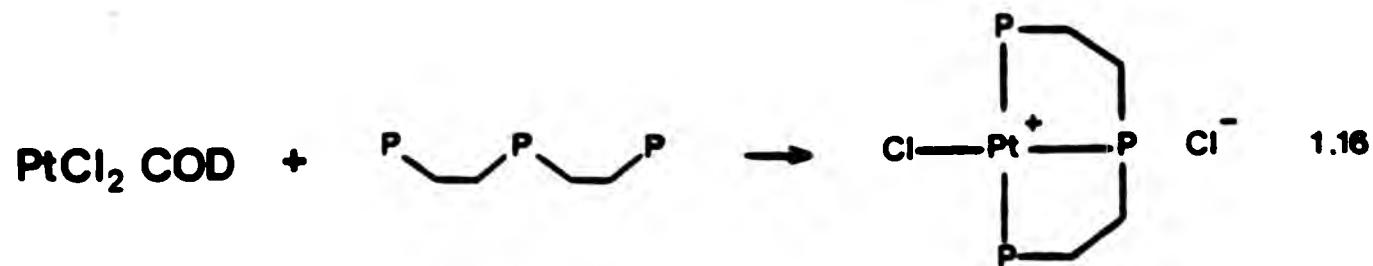


Fig 1.4

This partial coordination mode can also be exhibited by linear triphosphines in cases where replacement of certain groups on the metal is difficult³² (1.17). This is generally found to be so for dialkyl platinum and palladium species where replacement of the alkyl groups by phosphorus ligands is not favoured, and is in distinct contrast to

dihalo-platinum and palladium species (1.16).



For square-planar complexes full coordination of most tetradentate phosphine ligands is precluded by the high degree of strain required to adopt such an arrangement, although for octahedral metal complexes this constraint does not necessarily apply. In practice however, successive replacement of carbonyl groups by organophosphorus ligands gets progressively more difficult, and explanations of this usually involve discussions of the relative π -acidities of carbonyl and phosphorus ligands³³.

When a metal in a low oxidation state forms a complex involving metal + ligand σ -bonds stabilization occurs by delocalisation of some electron density on the metal back onto the ligand(s). This process involves overlap of a filled $d\pi$ metal orbital with a suitable vacant orbital on the ligand. Thus ligands with appropriate empty orbitals such as carbon monoxide (with a vacant $p\pi^*$ orbital) have the ability to relieve the metal atom of some of the electron density acquired by the σ -donation process and consequently to stabilize the complex. Such ligands are called π -acceptor ligands. Phosphorus ligands also show π -acceptor ability, the acceptor orbitals being the 3d-orbitals of

phosphorus, and therefore the overlap can be designated $d\pi-d\pi$. The extent of this back-donation depends to a high degree on the nature of the other groups on phosphorus. For instance, the highly electronegative fluorine atoms of PF_3 withdraw electrons from the phosphorus thus increasing the metal $d\pi$ -phosphorus $d\pi$ overlap. The result is that carbon monoxide and PF_3 are comparable in their π -bonding capacity and thus species such as $\text{M}(\text{PF}_3)_6$, ($\text{M}=\text{Cr}, \text{Mo}, \text{W}$), analogous to $\text{M}(\text{CO})_6$ are known³⁴. Organophosphorus ligands participate in $d\pi-d\pi$ overlap to a lesser extent than PF_3 , and as a result it is difficult to replace more than three carbonyl groups with organophosphorus ligands even when chelation is possible. A good example of this is the hexatertiary phosphine ligand 1,2-bis[bis(2-diphenylphosphinoethyl)-phosphino]ethane²⁴, (Fig. 1.5), which is a hexaphosphorus analogue of edta

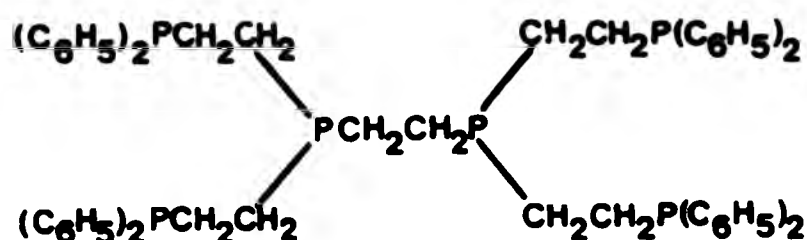
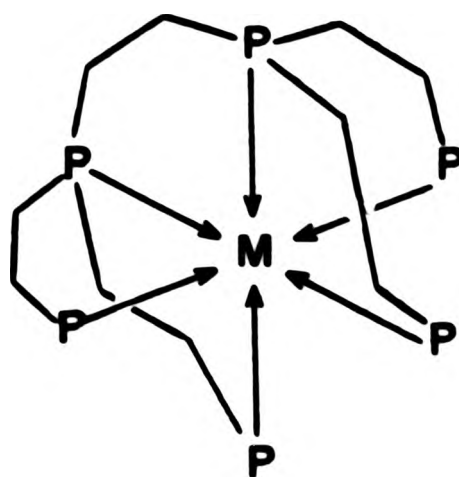
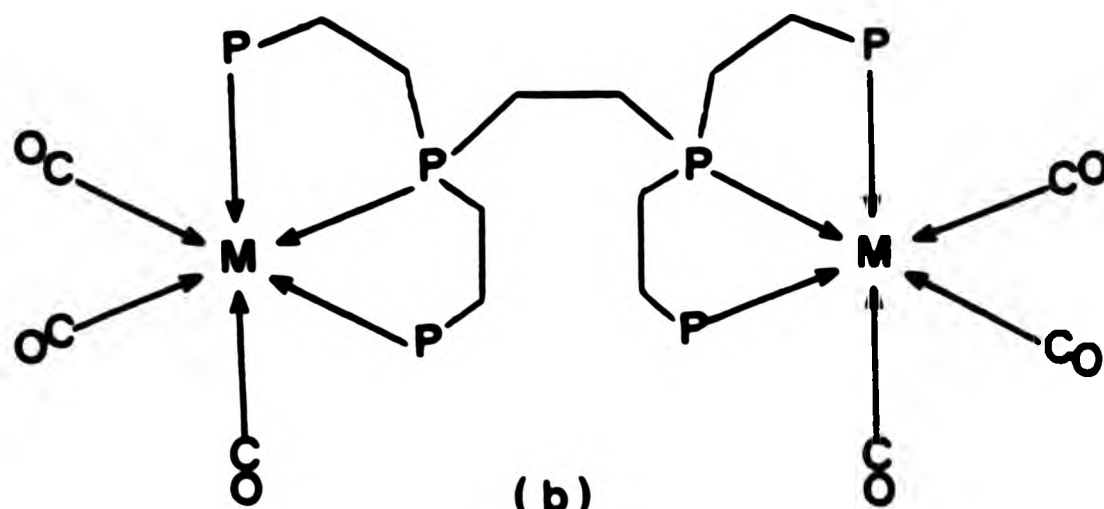


Fig 1.5

and could therefore expect to function as a hexadentate ligand fully coordinated to a single metal atom (Fig. 1.6a). However, because of the difficulty of complete carbonyl replacement, the bimetallic structure (Fig. 1.6b) is preferred. This tendency is typical of large polyphosphorus ligands which generally show a reluctance to coordinate more than three phosphorus atoms to a single metal centre³⁵.



(a)



(b)

Fig 1.6

3. N.M.R. Spectroscopy

(A) ^{31}P n.m.r.

The availability of the ^{31}P nucleus ($I = \frac{1}{2}$, abundance 100%) makes n.m.r. spectroscopy a highly effective tool for structural elucidation of phosphine ligands and their diamagnetic transition-metal complexes. Enough research has now been performed for values of n.m.r. parameters such as chemical shifts and coupling constants often to be used unambiguously to assign molecular structure and conformation. The following pages examine the factors affecting the magnitudes of these n.m.r. parameters in the types of molecule dealt with in this thesis.

(i) Factors Affecting ^{31}P Chemical Shifts

(a) Ligands

The characterisation of uncoordinated polydentate phosphine ligands by ^{31}P n.m.r. spectroscopy is generally straightforward. For monodentate organophosphorus ligands the chemical shifts of a given species can be fairly well estimated by consideration of group contributions³⁶, which are dependent on the type or types of organic group directly bonded to the phosphorus atom. Similar considerations apply to polyphosphorus species, for example, the ^{31}P chemical shifts of dppe and dppp follow closely those predicted by group contribution theory and are almost exactly those of Ph_2EtP and $\text{Ph}_2^{\text{n}}\text{PrP}$ respectively³⁷. The situation with dppm and related species is slightly different however because both steric factors due to the close proximity of the Ph_2P -groups and lone pair interactions play a significant role.

(b) Complexes

Although the characterisation of the ^{31}P chemical shifts of uncoordinated ligands was straightforward, the considerations when applied to their complexes are far more involved, but consequently give more

information with regard to molecular structure.

From a chemical point of view the ^{31}P chemical shift of a coordinated monodentate phosphine ligand is dependent on several factors. Generally speaking the ^{31}P chemical shift of a coordinated monodentate phosphine ligand will be to an appreciably higher frequency than that of the free ligand. The difference between the ^{31}P chemical shift of a coordinated phosphine ligand, $\delta(^{31}\text{P}_\text{C})$, and that of the free ligand $\delta(^{31}\text{P}_\text{F})$, is called the coordination chemical shift, Δ^{38} . It is dependent on the nature and the oxidation state of the metal, its stereochemical environment, and the nature of the groups in the positions cis and trans to the coordinated phosphorus atom. However, for a series of related complexes such as those in Table 1.1, Δ is fairly constant for a range of phosphorus ligands, and therefore for known structures it is often possible to predict closely the ^{31}P chemical shifts of coordinated ligands.

Table 1.1 ^{31}P chemical shift data for related cis PtCl_2L_2 species

L	$\delta(^{31}\text{P}_\text{C})/\text{ppm}$ ^a	$\delta(^{31}\text{P}_\text{F})/\text{ppm}$ ^a	Δ/ppm	Ref.
PPh_2Me	-1.2	-28.1	+26.9	40
PPh_2Et	+9.8	-12.5	+22.3	40
PPh_2Pr	+6.9	-17.6	+24.5	40
PPh_2Bu	+7.0	-17.1	+24.1	39
PPhPr_2	-2.7	-27.7	+25.0	39
PPhBu_2	-2.3	-26.2	+23.9	39

a. Relative to 85% $\text{H}_3\text{PO}_4 = 0.00 \text{ ppm}$.

A similar argument can also be employed for predictions of ^{31}P chemical shifts for polyphosphorus ligands coordinated in a monodentate

mode, although it must be remembered that for dppm and its analogues, coordination may radically alter any steric effects on $\delta(^{31}\text{P})$ and may also destroy any lone pair interactions between phosphorus atoms. This leads not only to difficulty in the prediction of ^{31}P chemical shifts for the coordinated phosphorus nucleus but can also bring about substantial changes in $\delta(^{31}\text{P})$ for the uncoordinated phosphorus.

The relationship between the ^{31}P chemical shift of a free ligand and that when chelated is, however, far more complicated. In order to best explain the relationship it is useful to introduce a new parameter, Δ_R , or ring-strain contribution, to chemical shift considerations^{40a}. This is simply defined as the difference between the coordination chemical shift, Δ , of a chelated diphosphine complex and that of an equivalent atom in a non-chelate complex. Thus Δ_R is a measure of the change in $\delta(^{31}\text{P})$ upon chelation (Table 1.2).

TABLE 1.2 ^{31}P nmr data for cis PtCl_2L_2 species

Ligand	$\delta(^{31}\text{P}_\text{C})/\text{ppm}$ ^a	$\delta(^{31}\text{P}_\text{F})/\text{ppm}$ ^a	Δ/ppm	Δ_R/ppm	Ref.
dppm	-64.3	-22.7	-41.6	-68.5	40
PPh_2Me	-1.2	-28.1	+26.9		
dppe	+45.3	-13.2	+58.5	+36.2	40
PPh_2Et	+9.8	-12.5	+22.3		
dppp	-5.6	-17.3	+11.7	-12.8	40
PPh_2Pr	+6.9	-17.6	+24.5		

a. Relative to 85% $\text{H}_3\text{PO}_4 = 0.0$ ppm

The values of Δ_R shown in this table exhibit a typical sequence for this series of ligands which in general demonstrate a large shielding effect for the highly-strained four-membered rings and to a lesser extent for the six-membered rings, but a deshielding effect for the

relatively unstrained five-membered rings^{40b}.

Although there is no adequate theory of Δ_R , a knowledge of this parameter is extremely valuable as an aid to the characterisation of chelate complexes. As will be demonstrated later in this thesis, ^{31}P chemical shifts for four- and five-membered chelate rings lie in mutually exclusive ranges for a given metal, and are therefore important for the determination of unknown structural features.

(ii) Factors affecting phosphorus-phosphorus coupling constants

(a) Free Ligands

For free polyorganophosphorus ligands the magnitudes of phosphorus-phosphorus couplings, $^n\text{J}(^{31}\text{P}-^{31}\text{P})$, are generally dependent on two factors:

- i. the number of bonds (n) through which the phosphorus-phosphorus coupling is transmitted;
- ii. the relative orientations of the lone-pairs on the two phosphorus atoms.

In general, values for $^n\text{J}(^{31}\text{P}-^{31}\text{P})$ decrease with increasing n (Table 1.3) and therefore serve as a useful guide in the characterisation of polyphosphorus ligands.

TABLE 1.3 $^n\text{J}(^{31}\text{P}-^{31}\text{P})$ values for diphosphine ligands
(Data from ref.54.)

Ligand	$ ^n\text{J}(^{31}\text{P}-^{31}\text{P}) /\text{Hz}$	n
dppm	125.0	2
dppe	33.6	3
dppp	1.0	4
dppb	0.0	5

The lone-pair orientational dependence of phosphorus-phosphorus coupling constants is somewhat more difficult to analyse. By a

combination of low temperature n.m.r. and x-ray studies Keat and co-workers⁴¹ suggest that for geminally related phosphorus nuclei cis conformations of lone-pairs such as that in Fig. 1.7a tend to be associated with large positive values of $^2J(^{31}\text{P}-^{31}\text{P})$ whereas conformation b leads to low negative values. They also find that when X carries a

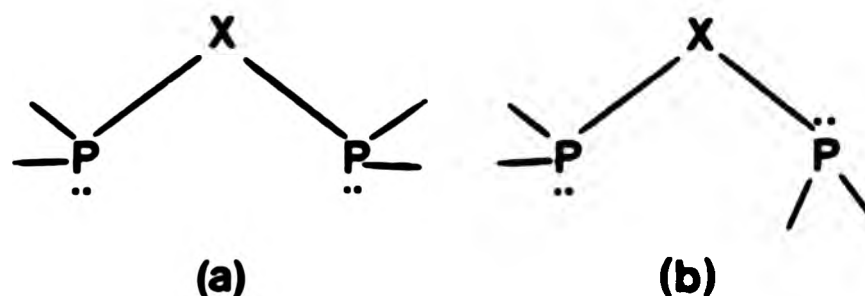


Fig 1.7

bulky group, such as tertiary-butyl, conformation b is more likely to predominate. Thus it is likely that for dppm the value of $^2J(^{31}\text{P}-^{31}\text{P})$, (+125.0 Hz) suggests a conformation close to a. However, this conformational dependence is itself dependent on n and thus while it is still important for discussions of $^3J(^{31}\text{P}-^{31}\text{P})$, longer range couplings are not significantly affected.

(b) Complexes of monodentate ligands

Many metal complexes are known that have more than one coordinated monodentate phosphine ligand, and the values of $^2J(^{31}\text{P}-\text{M}-^{31}\text{P})$ have been found to be dependent on three main factors.

1. Substituents on the phosphorus atom

The magnitude of a coupling to any given nucleus is now generally agreed to be to a large extent dependent on the s-electron density at that nucleus⁴². In the case of phosphorus ligands, electronegative substituents such as -F, -OR etc. tend to polarise the bond to phosphorus, thus in effect contracting the s-electron density closer to the

^{31}P nucleus which results in an effective increase in its s-electron density. As a consequence phosphorus-phosphorus couplings between PF_3 or P(OR)_3 ligands are generally significantly greater in magnitude than analogous couplings involving simple triaryl or trialkyl phosphines (Table 1.4). This is also the case for couplings between other nuclei and phosphorus (Table 1.5).

TABLE 1.4 Selected ^{31}P - ^{31}P coupling constants demonstrating dependence of $^2J(^{31}\text{P}$ - $^{31}\text{P})$ on electronegativity of substituents

Complex	$ ^2J(^{31}\text{P}$ - $^{31}\text{P}) /\text{Hz}$	Ref.
<u>trans</u> (CO) $_4\text{Mo}(\text{Bu}_3\text{P})(\text{Ph}_3\text{P})$	50.0	42a
<u>trans</u> (CO) $_4\text{Mo}(\text{Bu}_3\text{P})[(\text{PhO})_3\text{P}]$	112.0	42a
<u>trans</u> (CO) $_4\text{W}(\text{Bu}_3\text{P})(\text{Ph}_3\text{P})$	65.0	42a
<u>trans</u> (CO) $_4\text{W}(\text{Bu}_3\text{P})[(\text{PhO})_3\text{P}]$	112.0	42a
<u>trans</u> (CO) $_4\text{Mo}[\text{P(OMe)}_3]_2$	162 ± 5	43
<u>trans</u> (CO) $_4\text{Mo}(\text{PF}_3)_2$	312.0	43

TABLE 1.5 Selected n.m.r. data for a series of complexes $\text{W(CO)}_5\text{L}$

Ligand	$^1J(^{183}\text{W}$ - $^{31}\text{P})/\text{Hz}$	Ref.
PF_3	485	43
PCl_3	426	43
PBr_3	398	43
PI_3	334	43
P(OPh)_3	415	43
PPh_3	280	43

ii. The metal atom M

The dependence of $^2J(^{31}\text{P}-\text{M}-^{31}\text{P})$ on the nature of the metal atom is difficult to explain. The best studied series of phosphine complexes appears to be the derivatives of the group VIB metal carbonyls, and experimental results reveal that for a trans coupling $|^2J(^{31}\text{P}-\text{M}-^{31}\text{P})|$ decreases in the order $\text{W} > \text{Mo} > \text{Cr}$ whilst for a cis coupling the opposite is true $\text{Cr} > \text{Mo} > \text{W}$. This may be simply because the signs of the various coupling constants have not been taken into account since the limited amount of data available on the values of $^2J(^{31}\text{P}-^{31}\text{P})$ for analogous cis and trans complexes often reveal them as having opposite signs.

iii. Stereochemistry

The general rule that $|^2J(^{31}\text{P}-^{31}\text{P})_{\text{trans}}| \gg |^2J(^{31}\text{P}-^{31}\text{P})_{\text{cis}}|$ is dramatically demonstrated by square-planar complexes of palladium and platinum (Table 1.6).

TABLE 1.6 Comparison of $^2J(^{31}\text{P}-^{31}\text{P})$ for analogous cis and trans complexes of palladium and platinum

Complex	$ ^2J(^{31}\text{P}-\text{M}-^{31}\text{P}) /\text{Hz}$	Ref.
<u>cis</u> $\text{PdCl}_2(\text{PMe}_2\text{H})_2$	0	44
<u>trans</u> $\text{PdCl}_2(\text{PMe}_2\text{H})_2$	515	44
<u>cis</u> $\text{PtCl}_2[\text{P}(\text{OPh})_3](\text{PBu}_3)$	20	45
<u>trans</u> $\text{PtCl}_2[\text{P}(\text{OPh})_3](\text{PBu}_3)$	709	45

This rule is also followed for many other transition-metal complexes including $\text{Mo}(\text{O})$ and $\text{W}(\text{O})$ but not for $\text{Cr}(\text{O})$ where often $|^2J(^{31}\text{P}-^{31}\text{P})_{\text{cis}}| > |^2J(^{31}\text{P}-^{31}\text{P})_{\text{trans}}|$. Again, this may simply be due to a difference in signs between cis and trans phosphorus-phosphorus couplings for chromium where it is possible that the trans couplings are more positive than analogous cis couplings.

It is tempting to attribute the generally larger trans couplings to effects of $d\pi$ -bonding, but there are many cases where the rule is disobeyed (chromium), and also where π -bonding cannot take place (for instance couplings to protons) where the rule is followed nevertheless.

(c) Complexes Incorporating Chelating Ligands

Except for ligands such as $\text{Ph}_2\text{P}(\text{CH}_2)_n\text{PPh}_2$ where $n > 10$, the discussion of phosphorus-phosphorus coupling constants in chelate complexes can be confined to that of the cis arrangement. Grim et al.⁴⁶ have suggested that ^{31}P - ^{31}P coupling in such systems may be considered as a combination of two contributions: the 'through the metal' contribution, $^M J(^{31}\text{P}-^{31}\text{P})$, and the 'through the backbone' contribution, $^B J(^{31}\text{P}-^{31}\text{P})$. Values of $^M J(^{31}\text{P}-^{31}\text{P})$ can be estimated by consideration of a range of analogous non-chelate complexes and $^B J(^{31}\text{P}-^{31}\text{P})$ is likely to be of the order of that found in the free ligand. As previously mentioned $^n J(^{31}\text{P}-^{31}\text{P})$ decreases sharply with an increase in n for free ligands, and since in dppp $^4 J(^{31}\text{P}-^{31}\text{P})$ is almost negligible, the phosphorus-phosphorus couplings in its chelate complexes can be considered to be due to the through the metal contributions alone. For dppe, the presence of a low value for $J(^{31}\text{P}-^{31}\text{P})$ in its chelate complexes⁴⁶ leads to the conclusion that $^M J(^{31}\text{P}-^{31}\text{P})$ is approximately equal to $^B J(^{31}\text{P}-^{31}\text{P})$ but of opposite sign. It is likely that the contribution, $^B J(^{31}\text{P}-^{31}\text{P})$, is a modified value of $^n J(^{31}\text{P}-^{31}\text{P})$ in the free ligand, and that the extent of the modification will be dependent on the amount of ring strain (1.18),

$$^B J(^{31}\text{P}-^{31}\text{P}) = ^F J(^{31}\text{P}-^{31}\text{P}) + ^{RS} J \quad (1.18)$$

where $^F J(^{31}\text{P}-^{31}\text{P})$ is the value of the phosphorus-phosphorus coupling constant in the free ligand and $^{RS} J$ is the deviation in this coupling constant upon chelation. In the case of dppm it may be because this deviation is large for the highly strained four-membered chelate rings

that the magnitudes of $J(^{31}\text{P}-^{31}\text{P})$ in its chelate complexes are relatively low compared to that found in the free ligand⁴⁷.

(iii) Factors Affecting Metal-Phosphorus Couplings

For phosphine complexes of transition-metals such as molybdenum, tungsten, platinum, rhodium etc it is possible to determine values of $^1J(\text{M}-^{31}\text{P})$ relatively simply, and consideration of these values often helps in structural elucidation. In particular $^nJ(\text{M}-^{31}\text{P})$ is usually at least an order of magnitude greater for $n = 1$ than for $n > 1$.

For a given metal $^1J(\text{M}-^{31}\text{P})$ depends to a large extent on the nature of the phosphorus ligand (more specifically the electronegativities of its substituents) as discussed previously, and also on the nature of the groups trans to the this ligand.

A good discussion of the significance of the trans influence on such systems has been presented by Appleton et al.⁴⁸ They considered that within a related series of complexes such as those in Table 1.7

TABLE 1.7 Selected values of $^1J(^{195}\text{Pt}-^{31}\text{P})$ for a series of related complexes (Data from Ref 48a)

Complex	$^1J(^{195}\text{Pt}-^{31}\text{P})/\text{Hz}$	<u>Trans</u> group
<u>cis</u> Pt(Me)Cl(PEt ₃) ₂	4179	Cl
<u>cis</u> Pt(Me)Cl(PEt ₃) ₂	1719	Me
<u>cis</u> Pt(Ph)Cl(PEt ₃) ₂	4138	Cl
<u>trans</u> Pt(Me)Cl(PEt ₃) ₂	2821	(PEt ₃)
<u>trans</u> Pt(Ph) ₂ (PEt ₃) ₂	2824	(PEt ₃)
<u>cis</u> Pt(Me) ₂ (PEt ₃) ₂	1856	Me

the large variations in values of $^1J(^{195}\text{Pt}-^{31}\text{P})$ must be related to changes in the covalency of the platinum-phosphorus bond and in particular

to changes in the s-character of the bonding orbital used by platinum. These will be brought about by differences in trans-influence between the different mutually trans groups. The trans-influence of a ligand can be defined as the extent to which that ligand weakens the bond in the position trans to itself. This weakening can be considered as increasing the ionic character of the bond in the trans position which effects an increase in the s-electron density at the metal nucleus (in this case ^{195}Pt). Allen and Sze⁴⁹ have combined several sets of results and obtained a trans influence series (order of increasing value of $^1J(^{195}\text{Pt}-^{31}\text{P})$) as follows: $\text{Ph} > \text{Me} > \text{PR}_3 > \text{P(OR)}_3 > \text{CN} > \text{NR}_3 > \text{X}^-$ which is demonstrated by values shown in Table 1.7. Changes in $^1J(^{195}\text{Pt}-^{31}\text{P})$ upon altering the cis ligand are also seen to be far less important.

These arguments that involve the trans-influence to predict values of $^1J(^{31}\text{P}-\text{M})$ complexes of monodentate ligands, can also be applied to chelate complexes. Although $^1J(^{31}\text{P}-\text{M})$ values in chelates can differ quite substantially from those in analogous non-chelates, the dependence on the trans ligand does show a similar pattern. Distortions of the natural inter-bond angles at the phosphorus atoms due to ring-strain, with corresponding changes in s-electron density at the nucleus, may cause the differences between values of $^1J(^{31}\text{P}-\text{M})$ in analogous chelate and non-chelate metal complexes.

Other Nuclei

Although the use of ^{31}P n.m.r. spectroscopy to characterise structures of complexes of polyphosphorus ligands is extensive, n.m.r. studies of other nuclei can and often do play an important role in further structural elucidation. Much of the earlier work used proton n.m.r., but most of the molecules studied in this thesis have unduly complicated proton spectra, and this technique was not used to any great extent.

^{13}C n.m.r. spectroscopy is now a highly sophisticated analytical tool for the chemist and an ever-increasing volume of experimental data is available such that it is now possible to make fairly confident predictions of ^{13}C n.m.r. parameters by analogy with other previously known compounds, even for organometallic species⁵⁰. Thus, consideration of, for example, the ^{13}C n.m.r. spectra of the carbonyl region for metal carbonyl phosphine complexes can give unambiguous information on structure and geometry. Also, analysis of ^{13}C n.m.r. spectra in certain (usually symmetrical) cases can, by calculation, give values of ^{31}P n.m.r. parameters which cannot be determined simply by inspection of the ^{31}P n.m.r. spectra.

More recently, with the improvement in n.m.r. spectrometer sensitivity, it has been possible to study metal nuclei such as ^{195}Pt and ^{95}Mo directly, and in fact ^{195}Pt spectra for the new platinum complexes reported in this thesis were obtained routinely. Here again because of the rapidly increasing amount of data available for these and other nuclei^{51,52} it is now possible to use metal n.m.r. parameters to establish structures. Generally, metal chemical shifts lie in characteristic ranges for different stereochemistries, chelate ring sizes etc, and an examination of these and related phenomena appears in relevant chapters later in this thesis.

CHAPTER 2

NEW POLYPHOSPHORUS LIGANDS

1. INTRODUCTION

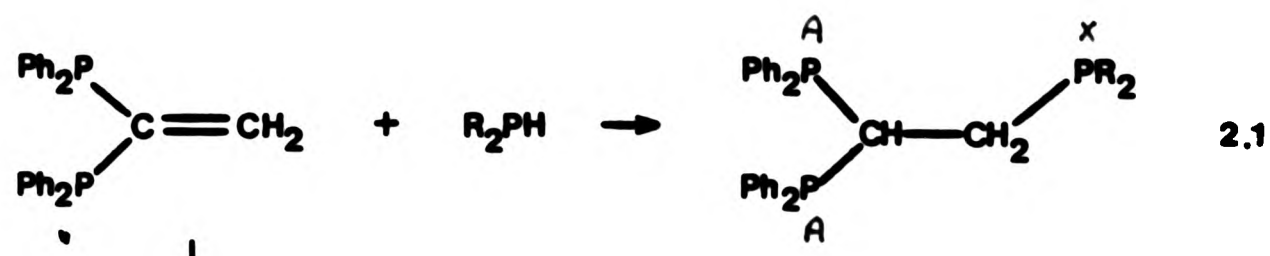
The aim of this work was to prepare a range of polyphosphorus ligands with the ability to exhibit a wide variety of coordinative behaviour. In particular emphasis was placed upon the design of ligands having the potential to demonstrate ring-size preferences upon chelation.

This chapter discusses the preparation and study by n.m.r. spectroscopy of new polyphosphorus ligands containing up to seven donor atoms. Subsequent chapters report transition-metal complexes and derivatives of these new ligands in a range of stereochemical environments.

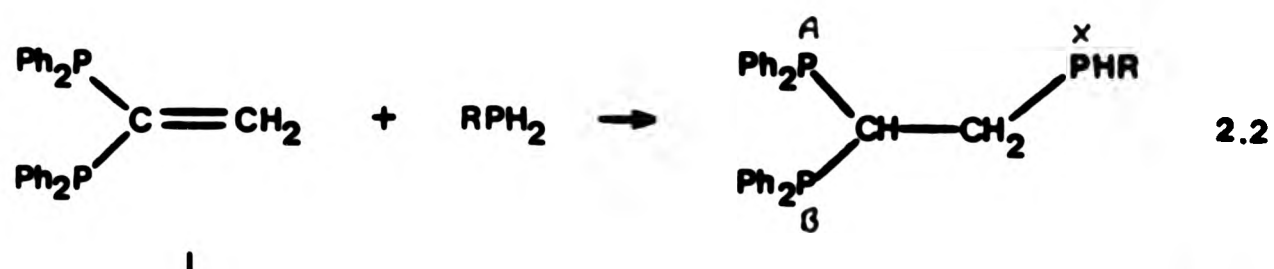
2. RESULTS AND DISCUSSION

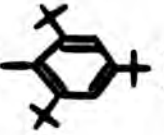
(A) Triphosphines and Related Species

The reaction between diphenylphosphine and an equimolar amount of 1,1-bis(diphenylphosphino)ethene, (I), in THF at room temperature with potassium tertiary butoxide catalyst resulted in immediate and virtually quantitative formation of 1,1,2-tris(diphenylphosphino)ethane (II). Similar reactions also occurred with Mes_2PH , $^t\text{Bu}_2\text{PH}$ and PhMePH to give the related triphosphine ligands (III - V) (Eq. 2.1) in varying yields as described in chapter 7. These reactions were also found to be applicable to a range of primary phosphines and then led to ready formation of ligands containing two tertiary phosphine atoms, and one secondary phosphine atom. (Eq. 2.2)



II - R = Ph
 III - R = Mesityl
 IV - R = ^tBu
 V - R = Ph/Me

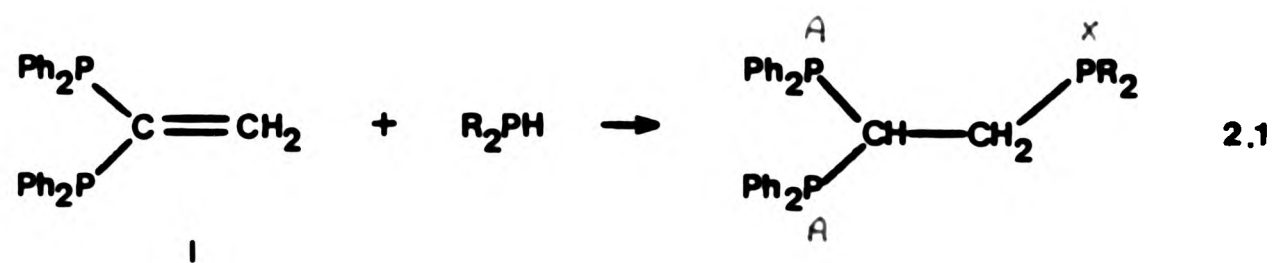


VI - R = Ph
 VII - R = (tri-^tBu)-Ph-()
 VIII - R = CH₂CH₂CN
 XIX - R = ⁿBu

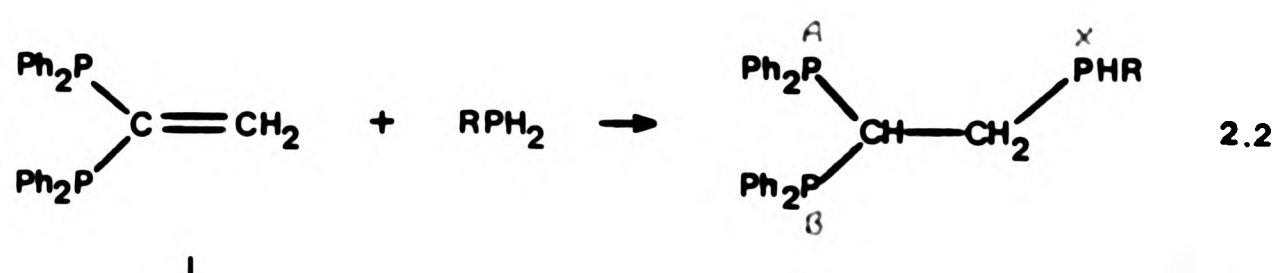
The ³¹P n.m.r. spectra of the reaction mixtures revealed virtually quantitative formation of the mixed tertiary/secondary species, suggesting that the phosphorus-hydrogen bonds in the new species are generally less reactive towards addition than the phosphorus-hydrogen bonds in the starting primary phosphines.

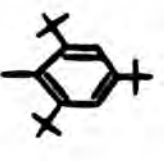
The new species II, VI and VII were isolated as air-stable white solids with sharp melting points and satisfactory elemental analyses (page 180).

By analogous methods, addition of diphenylphosphine to bis(diphenylphosphino)ethyne resulted in the formation of the new rigid tritertiary phosphine ligand 1,1,2-tris(diphenylphosphino)ethene (X) (Eq. 2.3)



II - R = Ph
 III - R = Mesityl
 IV - R = ^tBu
 V - R = Ph/Me

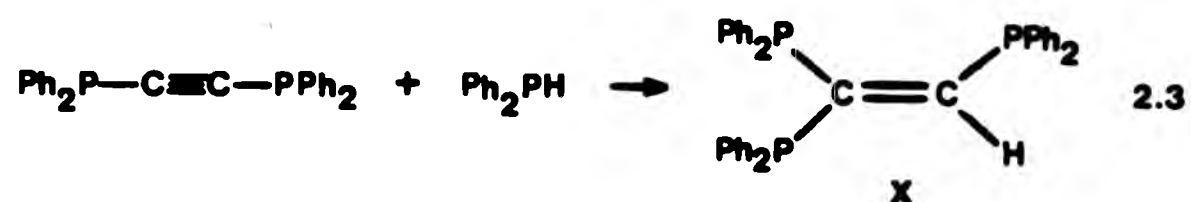


VI - R = Ph
 VII - R = (tri-^tBu)-Ph-()
 VIII - R = CH₂CH₂CN
 XIX - R = ⁿBu

The ³¹P n.m.r. spectra of the reaction mixtures revealed virtually quantitative formation of the mixed tertiary/secondary species, suggesting that the phosphorus-hydrogen bonds in the new species are generally less reactive towards addition than the phosphorus-hydrogen bonds in the starting primary phosphines.

The new species II, VI and VII were isolated as air-stable white solids with sharp melting points and satisfactory elemental analyses (page 180).

By analogous methods, addition of diphenylphosphine to bis(diphenylphosphino)ethyne resulted in the formation of the new rigid tritertiary phosphine ligand 1,1,2-tris(diphenylphosphino)ethene (X) (Eq. 2.3)



which was isolated as air-stable crystals. Further addition of diphenylphosphine to the double bond was found not to occur under these conditions, presumably owing to steric hindrance.

For compounds II - IV, rapid rotation about the carbon-carbon single bond results in chemical and magnetic equivalence of the two geminally related phosphorus nuclei and leads to these species having ^{31}P n.m.r. spectra characteristic of A_2X spin systems (Fig. 2.1). The presence of a chiral centre at the phosphorus atom X in compounds V - XIX, however, renders the two geminally-related phosphorus nuclei chemically and therefore magnetically inequivalent (Fig. 2.2) and because of

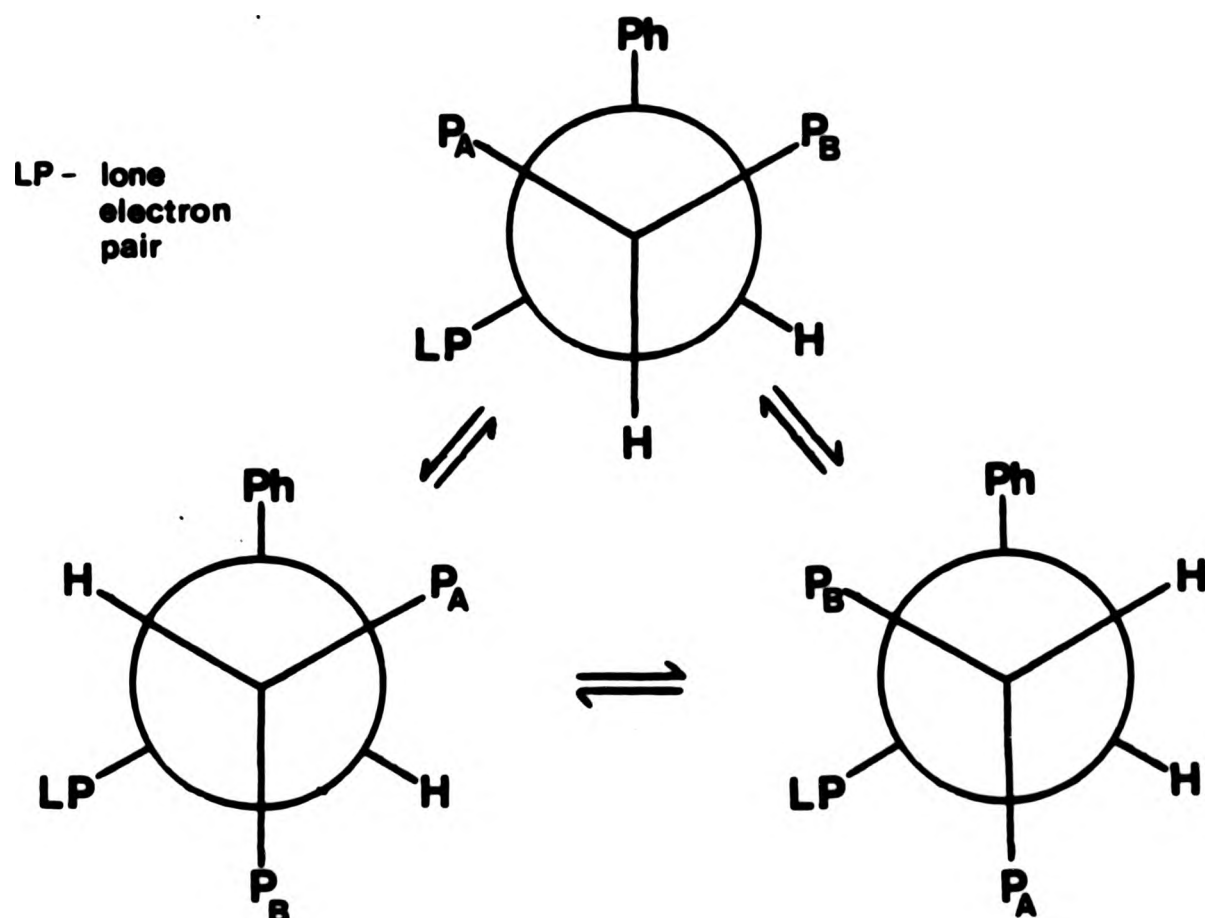


Fig 2.2 - Newman projection along the $\text{CH}-\text{CH}_2-\text{P}$ fragment of VI showing chemical inequivalence of P_A and P_B .

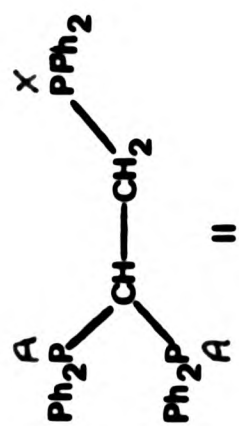


Fig 2.1 - ^{31}P N.M.R. spectrum of II recorded at 24.2 MHz.

24.4 Hz

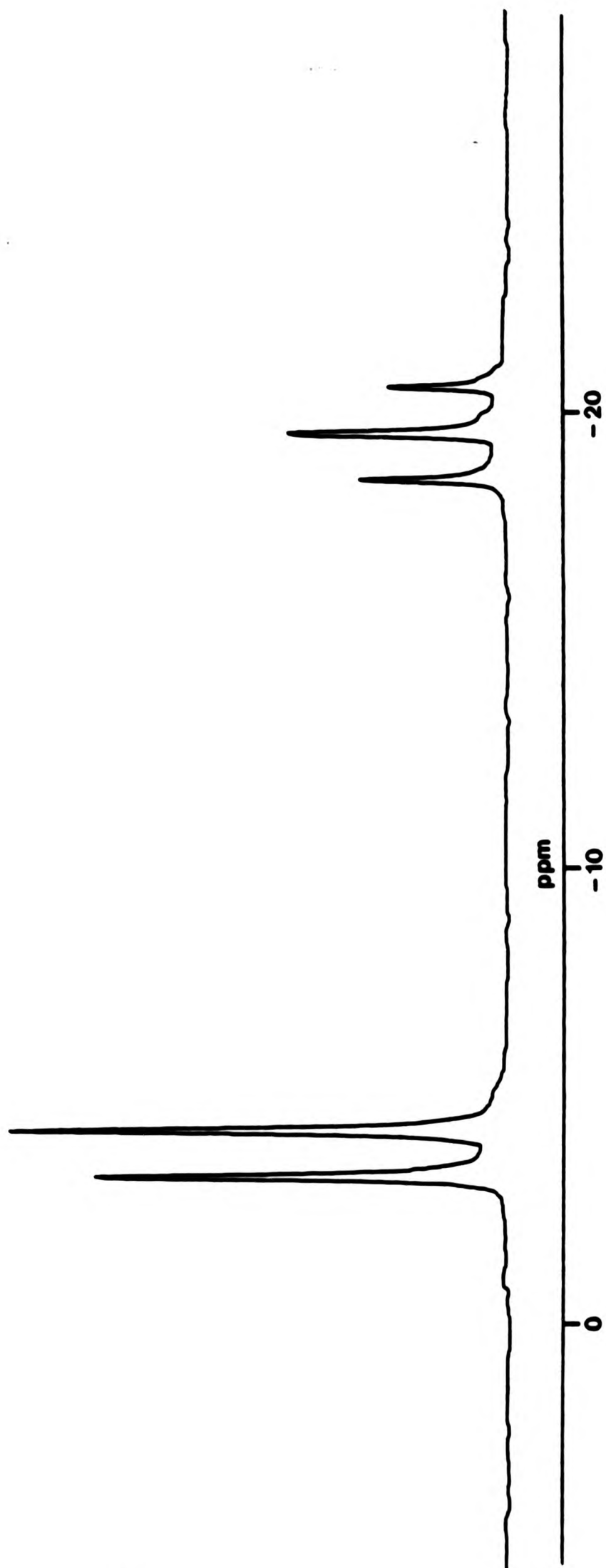
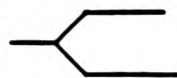
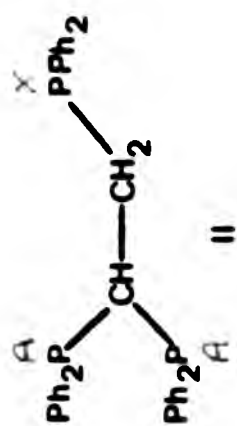
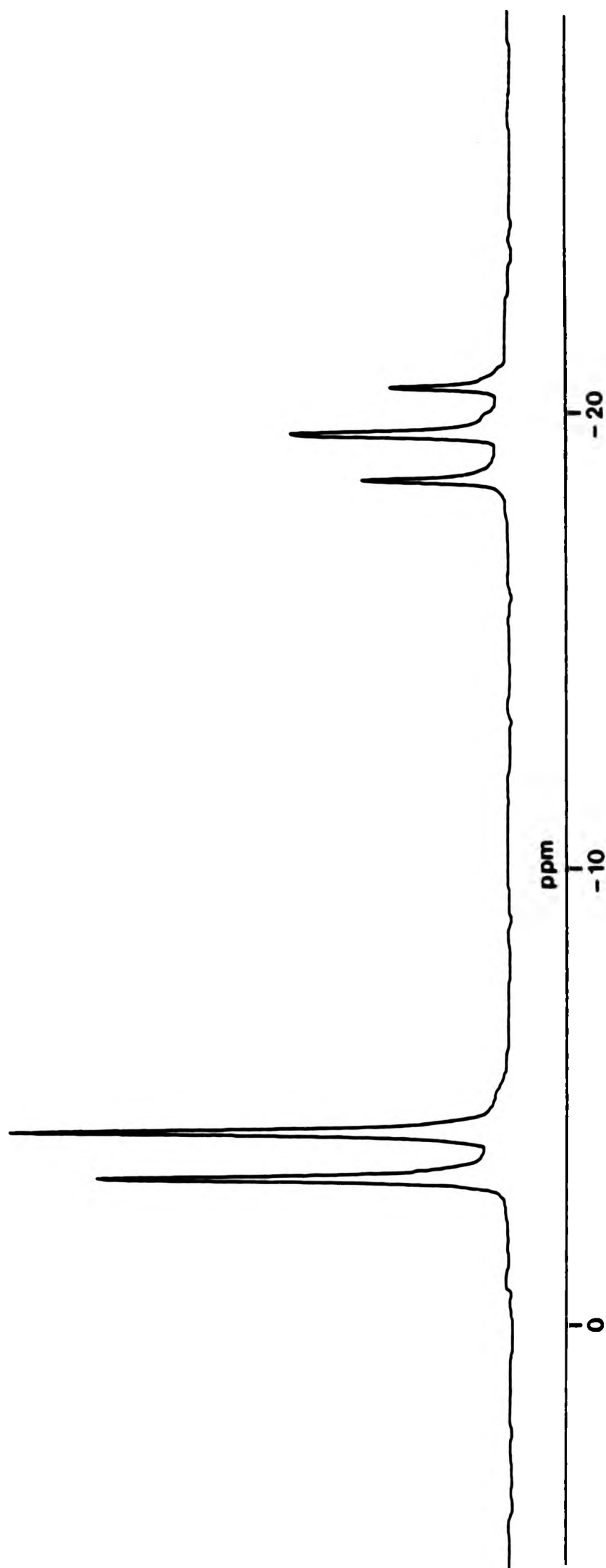
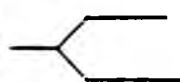


Fig 2.1 - ^{31}P N.M.R. spectrum of II recorded at 24.2 MHz.



24.4 Hz



this these species therefore give ABX ^{31}P n.m.r. spectra (Fig. 2.3) where A and B are the geminally related phosphorus nuclei. Analysis of these spectra⁵³ led to the ^{31}P n.m.r. parameters shown in Table 2.1 which show some interesting and important features as follows.

The chemical shifts of the geminal phosphorus nuclei A and B appear to be only slightly affected by changes in the nature of the vicinal phosphorus atom X, whereas the chemical shift of $\text{P}_{\bar{A}}$ is critically dependent on the types of group bonded to it³⁶.

For species that have A_2X spin systems $^2\text{J}(^{31}\text{P}-^{31}\text{P})$ cannot be determined by inspection of the ^{31}P n.m.r. spectra, but for species with chiral phosphorus nuclei $|^2\text{J}(\text{P}_\text{A}\text{P}_\text{B})|$ can be measured directly. Prior to the synthesis of VII it appeared that the magnitudes of $^2\text{J}(\text{P}_\text{A}\text{P}_\text{B})$ were virtually independent of the nature of P_X (112.3 Hz - 125.7 Hz), and comparable to that in dppm (125 Hz). However, the substantially reduced value of $|^2\text{J}(\text{P}_\text{A}\text{P}_\text{B})|$ for VII (58.6 Hz) suggests this is not the case. The conformational dependence of $^2\text{J}(^{31}\text{P}-^{31}\text{P})$ examined by Keat and co-workers⁴¹, described in Chapter 1, suggests that large values of $^2\text{J}(^{31}\text{P}-^{31}\text{P})$ are found for conformations such as that in Fig. 2.4(a), that low values are found in species preferring conformations similar to (b), and that conformation (b) predominates when X

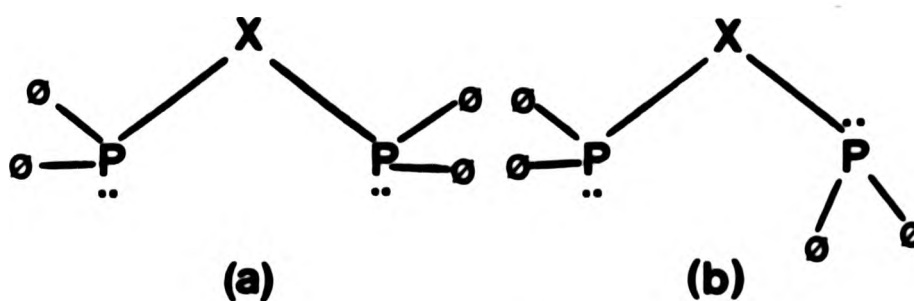


Fig 2.4

Fig 2.3 - ^{31}P N.M.R. spectrum of VII recorded at 36.2 MHz.

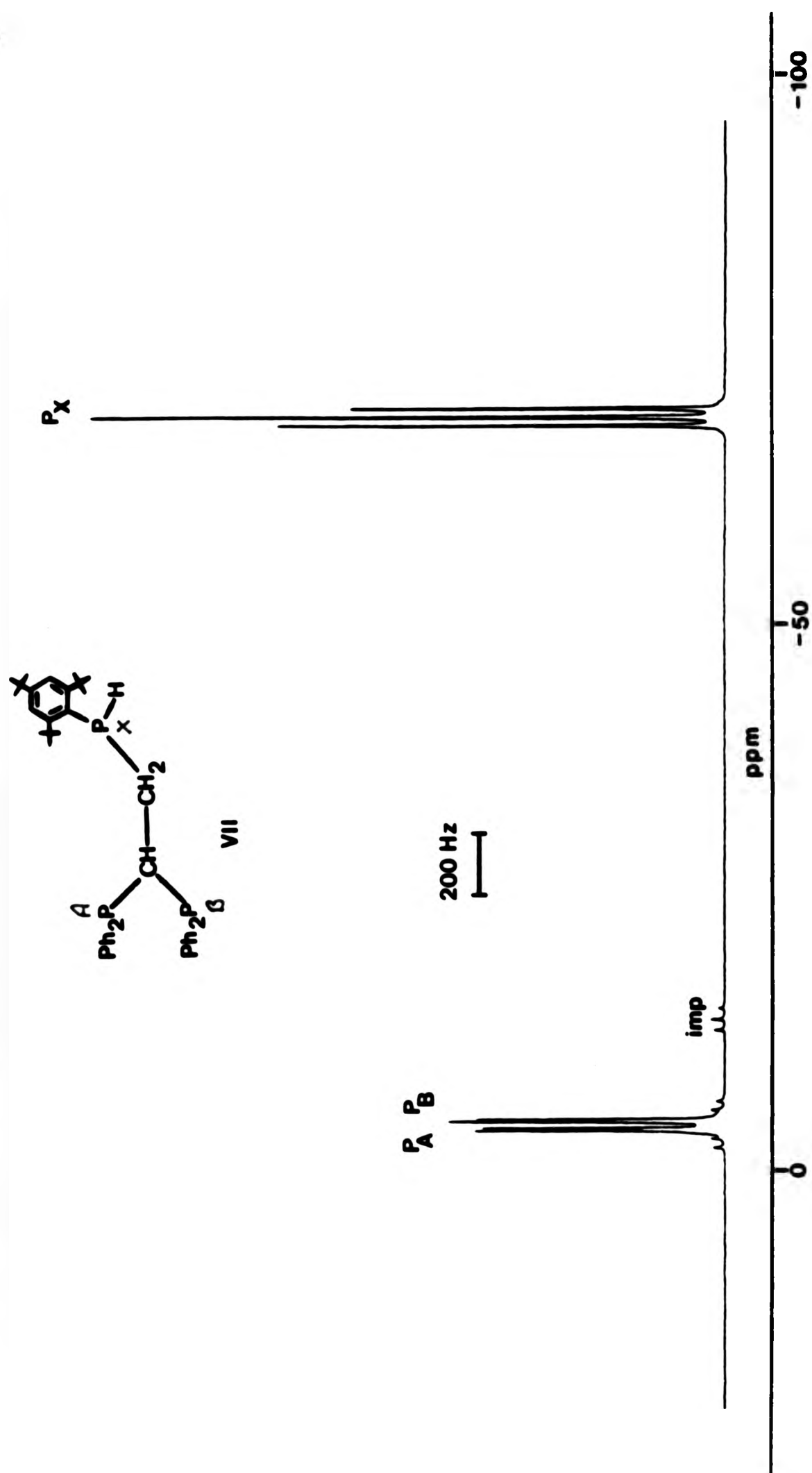


Fig 2.3 - ^{31}P N.M.R. spectrum of VII recorded at 36.2 MHz.

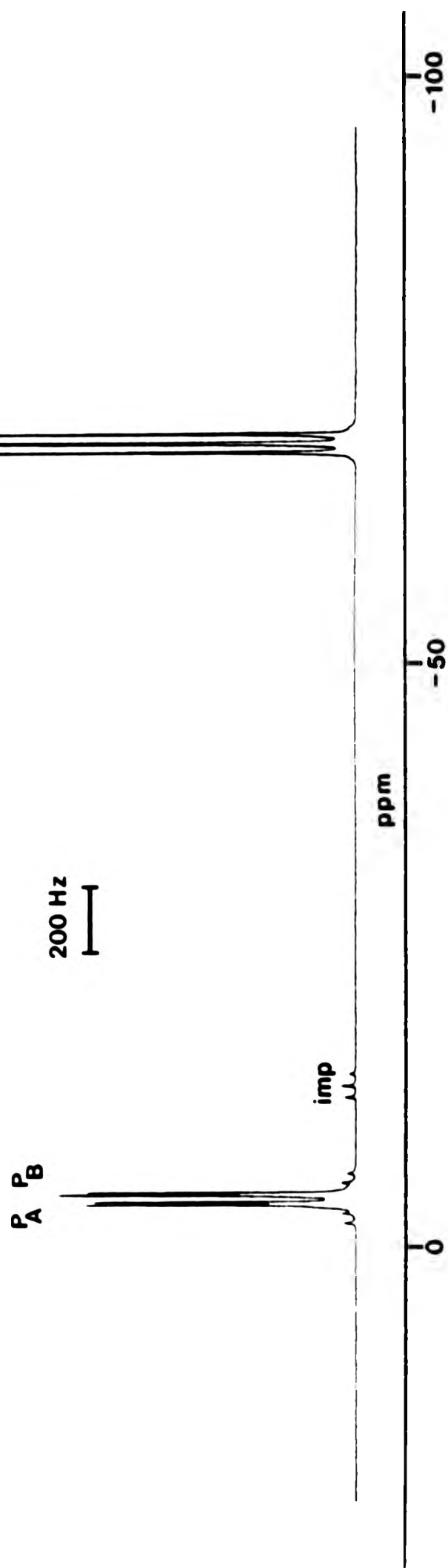
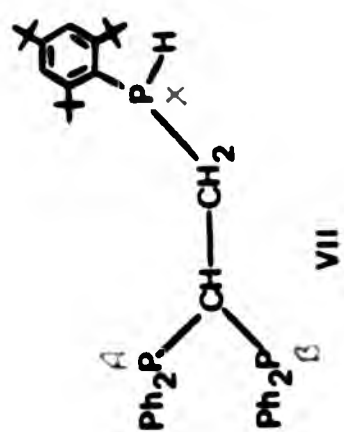


TABLE 2.1 ^{31}P n.m.r. data for the new triphosphine species

LIGAND	$\delta(^{31}\text{P}_\text{A})$ /ppm ^a	$\delta(^{31}\text{P}_\text{B})$ /ppm ^a	$\delta(^{31}\text{P}_\text{X})$ /ppm ^a	$ ^2\text{J}(\text{P}_\text{A}\text{P}_\text{B}) $ /Hz	$ ^3\text{J}(\text{P}_\text{A}\text{P}_\text{X}) $ /Hz	$ ^3\text{J}(\text{P}_\text{B}\text{P}_\text{X}) $ /Hz
II c	-4.0	-	-19.5	-	24.4	-
III c	-3.1	-	-24.3	-	32.9	-
IV d	+3.4	-	+58.3	-	7.9	-
V d	-3.5	-3.5	-37.0	b	20.8	20.8
VI c	-4.0	-5.7	-54.8	112.3	15.9	17.1
VII c	-3.7	-4.4	-69.0	58.6	29.3	28.1
VIII d	-3.8	-5.7	-70.1	124.5	19.6	20.1
IX d	-3.4	-5.8	-65.3	125.7	15.9	17.7

Notes (a) Relative to external 85% H_3PO_4 = 0.0 ppm.

(b) Not measurable from the ^{31}P n.m.r. spectrum.

(c) In CH_2Cl_2 at 25°C.

(d) In THF at 25°C.

bears a bulky group. This clearly may be the source of the relatively low value of $^2J(P_A P_B)$ in VII, where P_X bears the bulky tritertiarybutyl-phenyl group, and suggests that conformation (a) is preferred for VI, VIII and IX whilst conformation (b) is preferred for VII. One possible outcome of these differences in conformation is that for VII cis arrangements of lone pairs between P_A and P_X and between P_B and P_X are more likely than for species exhibiting conformation (a), and may explain the larger values of $^3J(^{31}P-^{31}P)$ in VII compared with those in VI, VIII and IX. Further evidence for these conformational differences comes from the temperature dependence of the various phosphorus-phosphorus coupling constants. A detailed ^{31}P n.m.r. study of VII (Fig 2.5) showed a steady decrease in $|^2J(P_A P_B)|$ and a simultaneous increase in $^3J(P_A P_X)$ with decreasing temperature. This clearly is only likely to occur when conformation (b) is preferred, and therefore adds weight to the suggestion that VII shows a preference for conformer (b).

For compound V the similarity of the ^{31}P chemical shifts of the geminal phosphorus nuclei leads to this ligand having a spectrum resembling an A_2X one and because of this $^2J(^{31}P_A-^{31}P_B)$ could not be determined.

(B) 1.1.2-tris(diphenylphosphino)ethene X

The ^{31}P n.m.r. spectrum of X (Fig. 2.6) is clearly that of an ABX spin-system and analysis leads to the following n.m.r. parameters: $\delta(^{31}P_A) = -5.4$ ppm, $\delta(^{31}P_B) = -25.7$ ppm, $\delta(^{31}P_X) = -0.9$ ppm, $|J(P_A P_B)| = 142.8$ Hz, $|J(P_A P_X)| = 1.5$ Hz, $|J(P_B P_X)| = 9.8$ Hz. Consideration of these values, however, does not permit an unambiguous assignment of resonances in the ^{31}P spectra to specific phosphorus nuclei in the molecule. It is tempting to assign the large phosphorus-phosphorus

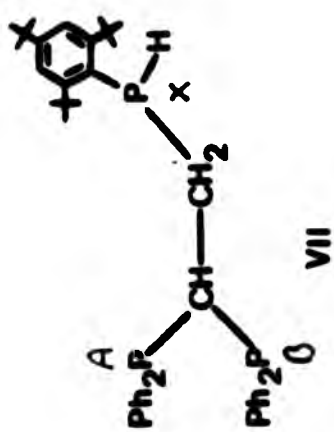
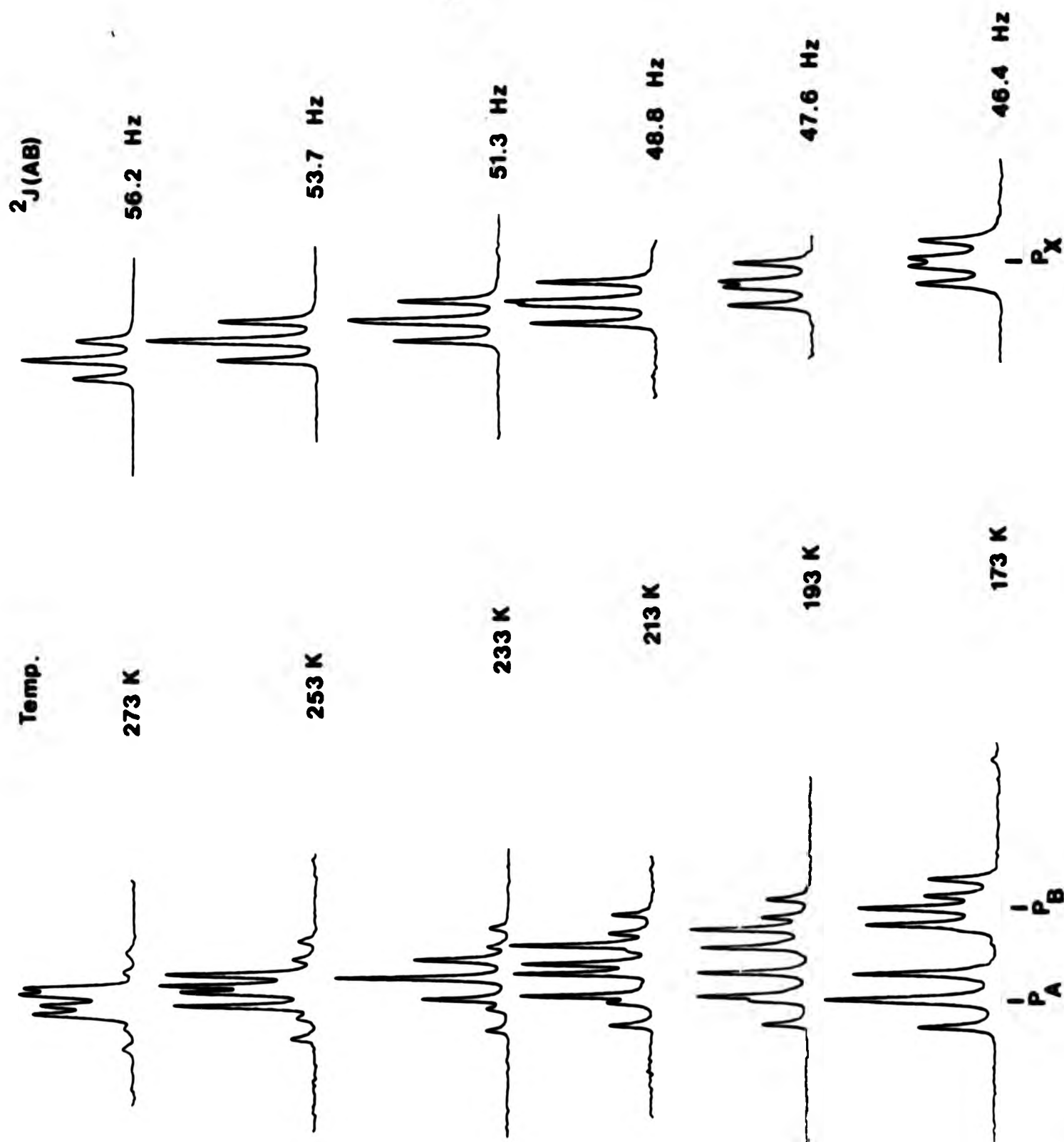


Fig 2.5

^{31}P N.M.R. spectra of VII showing the dependence of $^2J(\text{AB})$ on temperature.



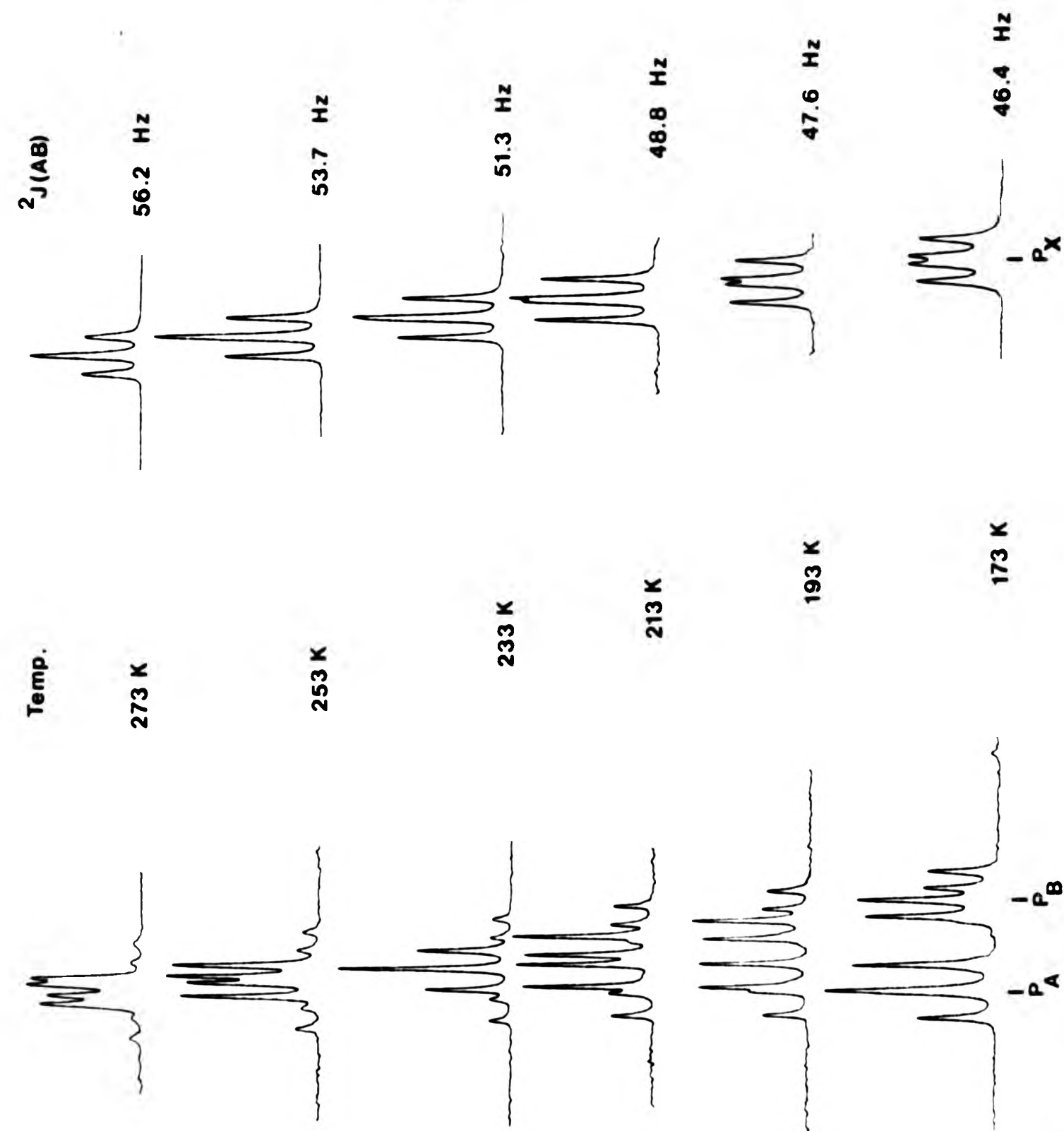


Fig 2.5

^{31}P N.M.R. spectra of VII showing the dependence of $^2J(\text{AB})$ on temperature.

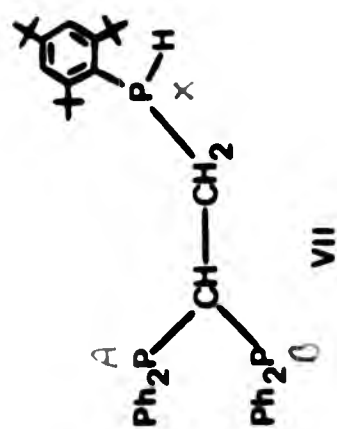
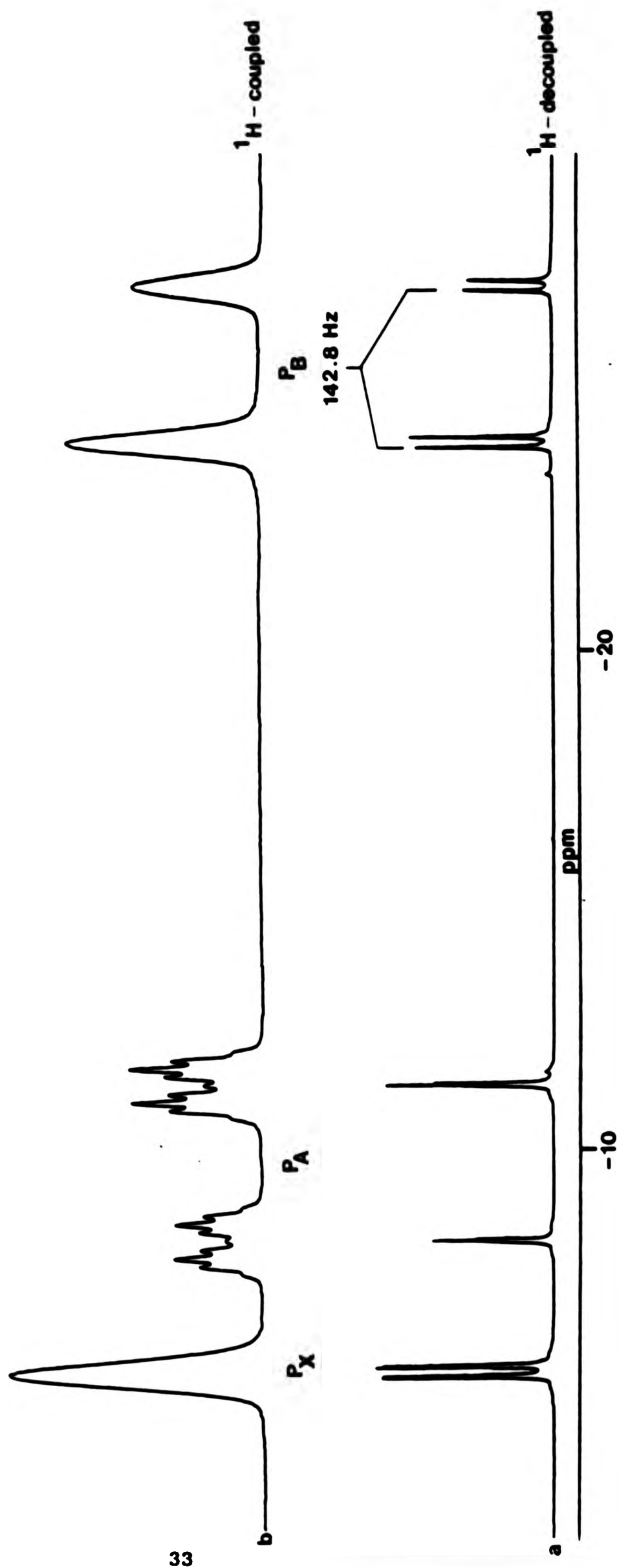
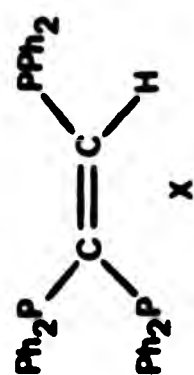


Fig 2.6 - ^{31}P N.M.R. spectra of the triphosphine ligand X

- a) fully proton-decoupled
- b) fully proton-coupled



coupling constant (142.8 Hz) to that between the geminally related phosphorus nuclei since in general $^2J(^{31}\text{P}-^{31}\text{P}) > ^3J(^{31}\text{P}-^{31}\text{P})$. However, Colquhoun and McFarlane⁵⁴ have indirectly obtained values of $J(^{31}\text{P}-^{31}\text{P})$ in a series of related substituted ethenes (Table 2.2) and from their

TABLE 2.2 ^{31}P n.m.r. data for some disubstituted ethenes

Compound	$\delta(^{31}\text{P})^a$ /ppm	$^nJ(^{31}\text{P}-^{31}\text{P})$ /Hz	n
$(\text{Ph}_2\text{P})_2\text{C}:\text{CH}_2$	-3.9	+98.0	2
<u>cis</u> $(\text{Ph}_2\text{P})\text{CH}:\text{CH}(\text{PPh}_2)$	-23.1	+105.5	3
<u>trans</u> $(\text{Ph}_2\text{P})\text{CH}:\text{CH}(\text{PPh}_2)$	-8.4	+13.4	3

Note: a Relative to external 85% $\text{H}_3\text{PO}_4 = 0.0$ ppm

results it would appear that this large value could equally well be attributed to the three-bond coupling between the phosphorus nuclei in a mutually cis arrangement since the values of $J(^{31}\text{P}-^{31}\text{P})$ for $(\text{Ph}_2\text{P})_2\text{C}:\text{CH}_2$ and cis $(\text{Ph}_2\text{P})\text{CH}:\text{CH}(\text{PPh}_2)$ are comparable. As previously mentioned, magnitudes of phosphorus-phosphorus coupling constants are dependent on the relative orientation of the lone pair on each phosphorus atom, and large positive values of $^nJ(^{31}\text{P}-^{31}\text{P})$ tend to result from conformations where the lone pairs are in a cis arrangement and because of this the presence of only one large phosphorus-phosphorus coupling constant in X provides evidence to suggest direct competition between conformations (a) and (b) in Fig. 2.7. Conformation (a) would lead to a large value of $^3J(^{31}\text{P}-^{31}\text{P}_{\text{cis}})$ and a small value of $^2J(^{31}\text{P}-^{31}\text{P}_{\text{gem}})$ whereas the opposite would result from conformer (b). It is reasonable that low values of $^3J(^{31}\text{P}-^{31}\text{P}_{\text{trans}})$ would be expected for both conformations, an assumption supported by the experimental value of 13.4 Hz

found in trans $(\text{Ph}_2\text{P})\text{CH}:\text{CH}(\text{PPh}_2)$.

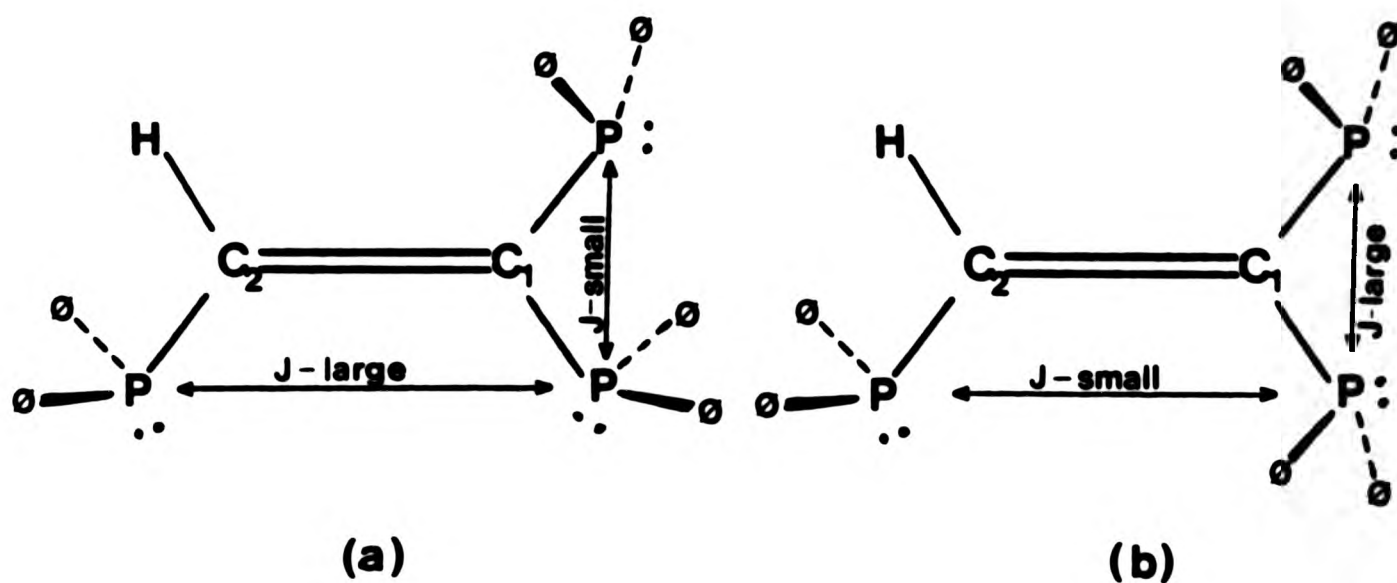
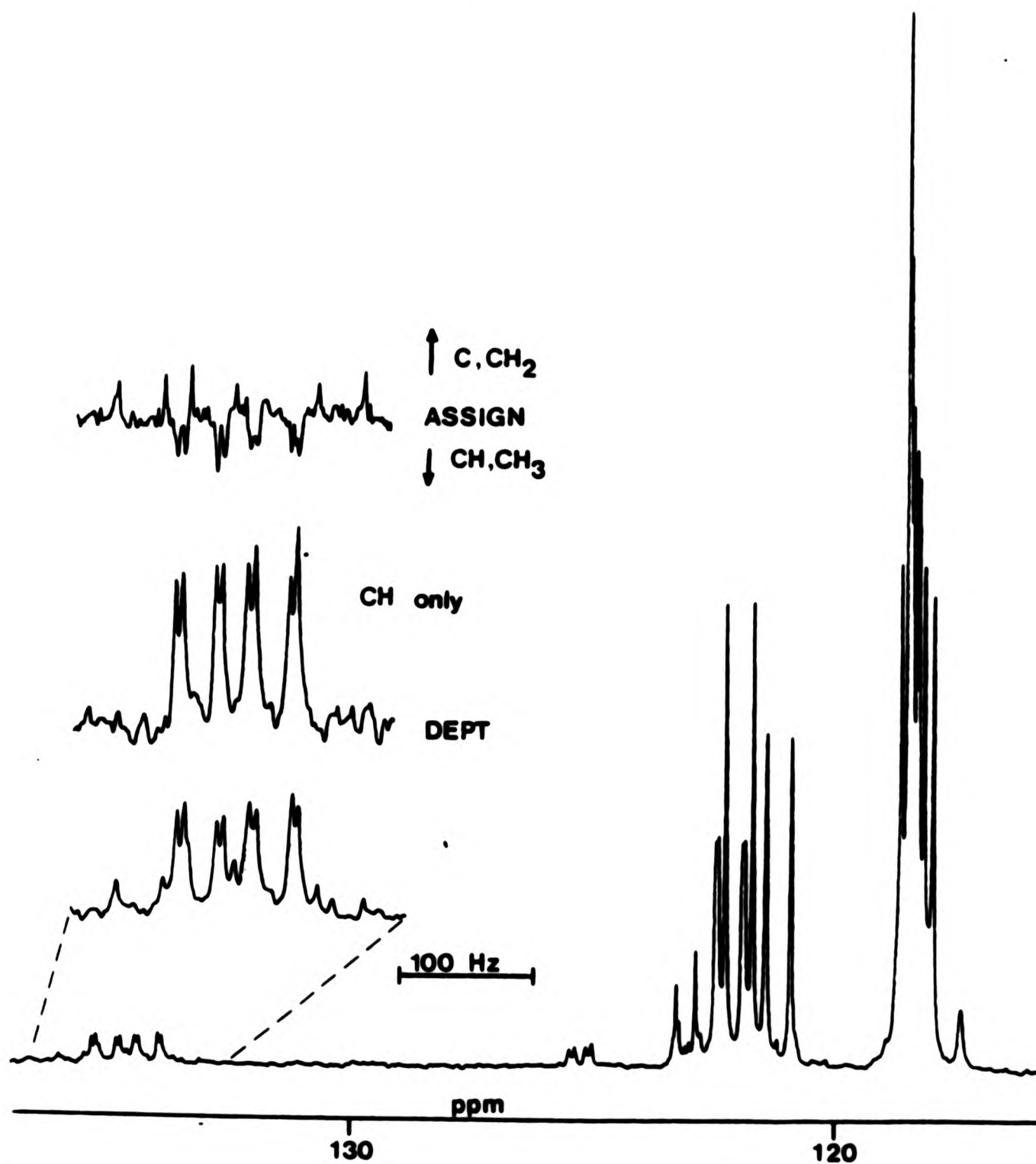
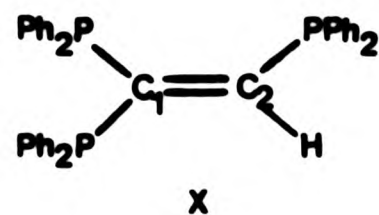


Fig 2.7

The proton-coupled ^{31}P n.m.r. spectrum of X (Fig. 2.6) shows that only the P_A resonance has a resolvable phosphorus-proton coupling. The doublet splitting (31.0 Hz) can only be assigned to coupling between P_A and the proton on C_2 but this still does not lead to a clear assignment. The assignment of the ^{31}P n.m.r. spectrum of X therefore required further characterisation of this ligand by investigation of the n.m.r. spectra given by other nuclei. The proton spectrum of X however was found to show only an unresolvable group of resonances due to the many inequivalent phenyl group protons and this masked the resonances due to the C_2 proton. Further study therefore concentrated on the ^{13}C n.m.r. spectrum of X which was found to be more amenable to investigation.

The ^{13}C n.m.r. spectrum of X (Fig. 2.8) shows clearly resonances due to C_1 and C_2 each coupled to the three phosphorus nuclei. C_1 and C_2 were distinguished by the characteristic one bond $^{13}\text{C}_2$ -proton coupling constant, $^1J(^{13}\text{C}_2-^1\text{H})$ (159.0 Hz), in the proton-coupled ^{13}C n.m.r. spectrum. In principle, assignments of phosphorus-carbon couplings

Fig 2.8
 ^{13}C N.M.R. spectrum of X showing an expansion of the C_1 and C_2 resonances, and the DEPT and ASSIGN experiments performed to confirm ^{13}C assignment.



may be made by direct observation of the ^{13}C satellites in the ^{31}P spectrum. However, problems of line shape combined with relatively low coupling-constants precluded this approach, and therefore assignments were made by a series of multiple-resonance (spin-tickling and selective decoupling) experiments.

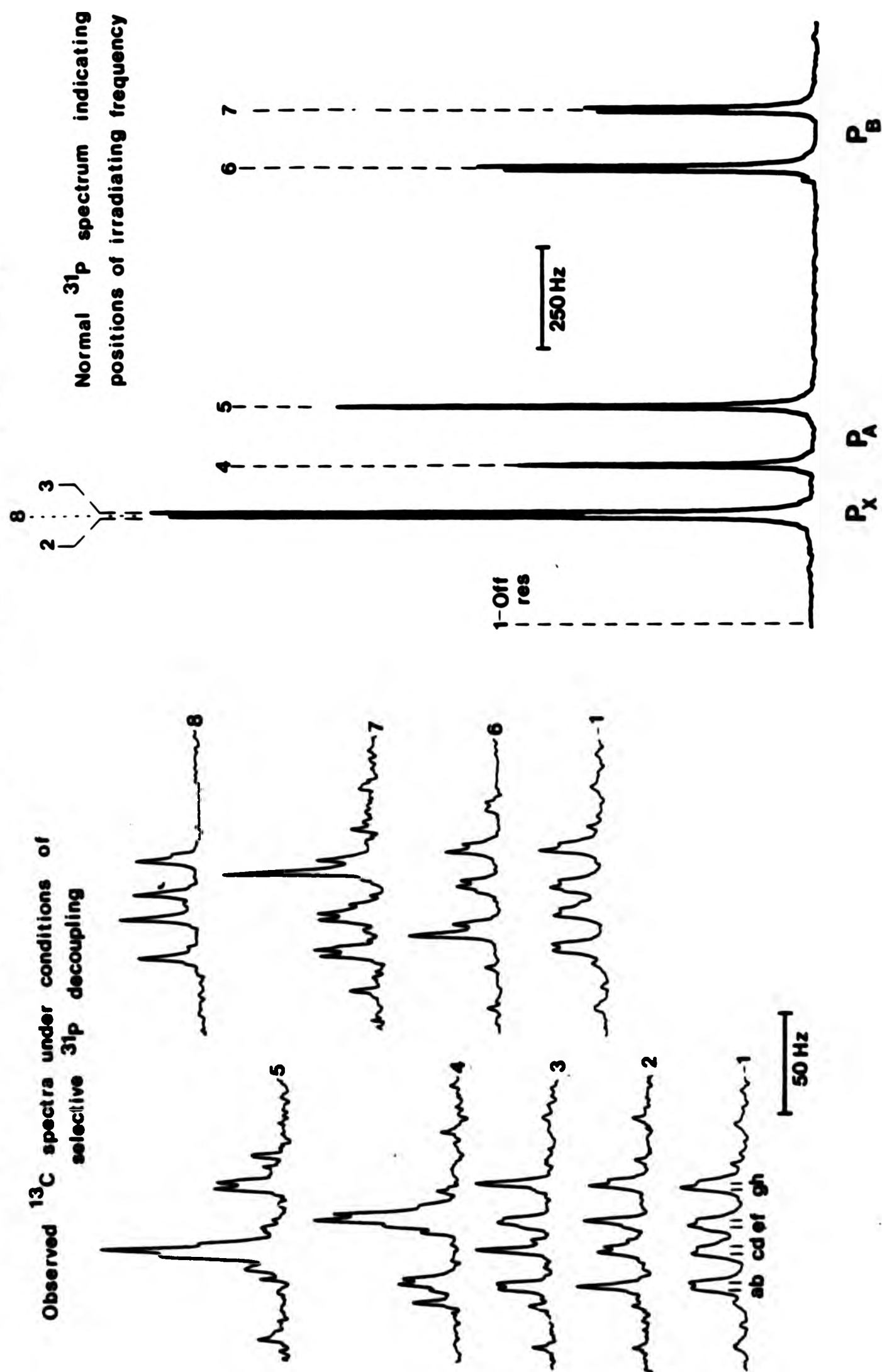
A discussion of the theory behind and the results obtainable from multiple-resonance experiments is provided in Appendix II and the following pages only detail and discuss the results of such experiments performed on this ligand.

The results of a series of selective decoupling experiments performed in order to assign the ^{31}P - $^{13}\text{C}_2$ couplings and to reveal sign information are shown in Fig. 2.9. Neglecting isotope effects on chemical shifts, each line labelled (2)-(7) in the ^{31}P spectrum also corresponds to the centre of the ^{13}C satellites for the species containing the same combination of phosphorus spin-states as the labelled transition. Irradiation at a frequency ν_2 corresponding to (8) involves a total decoupling of the ^{31}P - $^{13}\text{C}_2$ couplings for all combinations M_A and M_B , (the spin states of P_A and P_B) and as can be seen from spectrum (8) results in the collapse of the 3.1 Hz coupling and leads to the conclusion:

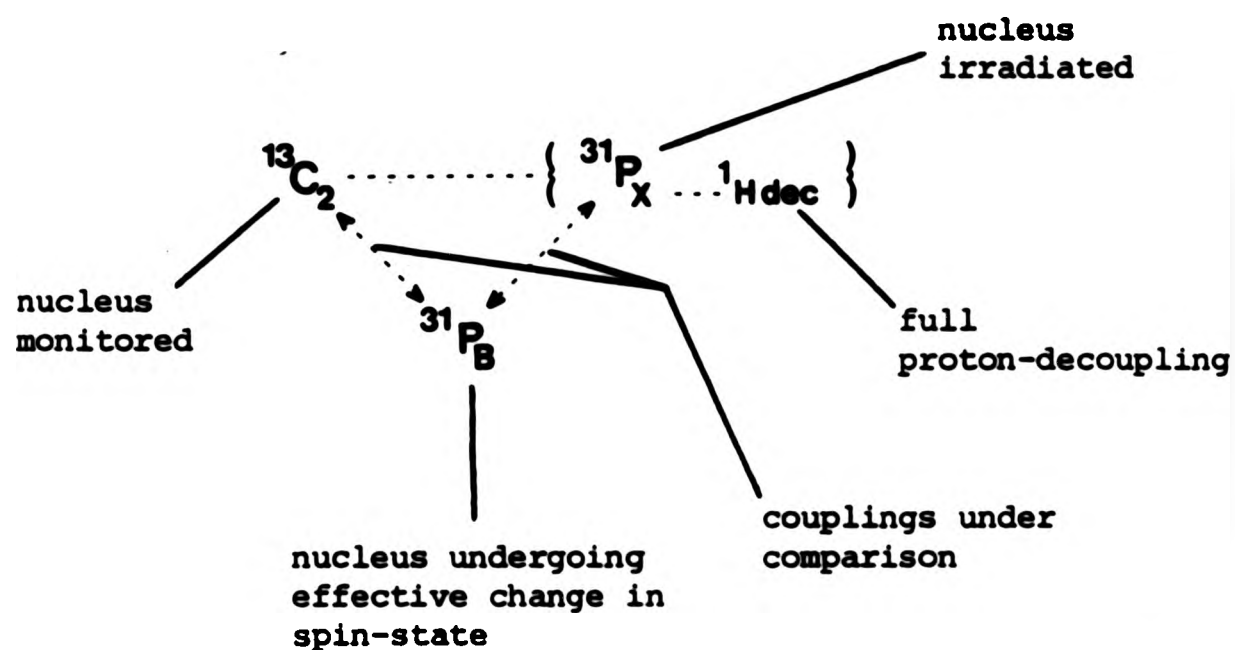
$$J(^{31}\text{P}_X - ^{13}\text{C}_2) = 3.1 \text{ Hz} \quad (2.3)$$

The two transitions labelled (2) and (3) in the ^{31}P spectrum of P_X correspond to the two different spin states of P_B since they are separated by $J(^{31}\text{P}_X - ^{31}\text{P}_B)$. Thus irradiation centred on line (2) collapses the $^{31}\text{P}_X$ - $^{13}\text{C}_2$ (3.1 Hz) couplings for one particular spin state of P_B (lines a,b and e,f in spectrum (2)) whilst irradiation centred on line (3) collapses those for the opposite spin state of P_B . Such an experiment therefore compares the signs of $J(^{31}\text{P}_B - ^{31}\text{C}_2)$ and

Fig 2.9 - Selective ^{31}P -decoupling experiments on the $^{13}\text{C}_2$ resonance of X.



$J(^{31}\text{P}_X - ^{31}\text{P}_B)$ and can be represented by the notation



The results of this experiment (spectra (2) and (3)) therefore are:

$$J(^{31}\text{P}_B ^{13}\text{C}_2) \text{ of the same sign as } J(^{31}\text{P}_B ^{31}\text{P}_X) \quad (2.4)$$

Total selective irradiation of P_A is not possible because its resonance frequencies cover too wide a range. However, a similar decoupling experiment as for P_X was performed by selective irradiation at frequencies centred on lines (4) and (5) resulting in spectra (4) and (5). Considerations similar to those of the previous experiment revealed:

$$J(^{31}\text{P}_A ^{13}\text{C}_2) = 31.0 \text{ Hz} \quad (2.5)$$

$$J(^{31}\text{P}_B ^{13}\text{C}_2) \text{ is of opposite sign to } J(^{31}\text{P}_A ^{31}\text{P}_B) \quad (2.6)$$

Analogous experiments for P_B (spectra (6) and (7)) gave

$$J(^{31}\text{P}_B ^{13}\text{C}_2) = 17.5 \text{ Hz} \quad (2.7)$$

$$J(^{31}\text{P}_A ^{13}\text{C}_2) \text{ same sign as } J(^{31}\text{P}_A ^{31}\text{P}_B) \quad (2.8)$$

An identical series of selective decoupling experiments was performed by observing $^{13}\text{C}_1$ and gave

$$J(^{31}\text{P}_\text{B} ^{13}\text{C}_1) = 19.7 \text{ Hz and of same sign as } J(^{31}\text{P}_\text{A} ^{31}\text{P}_\text{B}) \quad (2.9)$$

$$J(^{31}\text{P}_\text{A} ^{13}\text{C}_1) = 31.2 \text{ Hz of opposite sign to } J(^{31}\text{P}_\text{A} ^{31}\text{P}_\text{B}) \quad (2.10)$$

$$J(^{31}\text{P}_\text{X} ^{13}\text{C}_1) = 55.0 \text{ Hz sign unknown} \quad (2.11)$$

(The determination of the relative sign of $J(^{31}\text{P}_\text{X} ^{13}\text{C}_1)$ was not possible since irradiation centred on (3) also gave a large effect at (4) when the power level was high enough to decouple the 55.0 Hz coupling.)

The proton-coupled ^{31}P spectrum of X (Fig. 2.6) shows only one clearly resolved coupling, namely that of 31.0 Hz for $J(\text{P}_\text{A} - \text{H}(\text{C}_2))$, although the broadening of the P_B and P_X resonances suggests significant but smaller couplings to these nuclei. As already stated, direct observation of the C_2 proton by ^1H n.m.r. was not possible since the resonance of this proton lies in a position where it is masked by resonances of the thirty phenyl-protons. However, a two-dimensional (2-D) n.m.r. experiment is available that will display the proton resonance indirectly and in addition give relative sign information on its couplings to other nuclei. Since 2-D n.m.r. was not used to a great extent in this work the following discussion is limited to the points needed for an appreciation of the experiment actually performed.

The experiment performed on X involved the correlation of the $^{13}\text{C}_2$ resonances with those of its directly-bound proton and resulted in the C-H correlated 2-D spectrum (Fig. 2.10) of which a schematic contour plot is represented beneath (Fig. 2.11)^{54a}. The two axes correspond to the ^{13}C and ^1H resonance frequencies as labelled and a

Figs 2.10 , 2.11 - C₂ region of the ¹³C-¹H correlated 2-D spectrum of the triphosphine X.

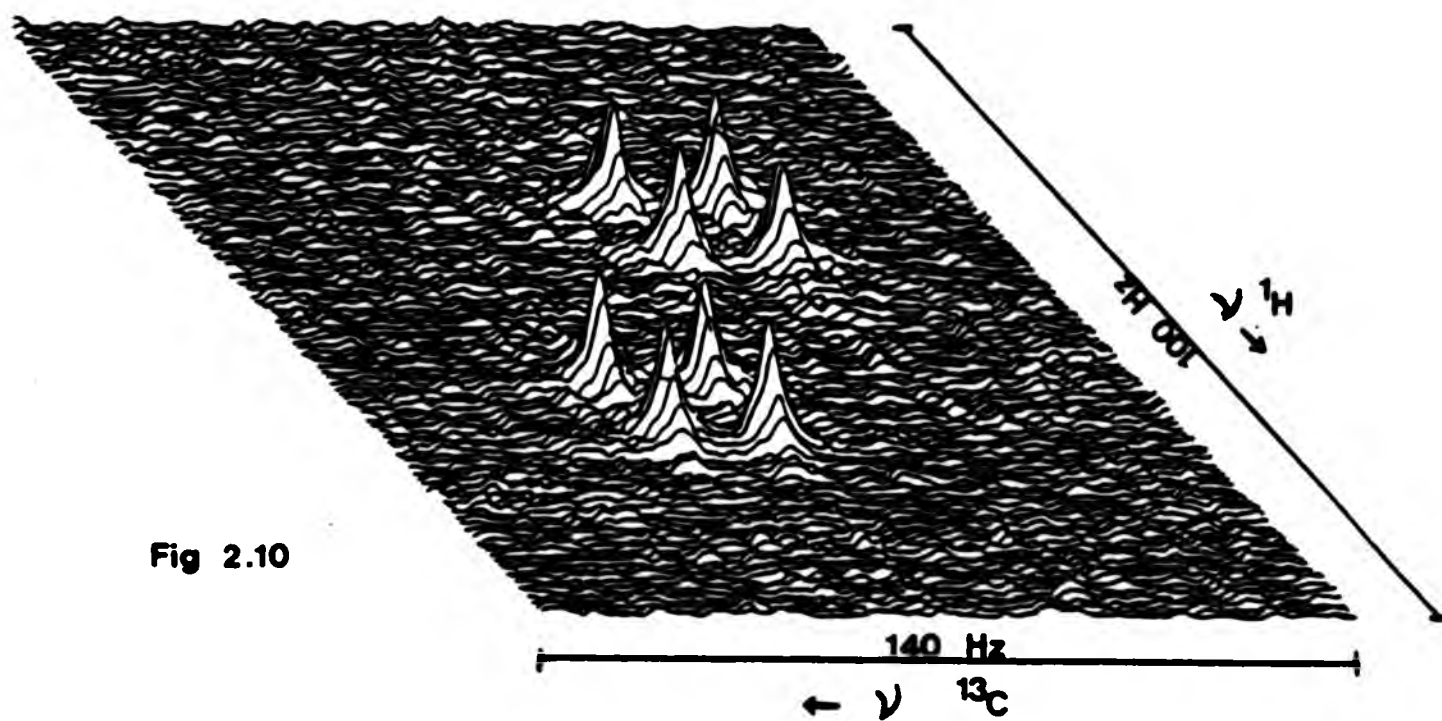


Fig 2.10

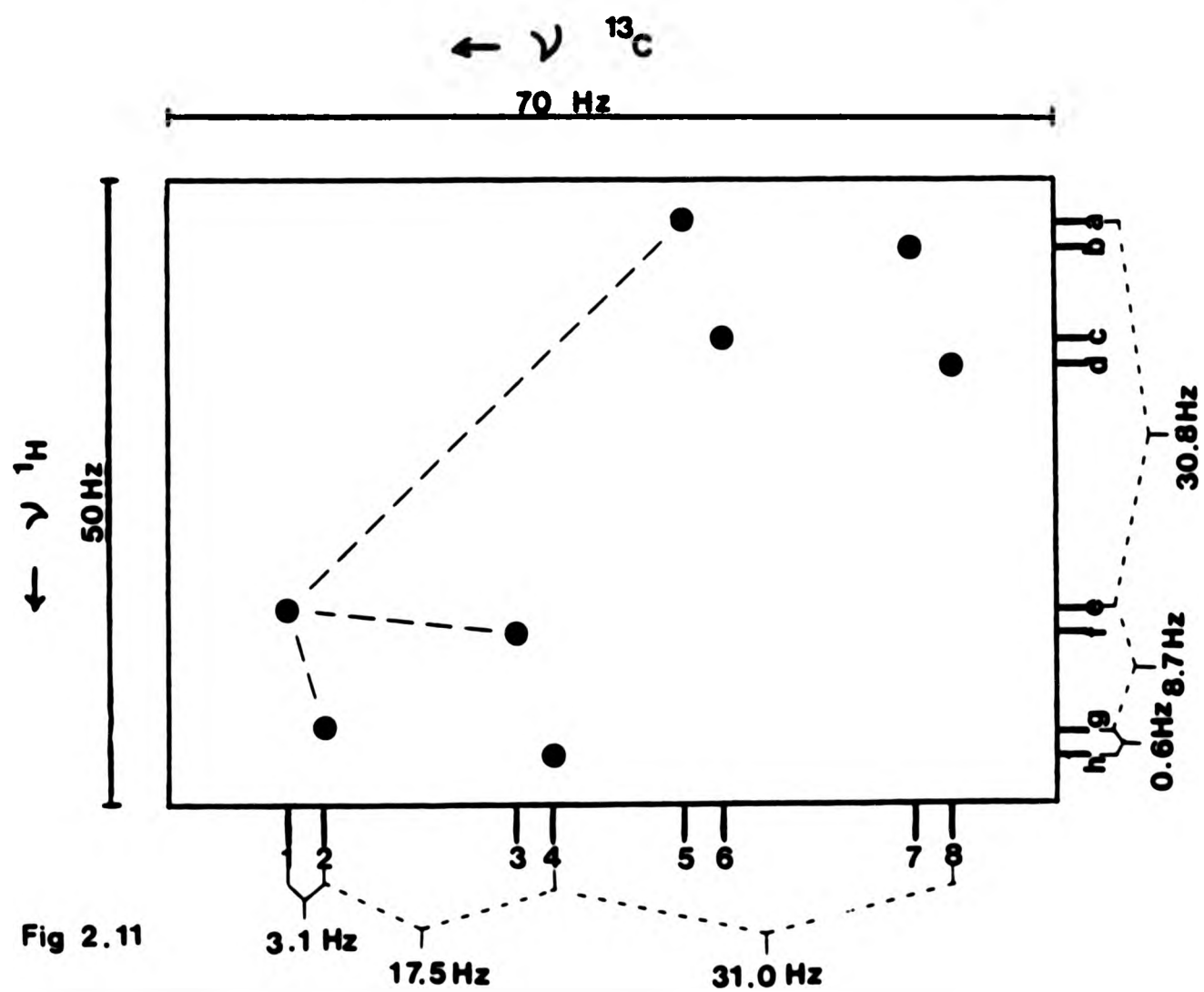


Fig 2.11

projection along the axes will display the phosphorus-coupled $^{13}\text{C}_2$ and $^1\text{H}_{\text{C}_2}$ spectra. It is clear from the contour representation that each transition in the ^{13}C spectrum is correlated with a single transition in the ^1H spectrum, each correlation occurring for a specific combination of all three phosphorus spin-states. Previous decoupling experiments had revealed that transitions (1) and (2) in the ^{13}C spectrum, separated by 3.1 Hz, correspond to the $^{31}\text{P}_{\text{X}}-^{13}\text{C}_2$ coupling. Thus the difference between transitions (1) and (2) merely reflect opposite spin-states of P_{X} . Inspection of Fig. 2.11 shows that transitions (1) and (2) are correlated with transitions e and g in the proton spectrum and therefore the separation between e and g of (8.7 Hz) corresponds to the previously unknown $^{31}\text{P}_{\text{X}}-^1\text{H}_{\text{C}_2}$ coupling. Furthermore, since the change of spin-state of P_{X} arising from a decrease in frequency from (1) - (2) is reflected by an increase in frequency for correlated transitions e and g the signs of $J(^{31}\text{P}_{\text{X}}-^1\text{H})$ and $J(^{31}\text{P}_{\text{X}}-^{13}\text{C}_2)$ must be opposite. Thus

$$J(^{31}\text{P}_{\text{X}}-^1\text{H}) = 8.7 \text{ Hz } \underline{\text{opposite}} \text{ sign to } J(^{31}\text{P}_{\text{X}}-^{13}\text{C}_2) \quad (2.12)$$

Similarly the $^{13}\text{C}_2$ transitions (1) and (3) separated by $J(^{31}\text{P}_{\text{B}}-^{13}\text{C}_2)$ are related by a change in spin-state of P_{B} and show correlation with transitions e and f in the ^1H spectrum which are separated by 0.6 Hz. Similar considerations as for the previous case reveal

$$J(^{31}\text{P}_{\text{B}}-^1\text{H}) = 0.6 \text{ Hz } \underline{\text{opposite}} \text{ sign to } J(^{31}\text{P}_{\text{B}}-^{13}\text{C}_2) \quad (2.13)$$

Finally, transitions (1) and (5), separated by $J(^{31}\text{P}_{\text{A}}-^{13}\text{C}_2)$ are correlated with transitions e and a in the ^1H spectrum which are separated by 30.8 Hz and therefore

$$J(^{31}\text{P}_{\text{A}}-^1\text{H}) = 30.8 \text{ Hz } \underline{\text{same}} \text{ sign as } J(^{31}\text{P}_{\text{A}}-^{13}\text{C}_2) \quad (2.14)$$

Thus the signs of the various phosphorus-phosphorus, phosphorus-carbon and phosphorus-proton couplings were determined relative to one another. In order to determine their absolute signs, therefore, it was only necessary to determine the absolute sign of any single coupling constant. To determine an absolute sign it is necessary to compare the unknown with a coupling of known sign such as $^1J(^{13}\text{C}-^1\text{H})$ which is known to be positive in all situations⁵⁵. Because of the appearance of the proton coupled ^{31}P spectrum of X (Fig. 2.6) a selective decoupling experiment of the type $^{13}\text{C}_2 \dots \{^{31}\text{P}_A\}$ was performed with results that are shown in Fig. 2.12. Consideration of spectra (2) and (3) of this experimental series leads to the conclusion

$$^1J(^{13}\text{C}_2-^1\text{H}) \text{ has the same sign as } J(^{31}\text{P}_B-^1\text{H}) \quad (2.15)$$

A combination of results 2.3 to 2.15 gave the n.m.r. parameters shown in Table 2.3.

TABLE 2.3 n.m.r. data for the new triphosphine X

Parameter	Phosphorus Nucleus P_1		
	P_A	P_B	P_X
$\delta(^{31}\text{P}_1)/\text{ppm}^a$	-5.4	-25.7	-0.9
$J(^{31}\text{P}_A-^{31}\text{P}_1)/\text{Hz}$	-	+142.8	$\pm 1.5^b$
$J(^{31}\text{P}_B-^{31}\text{P}_1)/\text{Hz}$	+142.8	-	-9.8
$J(^{31}\text{P}_X-^{31}\text{P}_1)/\text{Hz}$	$\pm 1.5^b$	-9.8	-
$J(^{31}\text{P}_1-^{13}\text{C}_1)/\text{Hz}$	-31.2	+19.7	$\pm 55.0^b$
$J(^{31}\text{P}_1-^{13}\text{C}_2)/\text{Hz}$	+31.1	-17.5	$\pm 3.1^b$
$J(^{31}\text{P}_1-^1\text{H})/\text{Hz}$	+30.8	+0.6	$\pm 8.7^b$

Notes: see over

Notes to
Table 2.3

- a Relative to external 85% $\text{H}_3\text{PO}_4 = 0.0$ ppm
b Sign not determined

Careful consideration of the results of the n.m.r. study performed on X led to the postulation that the assignment is as shown in Fig. 2.13 for the following reasons.

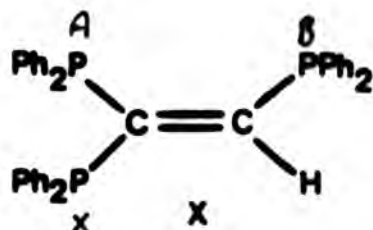


Fig 2.13

It is unlikely that the geminally related phosphorus nuclei (P_A and P_X) will have widely separated chemical shifts and therefore it was assumed that the resonance at -25.7 ppm arises from P_B . P_B shows a large coupling to one other phosphorus nucleus which by analogy with the related species in Table 2.2 must be P_A . The chemical shifts of P_A and P_X are therefore as shown in Table 2.3. Supporting evidence for this assignment comes from consideration of the other parameters shown in Table 2.3. The trans phosphorus-phosphorus (P_B - P_X) coupling of 9.8 Hz is comparable to that found in trans-1,2-bis(diphenylphosphino)ethene (13.0 Hz). Also, the largest phosphorus-proton coupling arises from the three-bond trans coupling to P_A rather than from the three-bond cis or two-bond geminal coupling, a situation reflected by analogous proton-proton couplings⁵⁶. Perhaps surprising is the very low value for the geminal P_A - P_X coupling constant (1.5 Hz) but it must be remembered that phosphorus-phosphorus couplings are critically dependent on lone-pair orientation and therefore conformer (a) (Fig. 2.7) is likely to be the preferred arrangement.

Notes to
Table 2.3

- a Relative to external 85% H_3PO_4 = 0.0 ppm
b Sign not determined

Careful consideration of the results of the n.m.r. study performed on X led to the postulation that the assignment is as shown in Fig 2.13 for the following reasons.

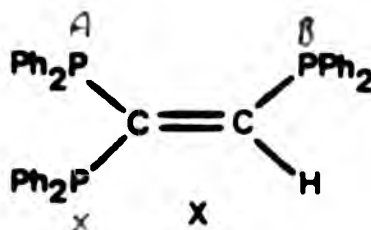
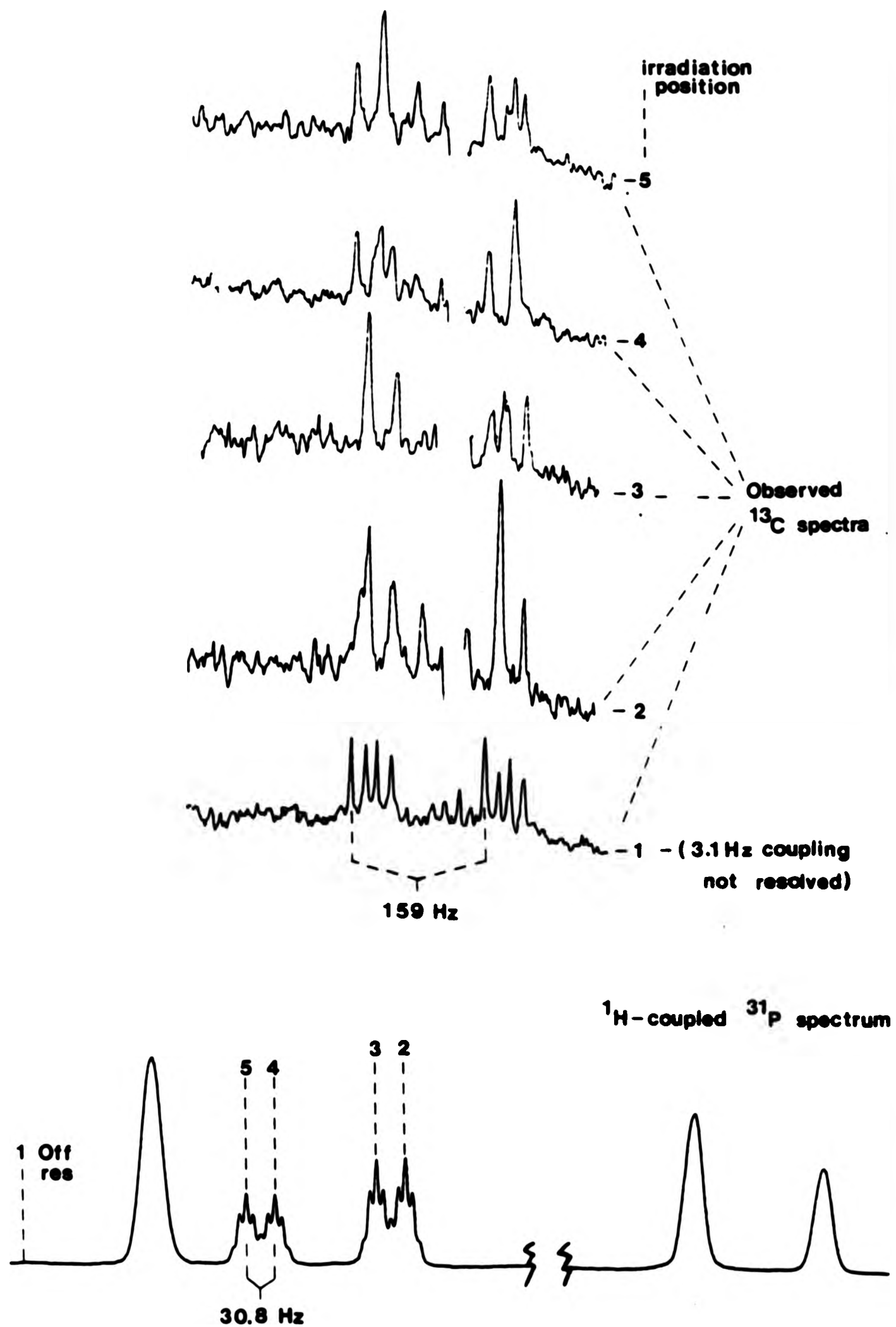


Fig 2.13

It is unlikely that the geminally related phosphorus nuclei (P_A and P_X) will have widely separated chemical shifts and therefore it was assumed that the resonance at -25.7 ppm arises from P_B . P_B shows a large coupling to one other phosphorus nucleus which by analogy with the related species in Table 2.2 must be P_A . The chemical shifts of P_A and P_X are therefore as shown in Table 2.3. Supporting evidence for this assignment comes from consideration of the other parameters shown in Table 2.3. The trans phosphorus-phosphorus (P_B - P_X) coupling of 9.8 Hz is comparable to that found in trans-1,2-bis(diphenylphosphino)ethene (13.0 Hz). Also, the largest phosphorus-proton coupling arises from the three-bond trans coupling to P_A rather than from the three-bond cis or two-bond geminal coupling, a situation reflected by analogous proton-proton couplings⁵⁶. Perhaps surprising is the very low value for the geminal P_A - P_X coupling constant (1.5 Hz) but it must be remembered that phosphorus-phosphorus couplings are critically dependent on lone-pair orientation and therefore conformer (a) (Fig. 2.7) is likely to be the preferred arrangement.

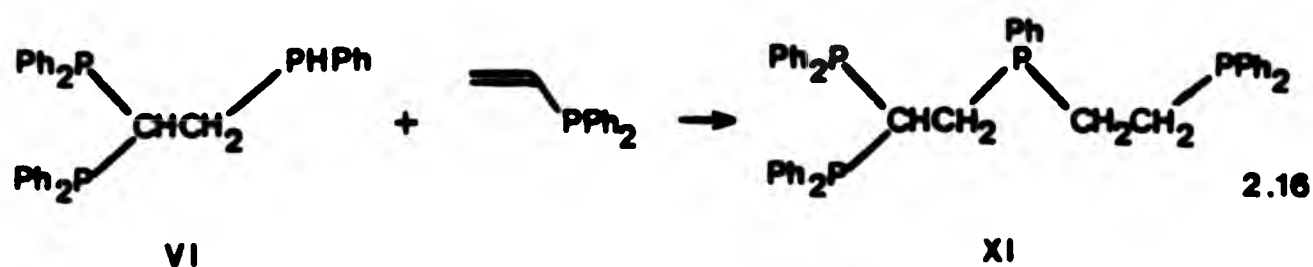
Fig 2.12 - Selective ^{31}P -decoupling experiments performed on the ^1H -coupled $^{13}\text{C}_2$ resonance of X.



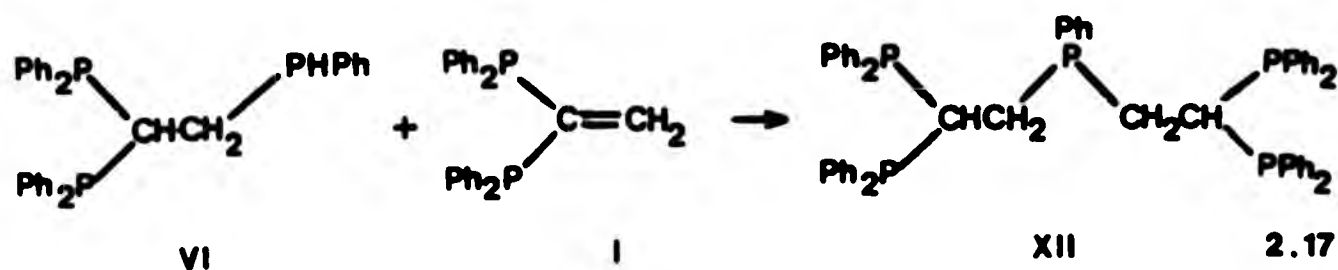
Further stronger evidence for this assignment comes from consideration of the ^{31}P n.m.r. spectra of some transition-metal complexes of X as discussed in Chapter 3.

(C) Tetra- and Pentatertiary Phosphines and Related Species

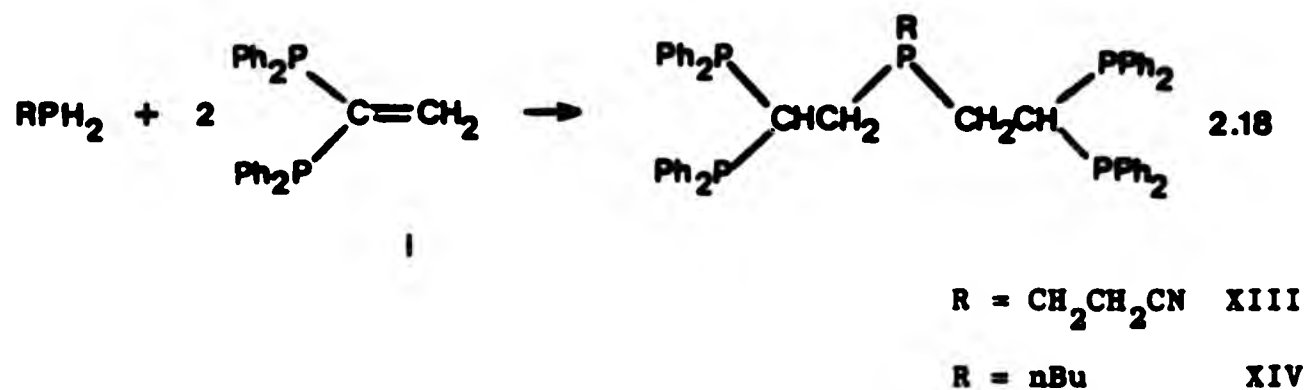
Although the phosphorus-hydrogen bonds in the triphosphine species VI - IX appear to be less reactive towards base-catalysed addition than those in the starting primary phosphines, they are nevertheless still capable of undergoing further addition reactions. Thus, reaction of VI with vinylidiphenylphosphine under similar conditions led to the formation of the new tetratertiary phosphine ligand XI (Eq. 2.16), which was again isolated as an air-stable white solid.



Similarly, reaction of VI with a further equivalent of 1,1-bis-diphenylphosphinoethene (I) or indeed reaction of phenylphosphine with two equivalents of the alkene resulted in rapid formation of the new pentatertiaryphosphine ligand XII (Eq. 2.17) which was isolated as

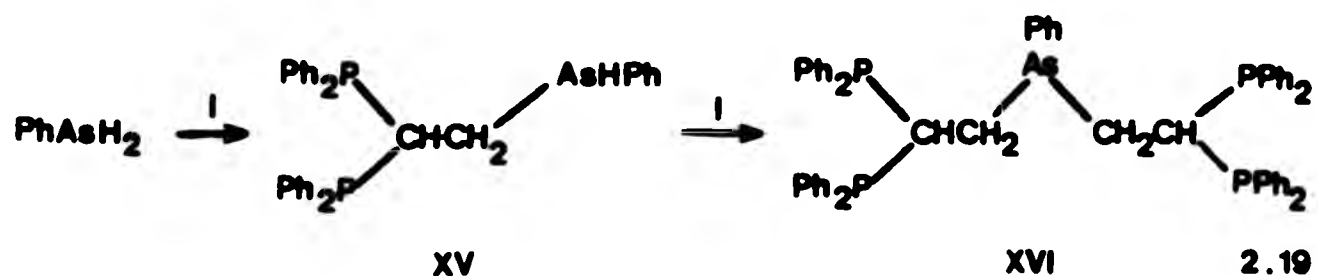


air-stable crystals with a sharp melting point and satisfactory elemental analysis. Other primary phosphines were found to undergo analogous reactions (Eq. 2.18) to give the related pentatertiary phosphine ligands XIII-XIV. However, the triphosphine ligand VII



underwent no further addition reactions either with vinylidiphenylphosphine or with 1,1-bis(diphenylphosphino)ethene, I, under these conditions or even under reflux (67°C), suggesting that the bulk of the tritertiarybutylphenyl group precludes further reaction.

Under similar conditions phenylarsine, PhAsH_2 , was found to undergo reactions analogous to those of phenyl phosphine (Eq. 2.19). Although the secondary arsino species XV decomposes rapidly in air, the



tetratertiaryphosphinearsino species XVI was isolated as air-stable crystals in good yield.

For the tetratertiary phosphine ligand XI the phosphorus atom M is chiral (Fig. 2.14) and therefore the two geminally related phosphorus nuclei are inequivalent. The ^{31}P n.m.r. spectrum of XI should

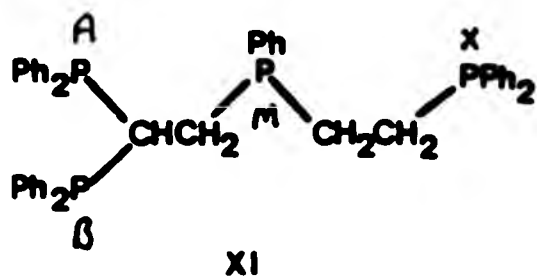


Fig 2.14

therefore be characteristic of an ABMX spin-system⁵³. However, the similarity of $\delta(^{31}\text{P}_\text{A})$ and $\delta(^{31}\text{P}_\text{B})$ results in the spectrum having an A_2MX appearance where $^3\text{J}(\text{P}_\text{A}\text{P}_\text{M}) = 20 \text{ Hz} = ^3\text{J}(\text{P}_\text{B}\text{P}_\text{M})$, and $^3\text{J}(\text{P}_\text{M}\text{P}_\text{X}) = 27.5 \text{ Hz}$, and where $^2\text{J}(\text{P}_\text{A}\text{P}_\text{B})$ could not be determined.

For the pentatertiary phosphine species (XII - XIV) the central phosphorus atom X (Fig. 2.15) is a prochiral centre. As in similar molecules containing chiral centres, this renders the geminally related phosphorus nuclei inequivalent but does not differentiate the pairs of geminal phosphorus nuclei.

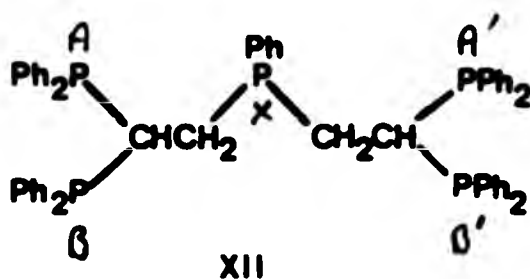


Fig 2.15

The ^{31}P n.m.r. spectra of these compounds are therefore characteristic of $\text{AA}'\text{BB}'\text{X}$ spin systems⁵³ in which the long range couplings $^6\text{J}(\text{P}_\text{A}\text{P}_\text{A}')$, $^6\text{J}(\text{P}_\text{A}\text{P}_\text{B}')$ and $^6\text{J}(\text{P}_\text{B}\text{P}_\text{B}')$ are zero (Fig. 2.16). Analysis of these spectra led to the parameters shown in Table 2.4.

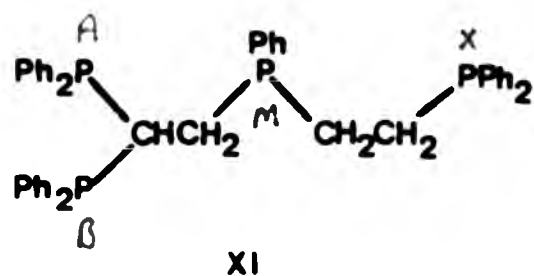


Fig 2.14

therefore be characteristic of an ABMX spin-system⁵³. However, the similarity of $\delta(^{31}\text{P}_\text{A})$ and $\delta(^{31}\text{P}_\text{B})$ results in the spectrum having an A_2MX appearance where $^3J(\text{P}_\text{A}\text{P}_\text{M}) = 20 \text{ Hz} = ^3J(\text{P}_\text{B}\text{P}_\text{M})$, and $^3J(\text{P}_\text{M}\text{P}_\text{X}) = 27.5 \text{ Hz}$, and where $^2J(\text{P}_\text{A}\text{P}_\text{B})$ could not be determined.

For the pentatertiary phosphine species (XII - XIV) the central phosphorus atom X (Fig. 2.15) is a prochiral centre. As in similar molecules containing chiral centres, this renders the geminally related phosphorus nuclei inequivalent but does not differentiate the pairs of geminal phosphorus nuclei.

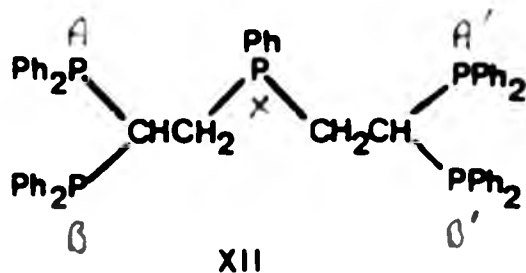


Fig 2.15

The ^{31}P n.m.r. spectra of these compounds are therefore characteristic of $\text{AA}'\text{BB}'\text{X}$ spin systems⁵³ in which the long range couplings $^6J(\text{P}_\text{A}\text{P}_{\text{A}'}), ^6J(\text{P}_\text{A}\text{P}_{\text{B}'})$ and $^6J(\text{P}_\text{B}\text{P}_{\text{B}'})$ are zero (Fig. 2.16). Analysis of these spectra led to the parameters shown in Table 2.4.

Fig 2.16 - ^{31}P N.M.R. spectrum of XII recorded at 24.2 MHz.

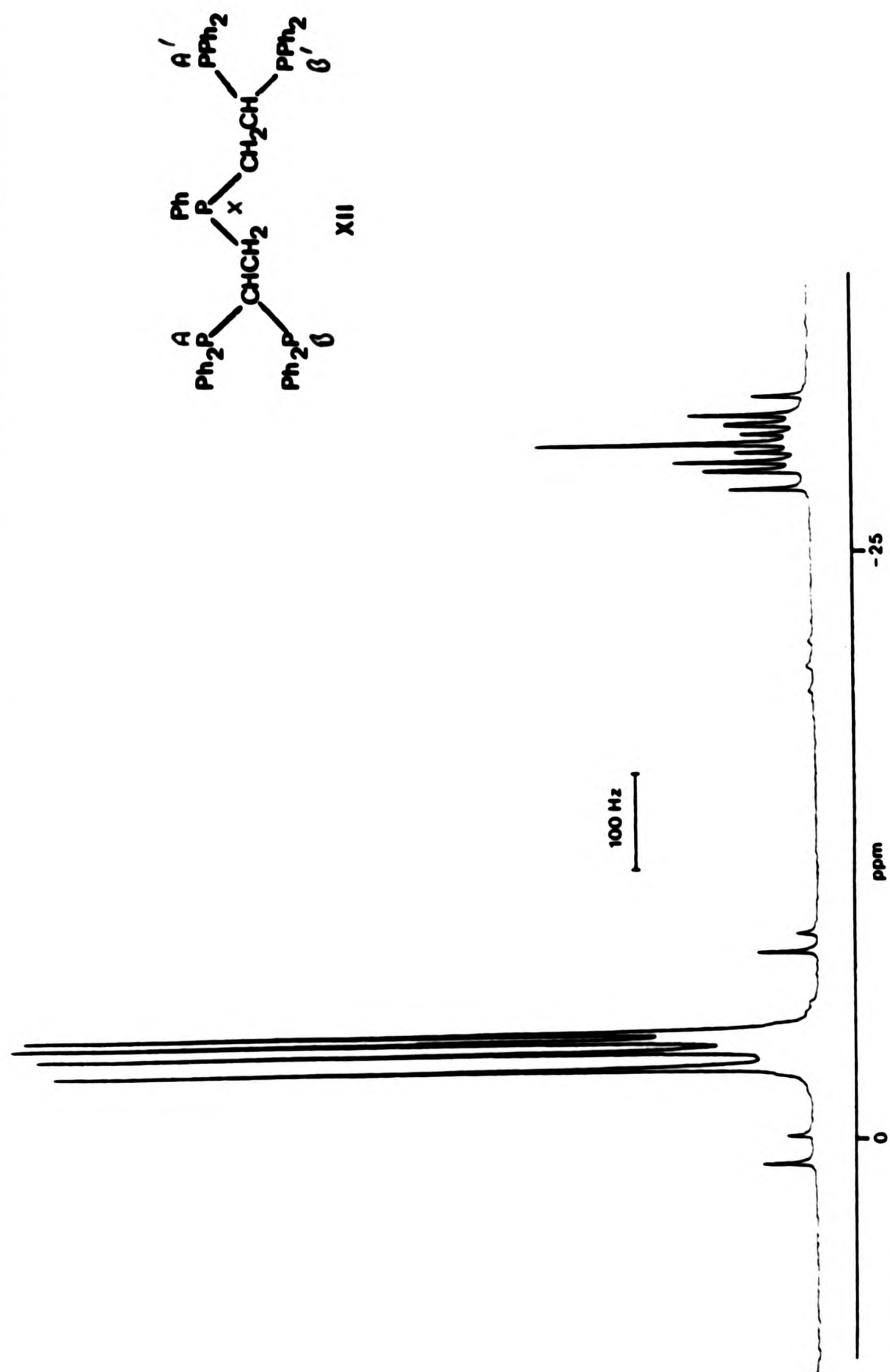


Fig 2.16 - ^{31}P N.M.R. spectrum of XII recorded at 24.2 MHz.

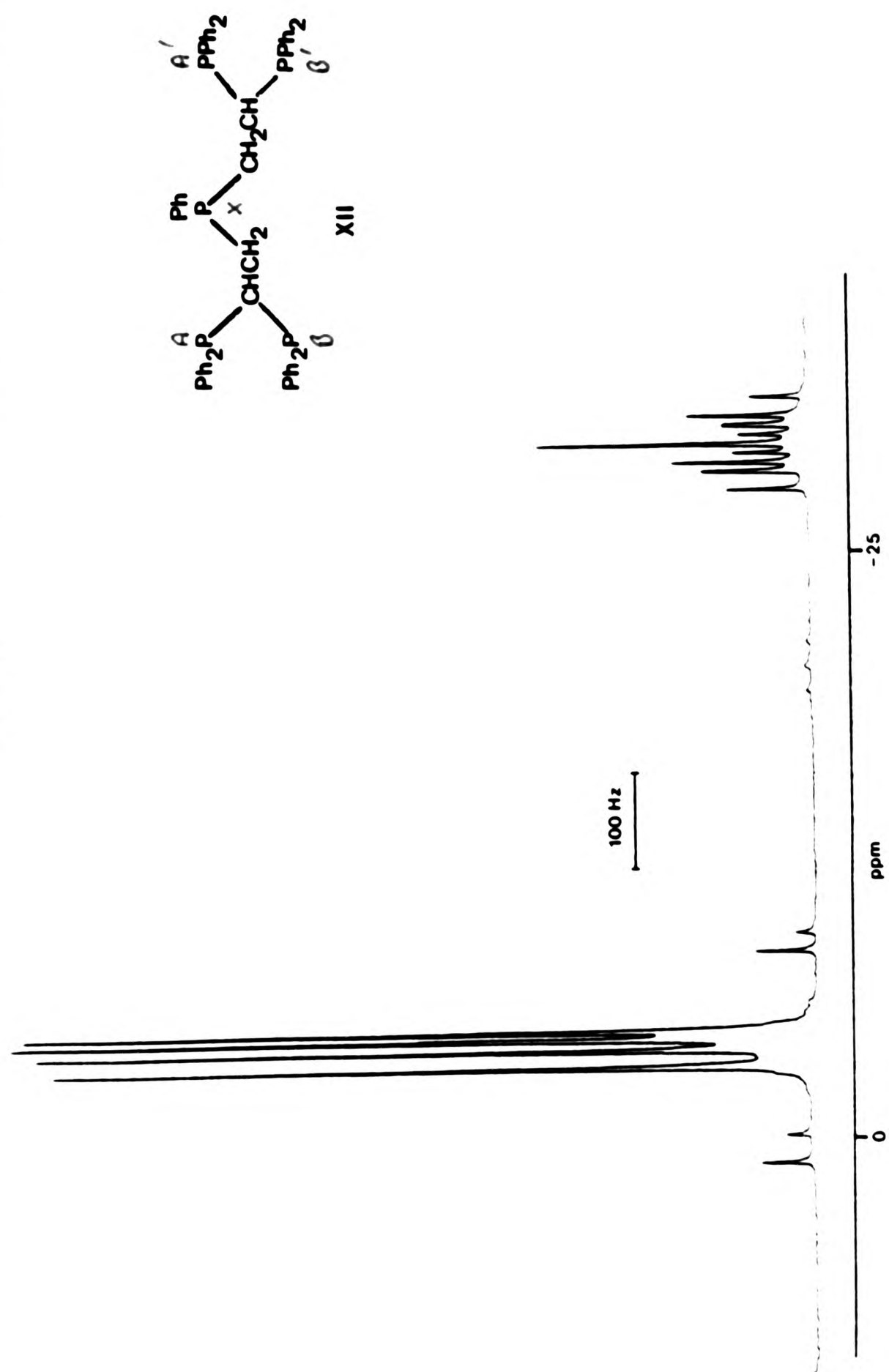


TABLE 2.4 ^{31}P n.m.r. data for the new pentaphosphine ligands

Ligand	$\delta(^{31}\text{P}_\text{A})$ /ppm ^a	$\delta(^{31}\text{P}_\text{B})$ /ppm ^a	$\delta(^{31}\text{P}_\text{X})$ /ppm ^a	$ ^2J(\text{P}_\text{A}-\text{P}_\text{B}) $ /Hz	$ ^3J(\text{P}_\text{A}-\text{P}_\text{X}) $ /Hz	$ ^3J(\text{P}_\text{B}-\text{P}_\text{X}) $ /Hz
XII ^b	-2.9	-4.8	-29.7	100.7	28.6	17.0
XIII ^b	-2.5	-4.0	-26.6	110.5	19.5	19.5
XIV ^b	-2.7	-3.3	-27.6	101.3	20.1	19.5

Notes ^a Relative to external 85% $\text{H}_3\text{PO}_4 = 0.0$ ppm

^b All longer range couplings = 0.0 Hz

The magnitudes of the coupling constants are in general comparable to analogous couplings in related triphosphine species (Table 2.1). However, for compound XII the relatively large difference in $^3J(P_A P_X)$ and $^3J(P_B P_X)$ may suggest a preferred configuration close to that of Fig. 2.17(a) or (b) where the dihedral angles for the P_A-P_X and P_B-P_X

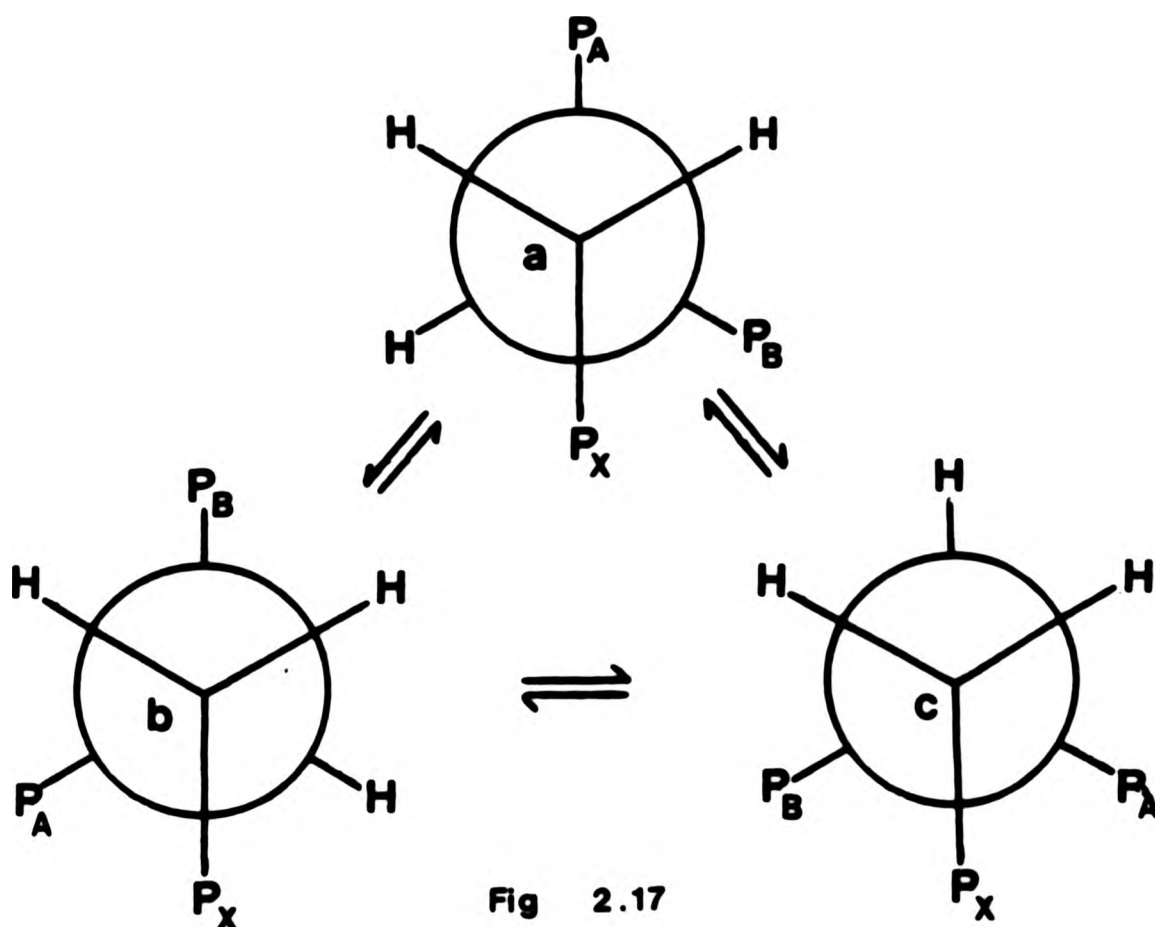


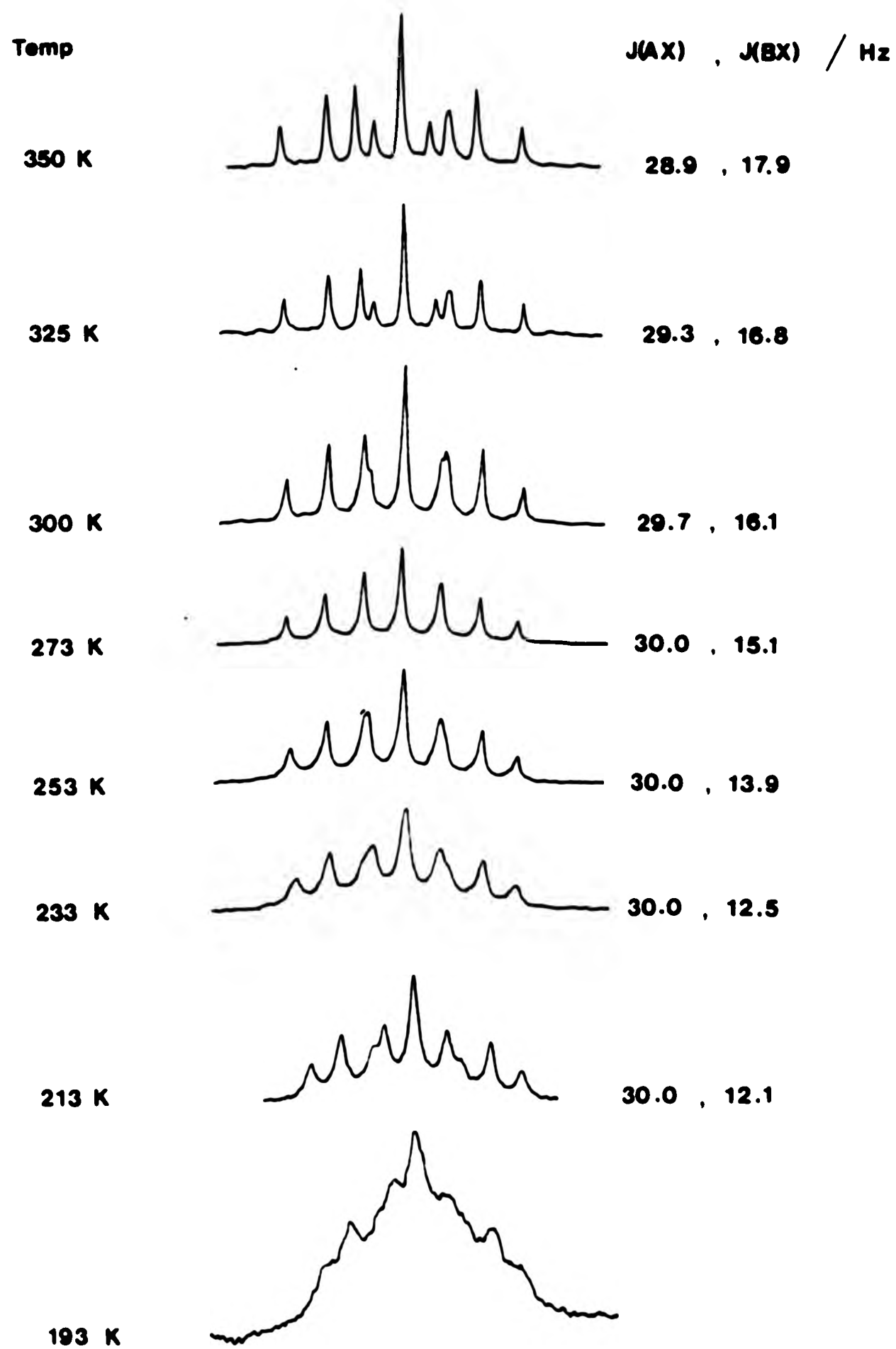
Fig 2.17
Newman projection along
the C-C bond of XII.

systems are different. A detailed n.m.r. study of XII (Fig. 2.18) showed an increased differentiation of $^3J(P_A-P_X)$ and $^3J(P_B P_X)$ with a decrease in temperature and helps to substantiate this suggestion.

The arsenic-containing species XV and XVI are both produced in the same reaction mixture and without prior knowledge their ^{31}P spectra are difficult to assign to a specific compound.

The secondary-arsino compound XV contains a chiral arsenic atom, and as in analogous triphosphine ligands this renders the geminally related phosphorus nuclei inequivalent so that this compound has an

Fig 2.18 - Temperature dependence of the P_x resonance of the pentaphosphine ligand XII showing differentiation of $J(AX)$ and $J(BX)$ at low temperature.



AB spin system. Similarly, the prochiral arsenic atom of XVI leads to this ligand having an AA'BB' spin system (Fig. 2.19). However,

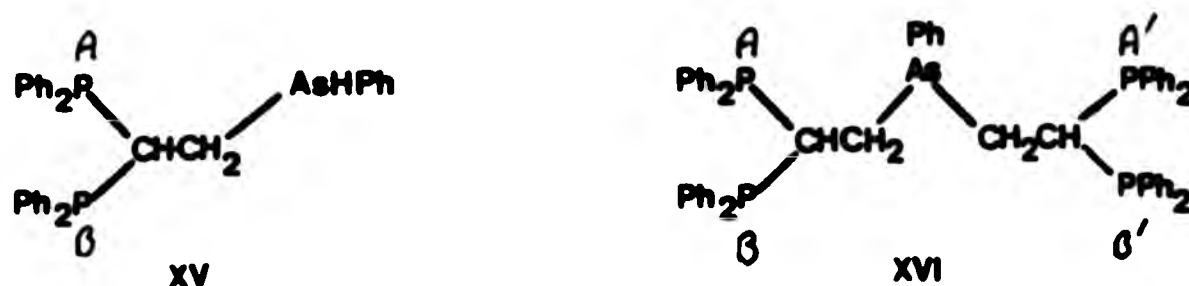


Fig 2.19

since there is negligible long range phosphorus-phosphorus coupling in this molecule its ^{31}P n.m.r. spectrum appears deceptively as a simple AB one⁵³. Since the spectra of both XV and XVI are consistent with either molecular structure the assignment of spectra to specific ligands was made only after careful consideration of the ^{31}P spectra of a range of reaction mixtures containing known proportions of both XV and XVI. Whilst the value of $|^2J(\text{P}_\text{A}\text{P}_\text{B})|$ (95.0 Hz) in XVI is comparable to that found in the phosphine analogue (XII) (100.7 Hz) the similarity of $\delta(\text{P}_\text{A})$ ^{and $\delta(\text{P}_\text{B})$} in XV precludes determination of $|^2J(\text{P}_\text{A}\text{P}_\text{B})|$ in this compound.

(D) Hexatertiary Phosphines

In an extension of the synthetic approach previously described the relatively recently prepared dissecondary phosphine species $\text{PhHP}(\text{CH}_2)_n\text{PPh}$ $n = 2,3$ underwent addition reactions to give the hexaphosphorus ligands XVIII and XIX (Eq. 2.20) as air-stable white solids. This reaction is likely to be applicable to dissecondary phosphines of any chain length thus leading to a series of hexatertiary-phosphine ligands, the most important member of which is likely to be

AB spin system. Similarly, the prochiral arsenic atom of XVI leads to this ligand having an AA'BB' spin system (Fig. 2.19). However,

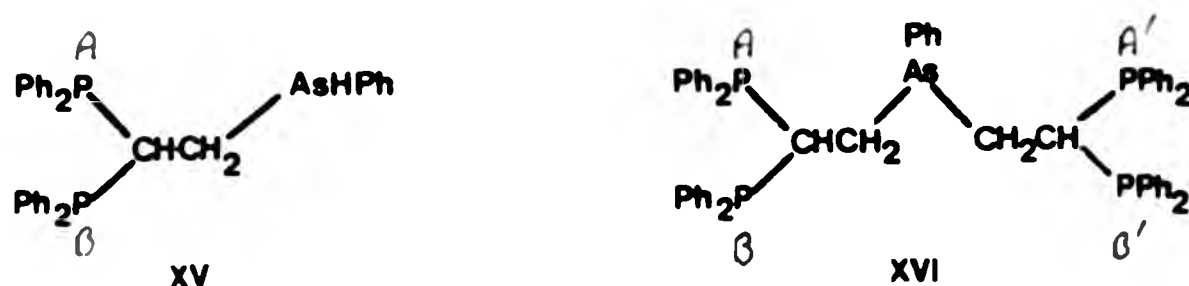
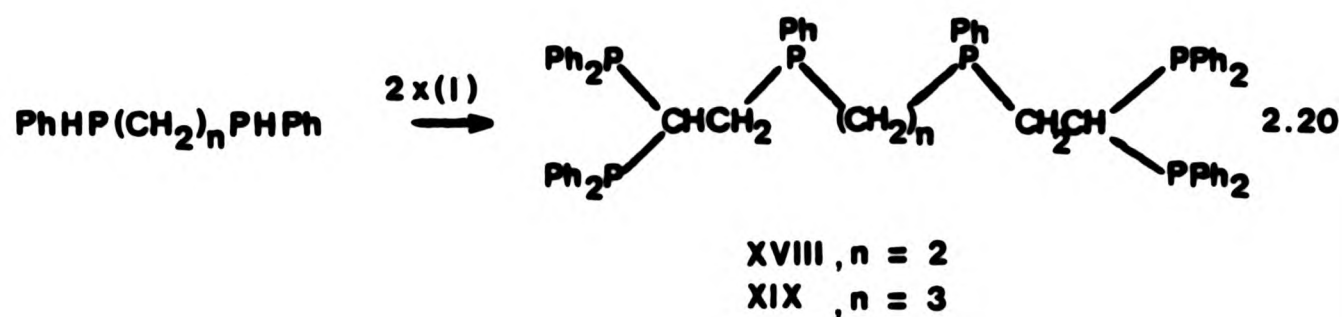


Fig 2.19

since there is negligible long range phosphorus-phosphorus coupling in this molecule its ^{31}P n.m.r. spectrum appears deceptively as a simple AB one⁵³. Since the spectra of both XV and XVI are consistent with either molecular structure the assignment of spectra to specific ligands was made only after careful consideration of the ^{31}P spectra of a range of reaction mixtures containing known proportions of both XV and XVI. Whilst the value of $|^2J(\text{P}_\text{A}\text{P}_\text{B})|$ (95.0 Hz) in XVI is comparable to that found in the phosphine analogue (XII) (100.7 Hz) the similarity of $\delta(^{31}\text{P}_\text{A})$ and $\delta(^{31}\text{P}_\text{B})$ in XV precludes determination of $|^2J(\text{P}_\text{A}\text{P}_\text{B})|$ in this compound.

(D) Hexatertiary Phosphines

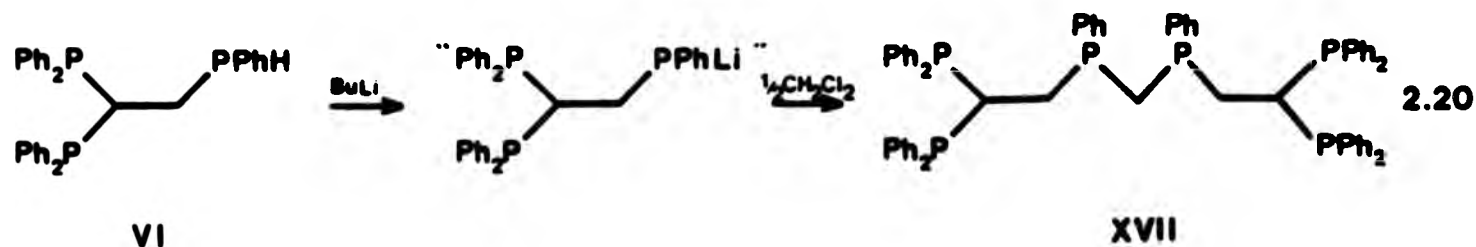
In an extension of the synthetic approach previously described the relatively recently prepared dissecondary phosphine species $\text{PhHP}(\text{CH}_2)_n\text{PPh}$ $n = 2, 3$ underwent addition reactions to give the hexaphosphorus ligands XVIII and XIX (Eq. 2.20) as air-stable white solids. This reaction is likely to be applicable to dissecondary phosphines of any chain length thus leading to a series of hexatertiary-phosphine ligands, the most important member of which is likely to be



the species where $n = 1$ (XVII). The inaccessibility of $\text{PhHPCH}_2\text{PPh}$, however, required the development of an alternative method of synthesis for this ligand from a suitable alkali-metal phosphide. Of the various methods available for the preparation of these reagents, the one of interest here is the reaction of a secondary phosphine with butyllithium (Eq. 2.21)^{57,58}. The exact nature of species such as



" R_2PLi " depends to a large extent on the solvent used and the organic group R ⁵⁹, but all are consistent in that they react with polyhaloalkanes⁶⁰ to give polyphosphorus species as previously described. This reaction was found also to be applicable to the triphosphine ligand VI in which the secondary phosphine atom was readily lithiated. Subsequent reaction with half an equivalent of dichloromethane led to the formation of the required hexatertiary phosphine XVII (Eq. 2.22) which



was isolated as an air-stable white solid.

The presence of two chiral centres at the central phosphorus atoms of these hexaphosphines results in these species each having two stereoisomers⁶¹. In the case where $n = 3$ the near zero four-bond coupling $^4J(P_X-P_{X'})$ (Fig. 2.20) results in this species deceptively

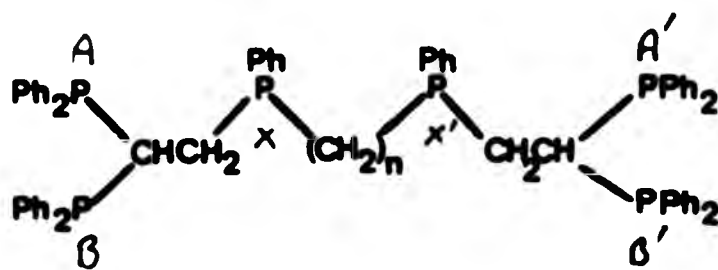


Fig 2.20

having a simple ABX ^{31}P spectrum (where both stereoisomers may be distinguished) (Fig. 2.21).

was isolated as an air-stable white solid.

The presence of two chiral centres at the central phosphorus atoms of these hexaphosphines results in these species each having two stereoisomers⁶¹. In the case where $n = 3$ the near zero four-bond coupling $^4J(P_X-P_X)$ (Fig. 2.20) results in this species deceptively

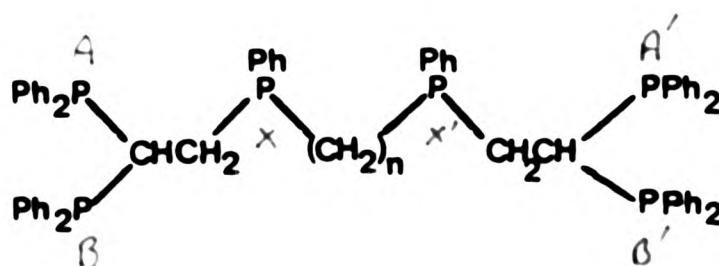


Fig 2.20

having a simple ABX ^{31}P spectrum (where both stereoisomers may be distinguished) (Fig. 2.21).

Fig 2.21 - ^{31}P N.M.R. spectrum of XIX recorded at 36.2 MHz showing the presence of the two diastereomers i and ii.

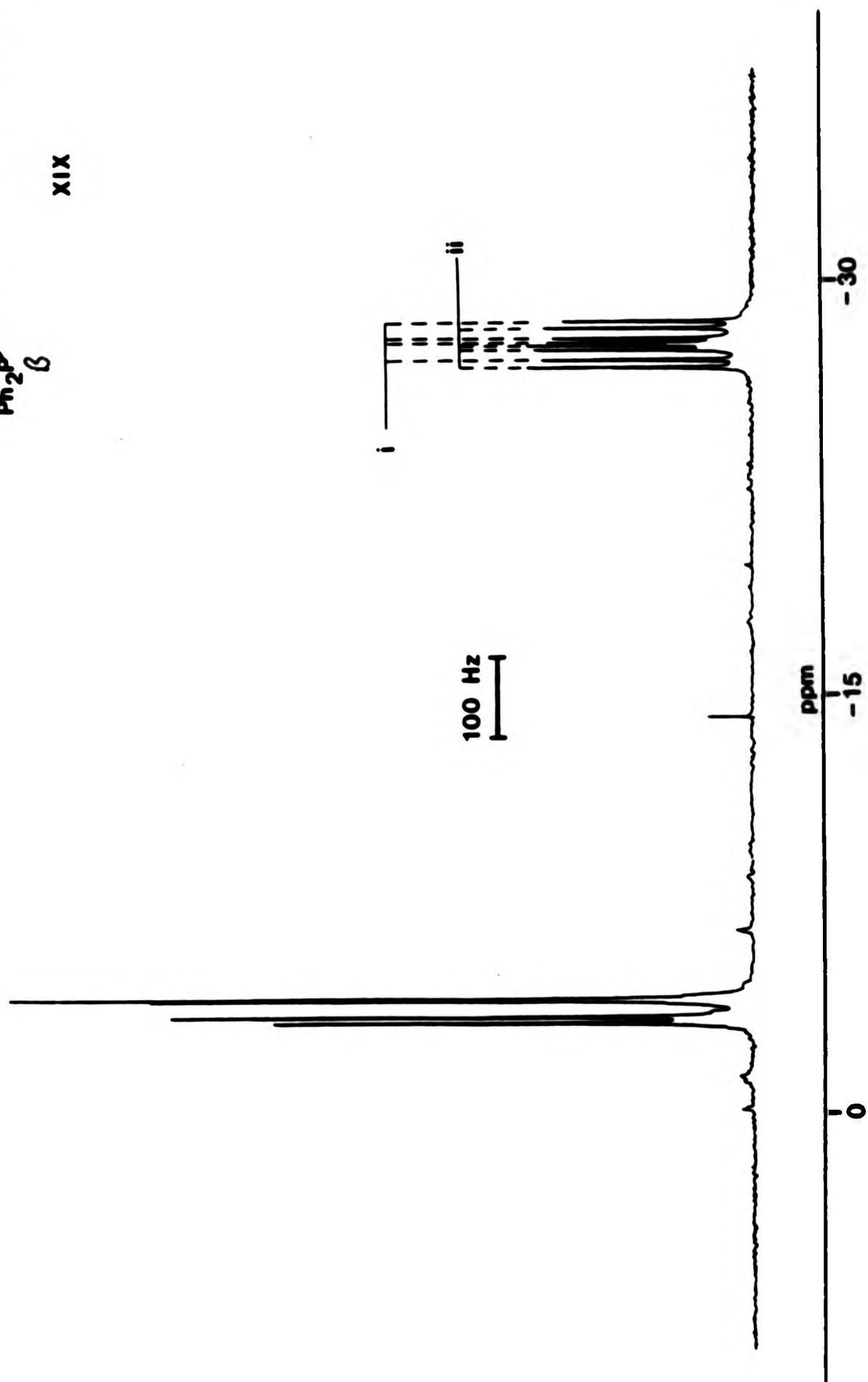
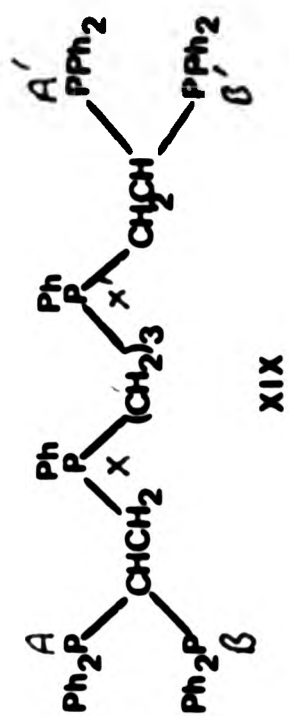
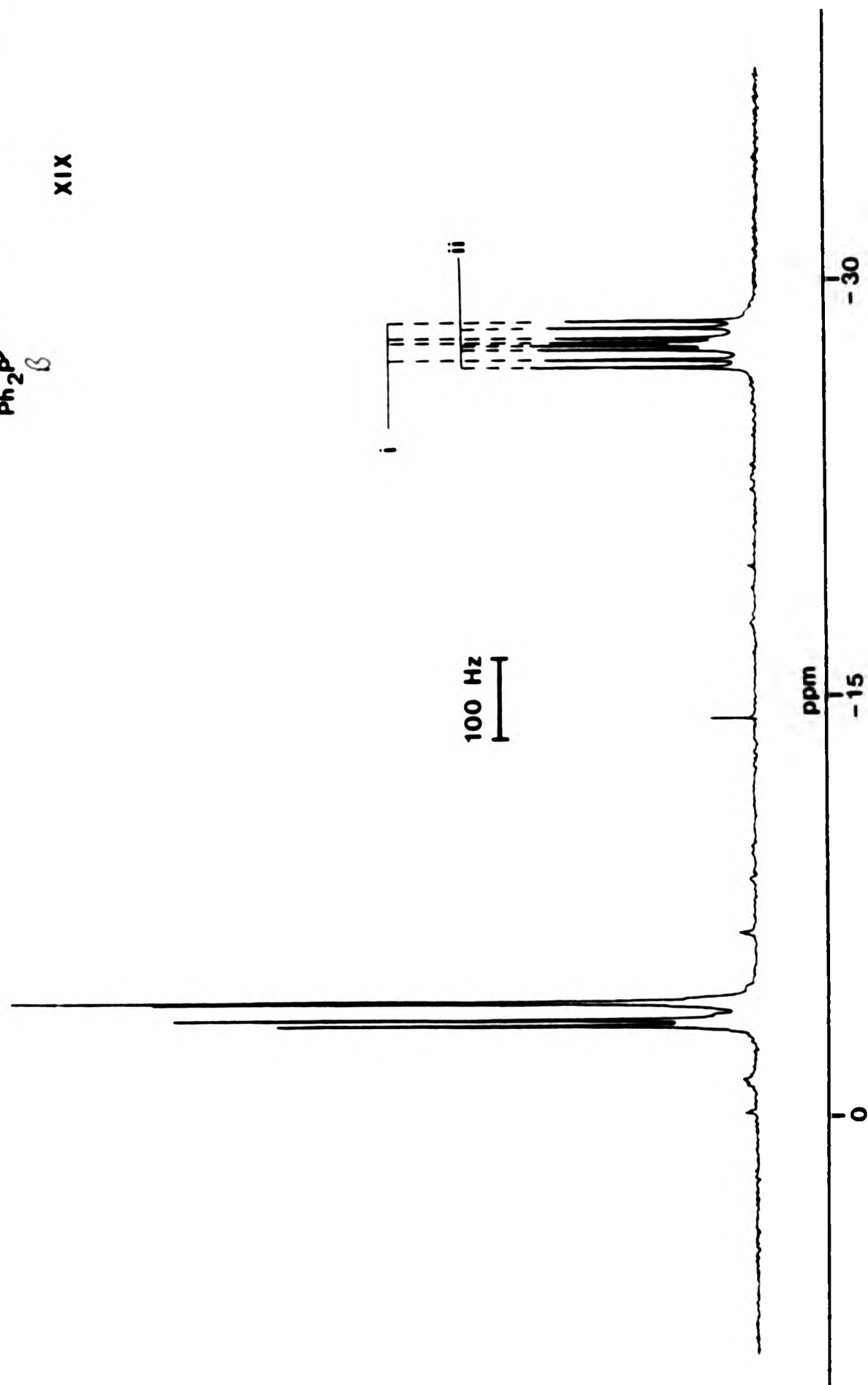
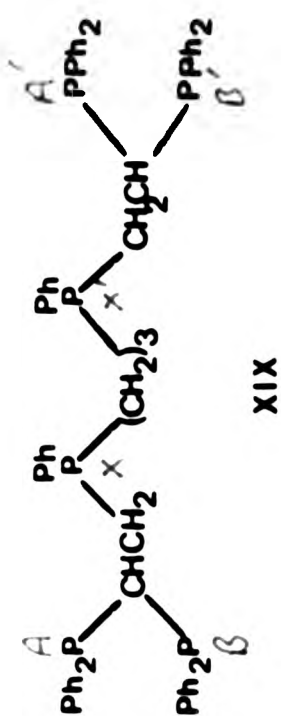
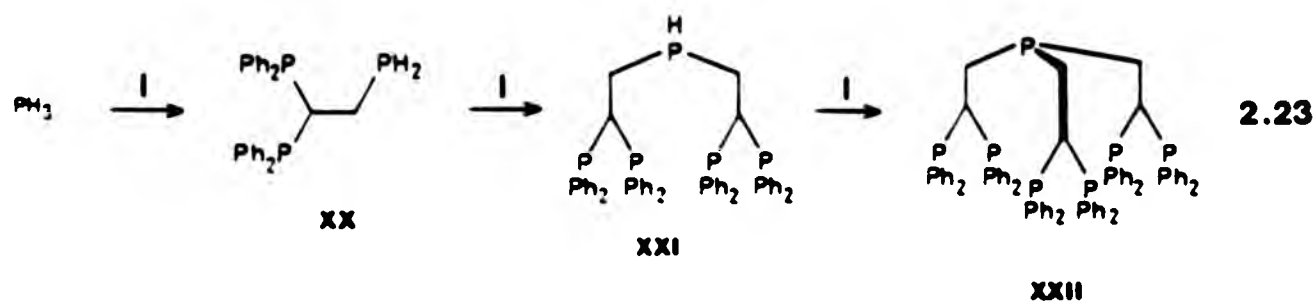


Fig 2.21 - ^{31}P N.M.R. spectrum of XIX recorded at 36.2 MHz showing the presence of the two diastereomers i and ii.



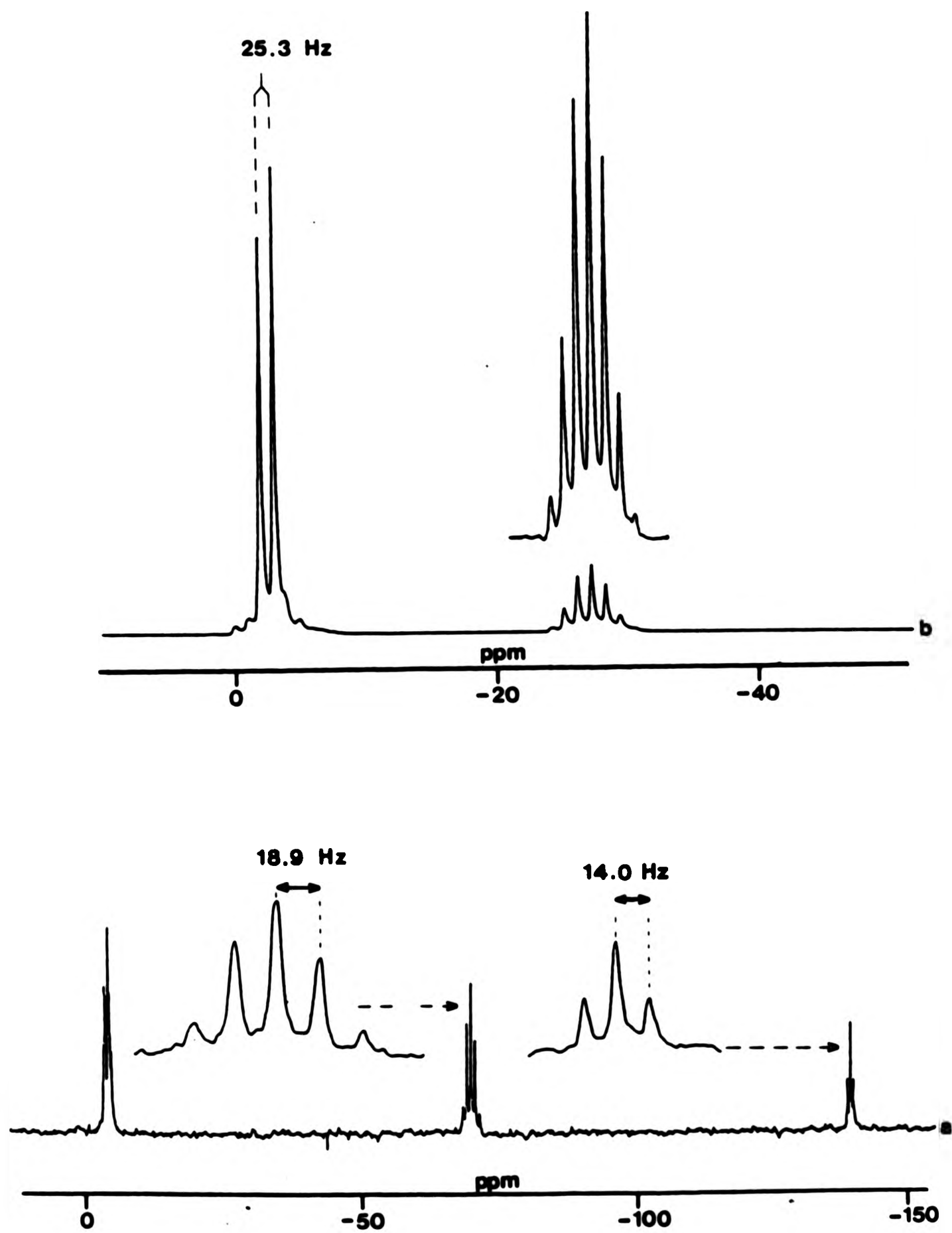
(E) Heptatertiary Phosphines

In a logical extension of the preparation of tri- and penta-
tertiary phosphines from secondary and primary phosphines respectively,
the reaction using phosphine, PH_3 , was found to lead to the formation
of the new heptatertiary phosphine tris (2,2-bis(diphenylphosphino)
ethyl)phosphine, (XXII), via a series of intermediates XX, XXI (Eq. 2.23),
all of which were identified in situ from their characteristic ^{31}P n.m.r.



spectra. Indeed the preparation of XII is facilitated by the use of ^{31}P
n.m.r. to monitor the reaction since it is difficult to control with
precision the amount of phosphine gas available. A ^{31}P n.m.r. spectrum
of the reaction mixture (Fig. 2.22) shows clearly the presence of the
intermediate species (Fig. 2.23) by the characteristic resonance due
to the hydrogen-bearing phosphorus nuclei X and yielded the n.m.r.
parameters shown in Table 2.6.

Fig 2.22 a) ^{31}P N.M.R. spectrum of the reaction mixture from the preparation of the heptaphosphine XXII
b) ^{31}P N.M.R. spectrum of the final product.



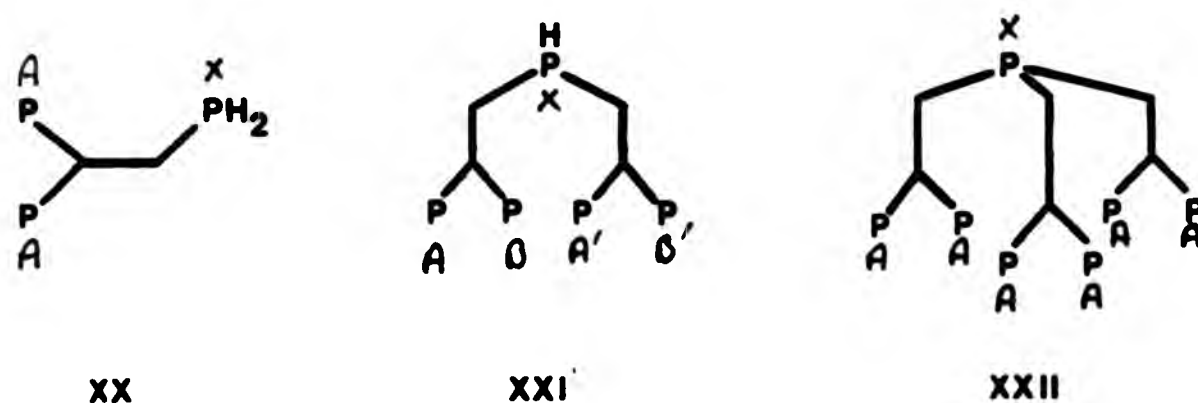


Fig 2.23 Phosphorus labelling system for the species XX-XXII

TABLE 2.6 ^{31}P n.m.r. data for the intermediates XX - XXII

Ligand	$\delta(^{31}\text{P}_X)$ ^a /ppm	$ ^3J(\text{P}_A\text{P}_X) $ /Hz ^b	$ ^3J(\text{P}_B\text{P}_X) $ /Hz ^c
XX	-139.5	14.0	-
XXI	-71.1	18.9	18.9
XXII ^d	-27.3	25.3	-

Notes a Relative to external 85% $\text{H}_3\text{PO}_4 = 0.00$ ppm

b $= ^3J(\text{P}_A, \text{P}_X)$

c $= ^3J(\text{P}_B, \text{P}_X)$

d $\delta(^{31}\text{P}_A) = -2.7$

The ^{31}P n.m.r. spectrum of the product XXII (Fig. 2.14) shows clearly an A_6X spin system ⁵³ with $|^3J(\text{P}_A\text{P}_X)| = 25.3$ Hz, all seven lines of the X-septet being visible. The increase in $|^3J(\text{P}_A\text{P}_X)|$ as successive protons are replaced on P_X may be due to changes in electronegativity but is more likely to be due to inter-bond angle distortions at the P_X atom ⁶³.

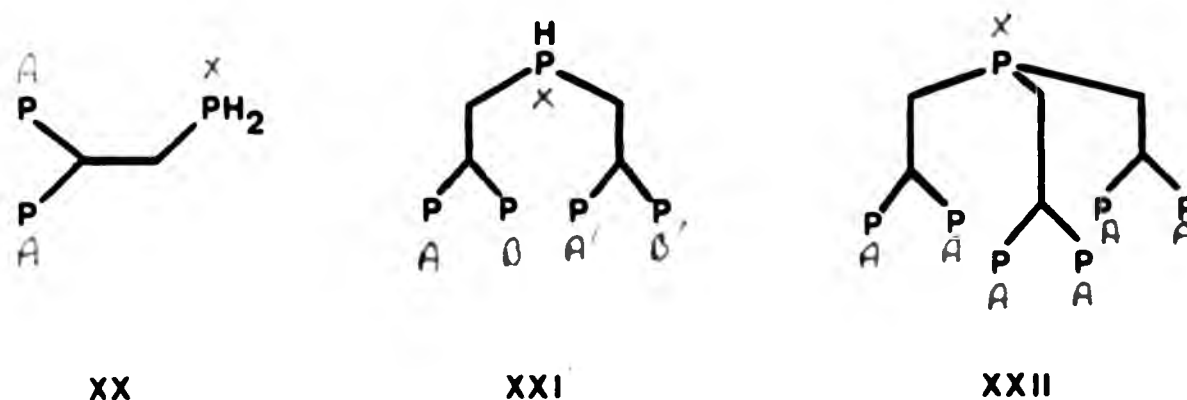


Fig 2.23 Phosphorus labelling system for the species XX-XXII

TABLE 2.6 ^{31}P n.m.r. data for the intermediates XX - XXII

Ligand	$\delta(^{31}\text{P}_X)$ ^a /ppm	$ ^3J(\text{P}_A\text{P}_X) $ /Hz ^b	$ ^3J(\text{P}_B\text{P}_X) $ /Hz ^c
XX	-139.5	14.0	-
XXI	-71.1	18.9	18.9
XXII ^d	-27.3	25.3	-

Notes a Relative to external 85% $\text{H}_3\text{PO}_4 = 0.00$ ppm

b $= ^3J(\text{P}_A, \text{P}_X)$

c $= ^3J(\text{P}_B, \text{P}_X)$

d $\delta(^{31}\text{P}_A) = -2.7$

The ^{31}P n.m.r. spectrum of the product XXII (Fig. 2.14) shows clearly an A_6X spin system ⁵³ with $|^3J(\text{P}_A\text{P}_X)| = 25.3$ Hz, all seven lines of the X-septet being visible. The increase in $|^3J(\text{P}_A\text{P}_X)|$ as successive protons are replaced on P_X may be due to changes in electronegativity but is more likely to be due to inter-bond angle distortions at the P_X atom ⁶³.

3. SUMMARY

The preparation of a series of related polyphosphorus ligands containing up to seven phosphorus atoms has been described. It will be noted that these ligands may be prepared under extremely mild conditions and are often air-stable crystalline materials consequently making them easy to handle and store. A feature of these ligands is their potential for forming complexes with chelate-rings of various sizes, and in particular XIX is of special interest in having the potential to form complexes with four, five and six-membered and larger rings.

CHAPTER 3

OCTAHEDRAL AND SQUARE-PLANAR TRANSITION-METAL COMPLEXES OF

1,1,2-TRIS(DIPHENYLPHOSPHINO)ETHANE AND RELATED TRIPHOSPHINE LIGANDS

1. INTRODUCTION

The new triphosphine ligands reported in the previous chapter have the potential to exhibit a wide range of new and unusual coordination modes. In order to study their coordinative behaviour a series of group VIB metal carbonyl and square-planar palladium and platinum complexes of these new ligands was prepared. This chapter discusses the syntheses of these complexes and examines the multi-element n.m.r. study which was undertaken in order to confirm their structural assignment.

2. OCTAHEDRAL COMPLEXES

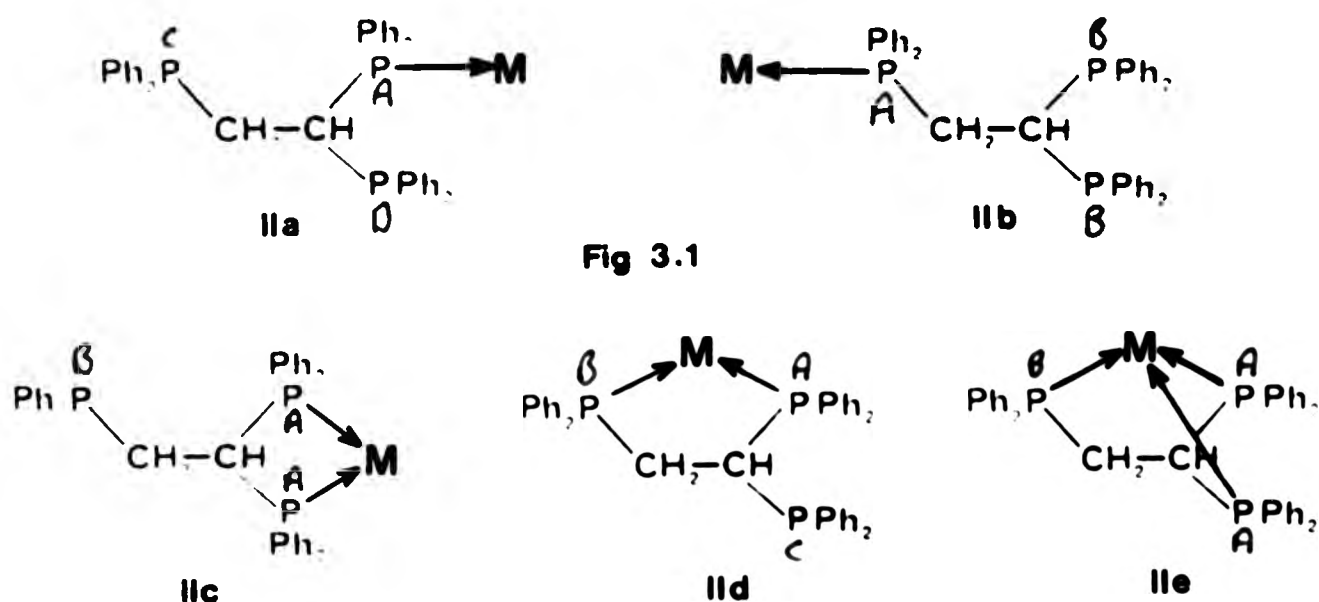
(A) Introduction

The ready availability of the group VI metal hexacarbonyls and the general air-stability of their phosphine complexes have made such species attractive for study and have prompted numerous reviews on the subject⁶⁴. Furthermore, n.m.r. spectroscopists have an interest in these metals since both molybdenum and tungsten have isotopes amenable to study by n.m.r. For these reasons a series of chromium, molybdenum and tungsten complexes of the new triphosphine ligands described in Chapter 2 was prepared in order to study the trends in both coordinative behaviour and n.m.r. parameters (a) within the group and (b) within the series of ligands.

(B) Results and Discussion

(1) 1,1,2-tris(diphenylphosphino)ethane (II)

This ligand (II) is of special interest as it has features of both dppm and dppe. The five possible monometallic coordination modes of (II) are shown in Fig. 3.1 (modes IIa - IIe) and in the present work complexes exhibiting all these modes were synthesised and characterised. In general, direct reaction between the free ligand and a group VIB metal



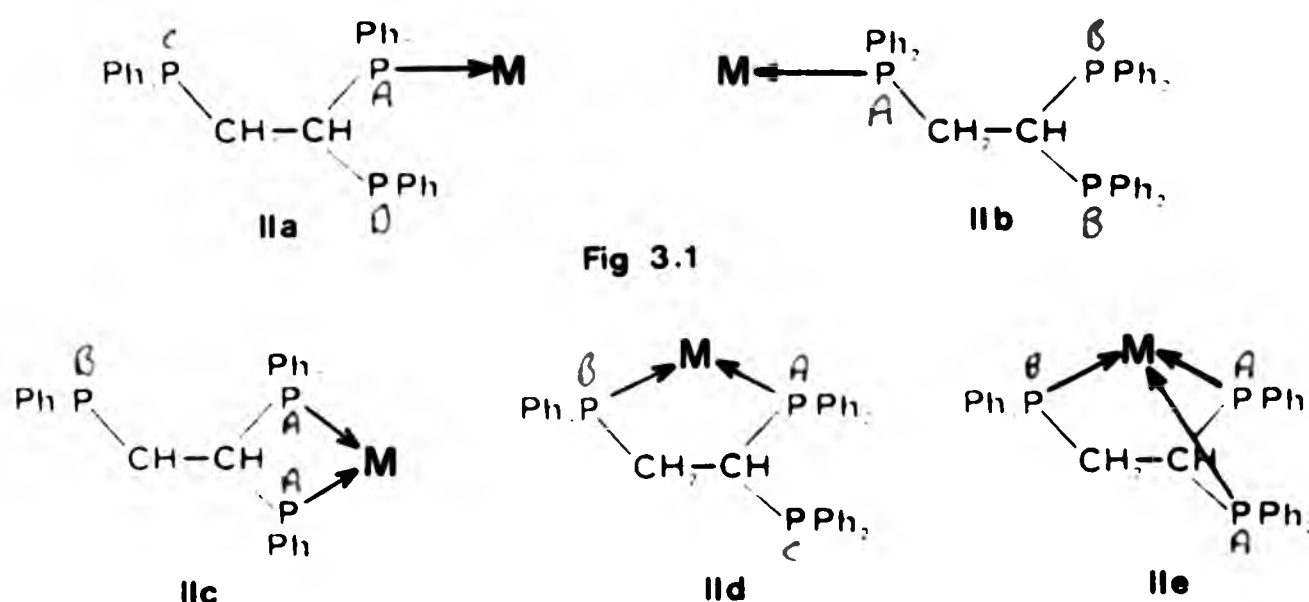
hexacarbonyl resulted in a mixture of complexes having the above and other polymetallic modes, and therefore a more selective synthetic approach was adopted.

The free ligand itself is prepared by the reaction of diphenylphosphine with 1,1-bis(diphenylphosphino)ethene (I), and similar reactions were found to occur for both monodentate (Ia) and bidentate chelate (Ib) forms of I, and these led to the selective syntheses of complexes exhibiting modes IIa and IIc (Eqs 3.1 and 3.2). At room temperature these reactions are rapid and proceed regiospecifically; under reflux conditions, however, partial rearrangements from IIa \rightarrow IIb and from IIc \rightarrow IId were found to occur. Complexes of structural type IId were made by a method (Eq 3.3) which is similar to Keiter's. ⁶⁵ ³¹P n.m.r. spectroscopy revealed that for chromium and tungsten, the reaction of Eq 3.3 led solely to the complex exhibiting mode IId, but for molybdenum the analogous

(B) Results and Discussion

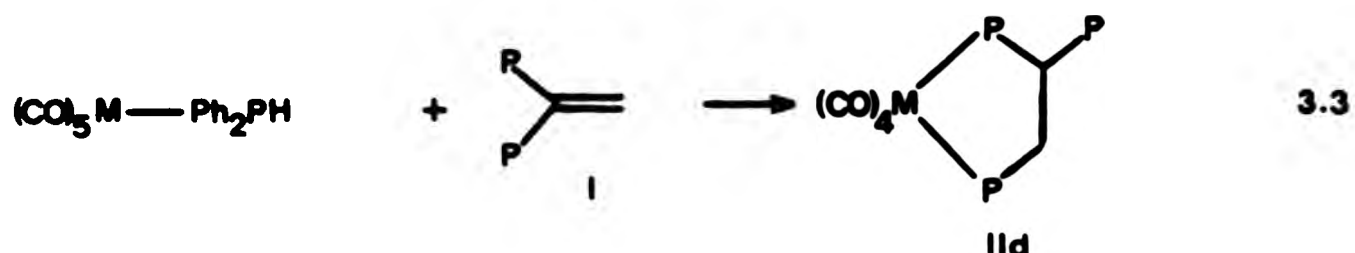
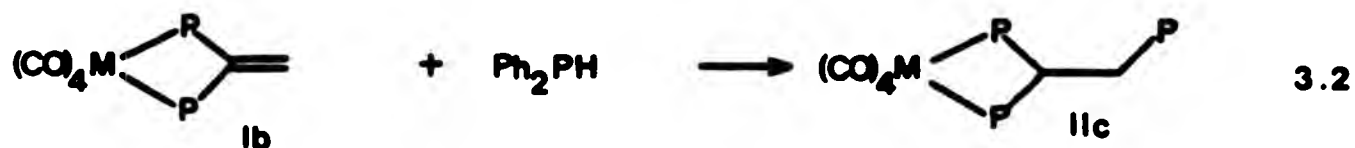
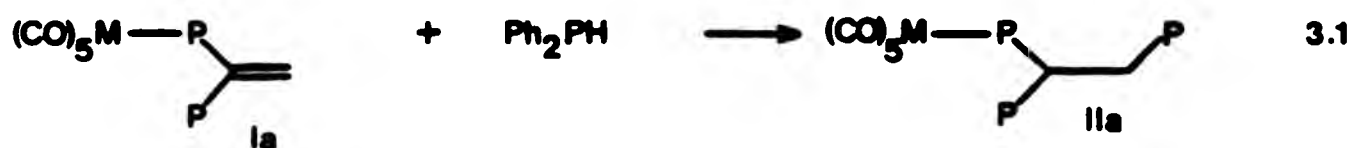
(i) 1,1,2-tris(diphenylphosphino)ethane (II)

This ligand (II) is of special interest as it has features of both dppm and dppe. The five possible monometallic coordination modes of (II) are shown in Fig. 3.1 (modes IIa - IIe) and in the present work complexes exhibiting all these modes were synthesised and characterised. In general, direct reaction between the free ligand and a group VIB metal



hexacarbonyl resulted in a mixture of complexes having the above and other polymetallic modes, and therefore a more selective synthetic approach was adopted.

The free ligand itself is prepared by the reaction of diphenylphosphine with 1,1-bis(diphenylphosphino)ethene (I), and similar reactions were found to occur for both monodentate (Ia) and bidentate chelate (Ib) forms of I, and these led to the selective syntheses of complexes exhibiting modes IIa and IIc (Eqs 3.1 and 3.2). At room temperature these reactions are rapid and proceed regiospecifically; under reflux conditions, however, partial rearrangements from IIa \rightarrow IIb and from IIc \rightarrow IId were found to occur. Complexes of structural type IId were made by a method (Eq 3.3) which is similar to Keiter's. ⁶⁵ ³¹P n.m.r. spectroscopy revealed that for chromium and tungsten, the reaction of Eq 3.3 led solely to the complex exhibiting mode IId, but for molybdenum the analogous



reaction produced a mixture of complexes having modes IIc and IId. This apparent equal preference of molybdenum to adopt four- and five-membered chelate-ring structures is also demonstrated by complexes of other ligands and is discussed later. The complexes of the tricoordinate ligand in mode IIc were prepared by direct reaction of the free ligand, II, with *fac*-M(CO)₃(RCN)₃, and ³¹P n.m.r. spectroscopy showed no indication of the formation of the related *mer* isomer. Complexes of mode IIb were found to be difficult to prepare selectively and therefore were not of isolated pure. Structural mode IIa was found to be overwhelmingly preferred to IIb; for example, treatment of the free ligand, II, with M(CO)₅.THF⁶⁶ resulted in a ca. 4:1 mixture of complexes having modes IIa and IIb. Also, reaction of M(CO)₅PPh₂H with I, which has the potential to give complexes of type IIb, was found not to proceed at room temperature, and under reflux conditions (67°C) resulted in the formation of complexes of structural type IId, as previously described.

The phosphine complexes M(CO)₅[IIa], M(CO)₄[IIc], M(CO)₄[IId] and M(CO)₃[IIe], where M = Cr, Mo, W, were generally obtained as white to yellow air-stable crystals with sharp melting points (pages 171-173).

Several of these complexes were also made by other methods, but since the isolation of the free ligand II is difficult it has been found generally better to build the coordinated ligand from the appropriate phosphine complex. This approach was found to be widely applicable in many subsequent reactions involving the larger ligands since it could be used to limit the isomeric divergence of complex formation. This series of complexes therefore demonstrates the ability of 1,1,2-tris(diphenylphosphino)ethane to form both four- and five-membered chelate-rings, and also to coordinate fully as in IIe, to produce complexes that would be expected to involve considerable strain.

A knowledge of the factors influencing ^{31}P chemical shifts in phosphine complexes as outlined in Chapter 1 made analysis of the ^{31}P n.m.r. spectra for the complexes IIa - IIe (e.g. Figs 3.2, 3.3) fairly straightforward, and led to the values of ^{31}P n.m.r. parameters shown in Tables 3.1 and 3.2.

Fig. 3.4 illustrates the pattern of coordination chemical shifts, Δ , (see page 14)³⁸ for these complexes and demonstrates nicely two important features.

- (i) A monotonic decrease in Δ as the group Cr, Mo, W is descended.
- (ii) For any particular metal the ranges of Δ do not overlap for the three types of coordinated phosphorus atom considered.

In the fully coordinated species IIe the phosphorus nuclei P_A are incorporated in both four- and five-membered rings and it is interesting that they exhibit Δ values in the region only associated with four-membered rings.

Perhaps more difficult to quantify are the various phosphorus-phosphorus coupling constants in the complexes IIa - IIe (Table 3.2). For the species of structural types IIa, IIb and IIc the various couplings appear to be dependent on conformational effects alone rather

Fig. 3.2 ^{31}P n.m.r. spectrum of $\text{W}(\text{CO})_4[\text{IIc}]$

Fig. 3.3 ^{31}P n.m.r. spectrum of $\text{Cr}(\text{CO})_5[\text{IIa}]$

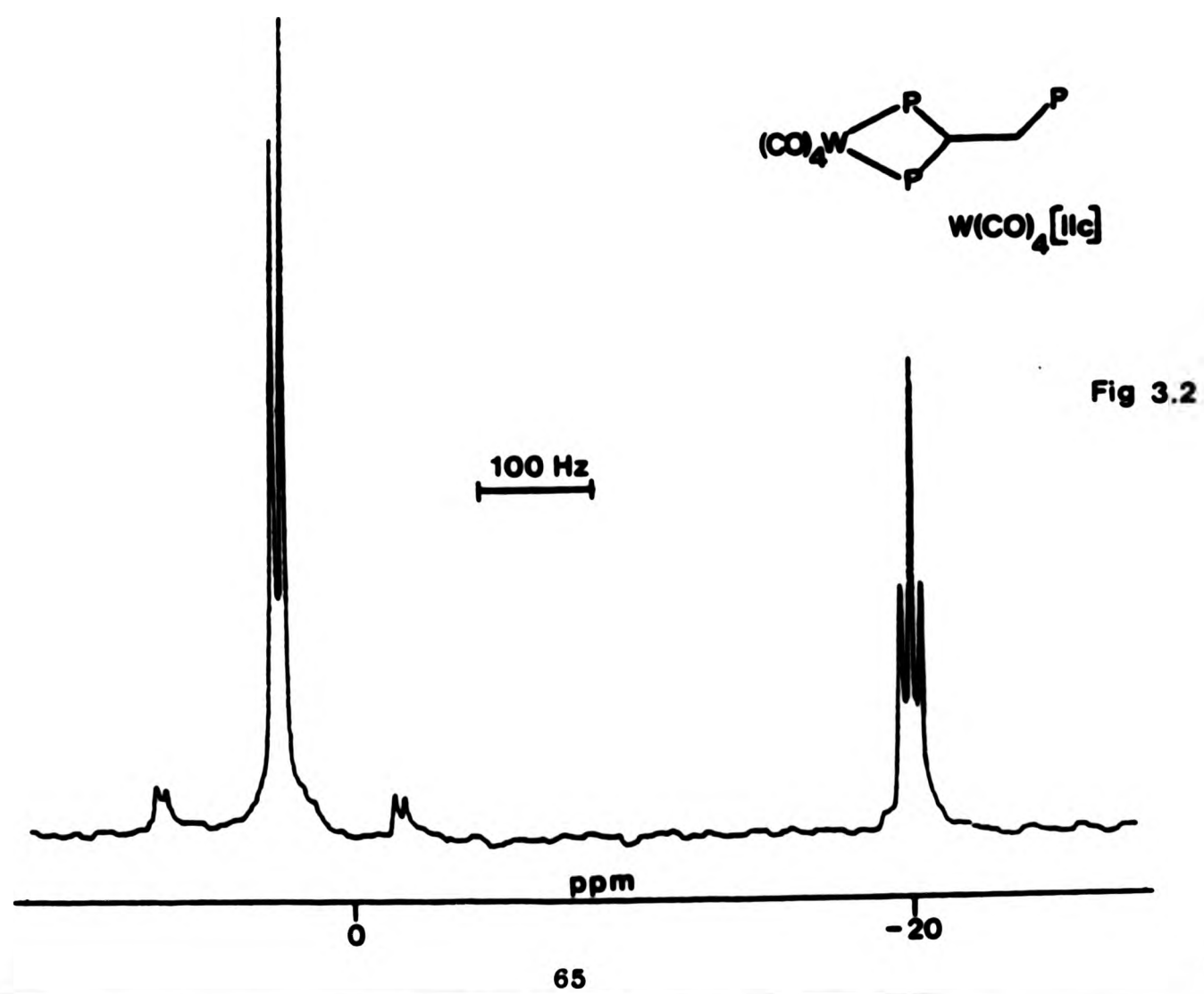
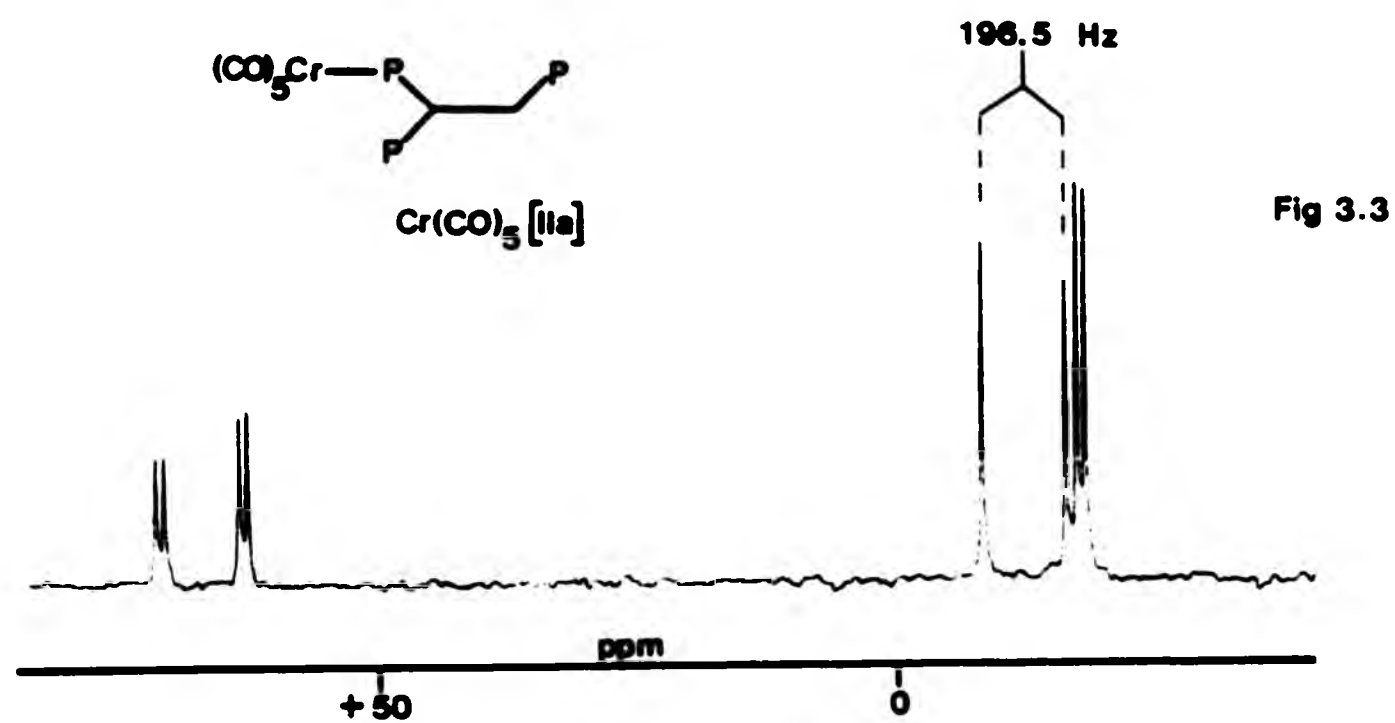


TABLE 3.1 ^{31}P chemical shift data for the group VIB metal carbonyl complexes of II

Complex	$\delta(^{31}\text{P}_\text{A})$ /ppm ^a	ΔP_A /ppm ^c	$\delta(^{31}\text{P}_\text{B})$ /ppm ^a	ΔP_B /ppm ^c	$\delta(^{31}\text{P}_\text{C})$ /ppm ^a
$\text{Cr}(\text{CO})_5$ [IIa]	+67.2	+70.8	-11.9	-	-17.3
$\text{Mo}(\text{CO})_5$ [IIa]	+50.0	+53.6	-10.5	-	-17.5
$\text{W}(\text{CO})_5$ [IIa]	+33.4	+37.0	-9.6	-	-17.5
$\text{Cr}(\text{CO})_5$ [IIb]	+49.6	+69.2	-3.7	-	-
$\text{Mo}(\text{CO})_5$ [IIb]	+30.2	+49.8	-4.2	-	-
$\text{W}(\text{CO})_5$ [IIb]	+12.0	+31.6	-3.9	-	-
$\text{Cr}(\text{CO})_4$ [IIc]	+50.5	+54.1	-19.3	-	-
$\text{Mo}(\text{CO})_4$ [IIc]	+26.8	+30.4	-19.5	-	-
$\text{W}(\text{CO})_4$ [IIc]	+2.7	+6.3	-20.0	-	-
$\text{Cr}(\text{CO})_4$ [IIId]	+87.5	+91.1	+69.4	+89.0	-15.9
$\text{Mo}(\text{CO})_4$ [IIId]	+64.8	+68.4	+47.4	+67.0	-14.8
$\text{W}(\text{CO})_4$ [IIId]	+49.5	+53.1	+32.7	+52.3	-15.6
$\text{Cr}(\text{CO})_3$ [IIe]	+50.3	+53.9	+61.4	+81.0	-
$\text{Mo}(\text{CO})_3$ [IIe]	+29.2	+32.8	+40.6	+60.2	-
$\text{W}(\text{CO})_3$ [IIe]	+11.7	+15.3	+28.1	+47.7	-

Notes a Relative to external 85% H_3PO_4 = 0.0 ppm

b See Fig. 3.1 for labelling system

c Coordination chemical shift

Fig. 3.4 Dependence of ^{31}P coordination chemical shift on ring-size and metal atom for group VI metal carbonyl complexes of II.

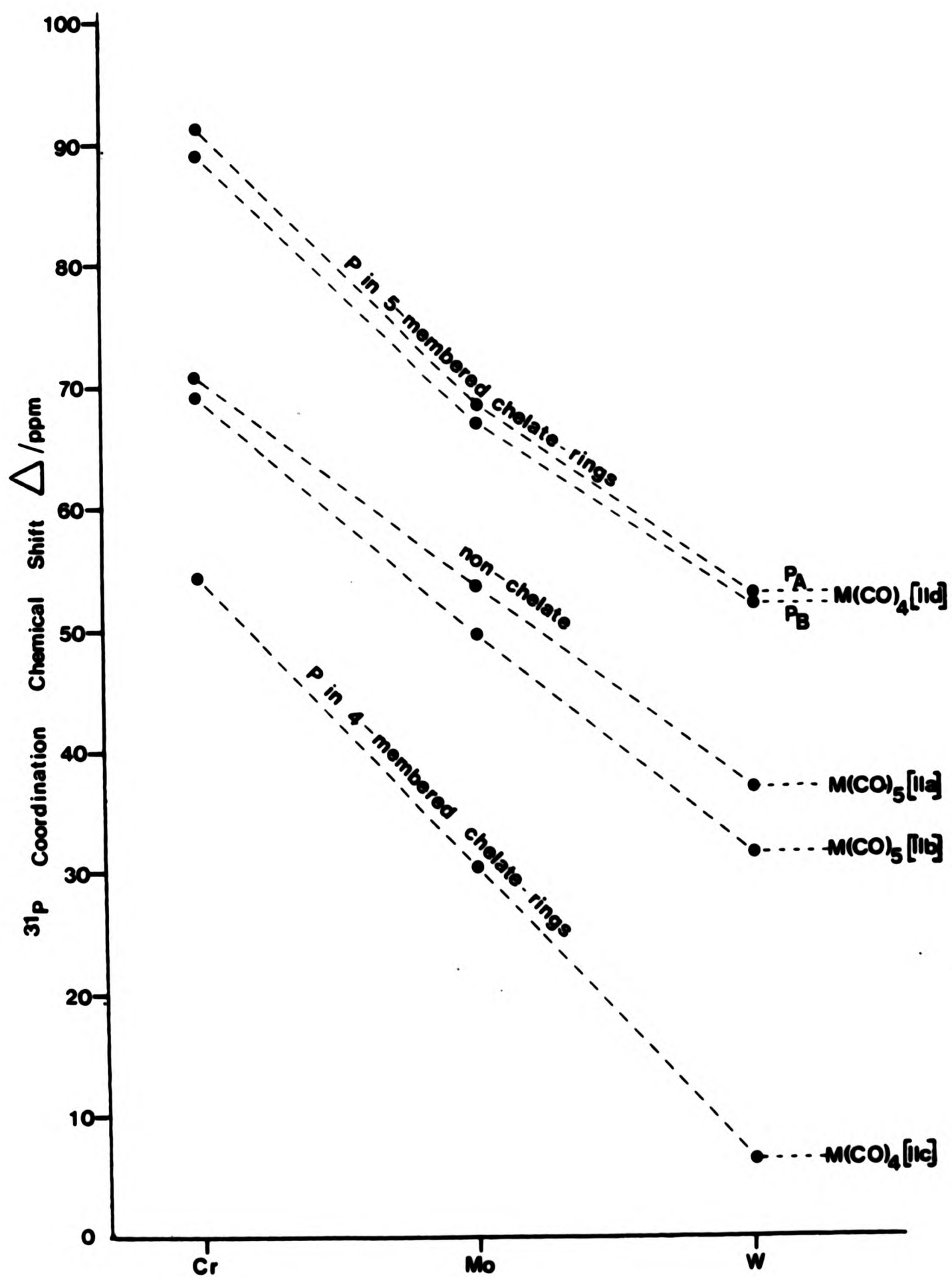


TABLE 3.2 ^{31}P - ^{31}P coupling constants for the group VIB metal carbonyl complexes of II

Complex ^a	$J(^{31}\text{P}_\text{A}-^{31}\text{P}_\text{B})$ ^b /Hz	$J(^{31}\text{P}_\text{A}-^{31}\text{P}_\text{C})$ ^b /Hz	$J(^{31}\text{P}_\text{B}-^{31}\text{P}_\text{C})$ ^b /Hz
$\text{Cr}(\text{CO})_5$ [IIa]	196.5	20.8	0.0
$\text{Mo}(\text{CO})_5$ [IIa]	213.6	19.5	0.0
$\text{W}(\text{CO})_5$ [IIa]	210.0	22.6	0.0
$\text{Cr}(\text{CO})_5$ [IIb]	3.1	-	-
$\text{Mo}(\text{CO})_5$ [IIb]	8.5	-	-
$\text{W}(\text{CO})_5$ [IIb]	7.3	-	-
$\text{Cr}(\text{CO})_4$ [IIc]	7.3	-	-
$\text{Mo}(\text{CO})_4$ [IIc]	7.3	-	-
$\text{W}(\text{CO})_4$ [IIc]	8.5	-	-
$\text{Cr}(\text{CO})_4$ [IIId]	20.8	25.9	1.8
$\text{Mo}(\text{CO})_4$ [IIId]	9.8	25.6	1.8
$\text{W}(\text{CO})_4$ [IIId]	1.5	29.5	2.4
$\text{Cr}(\text{CO})_3$ [IIe]	23.2	-	-
$\text{Mo}(\text{CO})_3$ [IIe]	12.2	-	-
$\text{W}(\text{CO})_3$ [IIe]	6.1	-	-

Notes a See Fig. 3.1 for labelling system

b Signs unknown

than on the nature of the metal, and it is only when coupling can occur through the metal itself, (IIId and IIe), that there are differences between complexes of the same structural type. Complexes of type IIId (Fig. 3.5) are the best examples where the values of $^3J(^{31}\text{P}_\text{B}-^{31}\text{P}_\text{C})$ and

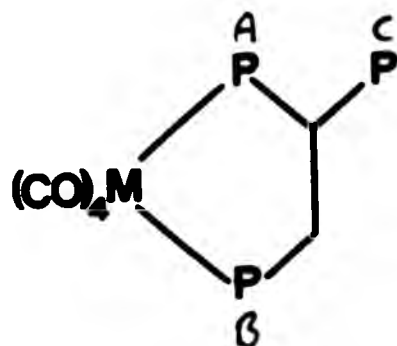


Fig 3.5

$^2J(^{31}\text{P}_\text{A}-^{31}\text{P}_\text{C})$ which do not involve through-the-metal coupling are comparable for each of chromium, molybdenum and tungsten, suggesting similar conformations. The decrease in magnitude of $J(^{31}\text{P}_\text{A}-^{31}\text{P}_\text{B})$ in IIId and similarly in IIe type complexes down the group must therefore, if conformational effects are the same for each complex, arise from differences in the through-the-metal couplings. As mentioned in Chapter 1, Grim et al.⁴⁶ have suggested that values of $^nJ(^{31}\text{P}-^{31}\text{P})$ within a chelate-ring structure can be considered as a sum of the "through-the-metal" and "through-the-backbone" contributions (Eq. 3.4).

$$^nJ(^{31}\text{P}-^{31}\text{P}) = M_J(^{31}\text{P}-^{31}\text{P}) + B_J(^{31}\text{P}-^{31}\text{P}) \quad (3.4)$$

Typical values of $M_J(^{31}\text{P}-^{31}\text{P})$ in such complexes are -41.0 Hz, -28.0 Hz and -22.0 Hz for chromium, molybdenum and tungsten respectively.⁴⁶ From the results of Table 3.2, therefore, it is possible to make approximate calculations of $B_J(^{31}\text{P}-^{31}\text{P})$, although in applying this equation it is essential to take into account signs of coupling constants. Since the signs of $J(^{31}\text{P}_\text{A}-^{31}\text{P}_\text{B})$ are not known, two sets of values for $B_J(^{31}\text{P}_\text{A}-^{31}\text{P}_\text{B})$ are possible for complexes of type IIId:

than on the nature of the metal, and it is only when coupling can occur through the metal itself, (IIId and IIe), that there are differences between complexes of the same structural type. Complexes of type IIId (Fig. 3.5) are the best examples where the values of $^3J(^{31}\text{P}_\text{B}-^{31}\text{P}_\text{C})$ and

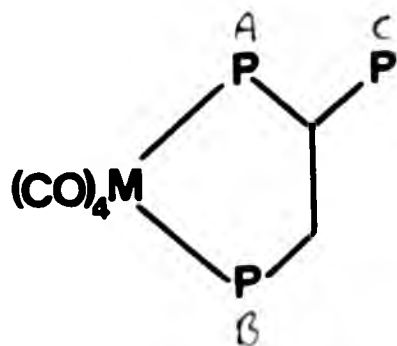


Fig 3.5

$^2J(^{31}\text{P}_\text{A}-^{31}\text{P}_\text{C})$ which do not involve through-the-metal coupling are comparable for each of chromium, molybdenum and tungsten, suggesting similar conformations. The decrease in magnitude of $J(^{31}\text{P}_\text{A}-^{31}\text{P}_\text{B})$ in IIId and similarly in IIe type complexes down the group must therefore, if conformational effects are the same for each complex, arise from differences in the through-the-metal couplings. As mentioned in Chapter 1, Grim et al⁴⁶ have suggested that values of $^nJ(^{31}\text{P}-^{31}\text{P})$ within a chelate-ring structure can be considered as a sum of the "through-the-metal" and "through-the-backbone" contributions (Eq. 3.4).

$$^nJ(^{31}\text{P}-^{31}\text{P}) = M_J(^{31}\text{P}-^{31}\text{P}) + B_J(^{31}\text{P}-^{31}\text{P}) \quad (3.4)$$

Typical values of $M_J(^{31}\text{P}-^{31}\text{P})$ in such complexes are -41.0 Hz, -28.0 Hz and -22.0 Hz for chromium, molybdenum and tungsten respectively.⁴⁶ From the results of Table 3.2, therefore, it is possible to make approximate calculations of $B_J(^{31}\text{P}-^{31}\text{P})$, although in applying this equation it is essential to take into account signs of coupling constants. Since the signs of $J(^{31}\text{P}_\text{A}-^{31}\text{P}_\text{B})$ are not known, two sets of values for $B_J(^{31}\text{P}_\text{A}-^{31}\text{P}_\text{B})$ are possible for complexes of type IIId:

- (i) if $J(^{31}\text{P}_\text{A} ^{31}\text{P}_\text{B})$ is positive, $^B J(^{31}\text{P}_\text{A} ^{31}\text{P}_\text{B}) = +61.8 \text{ Hz}, +37.8 \text{ Hz}$
and $+23.5 \text{ Hz}$ for Cr, Mo and W respectively;
- (ii) if $J(^{31}\text{P}_\text{A} ^{31}\text{P}_\text{B})$ is negative, $^B J(^{31}\text{P}_\text{A} ^{31}\text{P}_\text{B}) = +20.2 \text{ Hz}, +18.2 \text{ Hz}$
and $+20.5 \text{ Hz}$ for Cr, Mo and W respectively.

Since it is likely that conformational differences are small it is reasonable to assume that $^B J(^{31}\text{P}_\text{A} ^{31}\text{P}_\text{B})$ contributions within the IIId series are comparable. This is clearly the result if values of $J(^{31}\text{P}_\text{A} ^{31}\text{P}_\text{B})$ are negative for these complexes and leads to the prediction that $^B J(^{31}\text{P}_\text{A} ^{31}\text{P}_\text{B})$ is of the order of $+20 \text{ Hz}$ compared to 24.4 Hz in the free ligand. A similar treatment can be undertaken for the fully coordinated complexes of structural type IIe, and a summary of such calculations is given in Table 3.3.

TABLE 3.3

Complex Type	$^M J(^{31}\text{P}_\text{A} ^{31}\text{P}_\text{B})$ /Hz	$^B J(^{31}\text{P}_\text{A} ^{31}\text{P}_\text{B})$ /Hz	$J(^{31}\text{P}_\text{A} ^{31}\text{P}_\text{B})$ /Hz _{calc}	$J(^{31}\text{P}_\text{A} ^{31}\text{P}_\text{B})$ /Hz _{expt}
IIId - Cr	-41	+20	-21	± 20.8
- Mo	-28	+20	-8	± 9.8
- W	-22	+20	-2	± 1.5
IIe - Cr	-41	+16	-25	± 23.2
- Mo	-28	+16	-12	± 12.2
- W	-22	+16	-6	± 6.1
II - free ligand	0	24.4	24.4	24.4

⁹⁵Mo and ¹⁸³W n.m.r. data

The ¹⁸³W nucleus ($I = \frac{1}{2}$, nat. abundance 14.7%) has such low sensitivity to n.m.r. detection that many of the ¹⁸³W shieldings so far reported⁶⁷ have been determined by double-resonance methods related to spin-tickling (Appendix A). However, for quadrupolar nuclei such as ⁹⁵Mo ($I = \frac{5}{2}$, nat. abundance 15.7%) the very much shorter spin-lattice relaxation time, T_1 , permits rapid pulsing (ca 40 per sec. for ⁹⁵Mo) and therefore direct observation is preferable. Thus the ¹⁸³W and ⁹⁵Mo chemical shifts of these complexes were determined by multiple-resonance (³¹P-¹⁸³W, ¹H)) and direct observation methods respectively. Figs. 3.6 and 3.7 show examples of such experiments.

The ⁹⁵Mo and ¹⁸³W n.m.r. data for complexes of structural types IIa - IIe are given in Table 3.4.

TABLE 3.4 ⁹⁵Mo and ¹⁸³W n.m.r. data for complexes of II

Complex ^a	$\delta(^{95}\text{Mo})$ ^b /ppm	$^1J(^{95}\text{Mo}-^{31}\text{P})$ ^c /Hz	$\delta(^{183}\text{W})$ ^d /ppm	$^1J(^{183}\text{W}-^{31}\text{P})$ ^e /Hz
M(CO) ₅ [IIa]	+149	127	+239	249
M(CO) ₅ [IIb]	f	f	f	237
M(CO) ₄ [IIc]	+301	105	+502	205
M(CO) ₄ [IId]	+144	132 ^g , 132 ^h	+286	230 ^g , 230 ^h
M(CO) ₃ [IIe]	+352	110 ^g , 110 ^h	+558	178 ^g , 216 ^h

Notes a M = Mo, W

b Relative to $\delta(^{95}\text{Mo})$ for Mo(CO)₆ in THF = 0.0 ppm

c ± 5 Hz

d Relative to $\delta(^{183}\text{W})$ for W(CO)₆ in THF = 0.0 ppm
($\Sigma(^{183}\text{W})$ for W(CO)₆ taken as 4151878 Hz)

e ± 1 Hz

f Not determined

g $^1J(\text{M}-^{31}\text{P}_\text{A})$

h $^1J(\text{M}-^{31}\text{P}_\text{B})$

Figs 3.6 and 3.7 Direct ^{95}Mo observation and $^{31}\text{P}\{-^{183}\text{W}, ^1\text{H}\}$ experiments performed on $\text{Mo}(\text{CO})_3[\text{IIe}]$ and $\text{W}(\text{CO})_4[\text{IIc}]$ respectively.

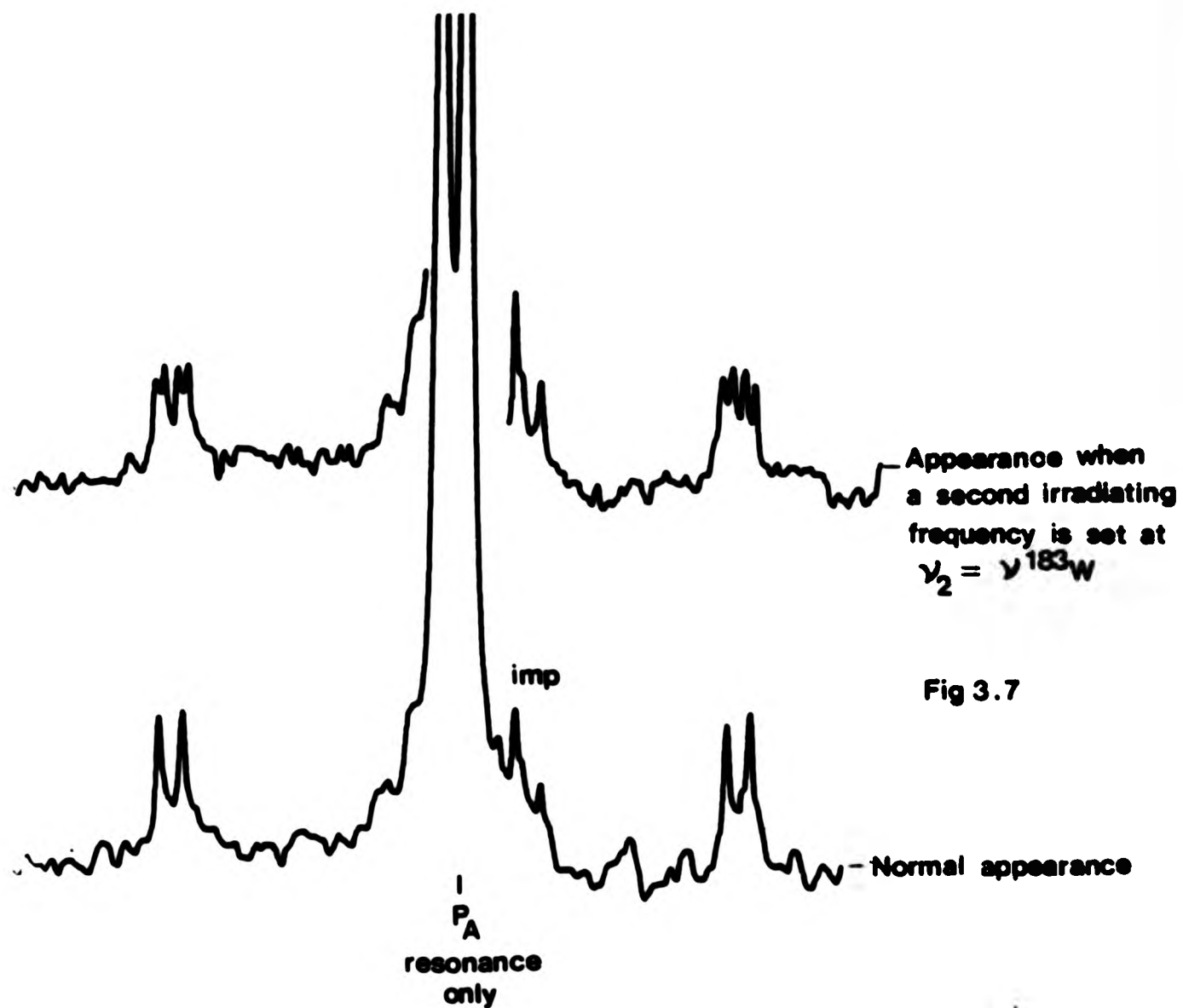


Fig 3.7

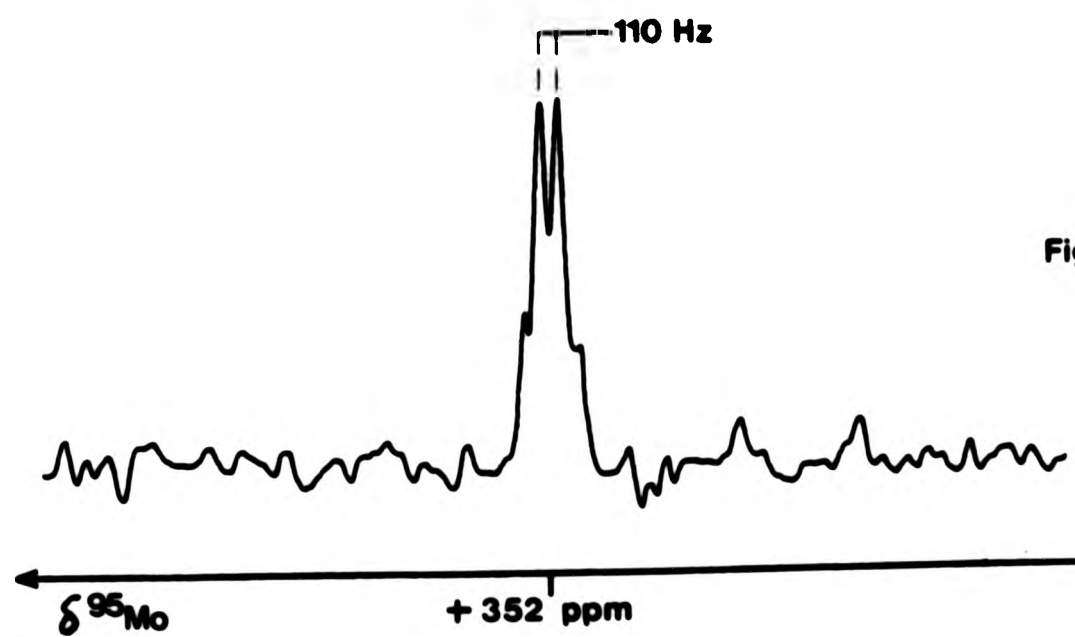


Fig 3.6

Inspection of this table reveals an approximately 1.7:1 ratio in values of metal chemical shifts for analogous tungsten and molybdenum complexes. This too is in conformity with previous results, and is of diagnostic value in that predictions of unknown metal chemical shifts are possible where analogous shifts are known for other metals.

According to Ramsey⁶⁸ the magnetic shielding of a nucleus in a molecule can be expressed as the sum of two components, σ^d (the diamagnetic term) and σ^p (the paramagnetic term) (Eq. 3.5)

$$\sigma = \sigma^d + \sigma^p \quad (3.5)$$

The first of these primarily arises from circulations of inner electrons of the atom and is therefore relatively little affected by changes in chemical bonds, whereas the second is due to restrictions of this circulation brought about by chemical bonding and it is believed that the trends in chemical shifts can largely be accounted for by variations in this term alone⁶⁹. According to Jameson and Gutowsky⁷⁰, the paramagnetic term may be expressed in the form of equation 3.6

$$\sigma^p = \frac{k}{\Delta E} (\langle r^{-3} \rangle_{np} P_1 + \langle r^{-3} \rangle_{nd} D_1) \quad (3.6)$$

where ΔE is the average excitation energy between ground and excited states

$\langle r^{-3} \rangle_{np}$ the radial expansion term is the average inverse cube of the distance (r) of the valence (n) p-electrons from the nucleus. (Similarly for nd electrons.)

P_1 and D_1 are a measure of the electron imbalance in the valence p and d-orbitals respectively.

Most treatments to date have concentrated on the p-orbital terms and this approach will be adopted here, although qualitative inclusion of d-orbitals would lead to similar results. Equation 3.6 may thus be simplified to

$$\sigma^p = \frac{k}{\Delta E} \langle r^{-3} \rangle_{np} P_1 \quad (3.7)$$

from which we may see that the ratio of tungsten and molybdenum chemical shifts is

$$\frac{\delta(^{183}\text{W})}{\delta(^{95}\text{Mo})} = \frac{\Delta E_{\text{Mo}}}{\Delta E_{\text{W}}} \left[\frac{\langle r^{-3} \rangle_{6p(\text{W})} P_1(\text{W})}{\langle r^{-3} \rangle_{5p(\text{Mo})} P_1(\text{Mo})} \right] \quad (3.8)$$

Electronic spectra for complexes of molybdenum and tungsten indicate the ratio of $\Delta E_{\text{Mo}}/\Delta E_{\text{W}}$ is close to unity⁷¹ and it is reasonable to expect values of P_1 to be constant for analogous complexes. Thus the main contribution to the 1.7:1 ratio appears to arise from the radial expansion terms of the appropriate p-orbitals although a greater significance of the d-orbital contribution in the case of tungsten could also bring about this effect.

Table 3.4 also contains values of $^1J(\text{M}-^{31}\text{P})$ for this series of complexes and shows an approximately 1.8:1 ratio for analogous tungsten and molybdenum species. Since the magnitudes of observed coupling constants depend on the magnetogyric ratios of the nuclei involved, the ratios of the reduced coupling constants $^1K(\text{M}-^{31}\text{P})$ ⁷² (Eq. 3.9) are more significant.

$$^1K(\text{A-B}) = \frac{4\pi^2 \cdot ^1J(\text{A-B})}{\gamma_{\text{A}} \cdot \gamma_{\text{B}} \cdot h} \quad (3.9)$$

Thus

$$\frac{^1K(^{183}\text{W}-^{31}\text{P})}{^1K(^{95}\text{Mo}-^{31}\text{P})} = \frac{^1J(^{183}\text{W}-^{31}\text{P}) \cdot \gamma_{\text{Mo}}}{^1J(^{95}\text{Mo}-^{31}\text{P}) \cdot \gamma_{\text{W}}} \quad (3.10)$$

The average ratio of reduced coupling constants for this series of complexes (ca. 2.9) can be interpreted in terms of the greater s-electron density at the tungsten nucleus when compared to analogous molybdenum species. Calculations of the relative s-electron densities at tungsten and molybdenum nuclei vary between 2.5⁷³ and 3.4⁷⁴ and therefore the

experimental value of 2.9 for these complexes shows a fair agreement.

(11) 1,1-bis(diphenylphosphino)-2-phenylphosphinoethane VI

The related triphosphine ligand, 1,1-bis(diphenylphosphino)-2-phenylphosphinoethane, VI, because of its similarity to II could be expected to show modes of coordination analogous to those of IIa - IIe. However, the inequivalence of the geminally related phosphorus atoms induced by the chiral secondary phosphine atom leads to further isomeric possibilities (e.g. Fig 3.8), and this is demonstrated by the reaction between

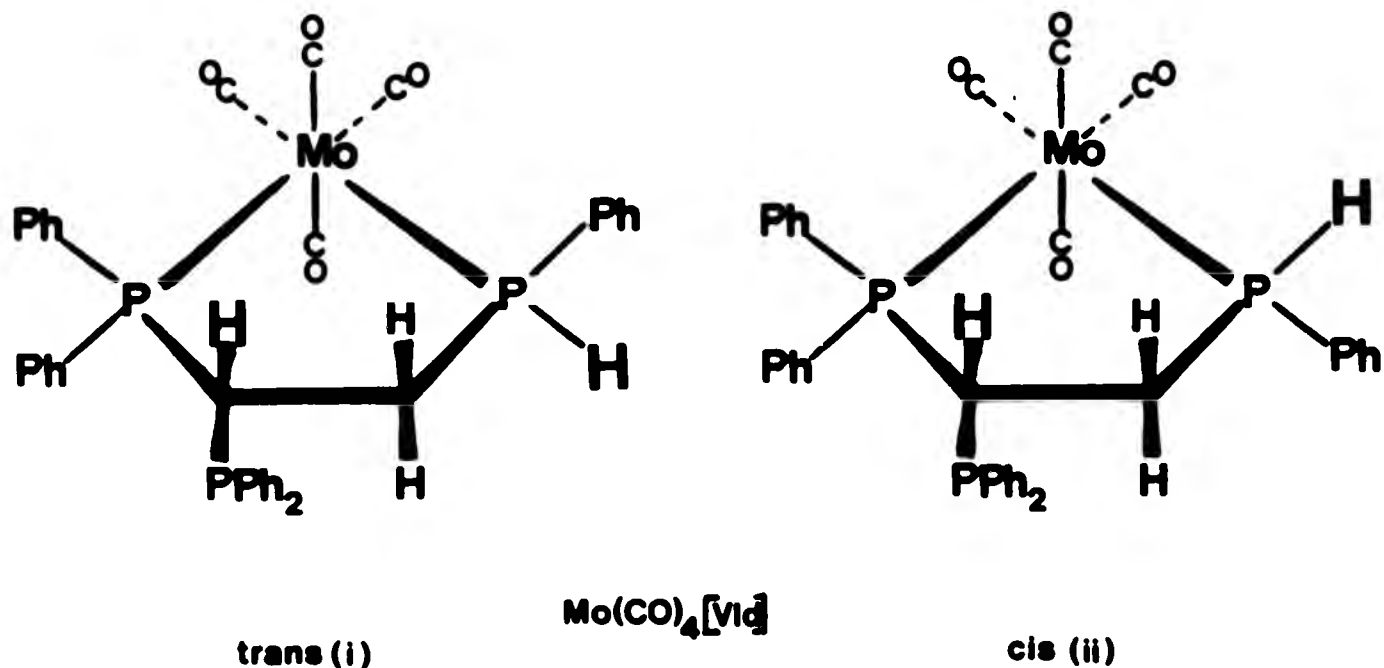


Fig 3.8

$\text{Mo(CO)}_4(\text{pip})_2$ and VI which was found to result in the formation of both the cis and trans isomers of VId and the corresponding four-membered ring structure VIc in approximately equal proportions. The presence of VIc, even after prolonged reflux demonstrates again the apparently equal preferences of molybdenum to form four and five-membered chelate

experimental value of 2.9 for these complexes shows a fair agreement.

(ii) 1,1-bis(diphenylphosphino)-2-phenylphosphinoethane VI

The related triphosphine ligand, 1,1-bis(diphenylphosphino)-2-phenylphosphinoethane, VI, because of its similarity to II could be expected to show modes of coordination analogous to those of IIa - IIe. However, the inequivalence of the geminally related phosphorus atoms induced by the chiral secondary phosphine atom leads to further isomeric possibilities (e.g. Fig 3.8), and this is demonstrated by the reaction between

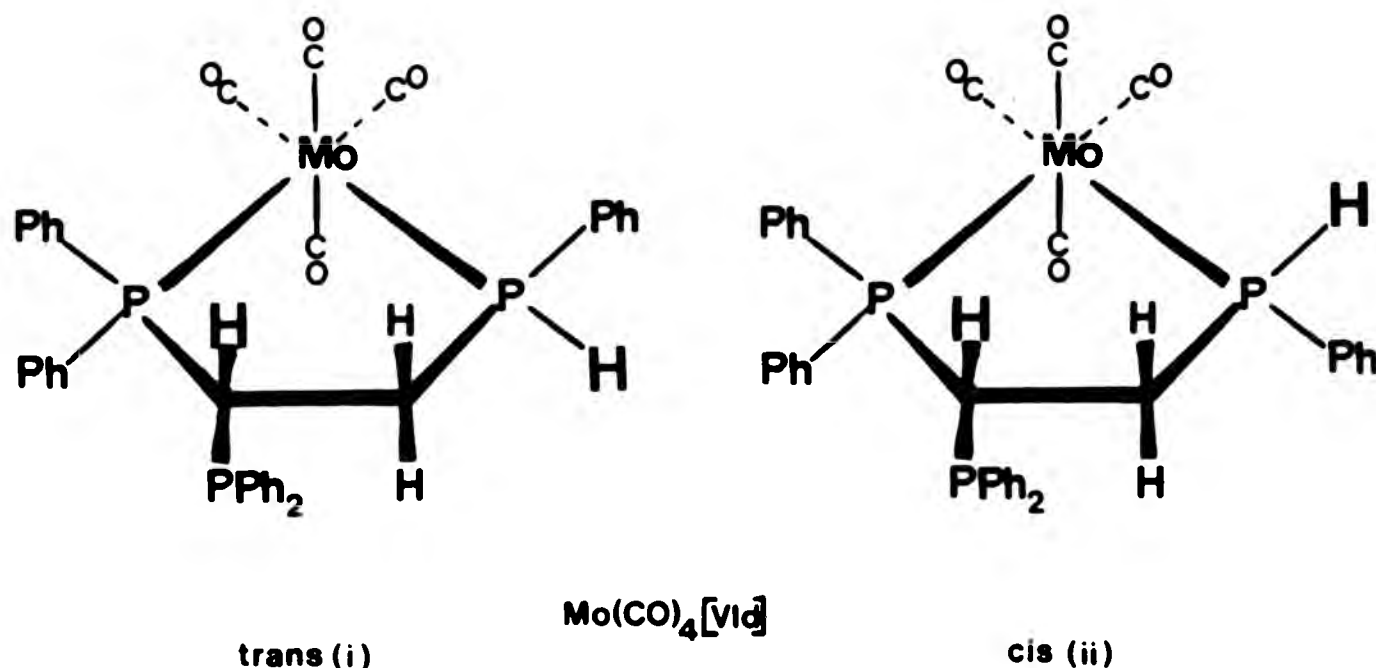


Fig 3.8

$\text{Mo(CO)}_4(\text{pip})_2$ and VI which was found to result in the formation of both the cis and trans isomers of VId and the corresponding four-membered ring structure VIc in approximately equal proportions. The presence of VIc, even after prolonged reflux demonstrates again the apparently equal preferences of molybdenum to form four and five-membered chelate

rings. The fully coordinated complex $\text{Mo(CO)}_3[\text{VIe}]$ (Fig. 3.9) may be prepared by a method analogous to that used for IIe and was isolated as yellow air-stable crystals.

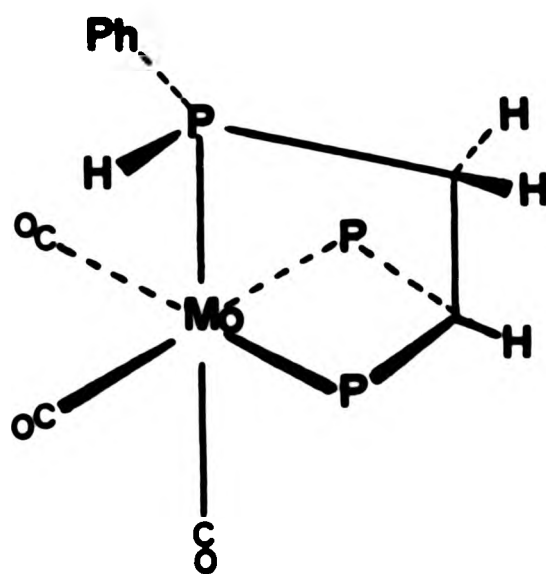


Fig 3.9



The ^{31}P n.m.r. spectra of these molybdenum complexes are relatively straightforward (e.g. Fig. 3.10) and can be analysed as ABX or AMX spin-systems. Such an analysis led to the values of n.m.r. parameters shown in Table 3.5. The geminally related phosphine atoms in these species generally have coordination chemical shift values, Δ , showing good agreement with those for similar complexes IIa - IIe. However, the values of Δ for the proton-bearing phosphorus atoms are lower, presumably owing to the larger effects of bond-angle distortions upon coordination.

Although these various modes of coordination may be distinguished by ^{31}P n.m.r., consideration of the parameters for the two isomeric complexes VI di) and VI dii) does not establish which set of parameters is associated with a particular isomer. Since values of

Fig. 3.10 ^{31}P n.m.r. spectrum of $\text{Mo(CO)}_3[\text{Vie}]$
recorded at 36.2 MHz

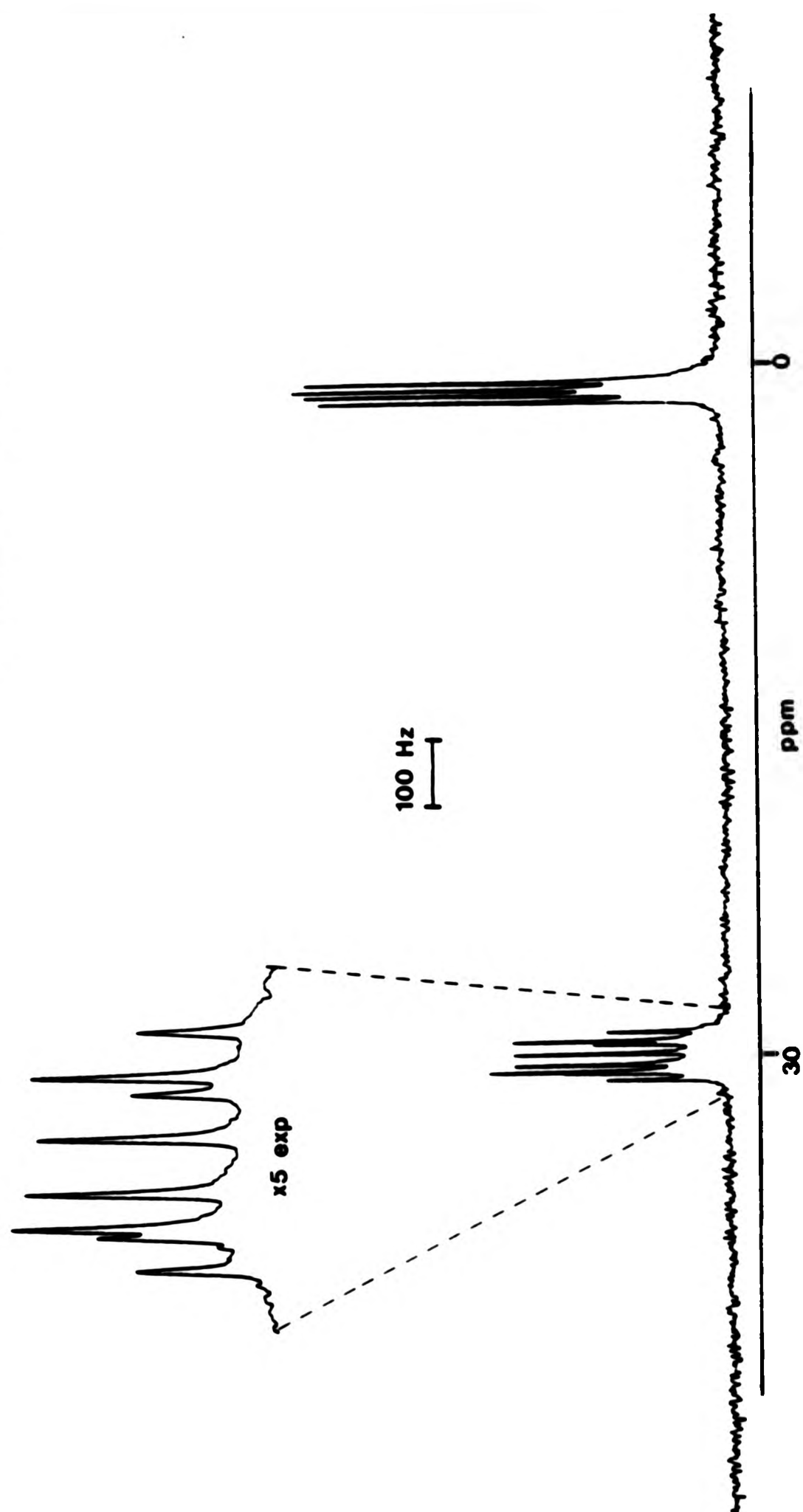


TABLE 3.5 ^{31}P n.m.r. data for molybdenum carbonyl complexes of VI

Complex	$\delta(^{31}\text{P}_\text{A})$ /ppm ^a	ΔP_A /ppm ^b	$\delta(^{31}\text{P}_\text{B})$ /ppm ^a	ΔP_B /ppm ^b	$\delta(^{31}\text{P}_\text{C})$ /ppm ^a	ΔP_C /ppm ^b	$\text{J}(\text{P}_\text{A}\text{P}_\text{B})$ /Hz	$\text{J}(\text{P}_\text{A}\text{P}_\text{C})$ /Hz	$\text{J}(\text{P}_\text{B}\text{P}_\text{C})$ /Hz
$\text{Mo}(\text{CO})_4[\text{VID}]^{\text{c,e}}$	+69.8	+73.7	+10.0	+64.8	-20.8	-	7.3	96.4	19.5
$\text{Mo}(\text{CO})_4[\text{VID}]^{\text{c,e}}$	+67.2	+73.0	+12.7	+67.5	-16.3	-	8.5	39.1	0
$\text{Mo}(\text{CO})_4[\text{VIC}]^{\text{c}}$	+26.0	+29.9	+26.0	+31.8	-53.6	-	d	3.7	3.7
$\text{Mo}(\text{CO})_3[\text{VIE}]^{\text{c}}$	+30.8	+34.7	+29.6	+35.4	+1.3	+56.1	13.7	11.0	19.5
VI Free ligand	-3.9	-	-5.8	-	-54.8	-	112.3	15.9	17.1

Notes a Relative to external 85% $\text{H}_3\text{PO}_4 = 0.0$ ppm

b Δ = coordination chemical shift

c See Fig. 3.11 for labelling system

d Not obtainable from ^{31}P spectrum

e Absolute configurations not known

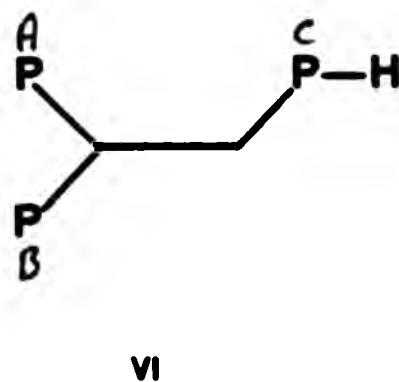
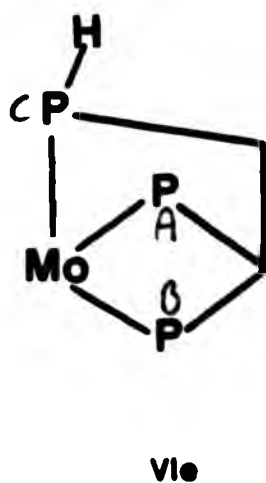
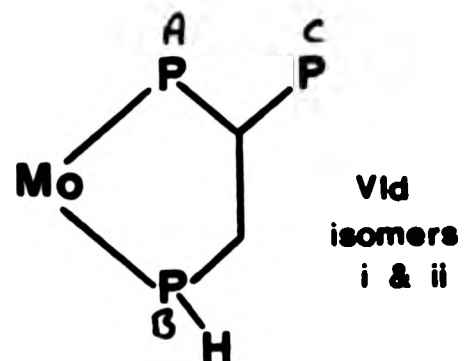
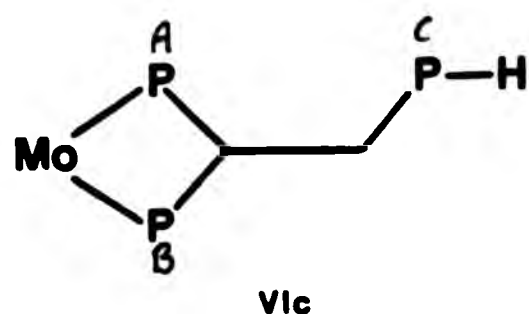


Fig 3.11

$J(^{31}\text{P}_\text{A} ^{31}\text{P}_\text{B})$ are similar for both isomers of Vld it is reasonable to deduce that the relationship between P_A and P_B is constant and therefore the difference in values of $^2J(\text{P}_\text{A}-\text{P}_\text{C})$ and to a lesser extent values of $^3J(\text{P}_\text{B}\text{P}_\text{C})$ between isomers result from the two possible orientations of P_C . It is surprising that the relatively small configurational differences between these two isomers (Fig. 3.7), is reflected by such a large difference in the values of $^2J(^{31}\text{P}_\text{A} ^{31}\text{P}_\text{C})$ (39.1 Hz and 96.4 Hz) in particular, since it would appear that the stereochemical relationship of P_A and P_C with respect to each other is virtually identical for both isomers. However, this sort of pattern is reproduced in similar isomeric complexes of the larger ligands which exhibit analogous configurational variations and is discussed further in later chapters.

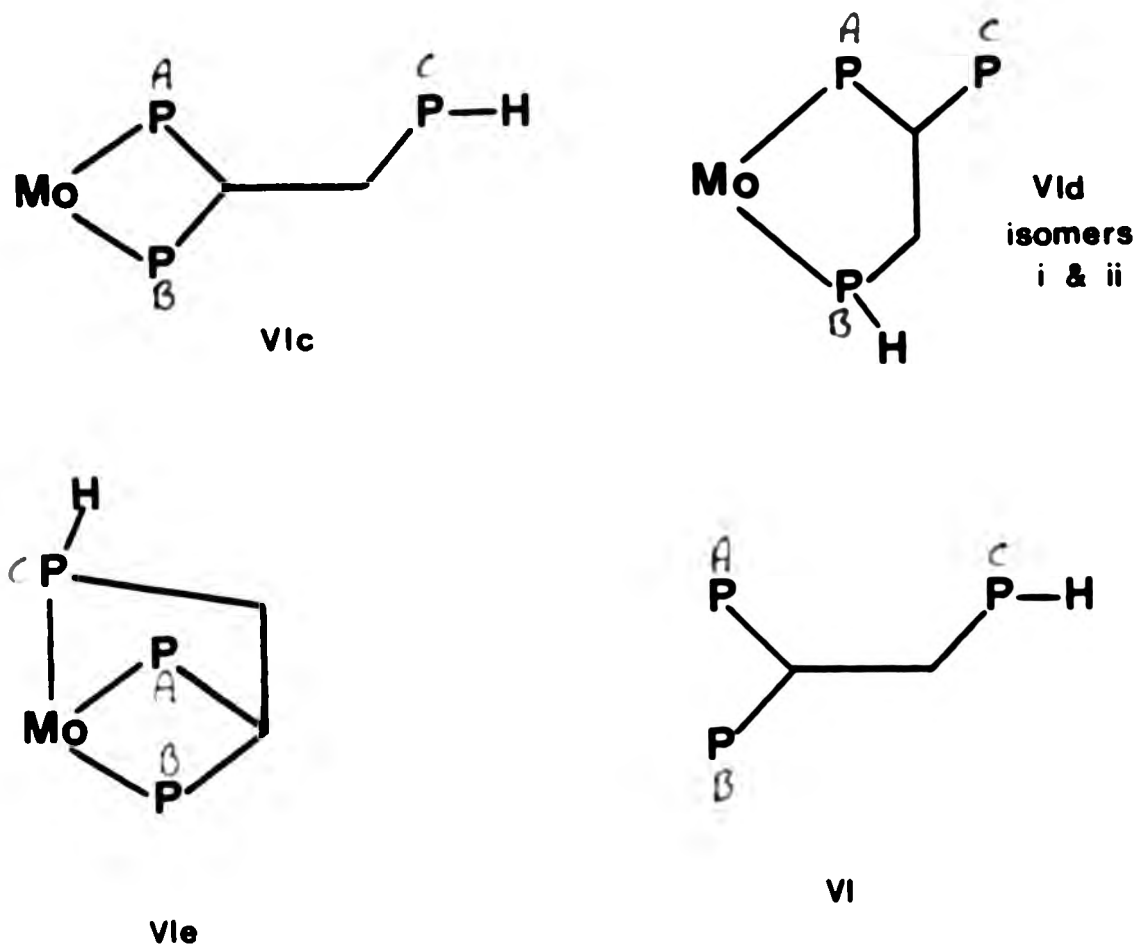


Fig 3.11

$J(^{31}\text{P}_\text{A} ^{31}\text{P}_\text{B})$ are similar for both isomers of VId it is reasonable to deduce that the relationship between P_A and P_B is constant and therefore the difference in values of $^2J(\text{P}_\text{A}-\text{P}_\text{C})$ and to a lesser extent values of $^3J(\text{P}_\text{B}-\text{P}_\text{C})$ between isomers result from the two possible orientations of P_C . It is surprising that the relatively small configurational differences between these two isomers (Fig. 3.7), is reflected by such a large difference in the values of $^2J(^{31}\text{P}_\text{A} ^{31}\text{P}_\text{C})$ (39.1 Hz and 96.4 Hz) in particular, since it would appear that the stereochemical relationship of P_A and P_C with respect to each other is virtually identical for both isomers. However, this sort of pattern is reproduced in similar isomeric complexes of the larger ligands which exhibit analogous configurational variations and is discussed further in later chapters.

(iii) 1,1,2-tris(diphenylphosphino)ethene X

The presence of the carbon-carbon double-bond in 1,1,2-tris(diphenylphosphino)ethene (X), alters its coordinative behaviour from that of the similar triphosphine ligands II and VI, particularly with regard to chelation. Reaction, therefore, of $\text{Mo(CO)}_4(\text{pip})_2$ with X was found to result in formation of an approximately 1:1 mixture of complexes exhibiting chelating modes Xc and Xd which are analogous to modes IIc and IId. (Fig. 3.12)

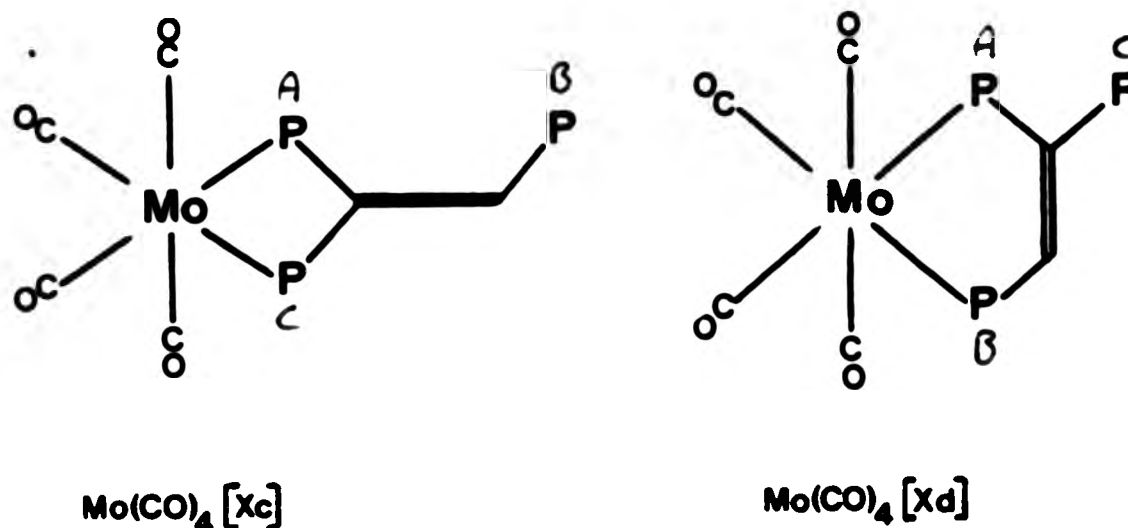


Fig 3.12

The presence of two inequivalent geminally related phosphorus atoms in X, however, results in this ligand having the potential, in principle, to form two isomers containing five-membered chelate rings as for the ligand VI. However, chelation involving coordination of the phosphorus atoms in the mutually trans positions was neither expected nor found to occur (it is unlikely that this type of chelation is exhibited by this ligand since 1,2-trans(diphenylphosphino)ethene is known to prefer monodentate coordination to chelation⁷⁵). Attempts to prepare the fully coordinated complex (analogous to complexes exhibiting mode

(iii) 1,1,2-tris(diphenylphosphino)ethene X

The presence of the carbon-carbon double-bond in 1,1,2-tris(diphenylphosphino)ethene (X), alters its coordinative behaviour from that of the similar triphosphine ligands II and VI, particularly with regard to chelation. Reaction, therefore, of $\text{Mo(CO)}_4(\text{pip})_2$ with X was found to result in formation of an approximately 1:1 mixture of complexes exhibiting chelating modes Xc and Xd which are analogous to modes IIc and IId. (Fig. 3.12)

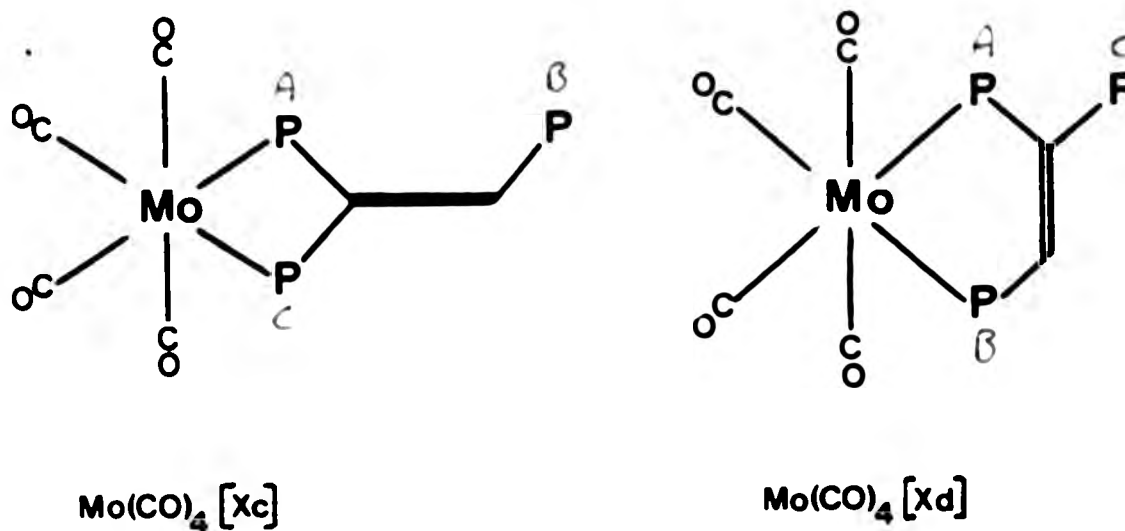


Fig 3.12

The presence of two inequivalent geminally related phosphorus atoms in X, however, results in this ligand having the potential, in principle, to form two isomers containing five-membered chelate rings as for the ligand VI. However, chelation involving coordination of the phosphorus atoms in the mutually trans positions was neither expected nor found to occur (it is unlikely that this type of chelation is exhibited by this ligand since 1,2-trans(diphenylphosphino)ethene is known to prefer monodentate coordination to chelation⁷⁵). Attempts to prepare the fully coordinated complex (analogous to complexes exhibiting mode

Ile) were not successful. However, this is to be expected, since the restriction of the double-bond prevents the phosphorus atoms occupying three coordination sites simultaneously.

Analysis of the ^{31}P n.m.r. spectra of these species was relatively straightforward and led to the values of n.m.r. parameters shown in Table 3.6. From the study of previous species prepared it is clear that any chemical shift difference between two inequivalent phosphorus nuclei in a free ligand is preserved upon coordination of both. For example, in the complexes exhibiting the coordination mode IId the chemical shift difference in the free ligand (15.9 ppm) is matched closely when coordinated (16.8 ppm for the tungsten complex), and a knowledge of this feature is useful for the following analysis. The ^{31}P n.m.r. spectrum of $\text{Mo}(\text{CO})_4[\text{Xc}]$ shows resonances due to the two coordinated phosphorus nuclei at +30.6 and +34.0 ppm, indicative of a four-membered chelate-ring structure. This 3.4 ppm shift difference could therefore be expected also to occur between the geminally related phosphorus nuclei in the free ligand X. Similarly the ^{31}P spectrum of Xd shows coordinated phosphorus nuclei at +74.1 and 53.7 ppm, characteristic of a five-membered chelate-ring structure, and this difference of 20.4 ppm should also be reflected in the free ligand. On this basis then, the ^{31}P assignment of X given in Fig. 2.13 must be the correct one since it indicates a difference of 4.5 ppm for the geminally related phosphorus nuclei and 20.3 ppm for the vicinally related phosphorus nuclei.

TABLE 3.6 ^{31}P n.m.r. data for molybdenum carbonyl complexes of X

Complex	$\delta(^{31}\text{P}_\text{A})^{\text{a}}$ /ppm	$\Delta_\text{C}^{\text{A}}$ /ppm	$\delta(^{31}\text{P}_\text{B})^{\text{a}}$ /ppm	$\Delta_\text{C}^{\text{B}}$ /ppm	$\delta(^{31}\text{P}_\text{C})^{\text{a}}$ /ppm	$\Delta_\text{C}^{\text{C}}$ /ppm	$J(\text{P}_\text{A}\text{P}_\text{B})$ /Hz	$J(\text{P}_\text{A}\text{P}_\text{C})$ /Hz	$J(\text{P}_\text{B}\text{P}_\text{C})$ /Hz
$\text{Mo}(\text{CO})_4[\text{Xc}]^{\text{b}}$	+30.6	+36.0	-30.8	-	+34.0	+34.9	9.5	83.6	10.7
$\text{Mo}(\text{CO})_4[\text{Xd}]^{\text{b}}$	+71.1	+79.5	+53.7	+79.4	-11.3	-	9.5	25.3	4.2
X	-5.4	-	-25.7	-	-0.9	-	142.8	1.5	9.8

Notes a Relative to external 85% $\text{H}_3\text{PO}_4 = 0.0$ ppm

b See Fig. 3.12 for labelling system

3. SQUARE-PLANAR COMPLEXES

(A) Introduction

The two principal oxidation states of platinum and palladium are +II and +IV, and while the +IV complexes are invariably six-coordinate octahedral, the +II state complexes are often four-coordinate square-planar⁷⁶. Pd^{II} and Pt^{II} show a preference for heavy donor atoms such as P, As, S and Se due to the formation of ligand-metal π -bonds by overlap of filled $d\pi$ (d_{xy} , d_{xz} , d_{yz}) orbitals on the metal with empty $d\pi$ orbitals on the donor atom.

The ability of palladium and platinum to form square-planar phosphine complexes including those involving chelating ligands^{77,78}, prompted investigation into similar complexes involving the new polydentate phosphorus ligands reported in Chapter 2.

(B) Results and Discussion

Treatment of $\text{PtCl}_2(\text{PhCN})_2$ with a stoichiometric amount of 1,1-bis(diphenylphosphino)ethene I at room temperature resulted in the formation of $\text{PtCl}_2[\text{Ib}]$ (Fig. 3.13). A similar reaction using the triphosphine ligand 1,1,2-tris(diphenylphosphino)ethane (II), resulted in the virtually quantitative formation of the platinum complex incorporating a

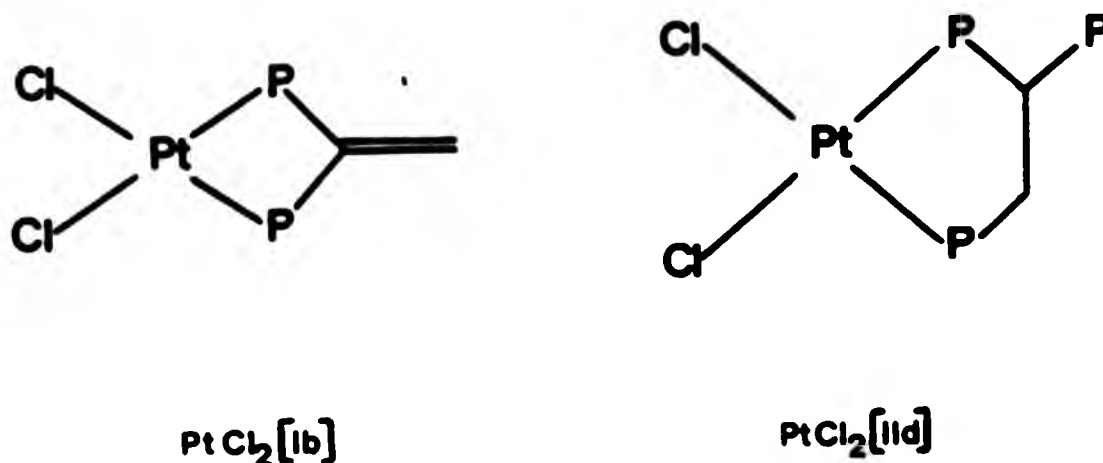


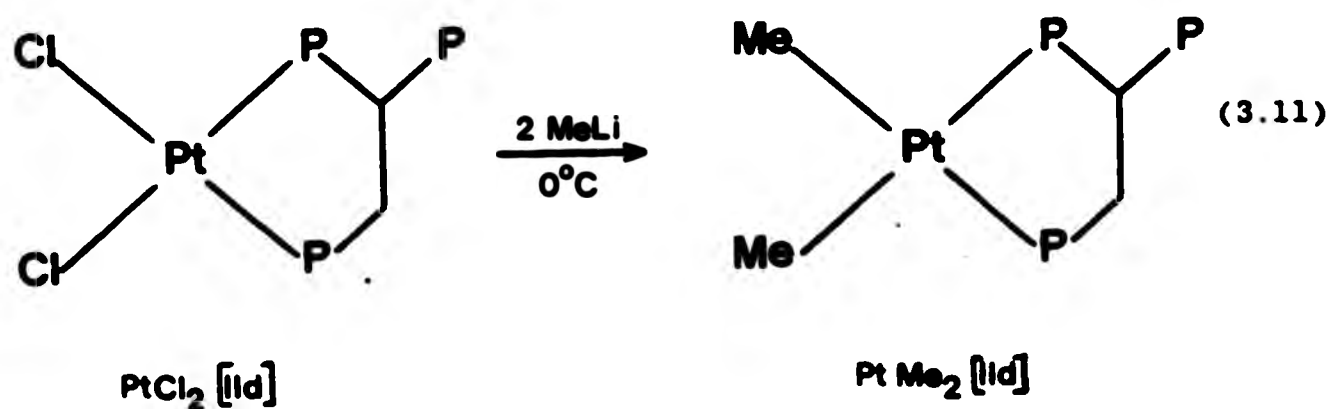
Fig 3.13

five-membered chelate-ring analogous to previously prepared octahedral complexes exhibiting coordination mode IId. (Fig. 3.13)

Under these conditions there was no evidence of formation of the isomer with a four-membered ring. Similar reactions were also undertaken for analogous palladium species.

Addition of diphenylphosphine across the double-bond of coordinated 1,1-bis(diphenylphosphino)ethene, I, has been described previously for group VI metal carbonyl complexes, and similar reactions were undertaken for $\text{PtCl}_2[\text{Ib}]$. Such reactions, however, resulted in formation of only the complex with a five-membered ring structure $\text{PtCl}_2[\text{IId}]$ rather than the expected complex with a four-membered ring, even at low temperatures. An explanation for this may be that the normally unoccupied positions above and below the metal/ligand plane are available for coordination in a five-coordinate reaction intermediate, thus providing a low energy pathway for rearrangement, a route obviously not available in octahedral complexes⁷⁹.

Replacement of the chlorine groups by methyl groups in such complexes was found to be readily achieved by treatment with methyllithium at 0°C and afforded the corresponding dimethyl complexes (Equation 3.11).



Mixed Me/Cl complexes were simply prepared by the reaction of $\text{Pt}(\text{Me})\text{Cl}[\text{COD}]$ with the appropriate ligand or by treatment of the dimethyl complexes with one equivalent of HCl prepared in situ. In

the case of $\text{Pt}(\text{Me})\text{Cl}[\text{IId}]$, however, there are two isomeric species (Fig. 3.14) which are formed in approximately equal proportions by each

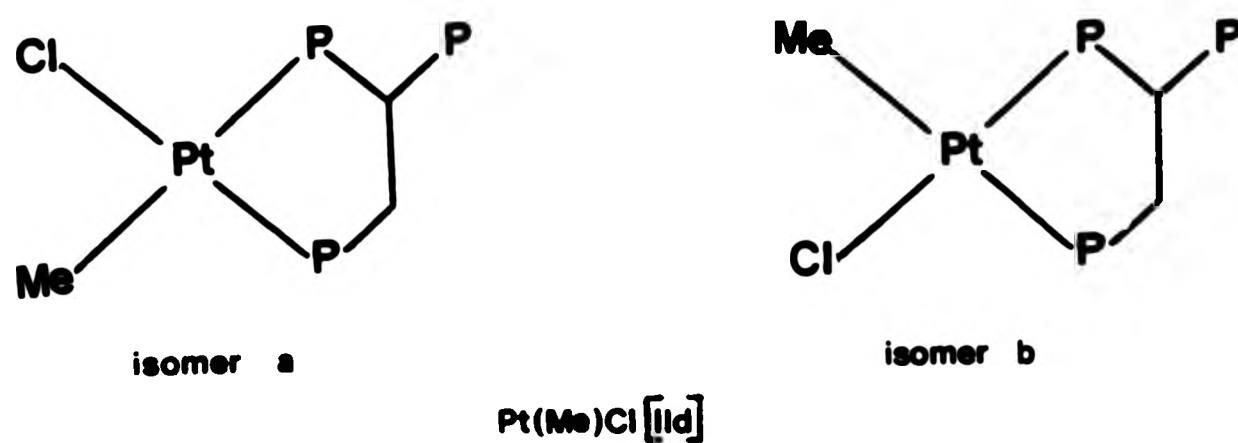
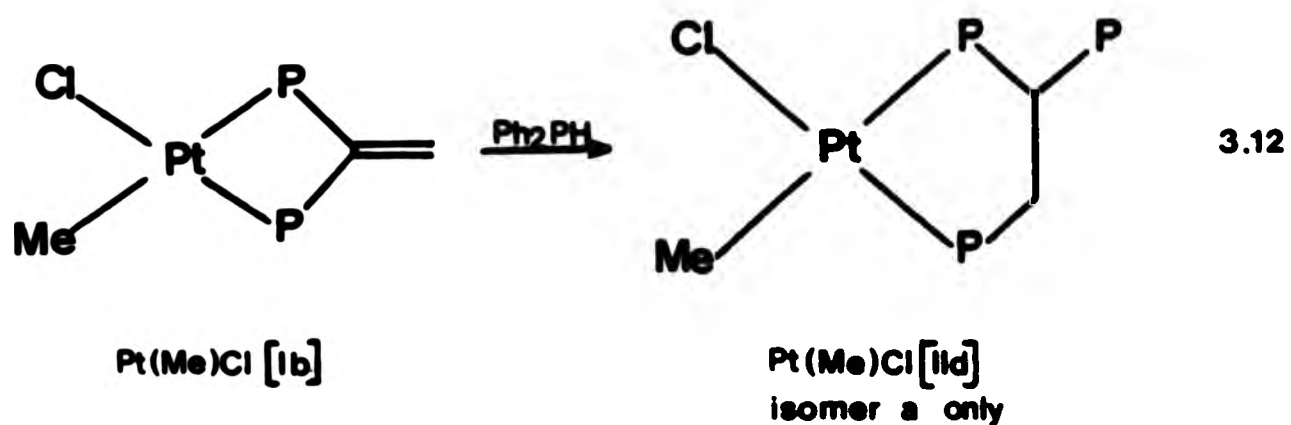
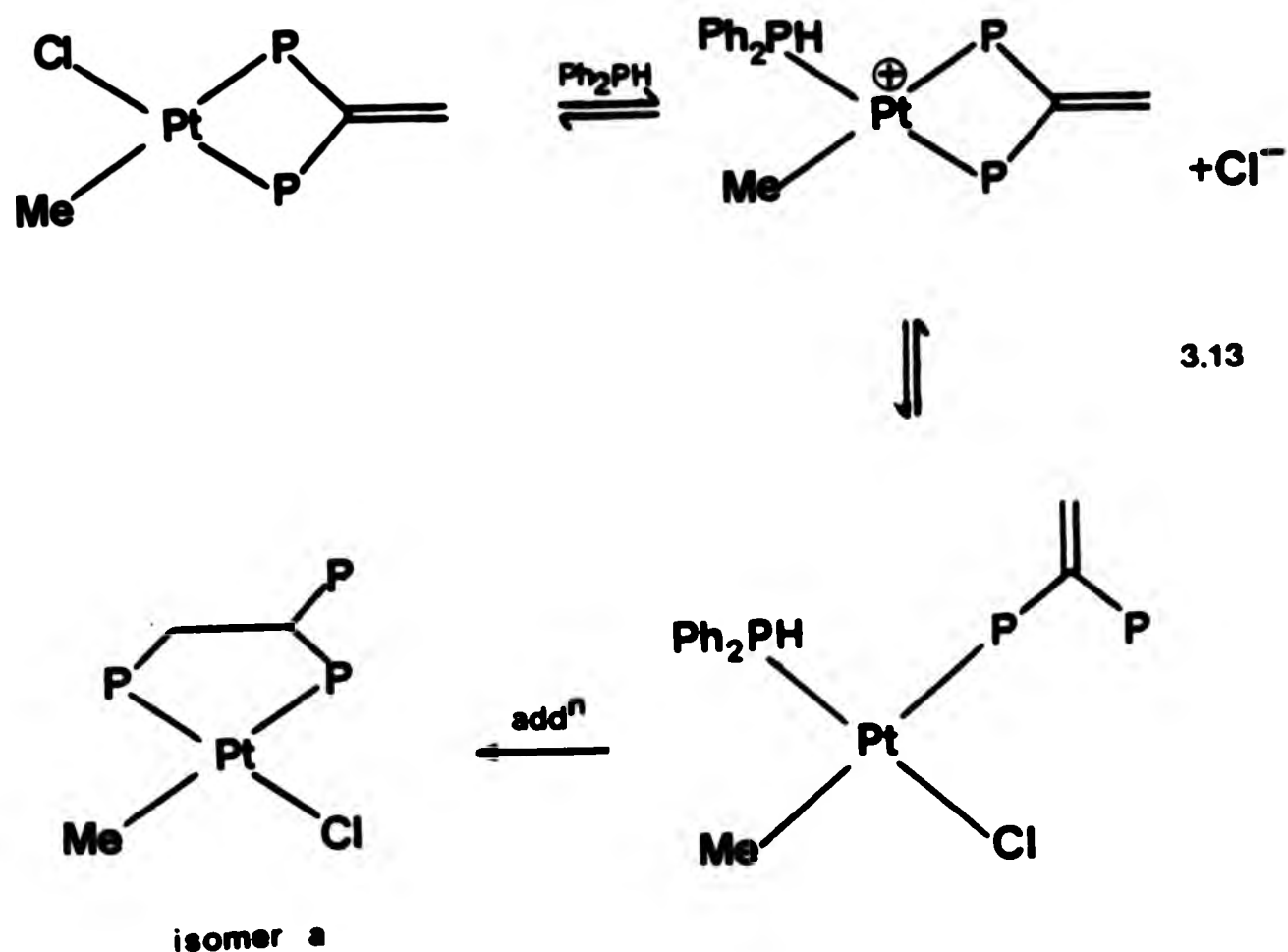


Fig 3.14

of the above methods. Addition of diphenylphosphine to the double-bond of $\text{Pt}(\text{Me})\text{Cl}[\text{Ib}]$, however, resulted in the formation of only isomer a) (Fig. 3.14) in good yield (Eq. 3.12) at room temperature.



In order to explain the apparent regiospecificity of this reaction a mechanism can be proposed invoking the different trans labilizing powers of different ligands as follows. (Eq 3.13)



Direct replacement of the chlorine group by diphenylphosphine is likely to labilise one of the chelated phosphorus atoms. This step is influenced by the greater trans-labilizing power of phosphorus than of a methyl group, and therefore the phosphorus atom trans to the diphenylphosphine ligand is labilized preferentially⁸⁰. Subsequent intramolecular addition then results in formation of isomer a) as the sole product. Other mechanisms involving five-coordinate intermediates may be proposed but all would lead to formation of isomer b) and are therefore inappropriate for this reaction.

The ³¹P n.m.r. spectra for the square-planar complexes of ligands I and II are generally straightforward and were analysed to give the values of n.m.r. parameters shown in Tables 3.7 and 3.8.

TABLE 3.7 N.m.r. data for some square-planar complexes of I

Complex	$\delta(^{31}\text{P})^a$ /ppm	$^1J(^{195}\text{Pt}-^{31}\text{P})$ /Hz
$\text{PtCl}_2[\text{Ib}]$	-32.3	3245
$\text{PtMe}_2[\text{Ib}]$	-19.3	1504
$\text{Pt}(\text{Me})\text{Cl}[\text{Ib}]^d$	-20.8 ^b , -14.6 ^c	3932 ^b , 1296 ^c
$\text{PdCl}_2[\text{Ib}]$	-21.6	-

- Notes
- a Relative to external 85% $\text{H}_3\text{PO}_4 = 0.0$ ppm
 - b Phosphorus trans to Cl
 - c Phosphorus trans to Me
 - d $^2J(^{31}\text{P}-^{31}\text{P}) = -34.2$ Hz - sign determined by the $^{195}\text{Pt}-\{^{31}\text{P}, ^1\text{H}\}$ experiment shown in Fig. 3.15.

As expected, complexes incorporating four-membered chelate rings have phosphorus chemical shifts in accordance with the ring-strain considerations proposed by Garou^{40b}.

In general, magnitudes of $^1J(^{195}\text{Pt}-^{31}\text{P})$ are critically dependent on the nature, or more specifically the trans influence of the species trans to phosphorus as described in Chapter 1⁴⁸. Fortunately in the present range of compounds the different trans ligands lie at the extremes of the trans-influence series⁴⁹; thus one-bond platinum-phosphorus couplings trans to chlorine are amongst the largest found whilst those trans to methyl groups are amongst the smallest. Hence assignment of the asymmetric complex $\text{Pt}(\text{Me})\text{Cl}[\text{Ib}]$ was made simply by consideration of the values of $^1J(^{195}\text{Pt}-^{31}\text{P})$. For this complex $^2J(^{31}\text{P}-^{31}\text{P})$ was measured directly from the ^{31}P spectrum (34.2 Hz) and subsequent $^{195}\text{Pt}-\{^{31}\text{P}, ^1\text{H}\}$ spin-tickling experiments (Fig. 3.15) showed its sign to be negative (relative to positive $^1J(^{195}\text{Pt}-^{31}\text{P})$).

Fig. 3.15 Results of the $^{195}\text{Pt}\{-^{31}\text{P}\}$ spin-tickling experiments performed on $\text{Pt}(\text{Me})\text{Cl}[\text{Ib}]$.

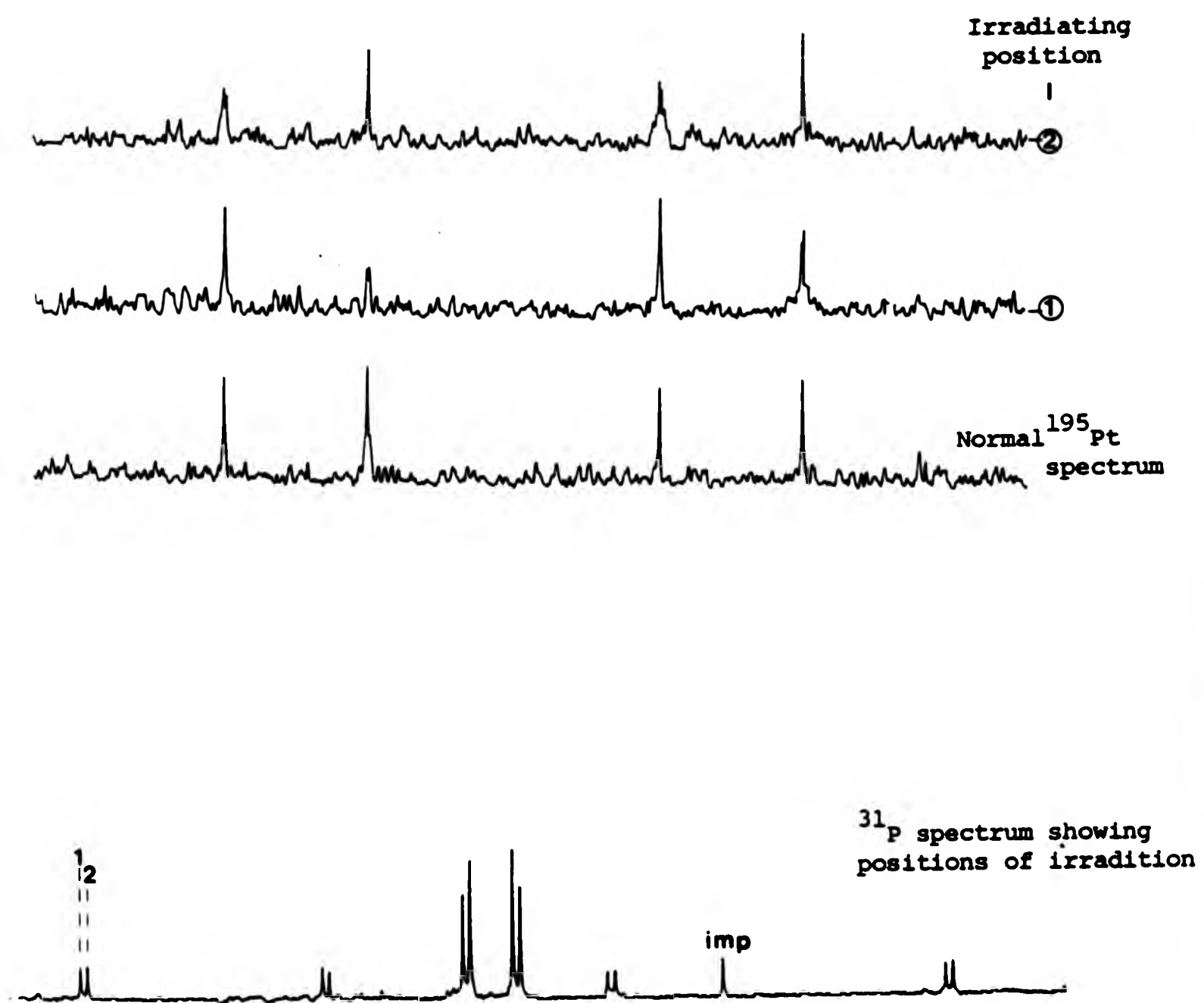


TABLE 3.8 ^{31}P n.m.r. data for the square-planar complexes of II

Complex ^b	$\delta(^{31}\text{P}_\text{A})$ /ppm ^a	$\delta(^{31}\text{P}_\text{M})$ /ppm ^a	$\delta(^{31}\text{P}_\text{X})$ /ppm ^a	$J(\text{P}_\text{A}\text{P}_\text{M})$ /Hz	$J(\text{P}_\text{A}\text{P}_\text{X})$ /Hz	$J(\text{P}_\text{M}\text{P}_\text{X})$ /Hz	$J(\text{PtP}_\text{A})$ /Hz	$J(\text{PtP}_\text{M})$ /Hz	$J(\text{PtP}_\text{X})$ /Hz
$\text{PtCl}_2[\text{IId}]$	+48.1	+33.6	-17.7	-7.7	+46.2	+13.5	+3631	+3630	+95.4
$\text{PtMe}_2[\text{IId}]$	+55.5	+37.8	-15.7	+2.0	+24.4	+13.7	+1773	+1820	+28.1
$\text{Pt}(\text{Me})\text{Cl}[\text{IId}]^c$	+53.3 ^e	+36.2 ^f	-16.6	+6.1	+29.3	+9.8	+1709 ^e	+4231 ^f	+36.6
$\text{Pt}(\text{Me})\text{Cl}[\text{IId}]^d$	+48.2 ^f	+36.2 ^e	-16.6	+6.7	+40.9	+15.2	+4230 ^f	+1754 ^e	+109
$\text{PdCl}_2[\text{IId}]$	+73.3	+58.8	-15.7	+9.8	+40.9	+18.3	-	-	-

Notes a Relative to external 85% $\text{H}_3\text{PO}_4 = 0.0$ ppm

b See Fig. 3.16 for labelling system

c Isomer a)

d Isomer b)

e Phosphorus trans to methyl

f Phosphorus trans to chlorine

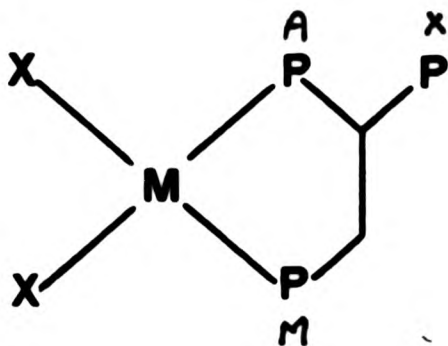


Fig 3.16

The complexes of palladium and platinum with a five-membered chelate-ring structure exhibit AMX ^{31}P spectra (e.g. Fig. 3.17) which show some interesting and important features. For the dichloro and dimethyl species, $\text{PtCl}_2(\text{IId})$ and $\text{PtMe}_2(\text{IId})$ the chemical shift difference of the two types of phosphorus (15.6 ppm in the free ligand) is well preserved upon coordination (14.5 ppm and 15.7 ppm respectively) and changing the trans ligand from chlorine to methyl has only a small effect on the chemical shifts of the coordinated phosphorus nuclei. Because of this, the two isomers of the mixed Me/Cl complex $\text{Pt}(\text{Me})\text{Cl}[\text{IId}]$ may be distinguished by their characteristic ^{31}P n.m.r. spectra since $\delta(^{31}\text{P}_\text{A})$ will always be to higher frequency than $\delta(^{31}\text{P}_\text{M})$, and measurement of $^1J(^{31}\text{P}-^{195}\text{Pt})$ reveals the nature of the group in the trans position. A series of $^{195}\text{Pt}---\{^{31}\text{P}, ^1\text{H}\}$ spin-tickling experiments were performed on the dichloro complex $\text{PtCl}_2[\text{IId}]$ in order to relate the signs of the various phosphorus-phosphorus coupling constants to the known positive $^1J(^{31}\text{P}-^{195}\text{Pt})$ (Fig. 3.18). Coupling between ^{195}Pt and $^{31}\text{P}_\text{X}$ is via the three-bond fragment $\{\text{Pt}-\text{P}_\text{A}-\text{C}-\text{P}_\text{X}\}$ and appears to depend on the nature of species trans to P_A in the same way as $^1J(^{195}\text{Pt}-^{31}\text{P}_\text{A})$. Theories regarding dependence of $^1J(^{195}\text{Pt}-^{31}\text{P})$ on the trans group outlined in Chapter 1 can be extended to longer range couplings provided factors influencing the stereochemistry of the fragment through which the

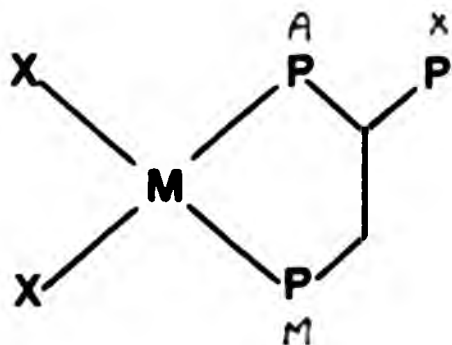


Fig 3.16

The complexes of palladium and platinum with a five-membered chelate-ring structure exhibit AMX ^{31}P spectra (e.g. Fig. 3.17) which show some interesting and important features. For the dichloro and dimethyl species, $\text{PtCl}_2(\text{IId})$ and $\text{PtMe}_2(\text{IId})$ the chemical shift difference of the two types of phosphorus (15.6 ppm in the free ligand) is well preserved upon coordination (14.5 ppm and 15.7 ppm respectively) and changing the trans ligand from chlorine to methyl has only a small effect on the chemical shifts of the coordinated phosphorus nuclei. Because of this, the two isomers of the mixed Me/Cl complex $\text{Pt}(\text{Me})\text{Cl}[\text{IId}]$ may be distinguished by their characteristic ^{31}P n.m.r. spectra since $\delta(^{31}\text{P}_\text{A})$ will always be to higher frequency than $\delta(^{31}\text{P}_\text{M})$, and measurement of $^1J(^{31}\text{P}-^{195}\text{Pt})$ reveals the nature of the group in the trans position. A series of $^{195}\text{Pt}---\{^{31}\text{P}, ^1\text{H}\}$ spin-tickling experiments were performed on the dichloro complex $\text{PtCl}_2[\text{IId}]$ in order to relate the signs of the various phosphorus-phosphorus coupling constants to the known positive $^1J(^{31}\text{P}-^{195}\text{Pt})$ (Fig. 3.18). Coupling between ^{195}Pt and $^{31}\text{P}_\text{X}$ is via the three-bond fragment $\{\text{Pt}-\text{P}_\text{A}-\text{C}-\text{P}_\text{X}\}$ and appears to depend on the nature of species trans to P_A in the same way as $^1J(^{195}\text{Pt}-^{31}\text{P}_\text{A})$. Theories regarding dependence of $^1J(^{195}\text{Pt}-^{31}\text{P})$ on the trans group outlined in Chapter 1 can be extended to longer range couplings provided factors influencing the stereochemistry of the fragment through which the

Fig. 3.17 ^{31}P n.m.r. spectrum of $\text{PdCl}_2(\text{lld})$ recorded at 24.2 MHz.

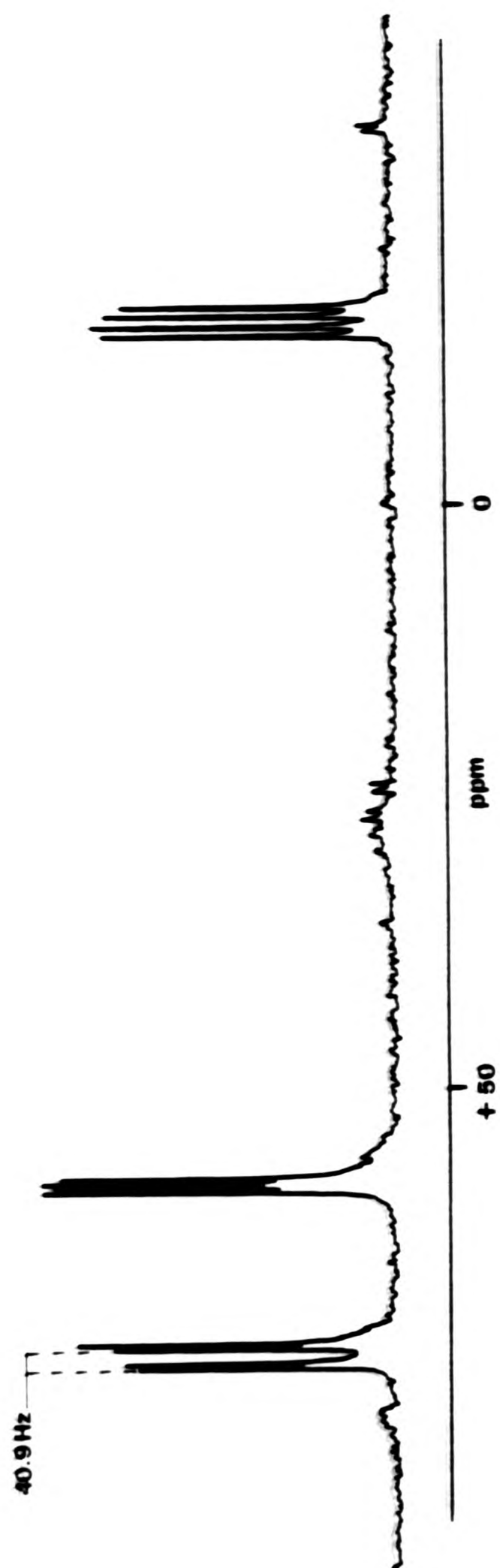
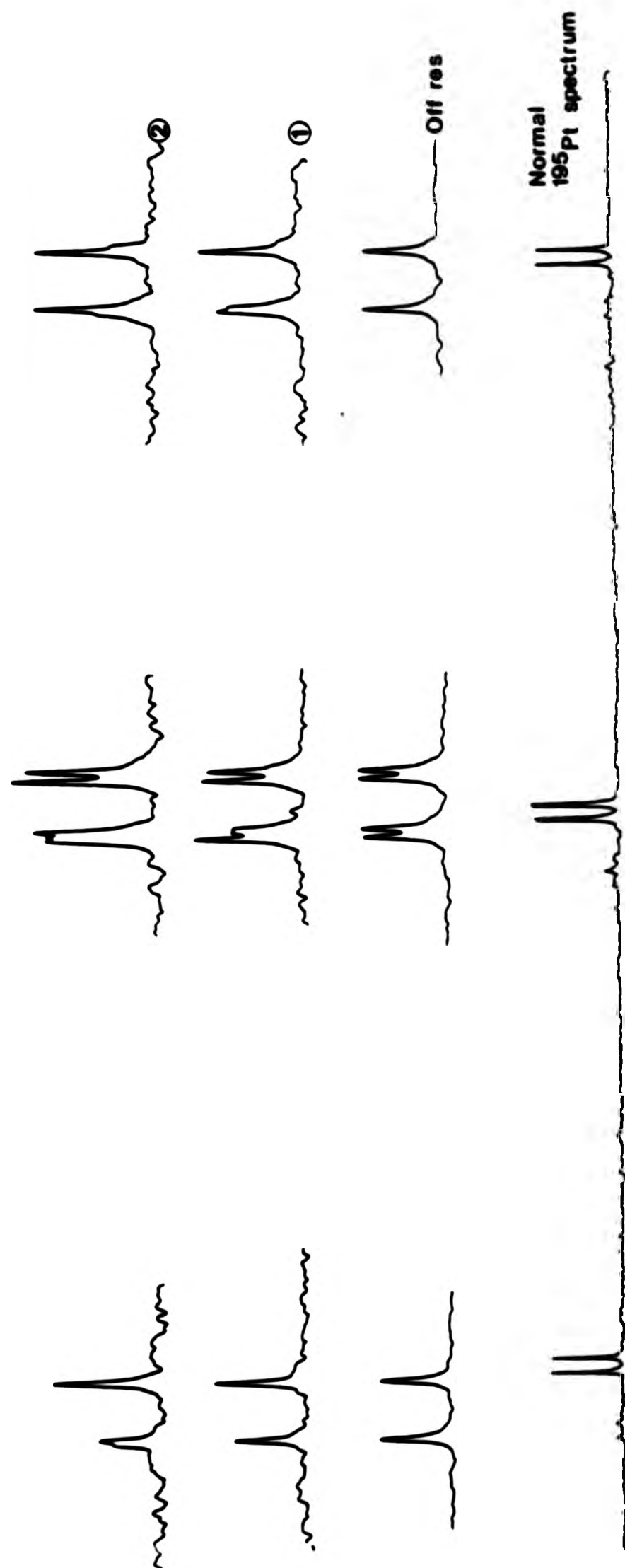


Fig. 3.18 $^{195}\text{Pt}-(^{31}\text{P}, ^1\text{H})$ spin tickling experiments performed on $\text{PtCl}_2(\text{IId})$. Spectra ① and ② show the results of irradiation at two frequencies separated by $J(\text{AM})$ in the ^{31}P spectrum.



coupling takes place are unchanged⁴⁸. The constancy of the various phosphorus-phosphorus coupling constants in this range of complexes suggests that this is indeed the case and therefore just as for $^1J(^{195}\text{Pt}-^{31}\text{P}_A)$, $^3J(^{195}\text{Pt}-^{31}\text{P}_X)$ is larger when P_A is trans to chlorine than when trans to methyl.

Reaction of $\text{Pt}(\text{PhCN})_2\text{Cl}_2$ with 1,1,2-tris(diphenylphosphino)ethene, (X), resulted in the formation of $\text{PtCl}_2[\text{Xd}]$ (Fig. 3.19) as the sole product. In contrast to molybdenum, no evidence was found for the formation of the corresponding structure with a four-membered ring $\text{PtCl}_2[\text{Xc}]$, and this demonstrates the preference of platinum for structures incorporating five-membered rings. A similar reaction was found to occur for analogous palladium species. The ^{31}P n.m.r. spectra of these complexes were analysed as AMX spin-systems as for the related molybdenum complexes, and led to the values of n.m.r. parameters in Table 3.9.

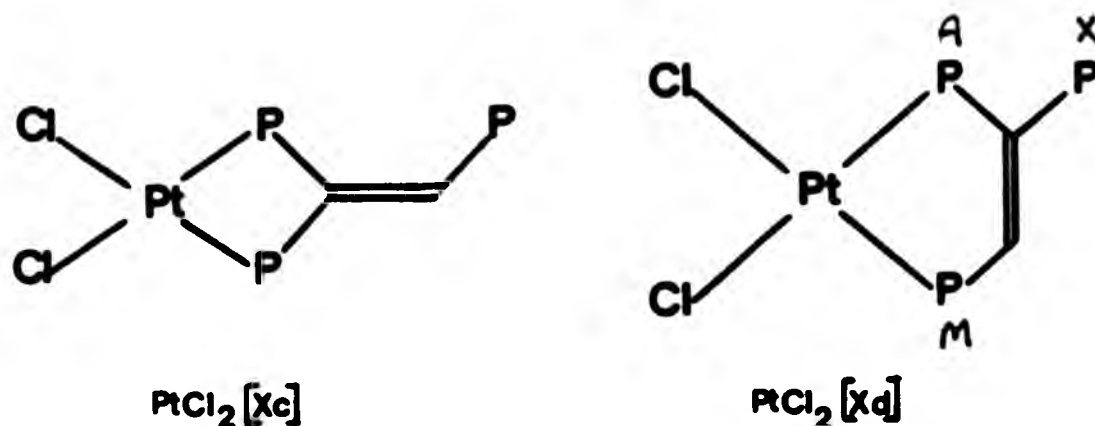


Fig 3.19

coupling takes place are unchanged⁴⁸. The constancy of the various phosphorus-phosphorus coupling constants in this range of complexes suggests that this is indeed the case and therefore just as for $^1J(^{195}\text{Pt}-^{31}\text{P}_\text{A})$, $^3J(^{195}\text{Pt}-^{31}\text{P}_\text{X})$ is larger when P_A is trans to chlorine than when trans to methyl.

Reaction of $\text{Pt}(\text{PhCN})_2\text{Cl}_2$ with 1,1,2-tris(diphenylphosphino)ethene, (X), resulted in the formation of $\text{PtCl}_2[\text{Xd}]$ (Fig. 3.19) as the sole product. In contrast to molybdenum, no evidence was found for the formation of the corresponding structure with a four-membered ring $\text{PtCl}_2[\text{Xc}]$, and this demonstrates the preference of platinum for structures incorporating five-membered rings. A similar reaction was found to occur for analogous palladium species. The ^{31}P n.m.r. spectra of these complexes were analysed as AMX spin-systems as for the related molybdenum complexes, and led to the values of n.m.r. parameters in Table 3.9.

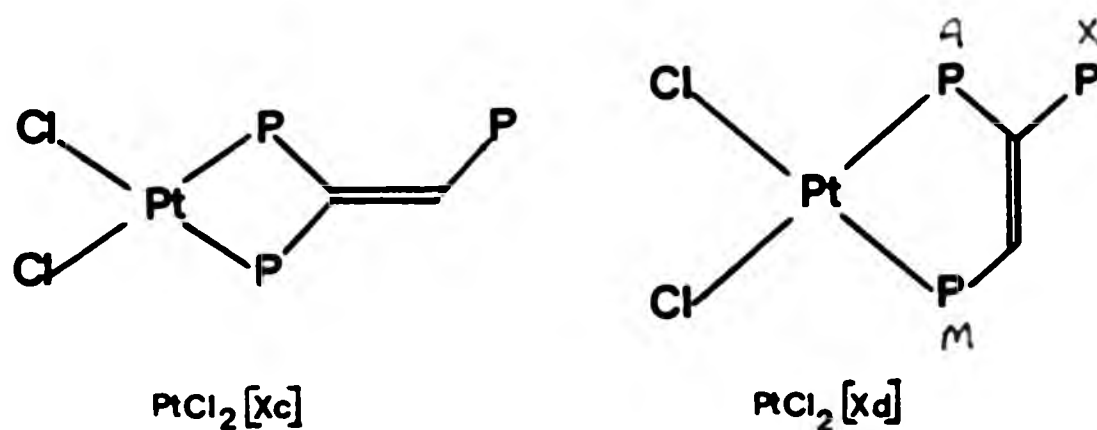


Fig 3.19

TABLE ^{31}P n.m.r. data for square-planar complexes of X

Complex	$\delta(^{31}\text{P}_\text{A})$ /ppm ^a	$\delta(^{31}\text{P}_\text{M})$ /ppm ^a	$\delta(^{31}\text{P}_\text{X})$ /ppm ^a	$J(\text{P}_\text{A}\text{P}_\text{M})$ /Hz	$J(\text{P}_\text{A}\text{P}_\text{X})$ /Hz	$J(\text{P}_\text{M}\text{P}_\text{X})$ /Hz	$J(\text{Pt-P}_\text{A})$ /Hz	$J(\text{Pt-P}_\text{M})$ /Hz	$J(\text{Pt-P}_\text{X})$ /Hz
$\text{PtCl}_2[\text{Xd}]^b$	+55.9	+40.9	-17.7	± 6.1	± 54.9	0.0	3603	3665	84.2
$\text{PdCl}_2[\text{Xd}]^b$	+80.0	+65.6	-14.9	± 18.3	± 47.7	0.0	-	-	-
X(free ligand)	-5.4	-25.7	-0.9	142.8	1.5	9.8	-	-	-

Notes a Relative to external 85% $\text{H}_3\text{PO}_4 = 0.0$ ppm

b See Fig. 3.19 for labelling system

These complexes have n.m.r. parameters comparable to those of the analogous molybdenum complexes previously prepared. As before, chelate-ring sizes may be determined by consideration of coordination chemical shifts although it is known from some of the complexes prepared earlier that these metals overwhelmingly prefer to adopt five-membered ring structures. It is interesting that in these species the largest phosphorus-phosphorus coupling constant arises from coupling between the geminally related phosphorus nuclei, in direct contrast to the free ligand X, and also that the value of $J(^{31}\text{P}_\text{A}-^{31}\text{P}_\text{M})$ is greatly reduced upon chelation. Previous workers have suggested that in similar complexes of dppe and related ligands, the relatively small magnitudes of $J(^{31}\text{P}-^{31}\text{P})$ may be attributed to contributions from 'through-the-metal' and 'through-the-backbone' components of approximately equal magnitude but of opposite sign as proposed by Grim⁴⁶, for five-membered ring structures⁸¹. Clearly for this ligand the value of $^3J(^{31}\text{P}_\text{A}-^{31}\text{P}_\text{M})$ (142.8 Hz) cannot be a sensible value for $^B J(^{31}\text{P}-^{31}\text{P})$ since analogous couplings in the complexes would then be expected to be of the order of 100 Hz. It is reasonable to suggest that the value of $^3J(^{31}\text{P}_\text{A}-^{31}\text{P}_\text{M})$ in the free ligand is in a sense an artificial one arising from the restricted orientations of the lone-pairs induced by the carbon-carbon double-bond, and that upon chelation this lone-pair interaction is removed and the 'through-the-backbone' coupling then reverts to a value similar to that in dppe and related species⁸².

¹⁹⁵Pt n.m.r.

Previous studies have shown a dependence of ¹⁹⁵Pt chemical shifts on chelate-ring size which is similar to the pattern of metal chemical shifts for related Mo and W complexes⁸³. Thus values of $\delta(^{195}\text{Pt})$

for four-membered chelate-ring structures are generally ca 700 ppm higher than those of analogous five-membered chelate ring complexes. Similar values have been found for the new complexes prepared here (Table 3.9). It is also clear that the replacement of chloride groups by methyl groups has a relatively small effect on $\delta^{195}\text{Pt}$ compared to the dependence on ring-size.

In general ^{195}Pt spectra were recorded in order to confirm structural assignment rather than as a diagnostic aid. However, the relative simplicity of the ^{195}Pt spectra enabled spin-tickling experiments of the type $^{195}\text{Pt} \dots \{^{31}\text{P}, ^1\text{H}\}^{84a}$ to be performed in order to determine the signs of various couplings within the same molecule as previously demonstrated.

TABLE 3.9 ^{195}Pt chemical shift data

COMPLEX	$\delta^{195}\text{Pt}^a/\text{ppm}$
$\text{PtCl}_2[\text{Ib}]$	+688.0
$\text{Pt}(\text{Me})\text{Cl}[\text{Ib}]$	+513.2
$\text{PtMe}_2[\text{Ib}]$	+577.0
$\text{PtCl}_2[\text{IIId}]$	-27.4
$\text{Pt}(\text{Me})\text{Cl}[\text{IIId}]$ isomer a)	-35.5
$\text{Pt}(\text{Me})\text{Cl}[\text{IIId}]$ isomer b)	-26.9
$\text{PtMe}_2[\text{IIId}]$	-57.7

Notes a) Relative to 21.4 MHz when the ^1H resonance of TMS is at exactly 100 MHz

CHAPTER 4

OCTAHEDRAL AND SQUARE-PLANAR TRANSITION-METAL COMPLEXES OF SOME NEW TETRA- AND PENTATERTIARY PHOSPHINE LIGANDS

1. INTRODUCTION

In the previous chapter the preparation and characterisation of a series of complexes of the new triphosphine ligands was described and a range of different coordination modes for these ligands was demonstrated. The present chapter extends this work by considering the comparable coordinative behaviour of the new tetra- and pentatertiary phosphine ligands introduced in Chapter Two. However, whereas in the case of the triphosphine ligands the number of different coordination modes is relatively small, the modes for the related pentaphosphine ligands are numbered in their hundreds. It was obviously not realistic to attempt to synthesise, isolate and characterise complexes exhibiting all these modes and therefore this chapter describes only a selection of the more interesting species.

2. OCTAHEDRAL COMPLEXES

(A) Introduction

For reasons previously mentioned the preparation of a complete range of group VIB metal carbonyl complexes of the pentatertiary phosphine ligand, bis-[2,2-bis(diphenylphosphino)ethyl]phenylphosphine (XII), was not attempted. Rather, a study was undertaken to extend the approach of selective isomer preparation with regard to complexes of this ligand, and to develop synthetic strategies required for the synthesis of complexes exhibiting some of its more unusual modes of

coordination. This section therefore does not systematically list the preparations of a complete series of complexes but gives an insight into the routes available to some selected complexes of XII.

(B) Results and Discussion

The two possible singly-coordinated modes of XII (XIIa and XIIb) are shown in Fig. 4.1 and are examples of linkage isomerism. However, the presence of two chiral centres (marked *) in XIIa leads to this

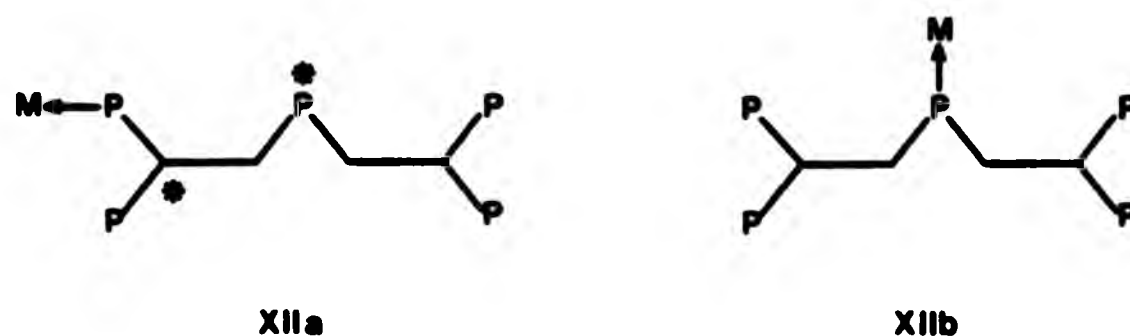
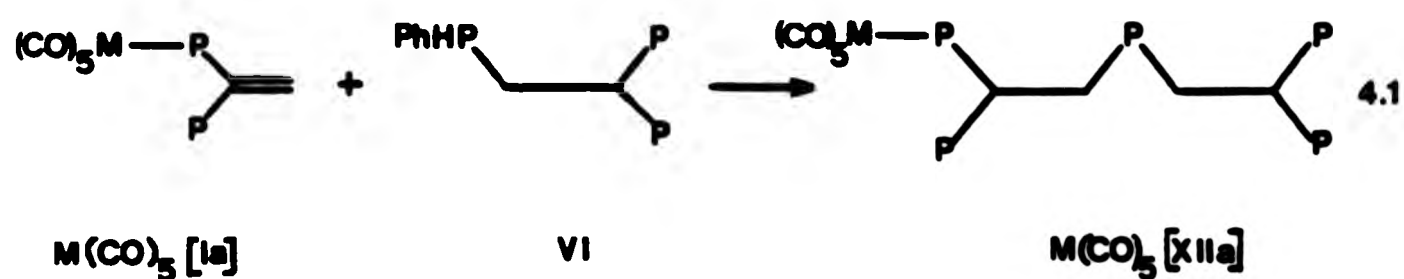


Fig 4.1

mode giving rise to two diastereomers which are chemically inequivalent and which can therefore, in principle, be distinguished by n.m.r. spectroscopy. Direct reaction between the free ligand XII and a metal substrate such as $M(CO)_5 \cdot THF$ was found to result in the formation of a mixture of complexes exhibiting so many of these and related poly-metallic modes (of which there is an even greater number) that characterisation was impossible. However, a selective reaction between the complex $M(CO)_5[1a]$ and the triphosphine species 1,1-bis-(diphenylphosphino)-(2-phenylphosphino)ethane, VI, resulted in the formation of approximately equal proportions of only the diastereomeric complexes exhibiting mode XIIa (Eq 4.1). The bonding of the metal group to one of the geminally related phosphorus atoms, as in XIIa, alters the phosphorus spin-system from that of the free ligand such that the ^{31}P spectra of both diastereomers of mode XIIa were characteristic



of ABMPX spin-systems (Fig. 4.2) and were analysed to give the n.m.r. parameters in Tables 4.1 and 4.2. The coordination chemical shifts

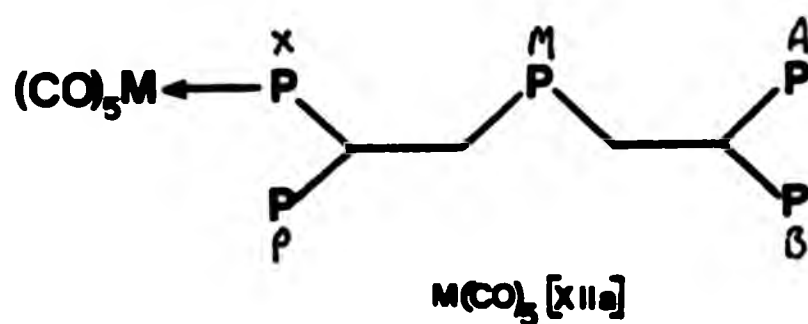


Fig 4.2

TABLE 4.1 ^{31}P chemical shifts for a series of complexes:
 $\text{M}(\text{CO})_5 [\text{XIIa}]$

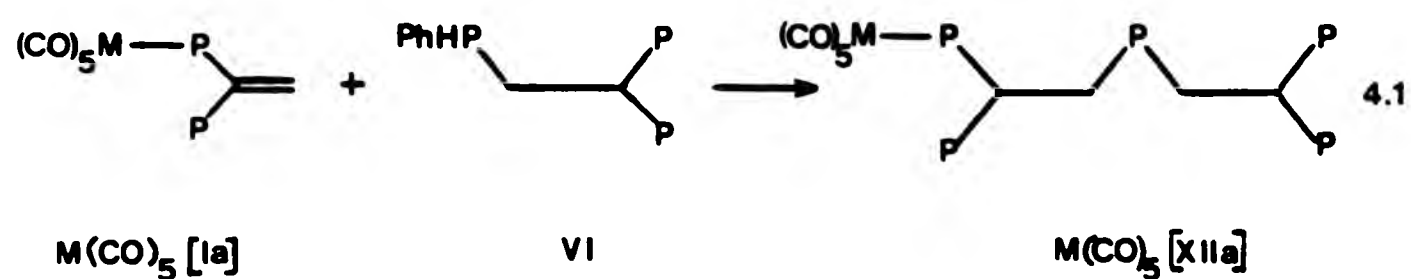
M	$\delta(^{31}\text{P}_\text{A})^b$ /ppm	$\delta(^{31}\text{P}_\text{B})^b$ /ppm	$\delta(^{31}\text{P}_\text{M})^b$ /ppm	$\delta(^{31}\text{P}_\text{P})^b$ /ppm	$\delta(^{31}\text{P}_\text{X})^b$ /ppm	Δp_X^c /ppm
Cr_1^a	-0.4	-4.3	-29.8	-12.4	+67.1	+70.0
Cr_2^a	d	d	-28.5	-12.0	+66.4	+71.2
Mo_1^a	-0.3	-3.8	-29.8	-11.3	+49.5	+52.4
Mo_2^a	d	d	-28.2	-10.4	+49.1	+53.9

Notes a See Fig. 4.2 for labelling system

b Relative to external 85% $\text{H}_3\text{PO}_4 = 0.0$ ppm

c Coordination chemical shift (see page 14)

d Not determined due to the complexity of the spectrum



of ABMPX spin-systems (Fig. 4.2) and were analysed to give the n.m.r. parameters in Tables 4.1 and 4.2. The coordination chemical shifts

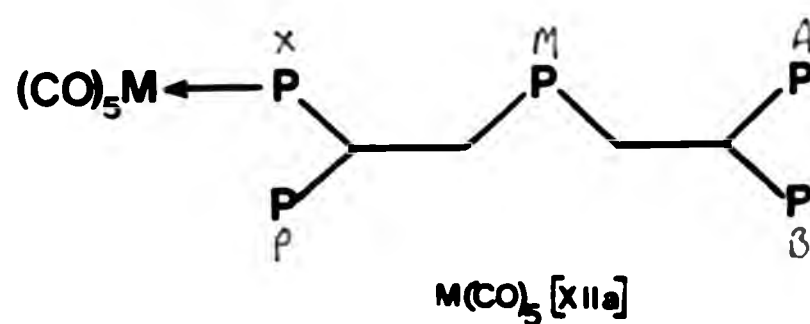


Fig 4.2

TABLE 4.1 ^{31}P chemical shifts for a series of complexes:
 $\text{M}(\text{CO})_5 [\text{XIIa}]$

M	$\delta(^{31}\text{P}_\text{A})^b$ /ppm	$\delta(^{31}\text{P}_\text{B})^b$ /ppm	$\delta(^{31}\text{P}_\text{M})^b$ /ppm	$\delta(^{31}\text{P}_\text{P})^b$ /ppm	$\delta(^{31}\text{P}_\text{X})^b$ /ppm	Δp_X^c /ppm
Cr_1^a	-0.4	-4.3	-29.8	-12.4	+67.1	+70.0
Cr_2^a	d	d	-28.5	-12.0	+66.4	+71.2
Mo_1^a	-0.3	-3.8	-29.8	-11.3	+49.5	+52.4
Mo_2^a	d	d	-28.2	-10.4	+49.1	+53.9

Notes a See Fig. 4.2 for labelling system

b Relative to external 85% $\text{H}_3\text{PO}_4 = 0.0$ ppm

c Coordination chemical shift (see page 14)

d Not determined due to the complexity of the spectrum

TABLE 4.2 ^{31}P - ^{31}P coupling constants for a series of complexes:
 $\text{M}(\text{CO})_5[\text{XIIa}]$

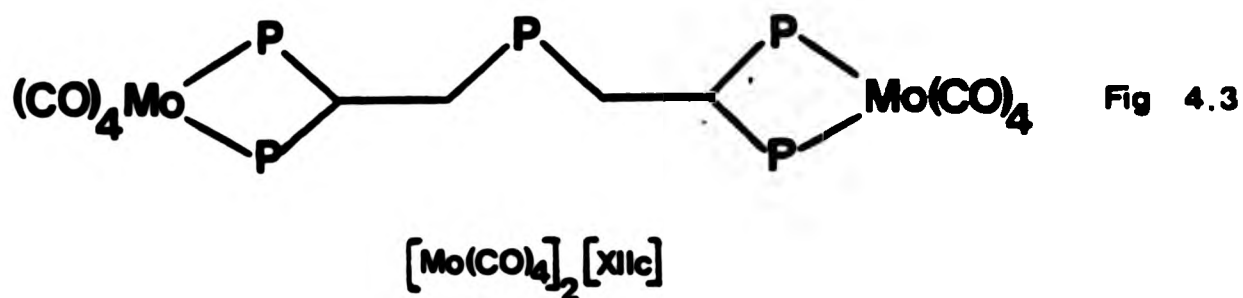
M	$ J(\text{P}_\text{A}-\text{P}_\text{B}) $ /Hz	$ J(\text{P}_\text{A}-\text{P}_\text{M}) $ /Hz	$ J(\text{P}_\text{B}-\text{P}_\text{M}) $ /Hz	$ J(\text{P}_\text{M}-\text{P}_\text{P}) $ /Hz	$ J(\text{P}_\text{M}-\text{P}_\text{X}) $ /Hz	$ J(\text{P}_\text{P}-\text{P}_\text{X}) $ /Hz
Cr_1^{a}	55.5	58.4	3.0	0.0	20.5	168.1
Cr_2^{a}	b	b	36.6	0.0	18.6	192.9
Mo_1^{a}	59.2	55.2	4.5	0.0	19.0	195.9
Mo_2^{a}	b	b	36.0	0.0	18.3	212.7

Notes a See Fig. 4.2 for labelling system

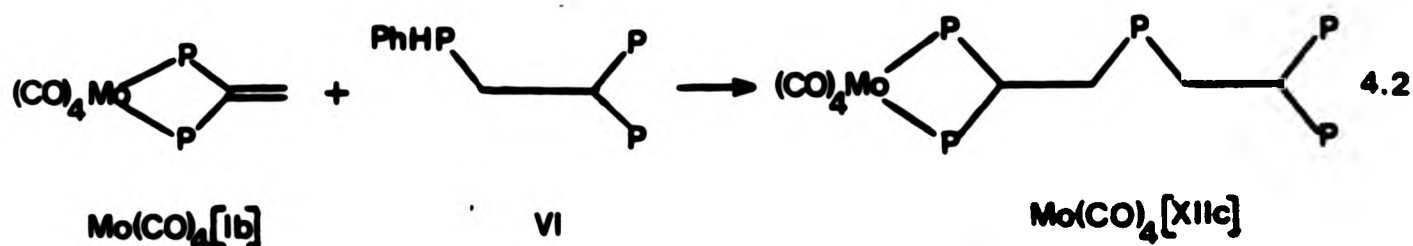
b Not determined due to complexity of the spectrum

of these complexes (ca +70 ppm and +50 ppm for chromium and molybdenum respectively) are consistent with a coordinated phosphorus atom not involved in chelation. Indeed the values of n.m.r. parameters associated with the $(\text{P}_\text{X}, \text{P}_\text{P}, \text{P}_\text{M})$ fragment bear a striking resemblance to those of analogous complexes of the triphosphine ligand II as described in the previous chapter. It also appears that each of the two diastereomeric forms has a characteristic configuration which is virtually independent of the nature of the metal atom and this results in different complexes of the same diastereomeric form exhibiting almost identical sets of n.m.r. parameters.

The number of different coordination modes incorporating a chelated form of XII in octahedral complexes is potentially very large, and it is therefore surprising that direct reaction between two equivalents of $\text{Mo}(\text{CO})_4[\text{pip}]_2$ and one equivalent of XII was found to result in the virtually quantitative formation of the bimetallic complex (Fig. 4.3) incorporating two independent four-membered chelate-rings. By contrast, reaction using equimolar amounts of $\text{Mo}(\text{CO})_4[\text{pip}]_2$ and XII resulted in



a mixture of the bimetallic and analogous monometallic complexes and left some free ligand unreacted. In order to achieve the selective preparation of the monometallic species $\text{M}(\text{CO})_4[\text{XIc}]$ it was therefore found better to utilize an addition reaction method (Eq 4.2) similar to the previous synthesis (Eq 4.1). Coordination mode XIc leads to

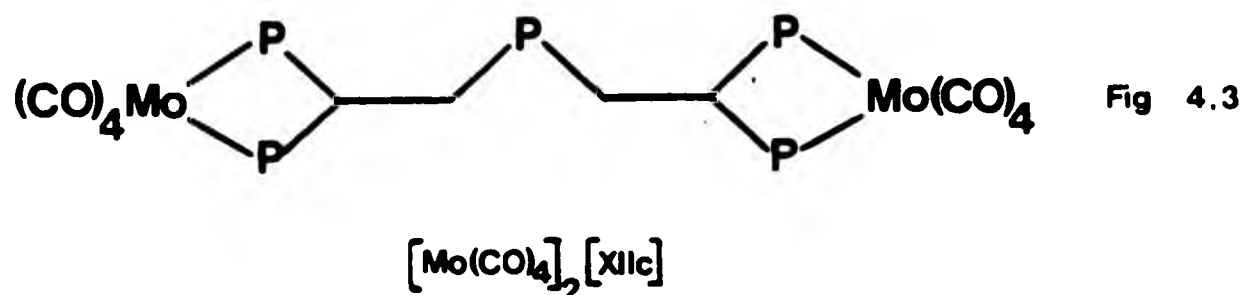


no diastereomers and therefore analysis of the ^{31}P spectra was generally straightforward and gave the parameters shown in Tables 4.3 and 4.4. The coordination chemical shift values in these complexes are clearly

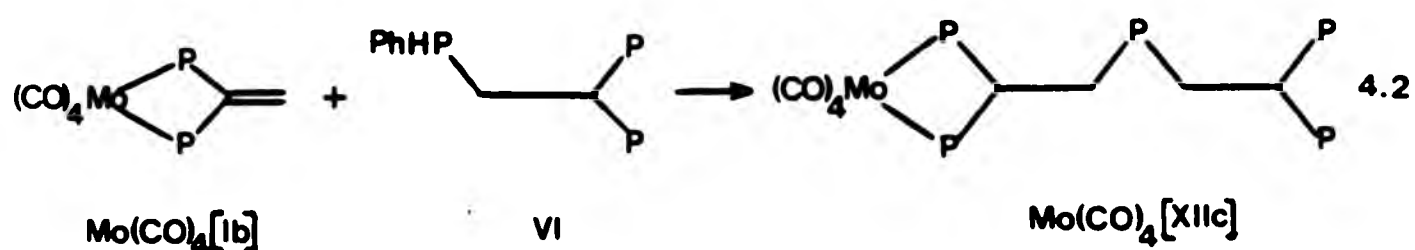


Fig 4.4

indicative of four-membered chelate-ring structures and are therefore consistent with the structures shown in Fig. 4.4. The comparability of all couplings (except $J(\text{P}_\text{A}\text{P}_\text{B})$) within the monometallic series suggests a consistent configuration throughout, and the variation in $J(\text{P}_\text{A}\text{P}_\text{B})$ is



a mixture of the bimetallic and analogous monometallic complexes and left some free ligand unreacted. In order to achieve the selective preparation of the monometallic species $\text{M}(\text{CO})_4[\text{XIIc}]$ it was therefore found better to utilize an addition reaction method (Eq 4.2) similar to the previous synthesis (Eq 4.1). Coordination mode XIIc leads to



no diastereomers and therefore analysis of the ^{31}P spectra was generally straightforward and gave the parameters shown in Tables 4.3 and 4.4. The coordination chemical shift values in these complexes are clearly



Fig 4.4

indicative of four-membered chelate-ring structures and are therefore consistent with the structures shown in Fig. 4.4. The comparability of all couplings (except $J(\text{P}_\text{A}\text{P}_\text{B})$) within the monometallic series suggests a consistent configuration throughout, and the variation in $J(\text{P}_\text{A}\text{P}_\text{B})$ is

TABLE 4.3 ^{31}P chemical shifts for a series of complexes
 $\text{M}(\text{CO})_4[\text{XIc}]$ and $\{\text{M}(\text{CO})_4\}_2[\text{XIc}]$

M	$\delta(^{31}\text{P}_\text{A})^b$ /ppm	ΔP_A /ppm	$\delta(^{31}\text{P}_\text{B})^b$ /ppm	ΔP_B /ppm	$\delta(^{31}\text{P}_\text{M})^b$ /ppm	$\delta(^{31}\text{P}_\text{X})^b$ /ppm	$\delta(^{31}\text{P}_\text{Y})^b$ /ppm
Cr ^a	+51.7	+54.6	+49.6	+54.4	-29.4	-2.8	-5.3
Mo ^a	+28.4	+31.3	+26.1	+30.9	-29.7	-2.6	-4.8
W ^a	+4.1	+7.0	+1.5	+6.3	-29.8	-2.5	-5.0
Mo ₂ ^{a,c}	+28.0	+30.9	+27.4	+32.2	-28.2	-	-

Notes a See Fig. 4.4 for labelling system

b Relative to external 85% $\text{H}_3\text{PO}_4 = 0.0$ ppm

c Bimetallic complex $\{\text{Mo}(\text{CO})_4\}_2[\text{XIc}]$

TABLE 4.4 ^{31}P - ^{31}P coupling constants for a series of complexes:
 $\text{M}(\text{CO})_4[\text{XIc}]$ and $\{\text{M}(\text{CO})_4\}_2[\text{XIc}]$

M	$ J(\text{P}_\text{A}-\text{P}_\text{B}) $ /Hz	$ J(\text{P}_\text{A}-\text{P}_\text{M}) $ /Hz	$ J(\text{P}_\text{B}-\text{P}_\text{M}) $ /Hz	$ J(\text{P}_\text{M}-\text{P}_\text{X}) $ /Hz	$ J(\text{P}_\text{M}-\text{P}_\text{Y}) $ /Hz	$ J(\text{P}_\text{X}-\text{P}_\text{Y}) $ /Hz
Cr ^a	10.0	3.6	8.8	36.4	16.8	83.5
Mo ^a	33.9	3.3	8.0	34.5	16.5	84.2
W ^{a,b}	41.2	4.0	9.5	36.4	16.4	83.2
Mo ₂ ^{a,d}	31.7	4.3	6.1	-	-	-

Notes a See Fig. 4.3 for labelling system

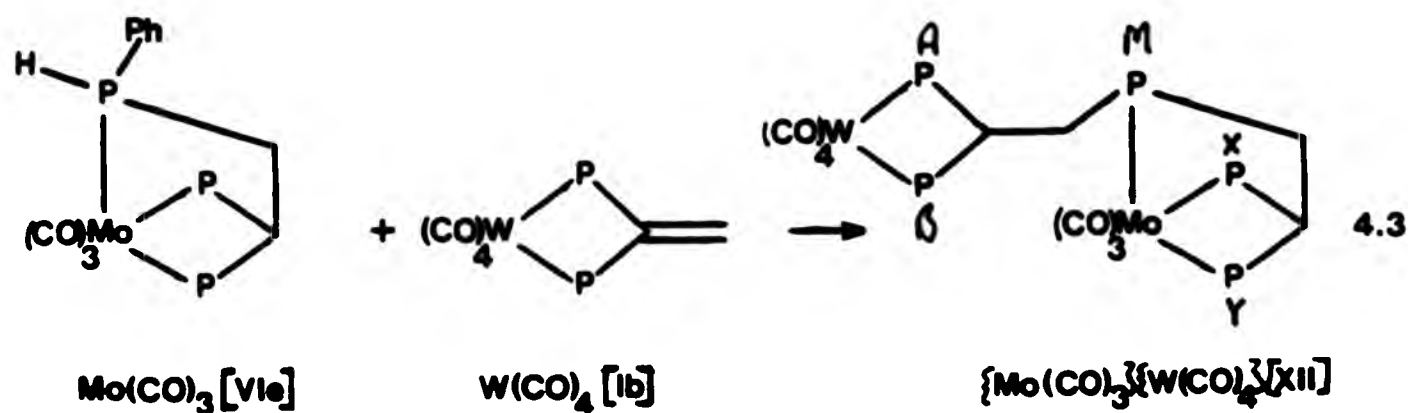
b $|J(^{183}\text{W}-^{31}\text{P}_\text{A})| = 204.2$ Hz: $|J(^{183}\text{W}-^{31}\text{P}_\text{B})| = 205.6$ Hz

c All longer range couplings = 0 Hz

d Bimetallic complex $\{\text{Mo}(\text{CO})_4\}_2[\text{XIc}]$

therefore probably attributable to different 'through-the-metal' contributions to the observed coupling constants as discussed previously.

The approach to selective isomer preparation as described so far may be extended by the use of complexes of the ligand VI as one of the reagents. Thus, reaction of $\text{Mo(CO)}_3[\text{VIe}]$ with $\text{W(CO)}_4[\text{Ib}]$ resulted in the formation of a fully-coordinated species (Eq 4.3) having no



diastereomers. Clearly, attempts to form this type of complex by more direct routes are unlikely to succeed since the number of isomeric products of direct reactions is overwhelming. The ^{31}P n.m.r. spectrum of this complex (Fig. 4.5) was analysed to give the n.m.r. parameters in Table 4.5. As for the previous complexes described in this chapter consideration of the coordination chemical shift values for this species allows an unequivocal assignment of the ^{31}P spectrum to the proposed structure. In addition, the presence of characteristic tungsten satellites confirms that this complex contains only two tungsten-bound phosphorus atoms and that rearrangement has not occurred to give a structure where the two metal atoms have interchanged.

TABLE 4.5 ^{31}P n.m.r. parameters for $\{\text{Mo}(\text{CO})_3\}(\text{W}(\text{CO})_4)_4[\text{XII}]$

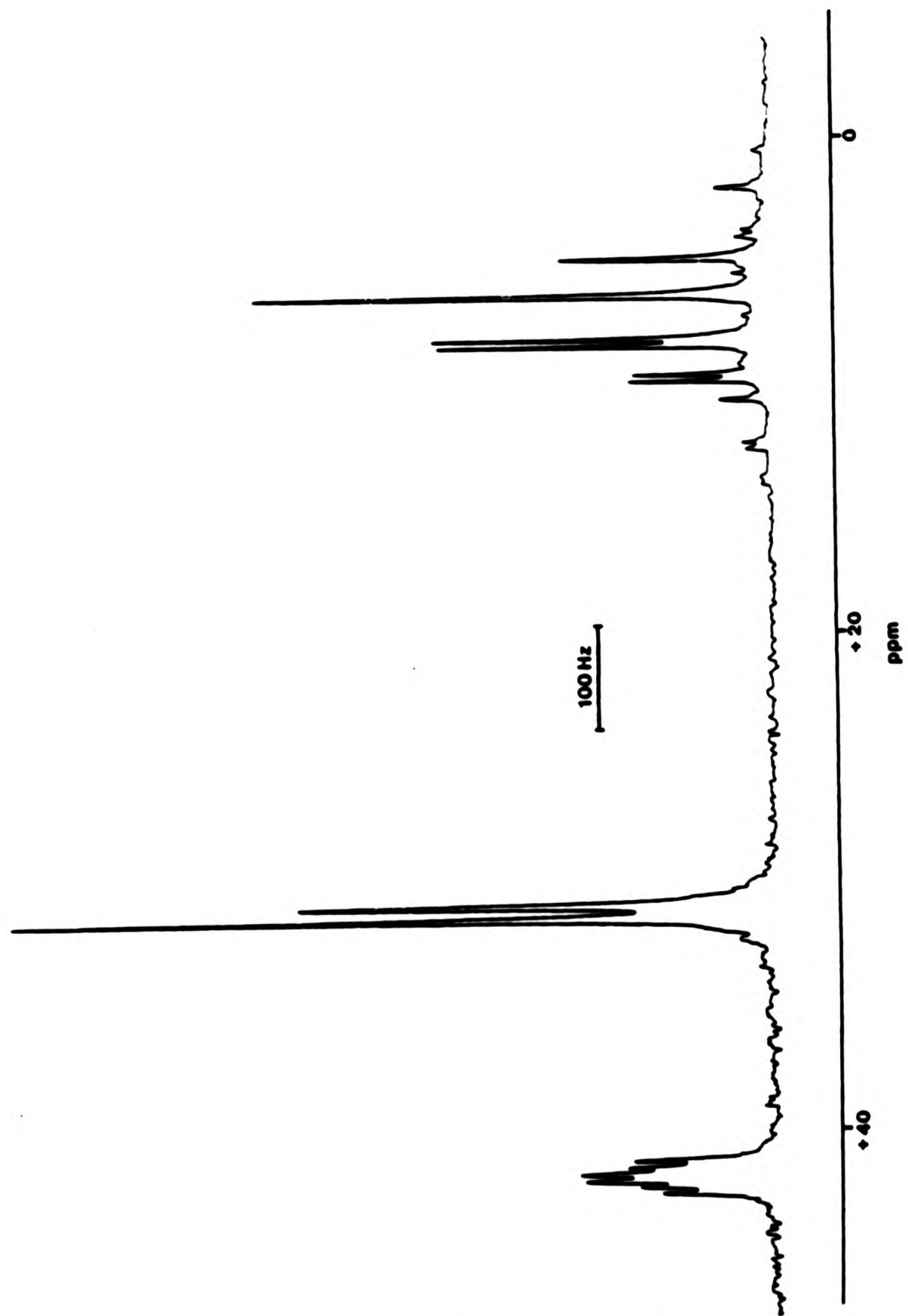
P_i ^b	$\delta(^{31}\text{P}_i)$ ^a /ppm	ΔP_i /ppm	$ J(P_A - P_i) $ /Hz	$ J(P_B - P_i) $ /Hz	$ J(P_M - P_i) $ /Hz	$ J(P_X - P_i) $ /Hz	$ J(P_Y - P_i) $ /Hz	$ J(^{183}\text{W} - P_i) $ /Hz
P_A	+8.9	+11.8	-	32.7	6.4	0	0	208.0
P_B	+6.3	+11.1	32.7	-	0.5	0	0	208.0
P_M	+41.7	+71.4	6.4	0.5	-	12.7	12.7	0
P_X	+30.9	+33.8	0	0	12.7	-	c	0
P_Y	+30.9	+35.7	0	0	12.7	c	-	0

Notes a Relative to external 85% $\text{H}_3\text{PO}_4 = 0.0$ ppm

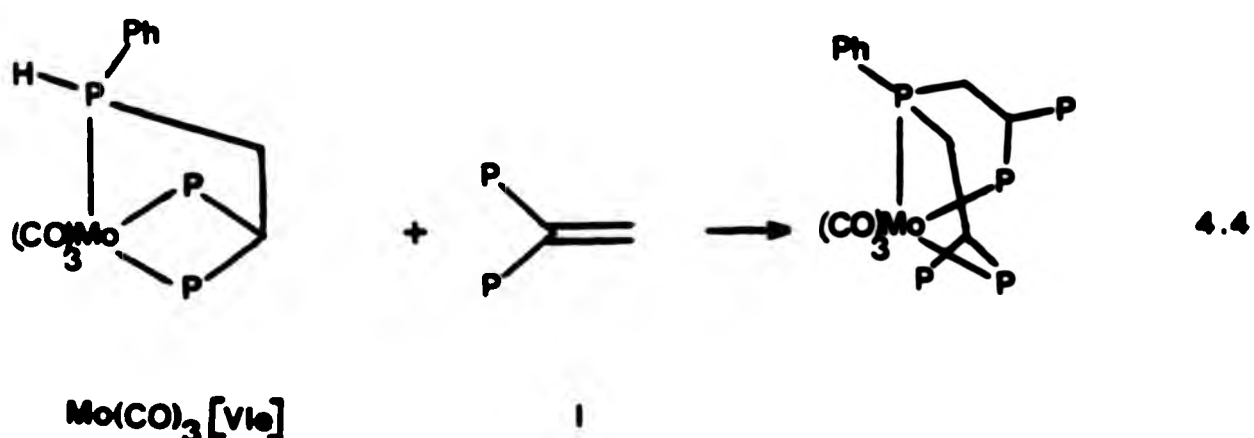
b See eq 4.3 for labelling system

c Not obtainable from ^{31}P n.m.r. spectrum

Fig 4.5 ^{31}P n.m.r. spectrum of $\{\text{Mo}(\text{CO})_3\}\{\text{W}(\text{CO})_4\}$ [XII] recorded at 24.2 MHz



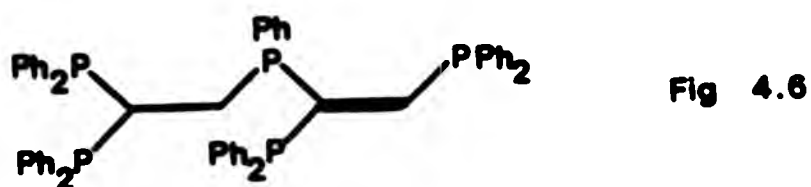
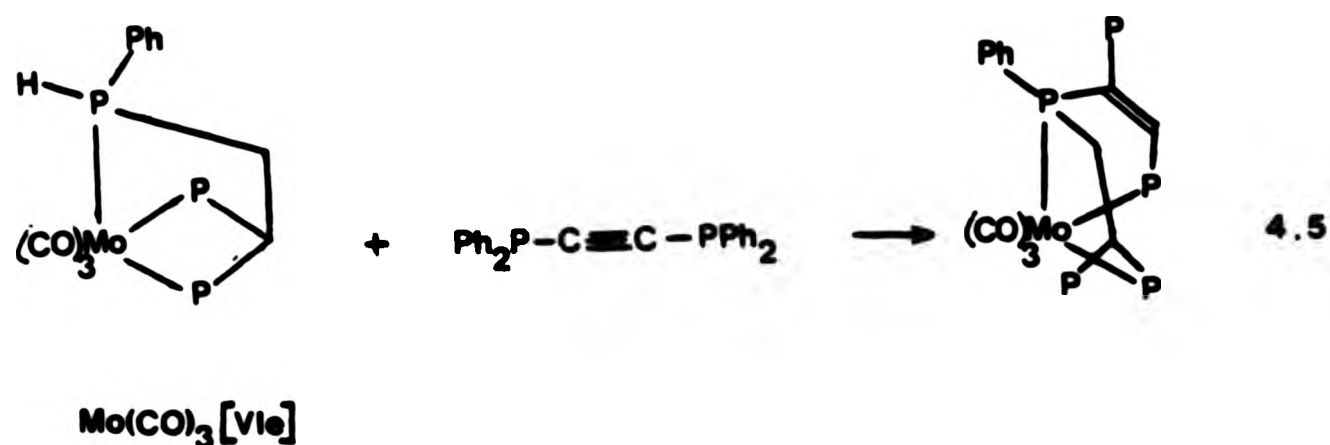
Although reaction between $\text{Mo(CO)}_3[\text{Vie}]$ and $\text{Cr(CO)}_5[\text{Ia}]$ did not occur under these conditions, presumably owing to steric hindrance, $\text{Mo(CO)}_3[\text{Vie}]$ and the free ligand **I** did react but the path followed was different from the previous reaction. It appears likely that after addition has taken place a rearrangement occurs rapidly under the reaction conditions (Eq 4.4) to give a structure which, in principle,



has three diastereomers. (It is reasonable to assume a fac structure since mer arrangements for related species are uncommon.) Two of these diastereomers can be expected to have AA'BB'X phosphorus spin-systems and the other an ABMXY spin-system. Thus the ^{31}P n.m.r. of these isomers are not only complicated in themselves but are also likely to overlap to an appreciable extent in a mixture. The ^{31}P spectrum of the product of this reaction is indeed of such complexity that it is impossible to analyse fully, but the positions of the various phosphorus resonances are consistent with the suggested structure.

This proposed rearrangement is also found in the following related case where analysis of the n.m.r. spectrum is somewhat easier and as a consequence provides better evidence for this sort of behaviour. Reaction of $\text{Mo(CO)}_3[\text{Vie}]$ with an equimolar amount of bis(diphenylphosphino)ethyne under similar conditions resulted in the formation of the complex shown in Eq 4.5 which is particularly interesting as it incorporates the otherwise unknown pentatertiary phosphine ligand shown

in Fig. 4.6. However, an analogous reaction between bis(diphenylphosphino)ethyne and the free ligand VI led instead to a mixture of products, none of which was the pentaphosphine hoped for. This



complex can have two diastereomeric structures although in the ^{31}P n.m.r. spectrum (Fig. 4.7) only one five-spin system with five inequivalent phosphorus nuclei was detected which could arise from either diastereomer. Considerations of molecular models indicate that neither isomeric structure is precluded by steric hindrance. This suggests a stereospecific reaction and indeed further experiments with molecular models were found to substantiate this. If the mechanism of the reaction is as proposed in Scheme 4.1, initial addition across the triple-bond would result in the formation of the intermediate (i). In this species phosphorus atom C is more likely to coordinate than phosphorus atom D since a relatively low-strained five-membered chelate ring will be formed. P_C , however, is then limited to direct replacement of P_B since the coordination site occupied by P_B is unavailable to it, owing to the strain inherent in

Fig. 4.7 ^{31}P n.m.r. spectrum recorded at 36.2 MHz of the reaction mixture resulting from the addition of bis(diphenylphosphino)-ethyne and $\text{Mo}(\text{CO})_3[\text{Vie}]$ (eq 4.5)

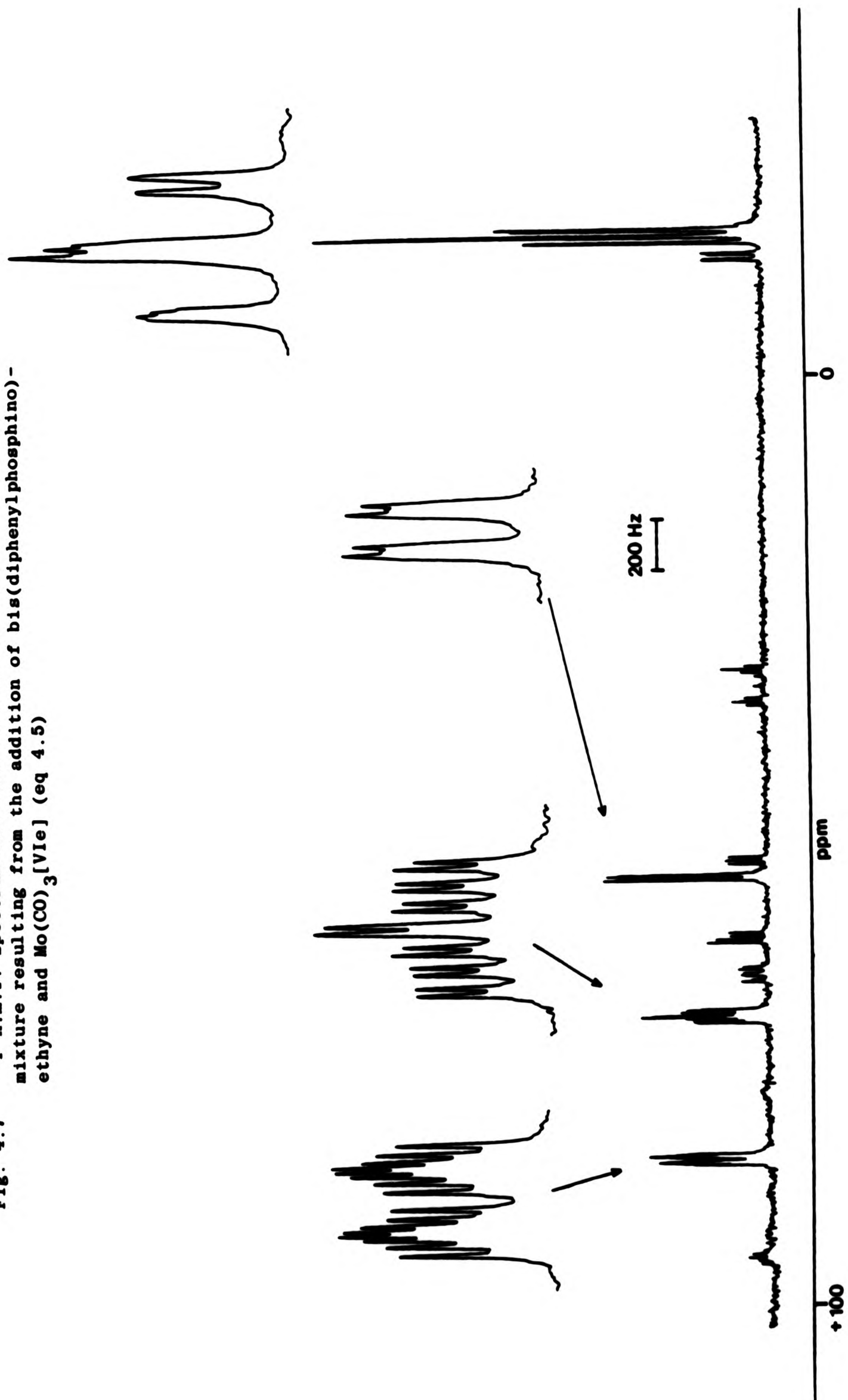


TABLE 4.6 ^{31}P n.m.r. parameters for the product of Eq. 4.5

P_i^a	$\delta(^{31}\text{P}_i)^b$ /ppm	$ J(P_A-P_i) $ /Hz	$ J(P_B-P_i) $ /Hz	$ J(P_C-P_i) $ /Hz	$ J(P_D-P_i) $ /Hz	$ J(P_E-P_i) $ /Hz
P_A	+84.0	-	8.2	3.7	25.0	6.4
P_B	+68.5	8.2	-	15.9	2.7	25.0
P_C	+53.6	3.7	15.9	-	1.5	1.0
P_D	-14.8	25.0	2.7	1.5	-	0
P_E	-15.5	6.4	25.0	1.0	0	-

Notes a See below for labelling system

b Relative to external 85% $\text{H}_3\text{PO}_4 = 0.0$ ppm

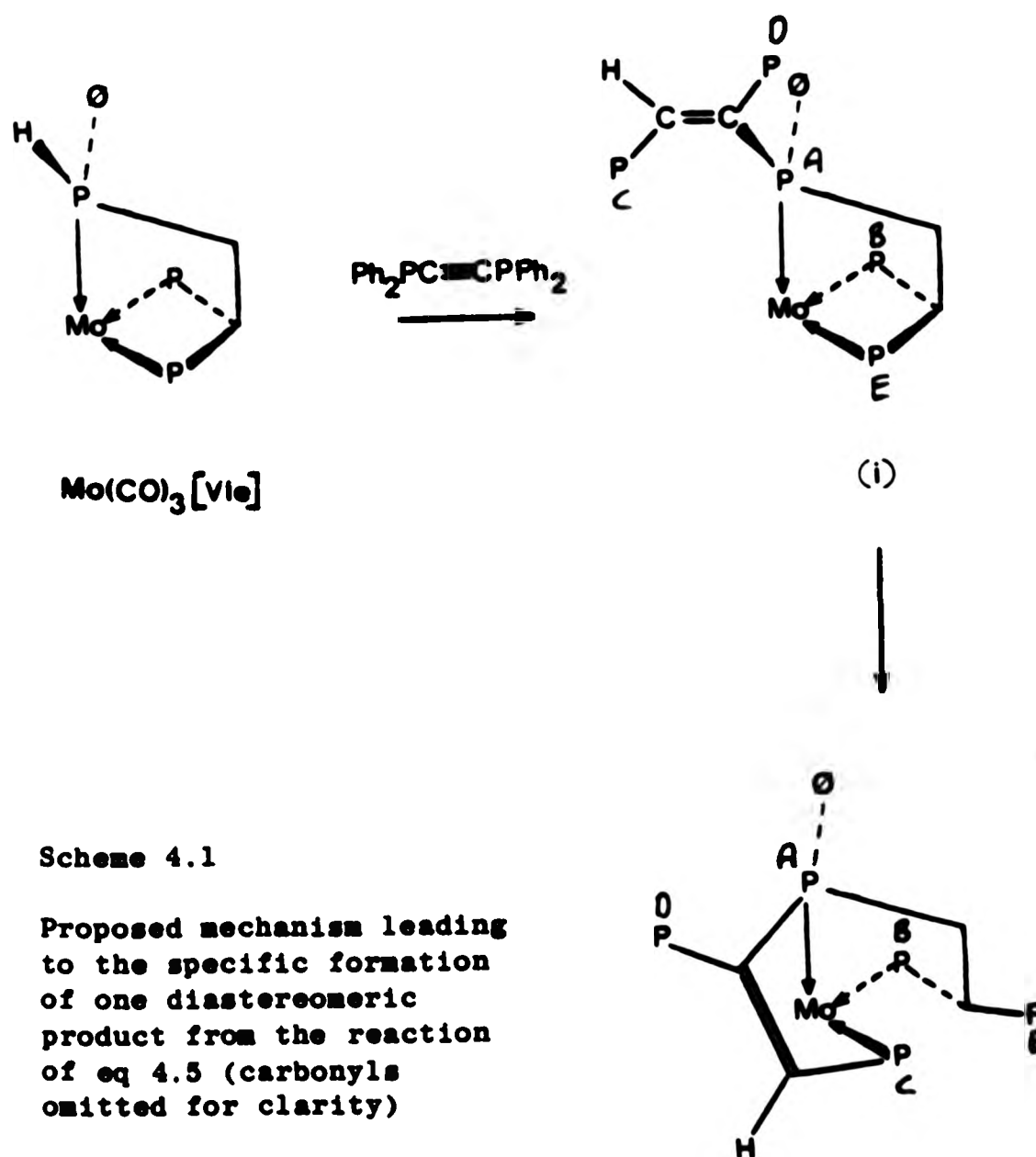
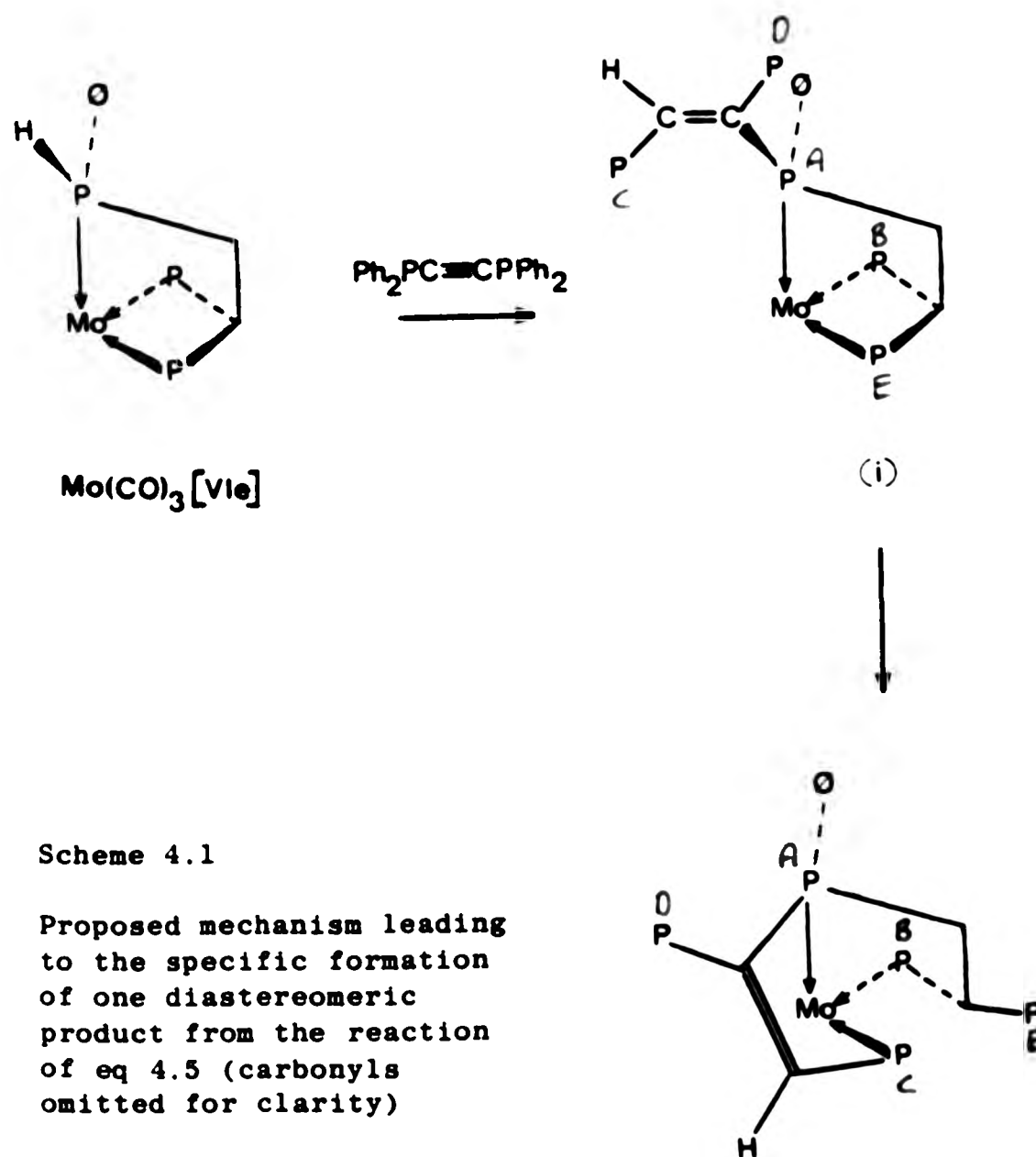


TABLE 4.6 ^{31}P n.m.r. parameters for the product of Eq. 4.5

P_i^a	$\delta(^{31}\text{P}_i)^b$ /ppm	$ J(P_A-P_i) $ /Hz	$ J(P_B-P_i) $ /Hz	$ J(P_C-P_i) $ /Hz	$ J(P_D-P_i) $ /Hz	$ J(P_E-P_i) $ /Hz
P_A	+84.0	-	8.2	3.7	25.0	6.4
P_B	+68.5	8.2	-	15.9	2.7	25.0
P_C	+53.6	3.7	15.9	-	1.5	1.0
P_D	-14.8	25.0	2.7	1.5	-	0
P_E	-15.5	6.4	25.0	1.0	0	-

Notes a See below for labelling system

b Relative to external 85% $\text{H}_3\text{PO}_4 = 0.0$ ppm



replacement of P_B . This mechanism would therefore lead to formation of only one diastereomer and is therefore likely to be applicable to this reaction. Discussion of the n.m.r. parameters for this complex is difficult since values for the corresponding ligand are obviously not available. However, chemical shifts are generally in the ranges expected and the values of $J(P_A P_C)$ and $J(P_A P_B)$ are small and therefore consistent with five-membered ring structures.

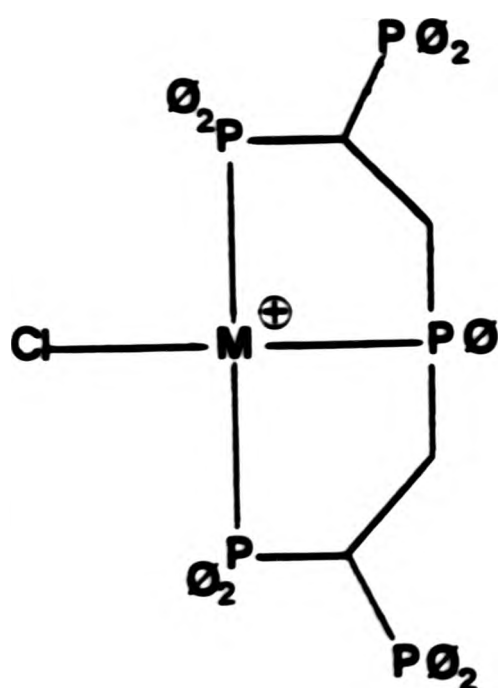
3. SQUARE-PLANAR COMPLEXES

(A) Introduction

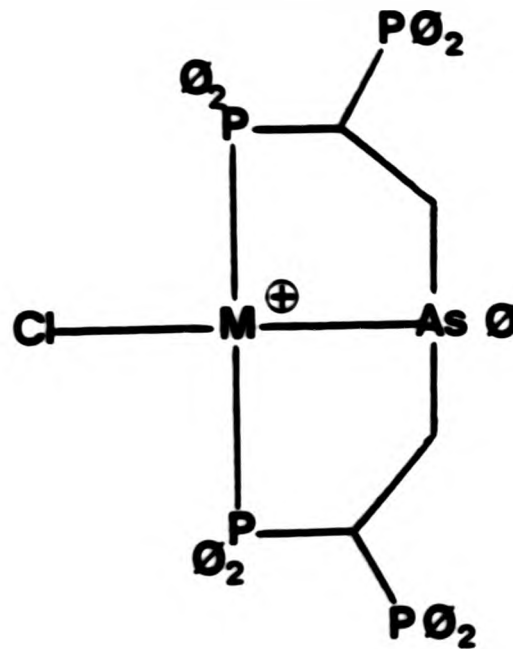
In an extension of the study of the coordinative behaviour of the triphosphine ligands described in Chapter Three the following section details the synthesis and characterisation of a series of square-planar palladium and platinum complexes of the new tetra- and penta-tertiary phosphine ligands. Emphasis has been placed on the discussion of the trends in n.m.r. parameters within the series, and the use of computer simulation techniques as an aid to assignment of intricate second-order spectra is also demonstrated.

(B) Results and Discussion

Treatment of $MCl_2(PhCN)_2$, ($M = Pd, Pt$), with an equimolar amount of bis-[2,2-bis(diphenylphosphino)ethyl]phenylphosphine, XII, in dichloromethane at room temperature resulted in rapid and virtually quantitative formation of the new ionic complexes $[MCl\{XII\}]^+Cl^-$ (Fig. 4.8a). Analogous reactions were found to occur for the related ligand bis-[2,2-bis(diphenylphosphino)ethyl]phenylarsine, XVI, to give the



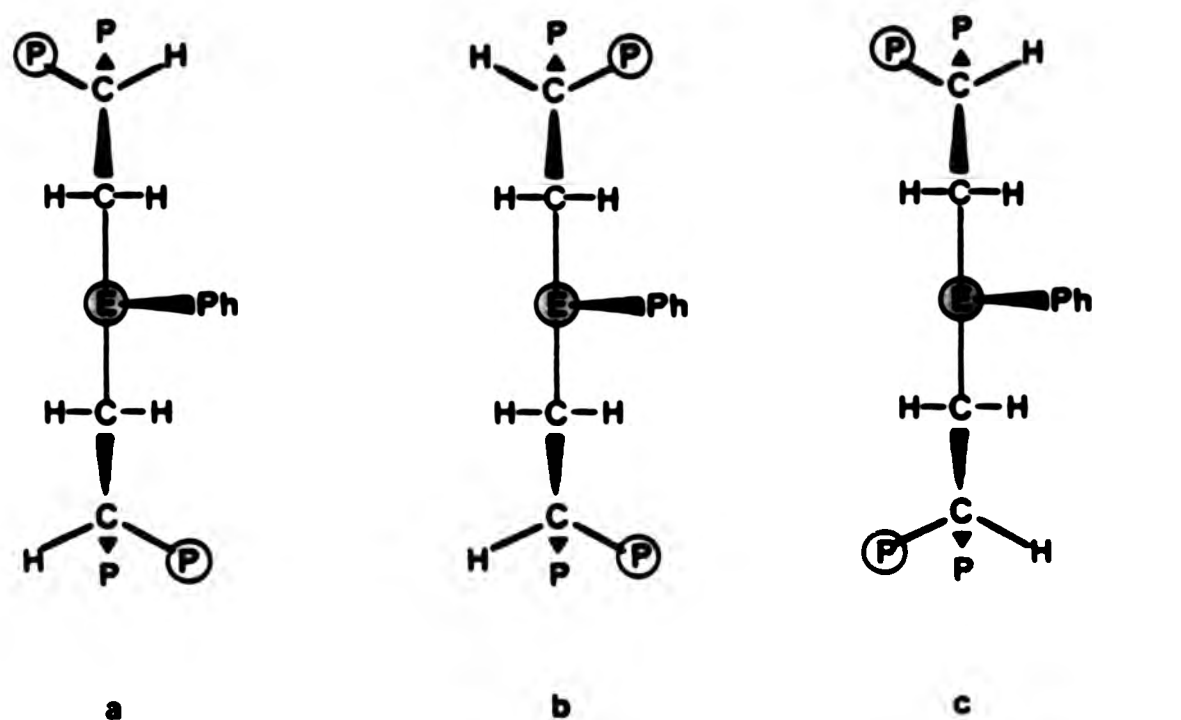
$[MCl\{XII\}]^+ Cl^-$
a



$[MCl\{XVI\}]^+ Cl^-$
b

Fig 4.8

arsenic-containing complexes $[MCl(XVI)]^+Cl^-$ shown in Fig. 4.8b. These reactions have the potential to yield three diastereomeric products (arising from the different relative orientations of the Ph_2P and Ph groups, (Fig. 4.9a) - c)) but in practice these were not obtained in



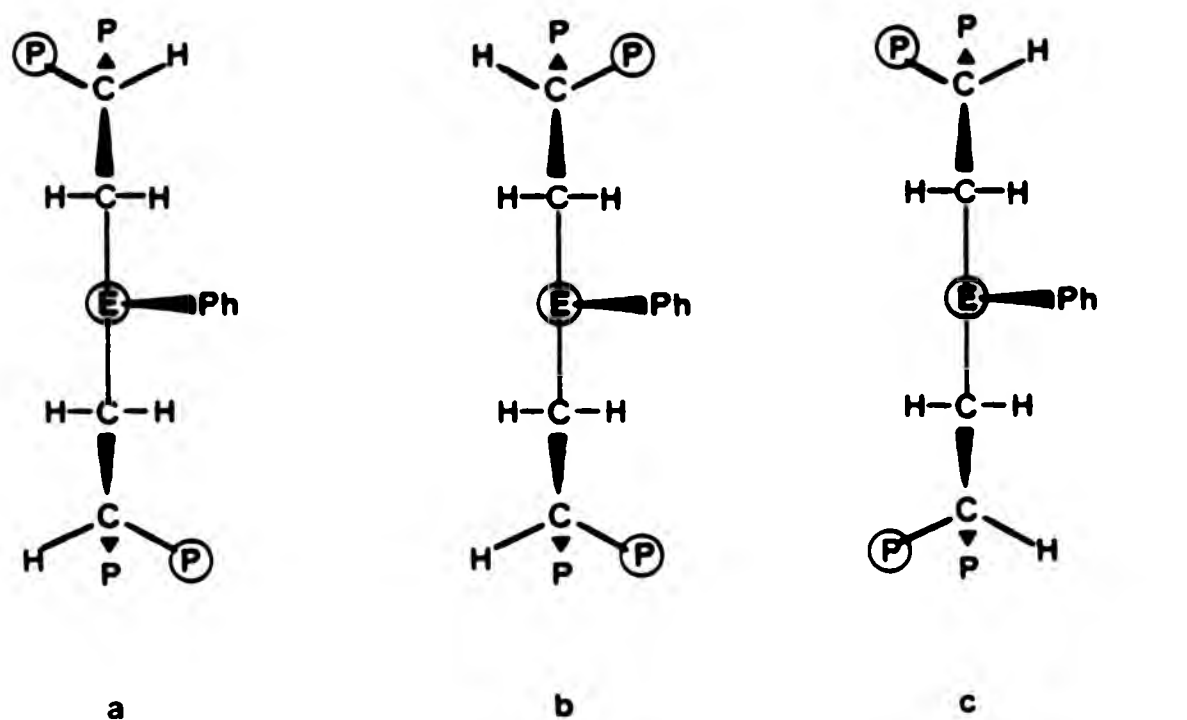
Projections along
E - M bond of
Fig 4.8

Fig 4.9

○ = Metal atom
E = P or As

the proportions expected on a simple statistical basis. Of the three structures shown in Fig. 4.9 it will be noticed that in structure a) all four terminal phosphorus nuclei are chemically and magnetically inequivalent. Thus complexes of this type would be expected to exhibit ABMXY ^{31}P spectra where A, B, X and Y are the terminal phosphorus nuclei (Fig. 4.10). Analogous diastereomeric complexes of the arsenic-containing ligand would therefore be expected to exhibit ABXY ^{31}P spectra. For reasons that will become clear later the diastereomers with ^{31}P spectra consistent with the asymmetric structure in Fig. 4.9a) will, for convenience, be termed type AB diastereomers. These AB diastereoisomers have been identified

arsenic-containing complexes $[MCl\{XVI\}]^+Cl^-$ shown in Fig. 4.8b. These reactions have the potential to yield three diastereomeric products (arising from the different relative orientations of the Ph_2P and Ph groups, (Fig. 4.9a) - c)) but in practice these were not obtained in

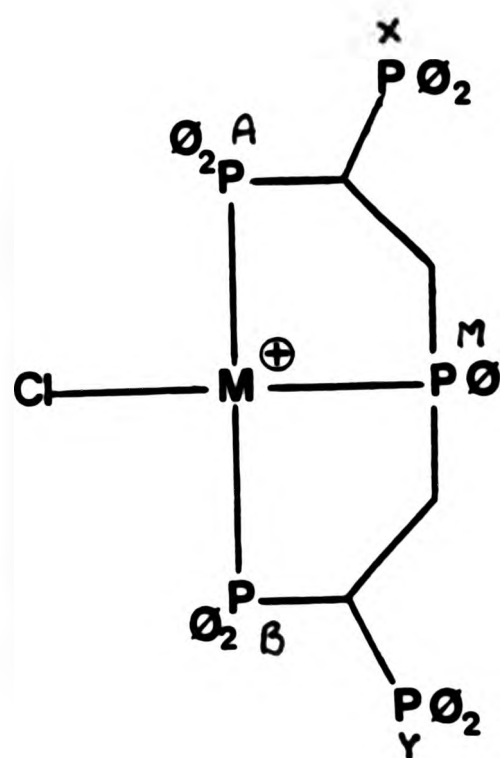


Projections along
E - M bond of
Fig 4.8

Fig 4.9

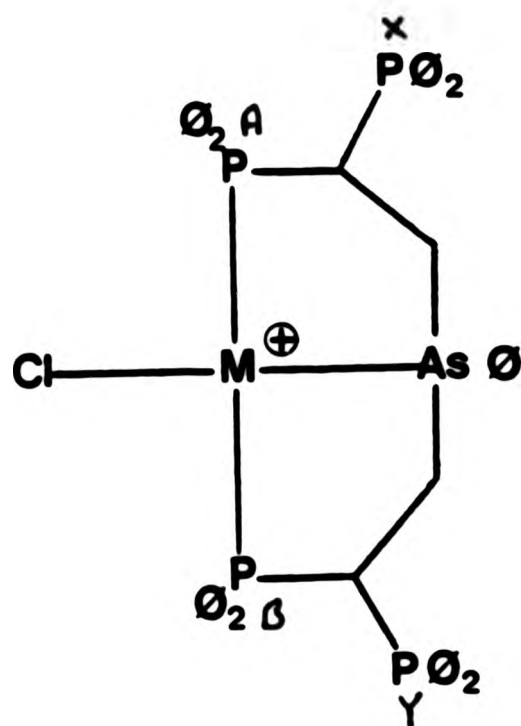
○ = Metal atom
E = P or As

the proportions expected on a simple statistical basis. Of the three structures shown in Fig. 4.9 it will be noticed that in structure a) all four terminal phosphorus nuclei are chemically and magnetically inequivalent. Thus complexes of this type would be expected to exhibit ABMXY ^{31}P spectra where A,B,X and Y are the terminal phosphorus nuclei (Fig. 4.10). Analogous diastereomeric complexes of the arsenic-containing ligand would therefore be expected to exhibit ABXY ^{31}P spectra. For reasons that will become clear later the diastereomers with ^{31}P spectra consistent with the asymmetric structure in Fig. 4.9a) will, for convenience, be termed type AB diastereomers. These AB diastereoisomers have been identified



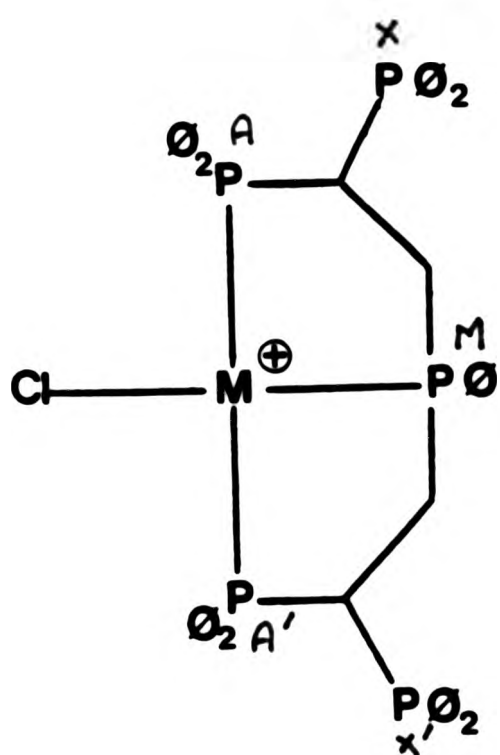
[MCl{XII}] Cl

a



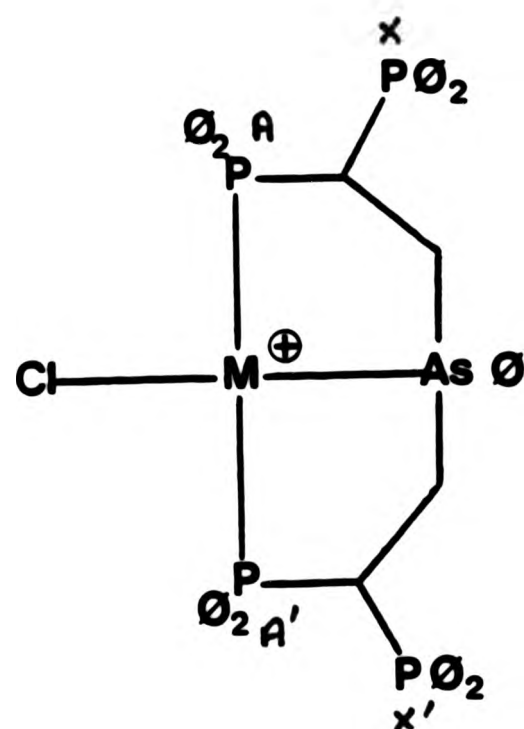
[MCl{XVI}] Cl

b



[MCl{XII}] Cl

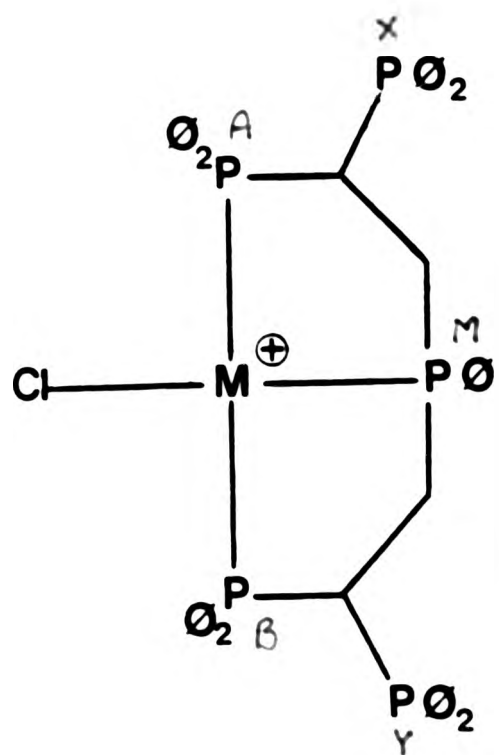
c



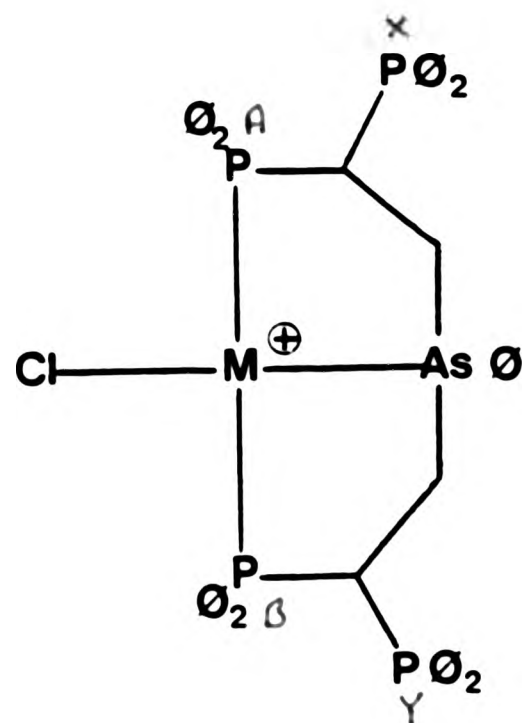
[MCl{XVI}] Cl

d

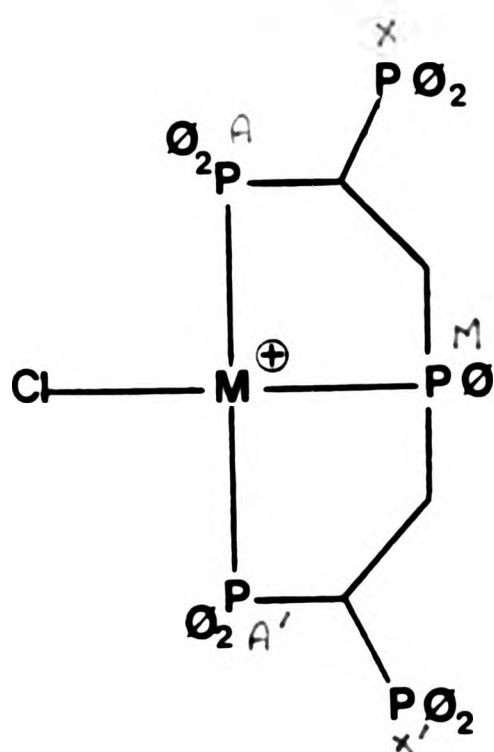
Fig. 4.10 Labelling system for:
 a) AB diastereomers of [MCl{XII}]Cl
 b) AB diastereomers of [MCl{XVI}]Cl
 c) A2 and B2 diastereomers of [MCl{XII}]Cl
 d) A2 and B2 diastereomers of [MCl{XVI}]Cl



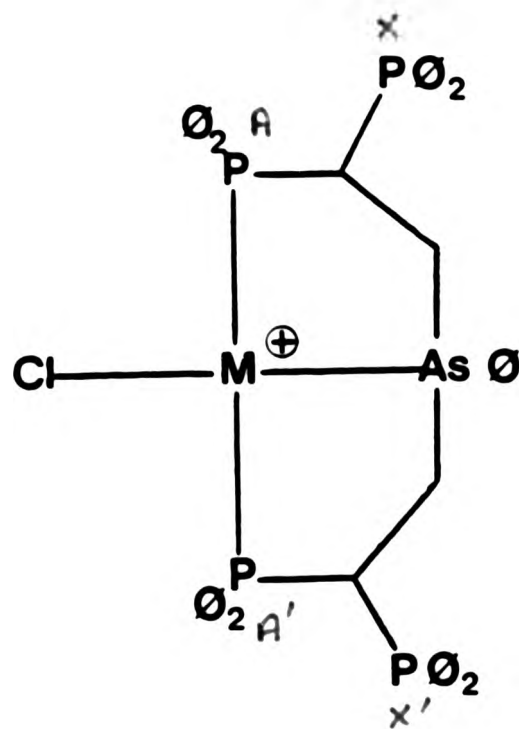
[MCl{XII}] Cl
a



[MCl{XVI}] Cl
b



[MCl{XII}] Cl
c



[MCl{XVI}] Cl
d

Fig. 4.10 Labelling system for:
a) AB diastereomers of [MCl{XII}]Cl
b) AB diastereomers of [MCl{XVI}]Cl
c) A2 and B2 diastereomers of [MCl{XII}]Cl
d) A2 and B2 diastereomers of [MCl{XVI}]Cl

for all four systems investigated and their ^{31}P n.m.r. parameters (Tables 4.7 and 4.8) display some interesting and important features. For the coordinated nuclei P_A and P_B in all these AB diastereomers there is a surprisingly large difference between the chemical shifts $\delta(\text{P}_\text{A})$ and $\delta(\text{P}_\text{B})$ (ca 18 ppm and 15 ppm for complexes of platinum and palladium respectively). Because of this it is possible to label the structures identically for each system by defining P_A as having the higher chemical shift of the two coordinated and terminal phosphorus nuclei. With this definition it is seen that $^2\text{J}(\text{P}_\text{A}\text{P}_\text{X})$ is characteristically of larger magnitude than $^2\text{J}(\text{P}_\text{B}\text{P}_\text{Y})$ whilst $^3\text{J}(^{195}\text{PtP}_\text{X})$ is characteristically smaller in magnitude than $^3\text{J}(^{195}\text{Pt-P}_\text{Y})$. Other parameters are less easy to quantify but are in general comparable for all four systems. It therefore appears that the AX and BY fragments each have different but highly characteristic sets of n.m.r. parameters, a feature which is important to recognize for the following examination of the other diastereomeric species produced by these reactions.

The reaction between $\text{PtCl}_2(\text{PhCN})_2$ and XII was found to result in the formation of a mixture of two of the three possible diastereomers of $[\text{PtCl}\{\text{XII}\}]\text{Cl}$: (i) the AB isomer characterised by its unique spin-system as described above; and (ii) another diastereomer which will be termed type B₂ for reasons which will become clear in the sequel. The B₂ diastereomer exhibits an AA'MXX' (Fig. 4.10) ^{31}P spectrum with the n.m.r. parameters shown in Table 4.9 and it is therefore consistent with both structures b) and c) of Fig. 4.9. The values of $\delta(^{31}\text{P}_\text{A})$ and $^3\text{J}(^{195}\text{Pt-P}_\text{X})$ for this species resemble the values characteristic of the BY fragment in its corresponding AB diastereomer and therefore since both coordinated geminally related nuclei in this symmetric diastereomer have chemical shifts in the

TABLE 4.7 ^{31}P n.m.r. parameters for the (AB) diastereomers of $[\text{MCl}(\text{XII})]\text{Cl}$
(structure a) of Fig. 4.9)

P_i^a	$\delta(^{31}\text{P}_i)^b$ /ppm	$ J(\text{P}_\text{A}\text{P}_i) $ /Hz	$ J(\text{P}_\text{B}\text{P}_i) $ /Hz	$ J(\text{P}_\text{M}\text{P}_i) $ /Hz	$ J(\text{P}_\text{X}\text{P}_i) $ /Hz	$ J(\text{P}_\text{Y}\text{P}_i) $ /Hz	$ J(^{195}\text{PtP}_i) $ /Hz
P_A	+61.1 / +65.1	- / -	381.2 / 406.6	1.6 / 9.0	90.3 / 83.4	12.0 / 14.6	2520.3 / -
P_B	+43.8 / +50.7	381.2 / 406.6	- / -	9.0 / 13.0	1.5 / 3.4	39.5 / 32.6	2424.6 / -
P_M	+71.6 / +99.3	1.6 / 9.0	9.0 / 13.0	- / -	8.3 / 11.4	0.0 / 0.0	3080.2 / -
P_X	-18.9 / -17.3	90.3 / 83.4	1.5 / 3.4	8.3 / 11.4	- / -	0.0 / 0.0	19.6 / -
P_Y	-12.1 / -10.8	12.0 / 14.6	39.5 / 32.6	0.0 / 0.0	0.0 / 0.9	- / -	85.0 / -

Notes:

a See Fig. 4.10 for
labelling system

b Relative to external
 $85\% \text{H}_3\text{PO}_4 = 0.0 \text{ ppm}$

Values shown top left
are for $\text{M} = \text{Pt}$

Values shown bottom
right are for $\text{M} = \text{Pd}$

TABLE 4.7 ^{31}P n.m.r. parameters for the (AB) diastereomers of $[\text{MCl}(\text{XII})\text{Cl}]$
(structure a) of Fig. 4.9)

P_i^a	$\delta(^{31}\text{P}_i)^b$ /ppm	$ J(\text{P}_i\text{P}_i) $ /Hz	$ J(\text{P}_i\text{P}_i) $ /Hz	$ J(\text{P}_i\text{P}_i) $ /Hz	$ J(\text{P}_i\text{P}_i) $ /Hz	$ J(\text{P}_i\text{P}_i) $ /Hz	$ J(\text{P}_i\text{P}_i) $ /Hz	$ J(^{195}\text{PtP}_i) $ /Hz
P_A	+61.1 / +65.1	- / -	381.2 / 406.6	1.6 / 9.0	90.3 / 83.4	12.0 / 14.6	2520.3 / -	- / -
P_B	+43.8 / +50.7	381.2 / 406.6	- / -	9.0 / 13.0	1.5 / 3.4	39.5 / 32.6	2424.6 / -	- / -
P_M	+71.6 / +99.3	1.6 / 9.0	9.0 / 13.0	- / -	8.3 / 11.4	0.0 / 0.0	3080.2 / -	- / -
P_X	-18.9 / -17.2	90.3 / 83.4	1.5 / 3.4	8.3 / 11.4	- / -	0.0 / 0.0	19.6 / -	- / -
P_Y	-12.1 / -10.8	12.0 / 14.6	39.5 / 32.6	0.0 / 0.0	0.0 / 0.0	- / -	85.0 / -	- / -

Notes:

a See Fig. 4.10 for
labelling system

b Relative to external
 $85\% \text{H}_3\text{PO}_4 = 0.0 \text{ ppm}$

Values shown top left
are for $\text{M} = \text{Pt}$

Values shown bottom
right are for $\text{M} = \text{Pd}$

TABLE 4.8 ^{31}P n.m.r. parameters for the 'AB' diastereomers (structure a)
Fig 4.9) of $[\text{MCl}(\text{XVI})]\text{Cl}$

P_i^a	$\delta(^{31}\text{P}_i)^b$ /ppm	$ J(\text{P}_i\text{P}_1) $ /Hz	$ J(\text{P}_i\text{P}_2) $ /Hz	$ J(\text{P}_i\text{P}_3) $ /Hz	$ J(\text{P}_i\text{P}_4) $ /Hz	$ J(^{195}\text{PtP}_i) $ /Hz
P_A	+61.8	-	394.3	74.6	12.2	2500.0
P_B	+43.9	394.3	-	4.0	39.1	2426.8
P_X	-15.3	74.6	4.0	-	0.0	45.8
P_Y	-8.1	12.2	39.1	0.0	-	90.1

Notes:

a See Fig. 4.10 for
labelling system

b Relative to external
 $85\% \text{H}_3\text{PO}_4 = 0.0 \text{ ppm}$

Values shown top left
are for $\text{M} = \text{Pt}$

Values shown bottom
right are for $\text{M} = \text{Pd}$

TABLE 4.8 ^{31}P n.m.r. parameters for the 'AB' diastereomers (structure a)
Fig 4.9) of $[\text{MCl}\{\text{XVI}\}\text{JCl}]$

P_i^a	$\delta(^{31}\text{P}_i)^b$ /ppm	$ J(\text{P}_i\text{P}_i) $ /Hz	$ J(\text{P}_i\text{P}_i) $ /Hz	$ J(\text{P}_i\text{P}_i) $ /Hz	$ J(\text{P}_i\text{P}_i) $ /Hz	$ J(^{195}\text{PtP}_i) $ /Hz
P_A	+61.8 / +65.2	- /	394.3 /	74.6 /	12.2 /	2500.0 /
P_B	+43.9 / +50.1	394.3 /	- /	4.0 /	39.1 /	2426.8 /
P_X	-15.3 / -13.8	74.6 /	4.0 /	- /	0.0 /	45.8 /
P_Y	-8.1 / -8.4	12.2 /	39.1 /	0.0 /	- /	90.1 /

Notes:

a See Fig. 4.10 for
labelling system

b Relative to external
 $85\% \text{H}_3\text{PO}_4 = 0.0 \text{ ppm}$

Values shown top left
are for $\text{M} = \text{Pt}$

Values shown bottom
right are for $\text{M} = \text{Pd}$

TABLE 4.9 ^{31}P n.m.r. parameters for the symmetric diastereomers of $[\text{MCl}(\text{XII})]\text{Cl}$ and $[\text{MCl}(\text{XVI})]\text{Cl}$ (structures b) and c) Fig. 4.9)

COMPLEX	Isotopic composition	M	E	$\delta(^{31}\text{P}_\text{A})$ /ppm	$\delta(^{31}\text{P}_\text{M})$ /ppm	$\delta(^{31}\text{P}_\text{X})$ /ppm	$ J(\text{P}_\text{A}\text{P}_\text{M}) $ /Hz	$ J(\text{P}_\text{M}\text{P}_\text{X}) $ /Hz	$ N $ /Hz	$ J(^{195}\text{Pt}-^{31}\text{P}_\text{A}) $ /Hz	$ J(^{195}\text{Pt}-^{31}\text{P}_\text{M}) $ /Hz	$ J(^{195}\text{Pt}-^{31}\text{P}_\text{X}) $ /Hz
$[\text{PtCl}(\text{XII})]\text{Cl}$	B_2	Pt	P	+48.1	+67.4	-12.6	8.8	0.0	57.9	2450.0	2997.0	91.0
$[\text{PdCl}(\text{XII})]\text{Cl}$	B_2	Pd	P	+53.8	+95.5	-12.1	13.2	2.9	57.2	-	-	-
$[\text{PtCl}(\text{XVI})]\text{Cl}$	B_2	Pt	As	+48.7	-	-10.1	-	-	63.5	2465.8	-	85.4
$[\text{PtCl}(\text{XVI})]\text{Cl}$	A_2	Pt	As	+57.9	-	-12.0	-	-	48.2	2445.0	-	78.0
$[\text{PdCl}(\text{XVI})]\text{Cl}$	B_2	Pd	As	+54.1	-	-10.3	-	-	68.4	-	-	-
$[\text{PdCl}(\text{XVI})]\text{Cl}$	A_2	Pd	As	+61.5	-	-12.3	-	-	39.1	-	-	-

Notes a See Fig. 4.10 for labelling system

b Relative to external 85% $\text{H}_3\text{PO}_4 = 0.0$ ppm

c See Appendix II

region of the P_B nuclei of the AB isomer this diastereomer is termed B₂ type. An analogous reaction was found to occur for the palladium analogue, and again was found to give a mixture of the AB diastereomer and corresponding B₂ isomers.

Reaction of $MCl_2(PhCN)_2$, ($M = Pt, Pd$), with the arsenic-containing ligand XVI was found to result in the formation of all three diastereomeric complexes of formula $[MCl\{XVI\}]^+Cl^-$ for both palladium and platinum. As for the previous complexes of XII both AB and B₂ diastereomers were identified by ^{31}P n.m.r. spectroscopy and as expected the third diastereomers exhibited n.m.r. parameters characteristic of those of the AX fragment of the corresponding AB diastereomers. These diastereomers are therefore termed the A₂ diastereomers, the analogues of which were not formed in the corresponding reactions of the pentaphosphine XII. This classification of the diastereomers now makes it possible to formulate Table 4.10 which shows the diastereomeric distribution pattern of the four reactions studied. It must be remembered,

TABLE 4.10 Approximate isomeric yields of the reactions forming complexes $[MCl\{XII\}]Cl$ and $[MCl\{XVI\}]Cl$ ($M = Pd, Pt$)

COMPLEX	ISOMERIC YIELD/(%)		
	AB	A ₂	B ₂
$[PtCl\{XII\}]Cl$	25	0	75
$[PdCl\{XII\}]Cl$	30	0	70
$[PtCl\{XVI\}]Cl$	40	5	55
$[PdCl\{XVI\}]Cl$	45	25	30

however, that whilst the AB diastereomers may be unequivocally assigned as having the structure of Fig. 4.9a) it is not possible to assign A₂

or \underline{B}_2 to either of the remaining structures since their spin-systems are identical.

In discussing the ^{31}P n.m.r. spectra of the different species it is convenient to treat the asymmetric (AB) and symmetric (\underline{B}_2 and \underline{A}_2) diastereomers separately since they have different spin-systems. The AB diastereomers exhibit ABMXY ^{31}P spectra for complexes of the penta-tertiaryphosphine ligand XII and ABXY spectra for complexes of the tetratertiary phosphine/arsine ligand XVI (Fig 4.10). The presence of the P_M nucleus merely gives rise to a simple doublet-splitting of the P_A , P_B , P_X and P_Y resonances and therefore the analyses of the two systems run along parallel lines. In general it was found possible to obtain a set of apparent values of the various ^{31}P n.m.r. parameters simply by inspection of the spectra. However, computer simulation of the n.m.r. spectra revealed that these were not always the true values. In such systems the presence of the large P_A - P_B coupling combined with the relative similarity of $\delta(^{31}\text{P}_\text{A})$ and $\delta(^{31}\text{P}_\text{B})$ leads to the partial averaging of certain coupling constants. In general this phenomenon leads to values of $J(\text{P}_\text{B}\text{P}_\text{X})$ read off the experimental spectrum being artificially high compared to the computer-generated values, and to values of $J(\text{P}_\text{A}\text{P}_\text{X})$ being correspondingly low. This problem was found to occur for all four AB diastereomers and computer simulation techniques were widely employed to obtain accurate values for the n.m.r. parameters (Tables 4.7 to 4.9). The parameters that define the AX and BY systems and indeed the other parameters are generally comparable for all four systems and this suggests similar configurations for them. Low values of $J(\text{P}_\text{A}\text{P}_\text{M})$ and $J(\text{P}_\text{B}\text{P}_\text{M})$ are consistent with other low values for five-membered chelate-ring systems as previously discussed. Phosphorus atom P_M is also characteristic in having a large positive coordination chemical shift ($\Delta = \text{ca } +100 \text{ ppm and } +130 \text{ ppm for}$

Pt and Pd respectively) which is therefore consistent with its being incorporated in two separate five-membered chelate-rings.

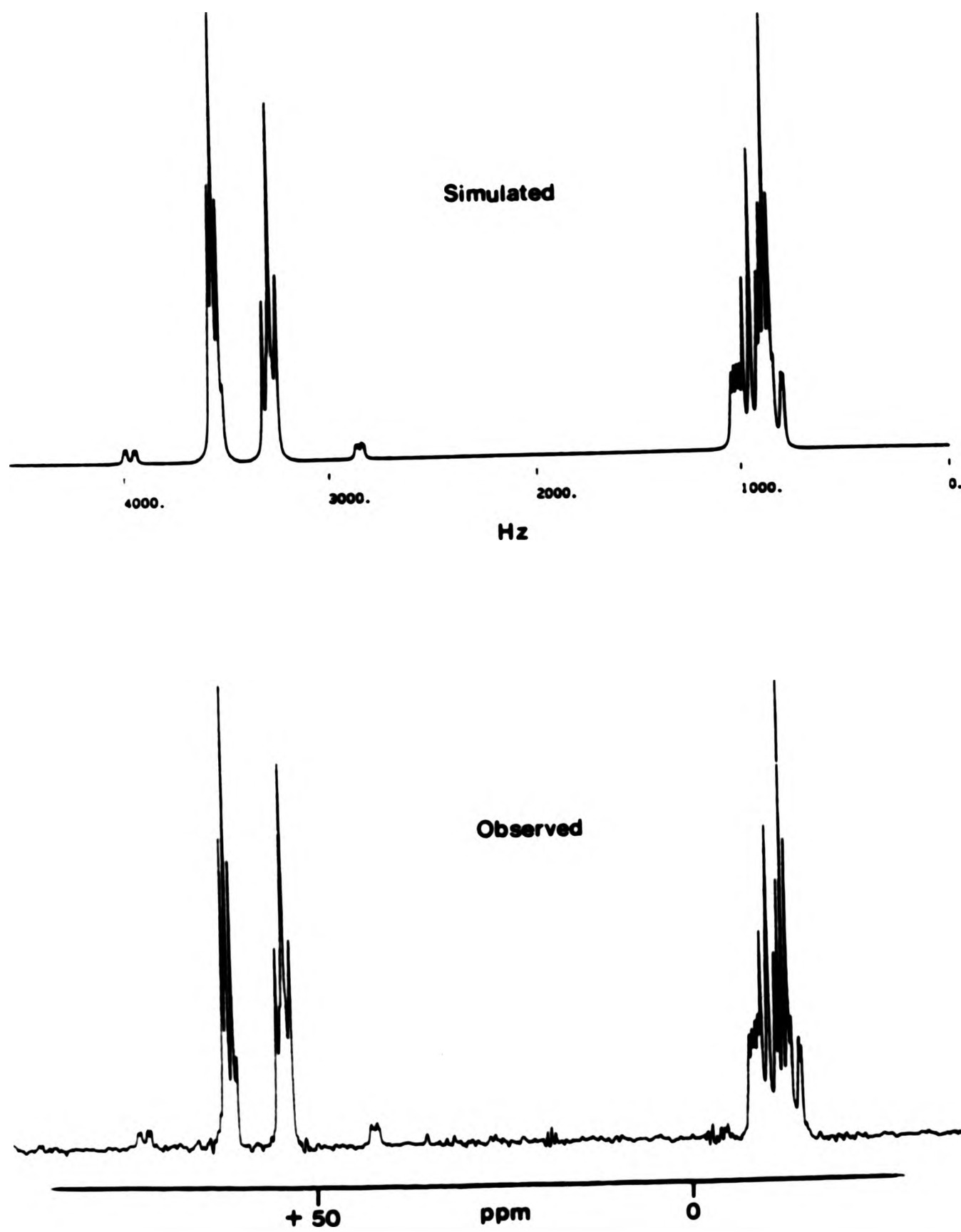
The \underline{A}_2 and \underline{B}_2 diastereomers have AA'MXX' and AA'XX' phosphorus spin-systems for complexes of XII and XVI respectively (Fig. 4.10). As for the previous cases the presence of P_M in complexes of XII merely results in the resonances of P_A and P_X being split into doublets, and therefore the analyses of both these systems are comparable. (A brief description of the appearance and analysis of AA'XX' spectra is given in Appendix II). In general, in these symmetrical systems the presence of a large P_A-P_A coupling and a small (zero) P_X-P_X coupling results in both the P_A and P_X resonances appearing deceptively as triplets or near triplets so that the observation of the weak outer lines required for a full analysis was not possible. In such cases it is possible to obtain accurately only the parameter $|N|$ which is defined by Eq 4.6

$$|N| = |J_{AX} + J_{AX'}| \quad (4.6)$$

although it is reasonable to assume $J(P_X P_{X'}) = 0$ Hz and that $J(P_A P_B) \approx 400$ Hz by analogy with corresponding \underline{AB} isomers. The deceptive simplicity of the spectra also prevents a breakdown of $|N|$ into its two component couplings although reasonable estimates of these may also be made by consideration of the \underline{AB} isomers.

The simplest ^{31}P spectrum to analyse at sight is that of $[\text{PdCl}\{\text{XVI}\}]^+\text{Cl}^-$ and this is therefore provided as an example in Fig. 4.11 along with a computer simulated ^{31}P spectrum. The AA' and XX' resonances of the symmetric \underline{A}_2 and \underline{B}_2 isomers appear deceptively as triplets for reasons previously described, and lie in chemical shift positions characteristic of their isomer type. This spectrum clearly demonstrates the applicability of the descriptive \underline{A}_2 , \underline{B}_2 and \underline{AB} terminology for these systems. The spectra of the other complexes

Fig. 4.11 Observed and simulated ^{31}P spectra of the diastereomeric mixture of $[\text{PdCl}\{\text{XVI}\}]\text{Cl}$



studied show analogous features but are more difficult to recognize at first sight due to the increased complexity of their spin-systems.

¹⁹⁵Pt n.m.r. data

The ¹⁹⁵Pt n.m.r. spectrum of [PtCl{XVI}]⁺Cl⁻ (Fig. 4.12) shows clearly the presence of all three diastereomers which were easily identified by their characteristic values of $\bar{J}({}^{195}\text{Pt}-{}^{31}\text{P})$. A ¹⁹⁵Pt spectrum of a mixture of isomers of [PtCl{XII}]⁺Cl⁻ was also found to be consistent with that expected from the structures of the complexes. These spectra confirm the values of $\bar{J}({}^{195}\text{Pt}-{}^{31}\text{P})$ for the different species and from them the ¹⁹⁵Pt chemical shifts were obtained (Table 4.11). The results indicate that $\delta({}^{195}\text{Pt})$ for the arsenic-

TABLE 4.11 ¹⁹⁵Pt chemical shifts for the platinum complexes of XII and XVI

Complex	Diastereomer type	$\delta({}^{195}\text{Pt})^a$ /ppm
[PtCl{XII}]Cl	AB	-280.4
[PtCl{XII}]Cl	B ₂	-311.9
[PtCl{XVI}]Cl	AB	-421.7
[PtCl{XVI}]Cl	A ₂	-449.0
[PtCl{XVI}]Cl	B ₂	-409.3

Notes a Relative to 21.4 MHz when the ¹H resonance of TMS is at exactly 100 MHz

containing complexes is generally of the order of 100-150 ppm to lower frequency than those of analogous pentaphosphine species. This appears to contradict results of previous workers for complexes of

Fig. 4.12 ^{195}Pt spectrum of $[\text{PtCl}(\text{XVI})]\text{Cl}$ recorded at 19.2 MHz showing the presence of the AB, A₂ and B₂ diastereomers

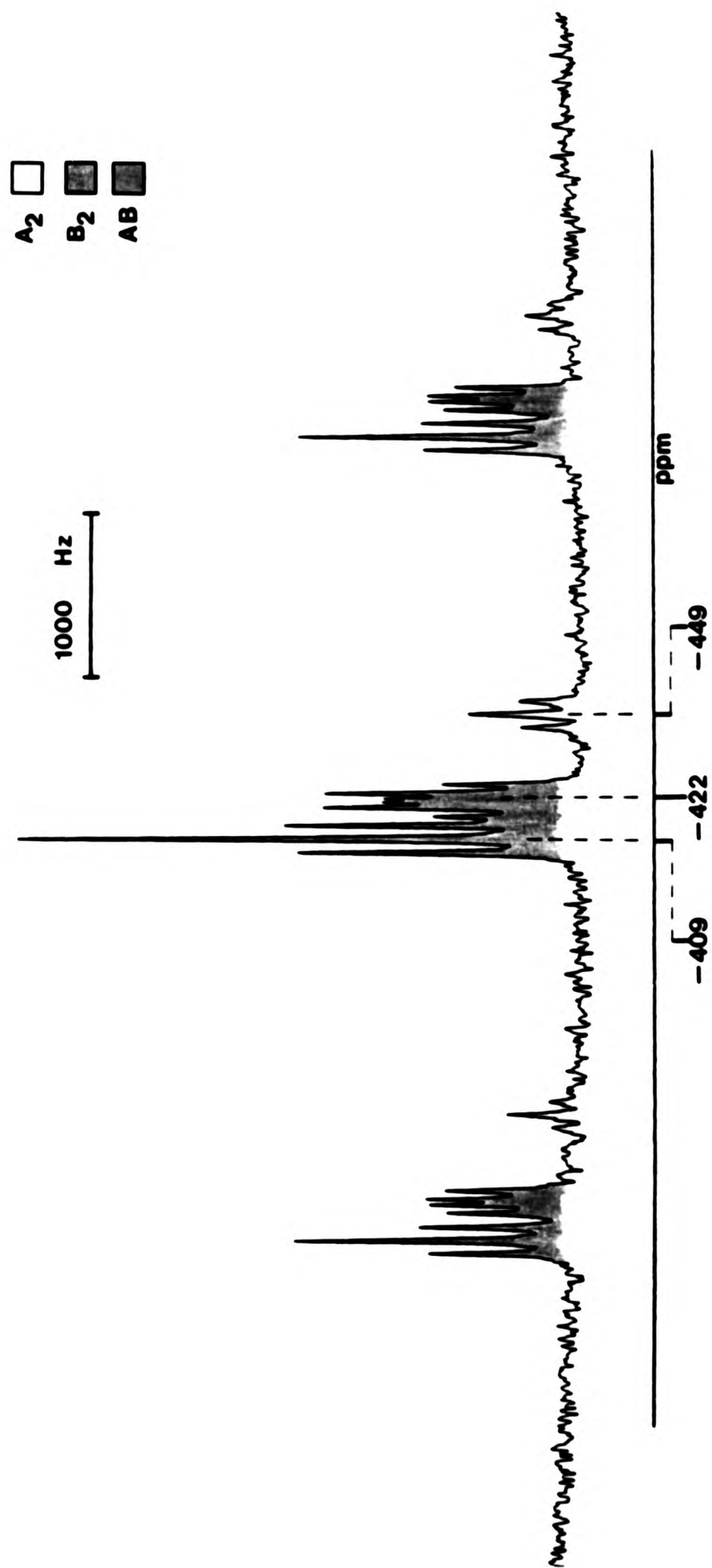
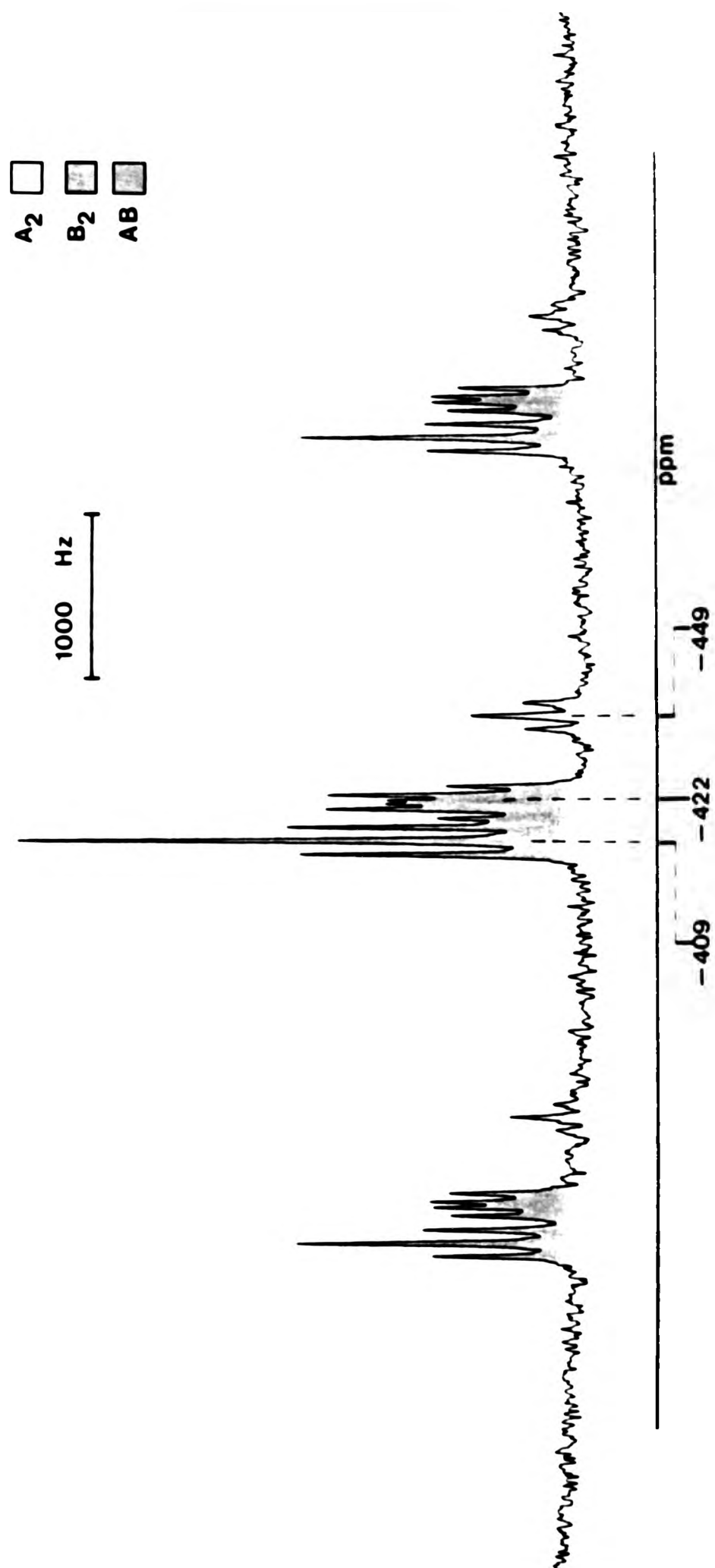


Fig. 4.12 ^{195}Pt spectrum of $[\text{PtCl}(\text{XVI})\text{Cl}]$ recorded at 19.2 MHz showing the presence of the AB, A2 and B2 diastereomers



non-chelating ligands which generally reveal an opposite effect of approximately the same magnitude^{85,86}. However it is possible that differences in ring-strain between analogous pentaphosphine and tetraphosphinoarsine complexes play a more significant role in the determination of chemical shifts and therefore these rather small effects are difficult to quantify.

CHAPTER 5

1,1-BIS(DIPHENYLPHOSPHINO)ETHENE (I) AS A BRIDGING LIGAND IN BINUCLEAR PALLADIUM AND PLATINUM COMPLEXES

1. INTRODUCTION

The recently discovered ability of the bidentate phosphine ligand bis(diphenylphosphino)methane, (dppm), to bridge two metal centres has led to a wealth of reported literature in this area and the range of different binuclear complexes of this sort is now extensive⁸⁷. This chapter begins with a brief review of the chemistry of some of the better-known binuclear complexes of dppm and then moves on to investigate the comparable bridging behaviour of the related ligand 1,1-bis(diphenylphosphino)ethene (I) which is of particular importance here as it is the precursor of the new polyphosphorus ligands reported in this thesis.

2. DPPM AS A BRIDGING LIGAND

The ability of dppm to form a variety of bridged bimetallic complexes such as that in Fig. 5.1 has been well documented. The best studied type of complex are the palladium and platinum species, and although many different syntheses are available for these^{88,89}, perhaps the simplest involves reaction between M(0) and M(II) compounds in the

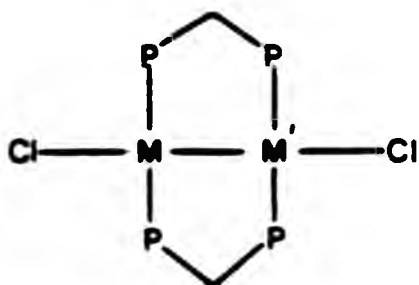
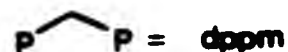


Fig 5.1



presence of the free ligand, dppm^{90} . These dppm bridged complexes are generally reactive in different ways:

(i) Insertion into the M-M bond

Small molecules such as CO , SO_2 etc can, under mild conditions, reversibly insert into the M-M bonds of bimetallic species to form the so-called 'A-frame' complexes as shown in Fig. 5.2^{91,92}. Other species such as CH_2 , CS_2 etc insert irreversibly under somewhat more forcing conditions⁹³⁻⁹⁵.

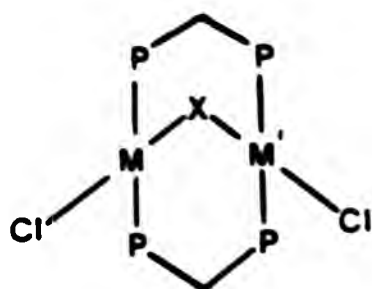


Fig 5.2



(ii) Displacement of terminal Cl ligands

The terminal chloride groups in these bridged complexes may be readily replaced by a wide range of neutral ligands such as NH_3 , PR_3 , pyridine etc to form ionic species that have generally been found to be better stabilised by large counter-ions such as $(\text{PF}_6)^-$ (Fig. 5.3)⁹⁶. Replacement of chloride groups on A-Frame complexes is also readily achieved in a similar manner⁹⁷.

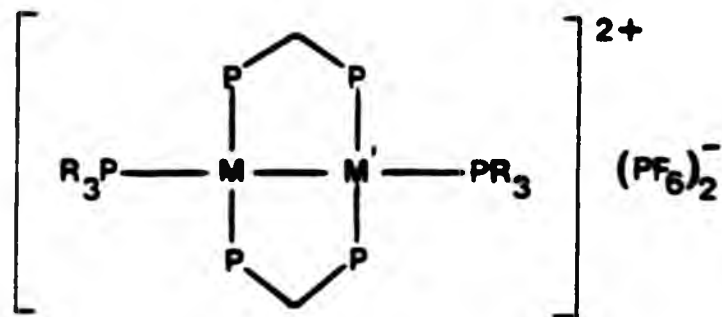
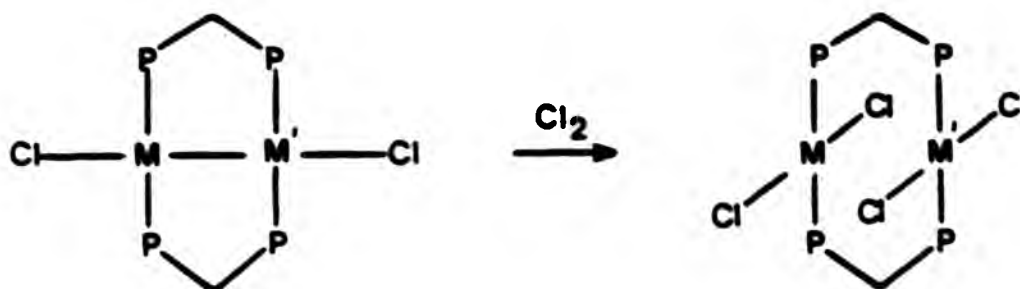


Fig 5.3

(iii) Oxidative addition

Oxidative addition reactions such as those shown below occur rapidly for Cl_2 , Br_2 and I_2 , and lead initially to species without a



M-M bond⁹⁸. However, these complexes gradually rearrange to simple monomeric products and therefore reactions such as these are of little significance in this chapter.

3. RESULTS AND DISCUSSION

(A) Syntheses

Treatment of equimolar amounts of $\text{Pd}_2(\text{dba})_3 \cdot \text{CHCl}_3$ and $\text{Pd}(\text{PhCN})_2\text{Cl}_2$ with two equivalents of 1,1-bis(diphenylphosphino)ethene, (I), in refluxing dichloromethane resulted in the formation of the new bridged dipalladium species $\text{Pd}_2\{\text{I}\}_2\text{Cl}_2$ (Fig. 5.4) as air-stable orange-red crystals in good yield. The reaction using $\text{Pt}(\text{PhCN})_2\text{Cl}_2$ in place of

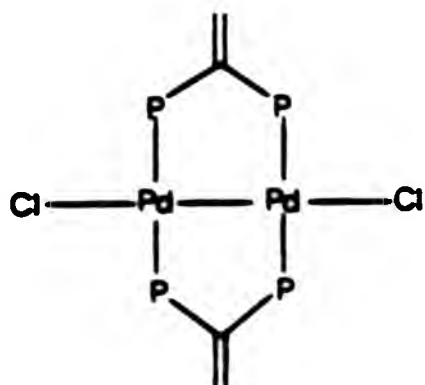
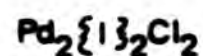


Fig 5.4

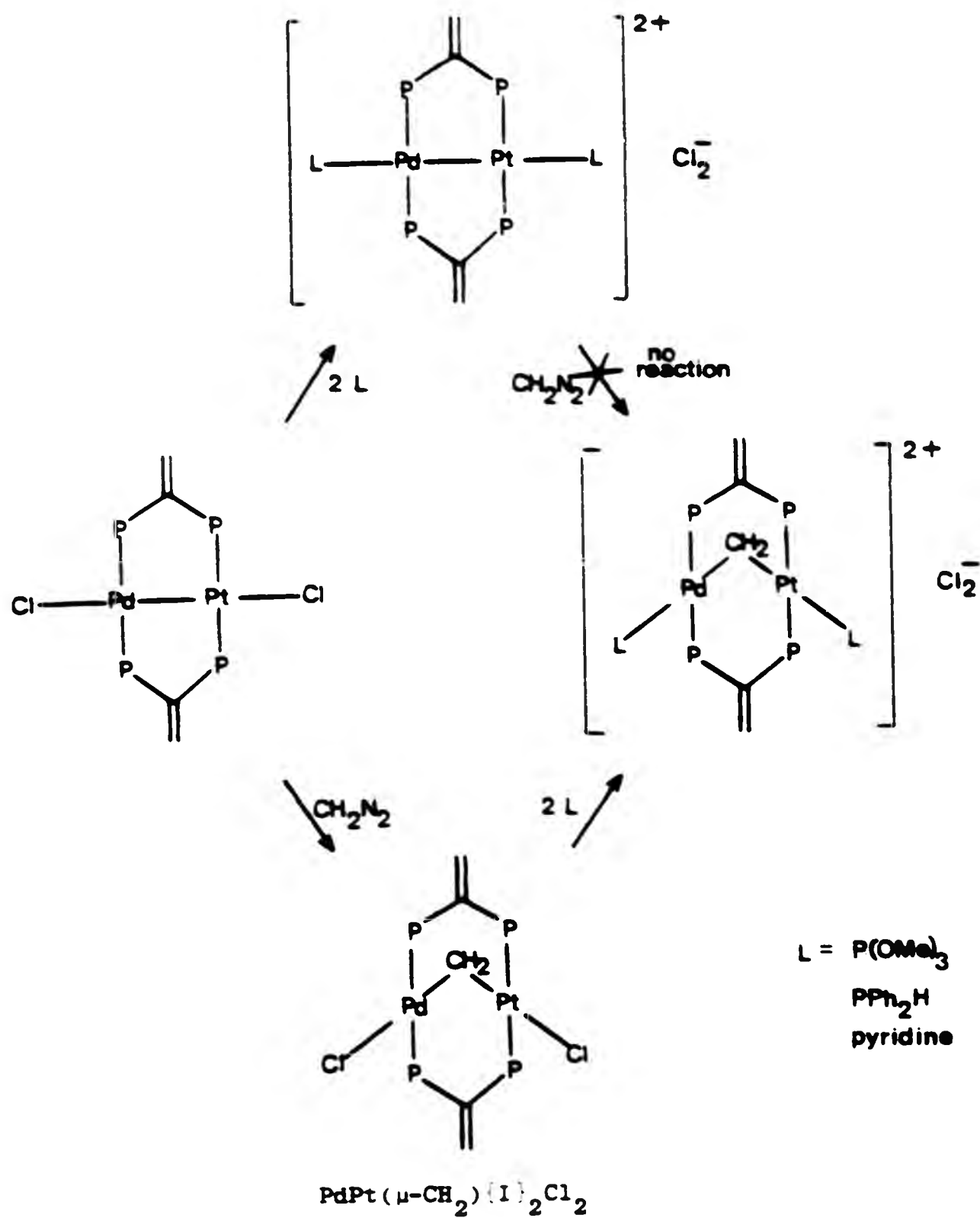


$\text{Pd}(\text{PhCN})_2\text{Cl}_2$ afforded the corresponding mixed metal complex $\text{PdPt}(\text{I})_2\text{Cl}_2$ as air-stable orange crystals in good yield.

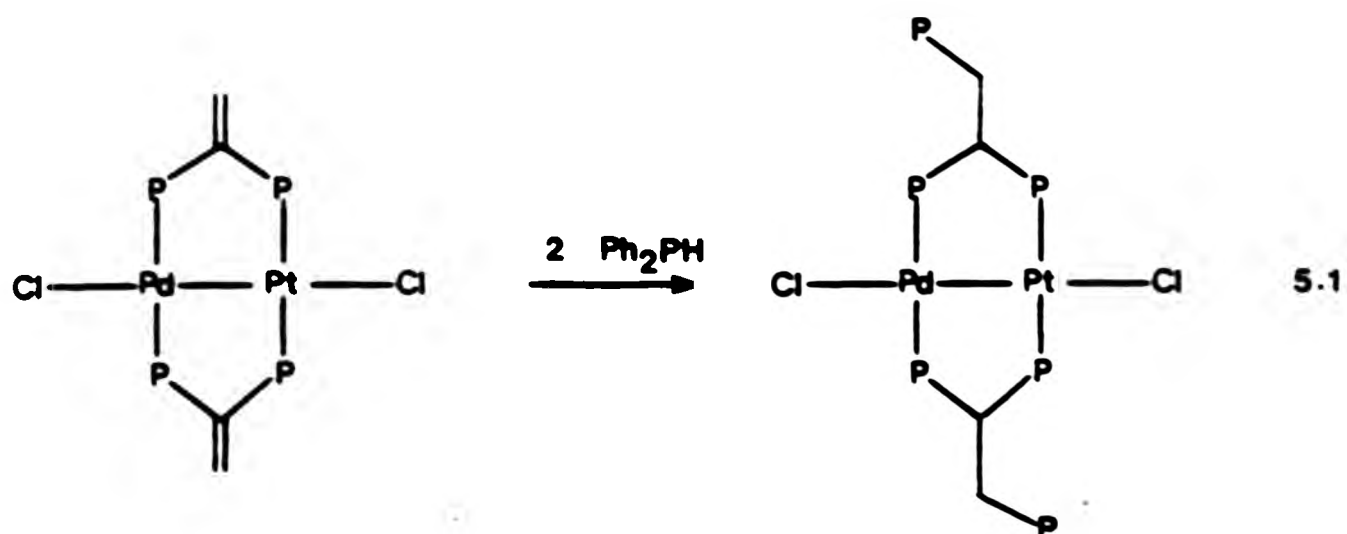
Treatment of $\text{PdPt}(\text{I})_2\text{Cl}_2$ with an excess of trimethylphosphite in methanol followed by the addition of excess ammonium hexafluorophosphate produced the new ionic complex $[\text{PdPt}(\text{I})_2\{\text{P}(\text{OMe})_3\}]^{2+}(\text{PF}_6)^{-}_2$ as air-stable red crystals. Similar reactions using diphenylphosphine or pyridine in place of trimethylphosphite were also found to occur, and the corresponding dipalladium complex was found to undergo analogous displacement reactions. (Scheme 5.1)

Treatment of $\text{PdPt}(\text{I})_2\text{Cl}_2$ with excess diazomethane in ether at low temperature resulted in the formation of the new A-frame complex $\text{PdPt}(\mu\text{-CH}_2)(\text{I})_2\text{Cl}_2$ (Scheme 5.1) as air-stable orange-yellow crystals. An analogous reaction is also available for the dipalladium complex, but treatment of the related ionic complexes with excess diazomethane failed to give the corresponding ionic A-frame species. (This apparent decrease in reactivity of the M-M bond upon replacement of the terminal chloride groups by neutral ligands has been previously reported for similar complexes of dppm^{96} . Treatment of $\text{PdPt}(\mu\text{-CH}_2)(\text{I})_2\text{Cl}_2$ with excess trimethylphosphite and subsequent addition of ammonium hexafluorophosphate, however, did result in the formation of the new ionic A-frame complex $[\text{PdPt}(\mu\text{-CH}_2)(\text{I})_2\{\text{P}(\text{OMe})_3\}]^{2+}(\text{PF}_6)^{-}_2$. (Scheme 5.1).

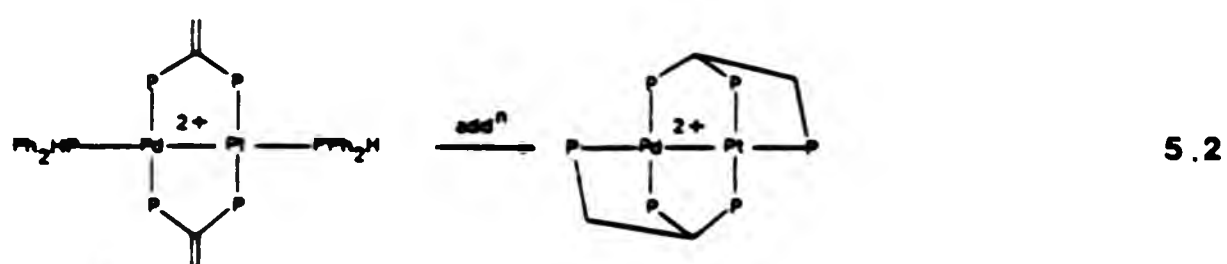
The presence of the carbon-carbon double bonds in these complexes provides the potential for a fourth type of reaction, namely, addition across the double bond to form bridged complexes incorporating the triphosphine ligand, 1.1.2-tris(diphenylphosphino)ethane, (II), (Eq. 5.D). Many attempts to form such complexes were undertaken but all produced deep-red products of low solubility which from their ^{31}P spectra appeared to be polymeric in nature. Internal addition reactions of



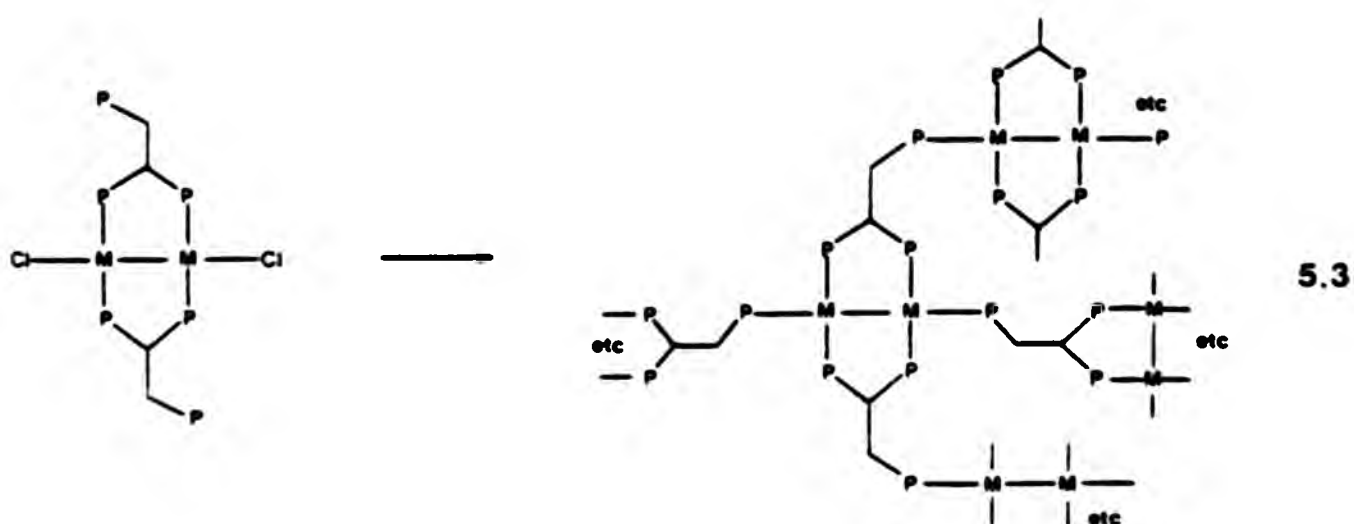
SCHEME 5.1 Reactions of $\text{PdPt}(\text{I})_2\text{Cl}_2$ and related species (analogous reactions occur for the corresponding dipalladium complexes)



the type shown in Eq. 5.2 were also attempted, but these led to similar polymeric products. From the ^{31}P spectra of the reaction mixtures it



was clear that addition had occurred since no proton-bearing phosphorus compounds were present, but a full analysis of these spectra was impossible. It is reasonable that replacement reactions involving the free phosphorus atom takes place after addition (Eq. 5.3) but the degree to which polymerisation may take place is unknown and the range of different species is potentially very large. Use of the free



ligand II as a starting reagent was also tried but this led, invariably, to the formation of monomeric species such as those described in Chapter Three.

(B) Characterisation by n.m.r.

Each of the dipalladium species $\text{Pd}_2\{\text{I}\}_2\text{Cl}_2$, $\text{Pd}_2(\mu\text{-CH}_2)\{\text{I}\}_2\text{Cl}_2$ and $[\text{Pd}_2\{\text{I}\}_2\{\text{pyr}\}_2](\text{PF}_6)_2$ contains four chemically equivalent phosphorus nuclei, and consequently their ^{31}P n.m.r. spectra consist of singlets revealing only the values of the chemical shift shown in Table 5.1. The ^{13}C spectra for these species are a little more informative. For instance, the ^{13}C spectrum of $[\text{Pd}_2\{\text{I}\}_2\{\text{pyr}\}_2]^{2+}(\text{PF}_6)_2$ (Fig. 5.5) shows the resonances due to the o, m and p phenyl-group carbons as simple quintets, indicative of large P-P couplings in the system⁵³. Insertion of a bridging CH_2 group into the molecule induces chemical inequivalence with respect to the two sides of the Pd_2P_4 plane of atoms (Fig. 5.6) resulting in two chemically inequivalent types of phenyl-group, and this is clearly demonstrated in the ^{13}C n.m.r. spectrum of $\text{Pd}_2(\mu\text{-CH}_2)\{\text{I}\}_2\text{Cl}_2$ (Fig. 5.7).

The dipalladium complexes that contain terminal phosphorus ligands have AA'A''A'''XX' phosphorus spin systems (Fig. 5.8). The appearance of spectra from these systems can be unduly complicated since large numbers of resonances are often coincident or nearly coincident. Thus, from the ^{31}P spectra of the two ionic complexes $[\text{Pd}_2\{\text{I}\}_2\{\text{P}(\text{OMe})_3\}_2]^{2+}(\text{PF}_6)_2^-$ and $[\text{Pd}_2\{\text{I}\}_2\{\text{PPh}_2\text{H}\}_2]^{2+}(\text{PF}_6)_2^-$ it was found possible to obtain only the chemical shifts of the two types of phosphorus present in the molecule (Table 5.1).

Fig. 5.5 ^{13}C spectrum of $[\text{Pd}_2(\text{I})_2(\text{pyr})_2](\text{PF}_6)_2$ recorded at 22.5 MHz

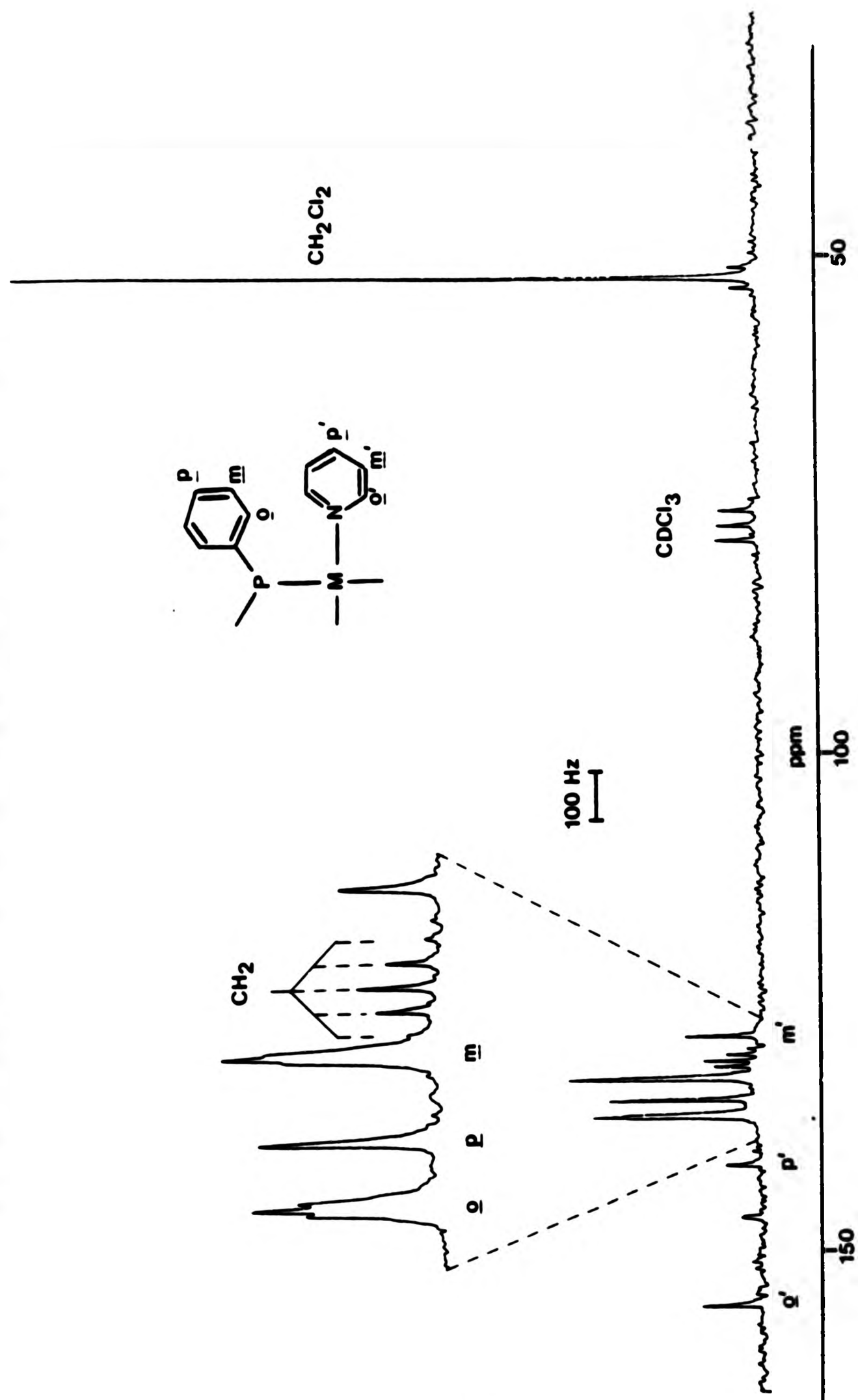


Fig. 5.6 Projection along the M-M bond in $\text{Pd}_2(\mu\text{-CH}_2)\{\text{I}\}_2\text{Cl}_2$

Fig. 5.7 ^{13}C spectrum of $\text{Pd}_2(\mu\text{-CH}_2)\{\text{I}\}_2\text{Cl}_2$ showing the two inequivalent types of phenyl groups

Fig 5.6

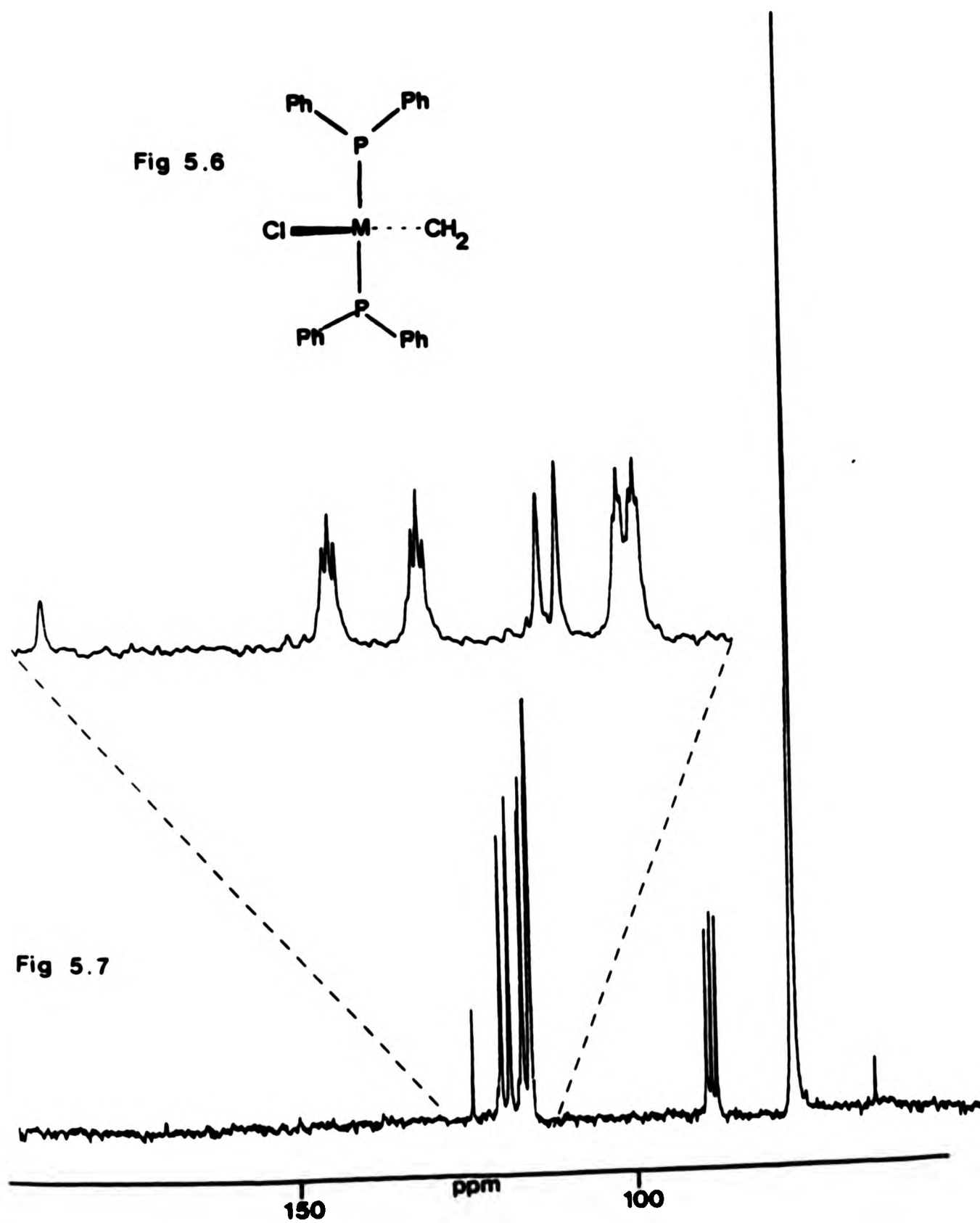
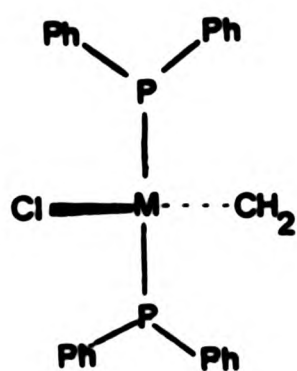


Fig 5.7

TABLE 5.1 ^{31}P chemical shifts for the dipalladium complexes of I

COMPLEX	$\delta(^{31}\text{P}_\text{A})^\text{b}$ /ppm	$\delta(^{31}\text{P}_\text{X})^\text{b}$ /ppm
$\text{Pd}_2\{\text{I}\}_2\text{Cl}_2$	+14.1	-
$\text{Pd}_2(\mu\text{-CH}_2)\{\text{I}\}_2\text{Cl}_2$	+26.2	-
$[\text{Pd}_2\{\text{I}\}_2(\text{pyr})_2](\text{PF}_6)_2$	+13.3	-
$[\text{Pd}_2\{\text{I}\}_2\{\text{P}(\text{OMe})_3\}_2](\text{PF}_6)_2$	+18.1	+98.7
$[\text{Pd}_2\{\text{I}\}_2(\text{PPh}_2\text{H})_2](\text{PF}_6)_2$	+17.1	-19.7

Notes: a See Fig. 5.8 for labelling system.

b Relative to external 85% $\text{H}_3\text{PO}_4 = 0.0$ ppm

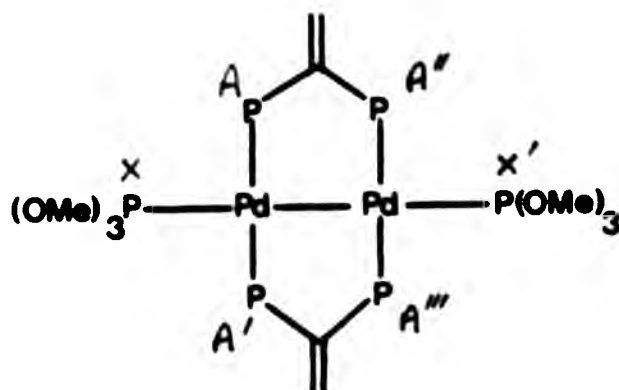


Fig 5.8

The ^{31}P spectrum of $\text{PdPt}\{\text{I}\}_2\text{Cl}_2$ (Fig. 5.9) may be readily analysed by inspection of the resonances due to phosphorus in molecules containing the ^{195}Pt isotope ($I = \frac{1}{2}$ nat. abundance 33.8%)⁹⁹. The presence of this isotope brings about large effective chemical shift changes of the phosphorus nuclei thus simplifying analysis of the spectrum. These well separated features (shaded blue) each correspond to one half of an AA'XX' spectrum and thus were analysed by inspection⁵³ (see Appendix II) giving the parameters shown in Table 5.2.

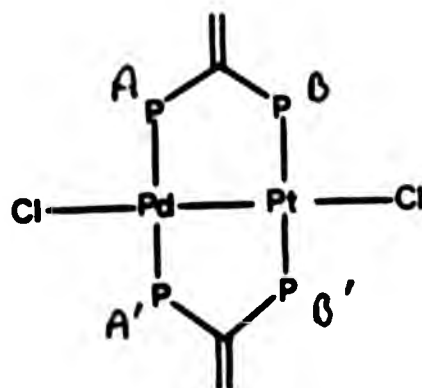


Fig 5.10

Fig. 5.9 Observed and simulated ^{31}P
spectra of $\text{PdPt}(\text{I})_2\text{Cl}_2$

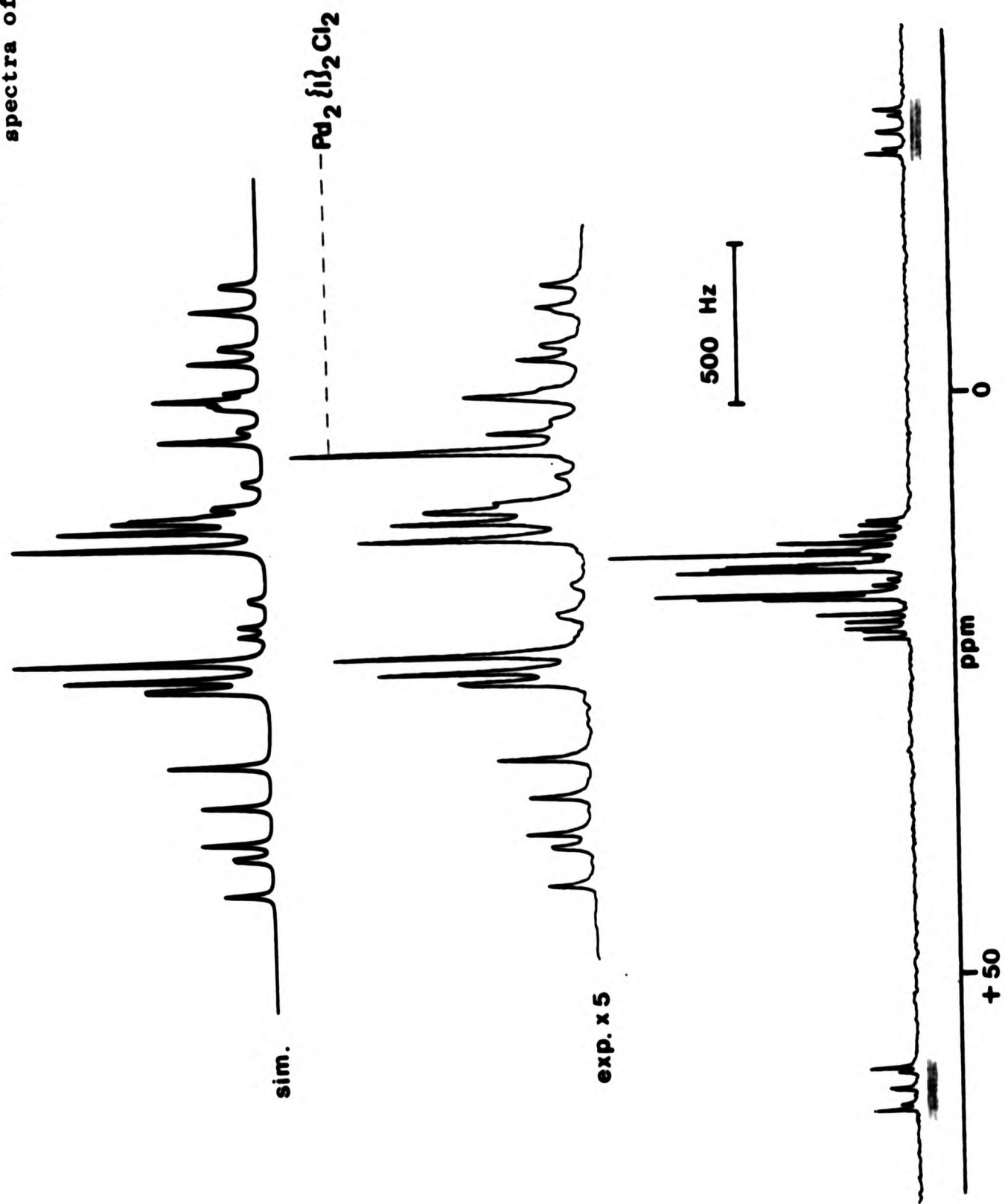


TABLE 5.2 ^{31}P n.m.r. data for some mixed Pd/Pt complexes of I

Complex ^a	$\delta(^{31}\text{P}_\text{A})$ ^b /ppm	$\delta(^{31}\text{P}_\text{B})$ ^b /ppm	$ J(\text{P}_\text{A}\text{P}_\text{B}) $ /Hz	$ J(\text{P}_\text{A}\text{P}_\text{B},.) $ /Hz	$J(^{195}\text{Pt}-\text{P}_\text{A})$ /Hz	$J(^{195}\text{Pt}-\text{P}_\text{B})$ /Hz
$\text{PdPt}\{\text{I}\}_2\text{Cl}$ ^c	+14.1	+19.1	119.5	14.5	-68.4	+2976
$[\text{PdPt}\{\text{I}\}_2(\text{pyr})_2](\text{PF}_6)_2$ ^c	+9.8	+18.8	120.9	15.3	-78.5	+2880
$\text{PdPt}(\mu\text{-CH}_2)\{\text{I}\}_2\text{Cl}_2$ ^c	+22.5	+26.1	71.8	10.0	0	+3262

Notes a See Fig. 5.10 for labelling system

b Relative to external 85% $\text{H}_3\text{PO}_4 = 0.0$ ppmc $J(\text{P}_\text{A}\text{P}_\text{B},.) \sim J(\text{P}_\text{B}\text{P}_\text{B},.) \sim 400$ Hz

In general the ^{31}P n.m.r. parameters are little affected by a change of terminal group from $\text{Cl} \rightarrow \text{pyr}$, and this feature is repeated for complexes containing terminal phosphorus groups (see later).

Large effects are however found upon insertion of CH_2 into the Pd-Pt bond. In the Pd-Pt bonded species values of $J(\text{P}_\text{A}\text{P}_\text{B})$ may be considered as the sum of two components; $^2J(\text{P}_\text{A}\text{P}_\text{B})$ through the carbon atom and $^3J(\text{P}_\text{A}\text{P}_\text{B})$ through the metal-metal bond. Removal of this 'through-the-metals' coupling route upon insertion of CH_2 may account for the observed decrease in $J(\text{P}_\text{A}\text{P}_\text{B})$ although the effects of changing the $\text{P}_\text{A}-\text{C}-\text{P}_\text{B}$ inter-bond angle may also be important. It is interesting that the sign of $J(^{195}\text{Pt}-\text{P}_\text{A})$ in all the Pd-Pt bonded species is negative. These couplings may also be considered as the sum of two components; $^2J(\text{Pt}-\text{Pd}-\text{P}_\text{A})$ and $^3J(\text{Pt}-\text{P}_\text{A}-\text{C}-\text{P}_\text{A})$. From other related complexes (e.g. $\text{PtCl}_2[\text{X}]\text{d}$) it was found that $^3J(^{195}\text{Pt}-^{31}\text{P})$ is generally of the order of +80 Hz and it is therefore possible that the 'through the metals' coupling component is of the order of -150 Hz. Conversion of this two bond route into a three bond route by insertion of CH_2 will obviously radically affect the magnitude of one of the contributions to the coupling, and thus the zero value of $J(^{195}\text{Pt}-\text{P}_\text{A})$ observed in $\text{PdPt}(\mu\text{-CH}_2)\{\text{I}\}_2\text{Cl}_2$ may arise from the two contributions having equal magnitudes but opposite signs. Overall therefore it is clear that changes of terminal group do not greatly affect n.m.r. parameters but that insertion reactions do.

If the terminal chloride groups are replaced by phosphorus-containing ligands as in $[\text{PdPt}\{\text{I}\}_2\{\text{P}(\text{OMe})_3\}](\text{PF}_6)_2$ the six phosphorus atoms in the molecule constitute an ABXX'YY' spin-system (Fig. 5.12)⁵³. As for the previous cases the ^{31}P n.m.r. spectrum of this complex (Fig. 5.13) was analysed by consideration of the ^{195}Pt satellites and gave the n.m.r. parameters shown in Tables 5.3 and 5.4. These tables also

Fig. 5.13 ^{31}P spectrum of $[\text{PdPt}\{\text{I}\}_2\{\text{P}(\text{OMe})_3\}_2](\text{PF}_6)_2$
recorded at 36.2 MHz

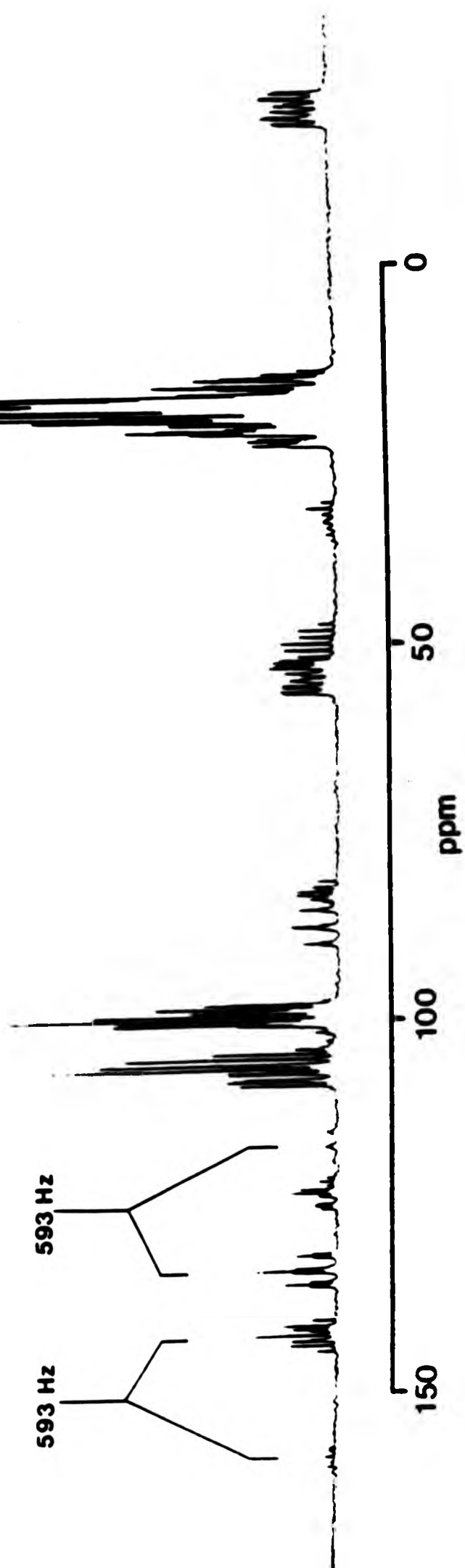
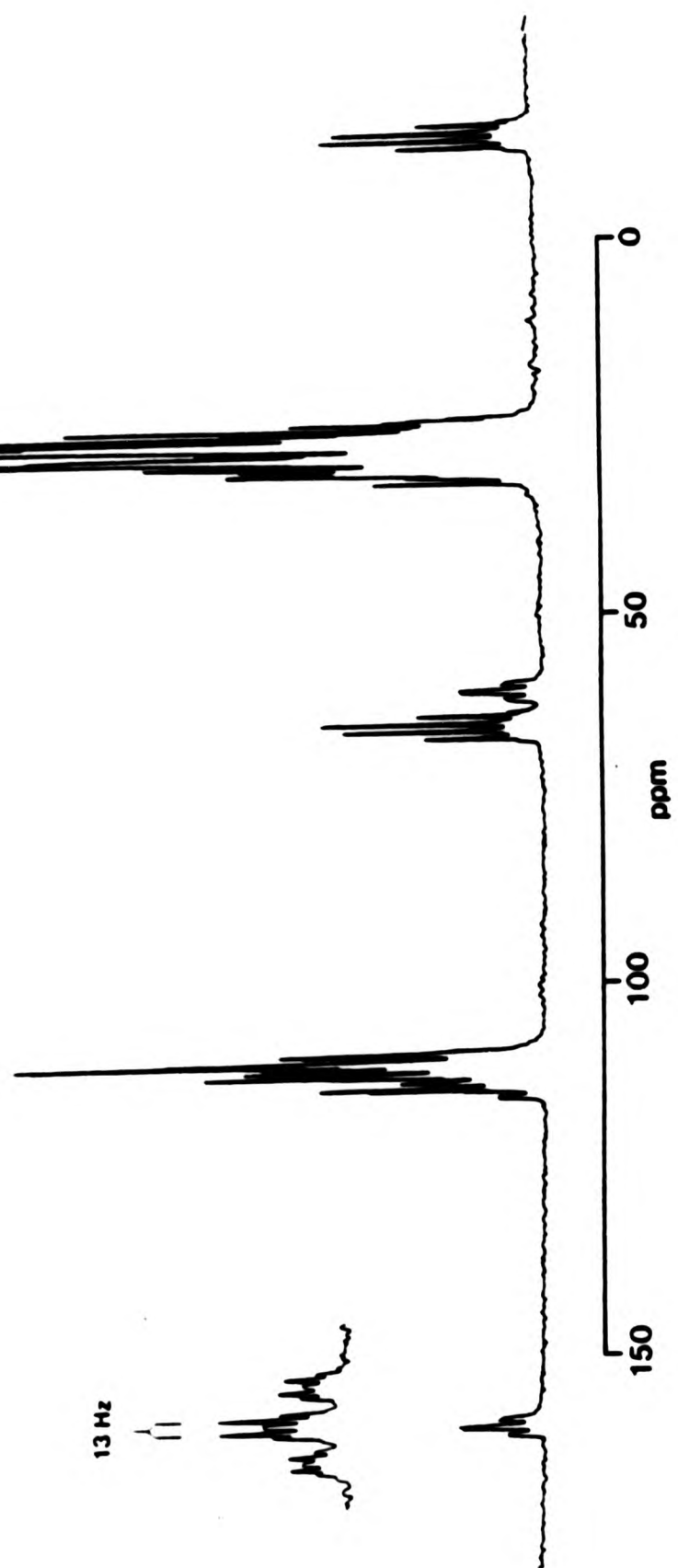


Fig. 5.14 ^{31}P spectrum of $[\text{PdPt}(\mu\text{-CH}_2)\{\text{I}\}_2\{\text{P}(\text{OMe})_3\}_2](\text{PF}_6)_2$
recorded at 36.2 MHz



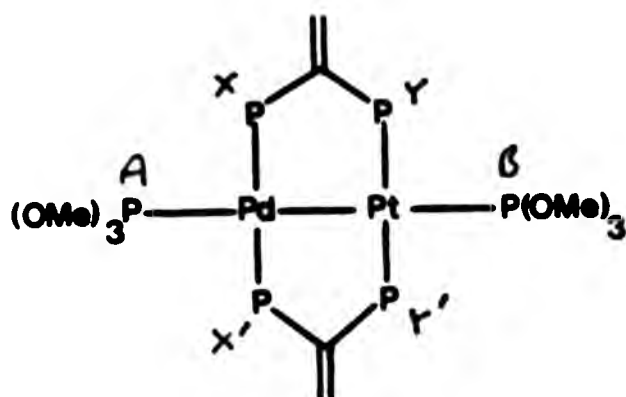


Fig 5.12

TABLE 5.3 ^{31}P chemical shift data for some mixed Pd/Pt complexes of I

Complex ^a	$\delta(^{31}\text{P}_\text{A})$ /ppm	$\delta(^{31}\text{P}_\text{B})$ /ppm	$\delta(^{31}\text{P}_\text{X})$ /ppm	$\delta(^{31}\text{P}_\text{Y})$ /ppm
$[\text{PdPt}\{\text{I}\}_2\{\text{P}(\text{OMe})_3\}_2](\text{PF}_6)_2$	+110.0	+94.6	+19.9	+16.6
$[\text{PdPt}\{\text{I}\}_2(\text{PPh}_2\text{H})_2](\text{PF}_6)_2$	-16.8	-10.6	+16.8	+16.2
$[\text{PdPt}(\mu\text{-CH}_2)\{\text{I}\}_2\{\text{P}(\text{OMe})_3\}_2](\text{PF}_6)_2$	+115.0 ^c	+110.7	+32.0 ^c	+27.2

Notes a See Fig. 5.12 for labelling system

b Relative to external 85% $\text{H}_3\text{PO}_4 = 0.0$ ppm

c ± 2 ppm - accurate values could not be obtained due to the complexity of the spectrum

give the parameters derived from the spectra of the related complexes $[\text{PdPt}(\mu\text{-CH}_2)\{\text{I}\}_2\{\text{P}(\text{OMe})_3\}_2](\text{PF}_6)_2$ (Fig. 5.14) and $[\text{PdPt}\{\text{I}\}_2(\text{PPh}_2\text{H})_2](\text{PF}_6)_2$ which have similar spin-systems. Of particular interest in these species are the values of $J(\text{P}_\text{A}-\text{P}_\text{B})$. The difference between $J(\text{P}_\text{A}-\text{P}_\text{B})$ for $[\text{PdPt}\{\text{I}\}_2\{\text{P}(\text{OMe})_3\}_2](\text{PF}_6)_2$ and $[\text{PdPt}\{\text{I}\}_2(\text{PPh}_2\text{H})_2](\text{PF}_6)_2$, (593 and 225 Hz respectively) probably arises mainly from the different s-electron densities at the two phosphorus nuclei arising from different substituent electronegativities as described in Chapter One⁴². The large value

TABLE 5.4 ^{31}P coupling constants for some mixed Pd/Pt complexes of I

Complex ^a	$ J(\text{P}_\text{A}\text{P}_\text{B}) $ /Hz	$ J(\text{P}_\text{A}\text{P}_\text{X}) $ /Hz	$ J(\text{P}_\text{A}\text{P}_\text{Y}) $ /Hz	$ J(\text{P}_\text{B}\text{P}_\text{X}) $ /Hz	$ J(\text{P}_\text{B}\text{P}_\text{Y}) $ /Hz	$ J(\text{P}_\text{X}\text{P}_\text{Y}) $ /Hz	$ J(\text{P}_\text{X}\text{P}_\text{Y}') $ /Hz	$ J(\text{Pt-P}_\text{A}) $ /Hz	$ J(\text{Pt-P}_\text{B}) $ /Hz	$ J(\text{Pt-P}_\text{X}) $ /Hz	$ J(\text{Pt-P}_\text{Y}) $ /Hz
$[\text{PdPt}(\text{I})_2\{\text{P}(\text{OMe})_3\}_2](\text{PF}_6)_2$	593.0	89.0	7.8	66.3	33.1	110.0	12.0	1215	3765	0	2723
$[\text{PdPt}(\text{I})_2(\text{PPh}_2)_2](\text{PF}_6)_2$	225.0	44.5	5.8	21.1	24.2	110.0	10.0	893	1945	0	2702
$[\text{PdPt}(\mu\text{-CH}_2)(\text{I})_2\{\text{P}(\text{OMe})_3\}_2](\text{PF}_6)_2$	12.6	70.0	0	4.9	37.5	68.0	5.0	78.0	3557	16.7	2845

of $J(P_A P_B)$ in the $P(OMe)_3$ complex (593.0 Hz) gives rise to a readily identifiable AB pattern of multiplets in its ^{31}P spectrum (Fig. 5.13). Upon insertion of CH_2 this value of 593 Hz is drastically reduced to 12.6 Hz (Fig. 5.14). $J(P_X P_Y)$ and $J(P_X P_{Y'})$ in all these complexes are generally comparable to analogous couplings in the related species containing terminal chloride or pyridine groups, and thus confirm their independence of the nature of the terminal group. Also of interest in these complexes are the values of the various phosphorus-platinum couplings. As expected couplings involving the phosphorus of trimethylphosphite ligands are appreciably greater in magnitude than analogous couplings to the phosphorus of diphenylphosphine ligands and in these complexes the signs of $J(^{195}Pt-P_A)$ can be deduced as positive (relative to positive $J(^{195}Pt-P_B)$) simply by inspection of the spectra. Again, insertion of CH_2 to form $[PdPt(\mu-CH_2)(I)_2\{P(OMe)_3\}_2](PF_6)_2$ manifests itself by a significant decrease in $J(^{195}Pt-P_A)$ from 1215 Hz to 78 Hz. Perhaps surprising are the zero or near-zero values of $J(^{195}Pt-P_X)$; in related complexes (Table 5.2) these were found to be ca -70 Hz. Confirmation of these zero couplings was obtained from the ^{195}Pt spectra of these complexes, and may indicate that changes of terminal group do have an effect on these couplings.

^{195}Pt n.m.r. data

^{195}Pt n.m.r. spectra were obtained for the three complexes $PdPt(I)_2Cl_2$, $[PdPt(I)_2\{P(OMe)_3\}_2](PF_6)_2$ and $[PdPt(\mu-CH_2)(I)_2\{P(OMe)_3\}_2](PF_6)_2$ as a confirmation of structural assignments, and the ^{195}Pt chemical shifts are shown in Table 5.5. The spectrum of $PdPt(I)_2Cl_2$ consists of a simple triplet of triplets which is consistent with the structure of Fig. 5.10 and thus confirms the values of $J(^{195}Pt-P)$ shown in Table 5.2. The ^{195}Pt spectrum of $[PdPt(\mu-CH_2)(I)_2\{P(OMe)_3\}_2](PF_6)_2$

(Fig. 5.15) is also a simple first-order one exhibiting doublet splittings of 3557 Hz and 78 Hz and triplets with splittings of 2845 Hz and 16.7 Hz; this spectrum is thus consistent with the structure shown in Fig. 5.16. However, in the related complex with a Pd-Pt bond, $[\text{PdPt}\{\text{I}\}_2\{\text{P}(\text{OMe})_3\}_2](\text{PF}_6)_2$, the presence of a large value of $J(\text{P}_\text{A}\text{P}_\text{B})$ combined with the similarity of $\delta(^{31}\text{P}_\text{A})$ and $\delta(^{31}\text{P}_\text{B})$ produces an appreciable degree of second-order character in the ^{195}Pt n.m.r. spectrum (Fig. 5.17). It was found that a computer-generated spectrum, using the n.m.r. parameters derived from the ^{31}P spectrum, matched the experimental spectrum and this therefore provided both confirmation of structure and assignment of the spin-system.

TABLE 5.5

Complex	$\delta(^{195}\text{Pt})^a$
$\text{PdPt}\{\text{I}\}_2\text{Cl}_2$	-31.3
$[\text{PdPt}\{\text{I}\}_2\{\text{P}(\text{OMe})_3\}_2](\text{PF}_6)_2$	-186.8
$[\text{PdPt}(\mu\text{-CH}_2)\{\text{I}\}_2\{\text{P}(\text{OMe})_3\}_2](\text{PF}_6)_2$	-282.3

Notes a Relative to 21.4 MHz when ^1H resonance of TMS is at exactly 100 MHz.

Fig. 5.15 ^{195}Pt spectrum of $[\text{PdPt}(\mu\text{-CH}_2)(\text{I})_2(\text{P}(\text{OMe})_3)_2](\text{PF}_6)_2$
recorded at 19.2 MHz

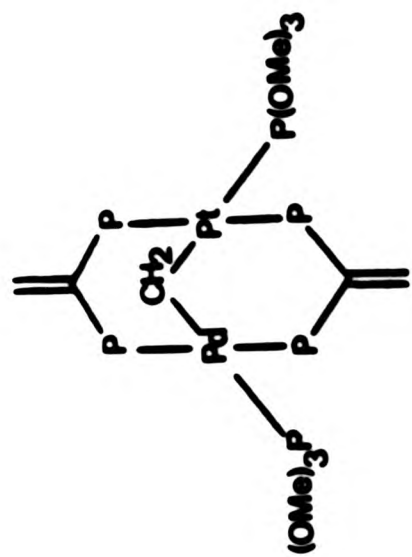


Fig 5.16

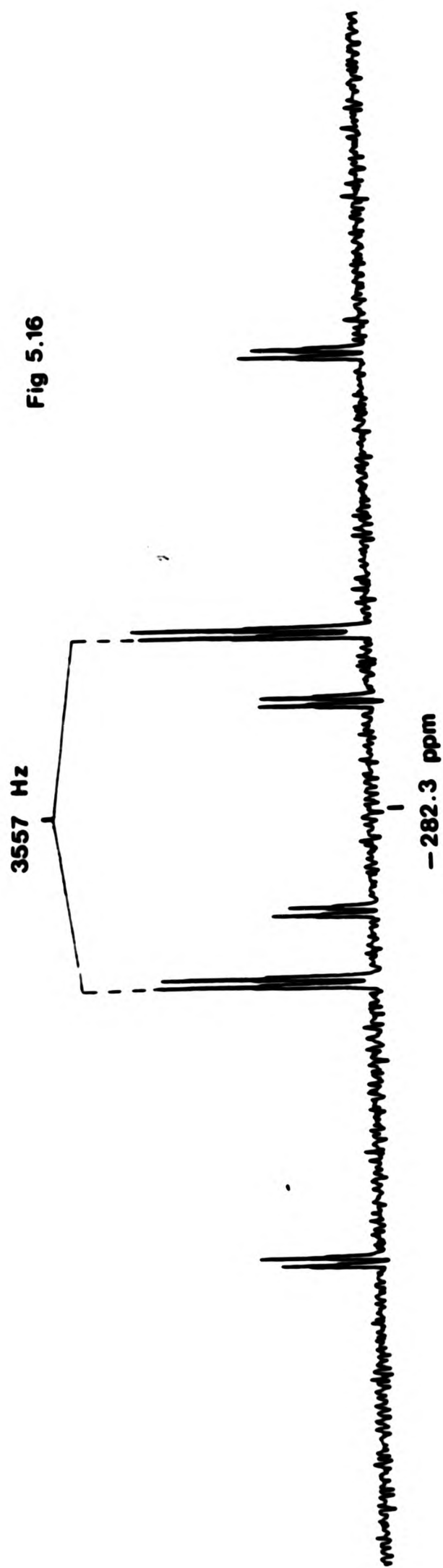
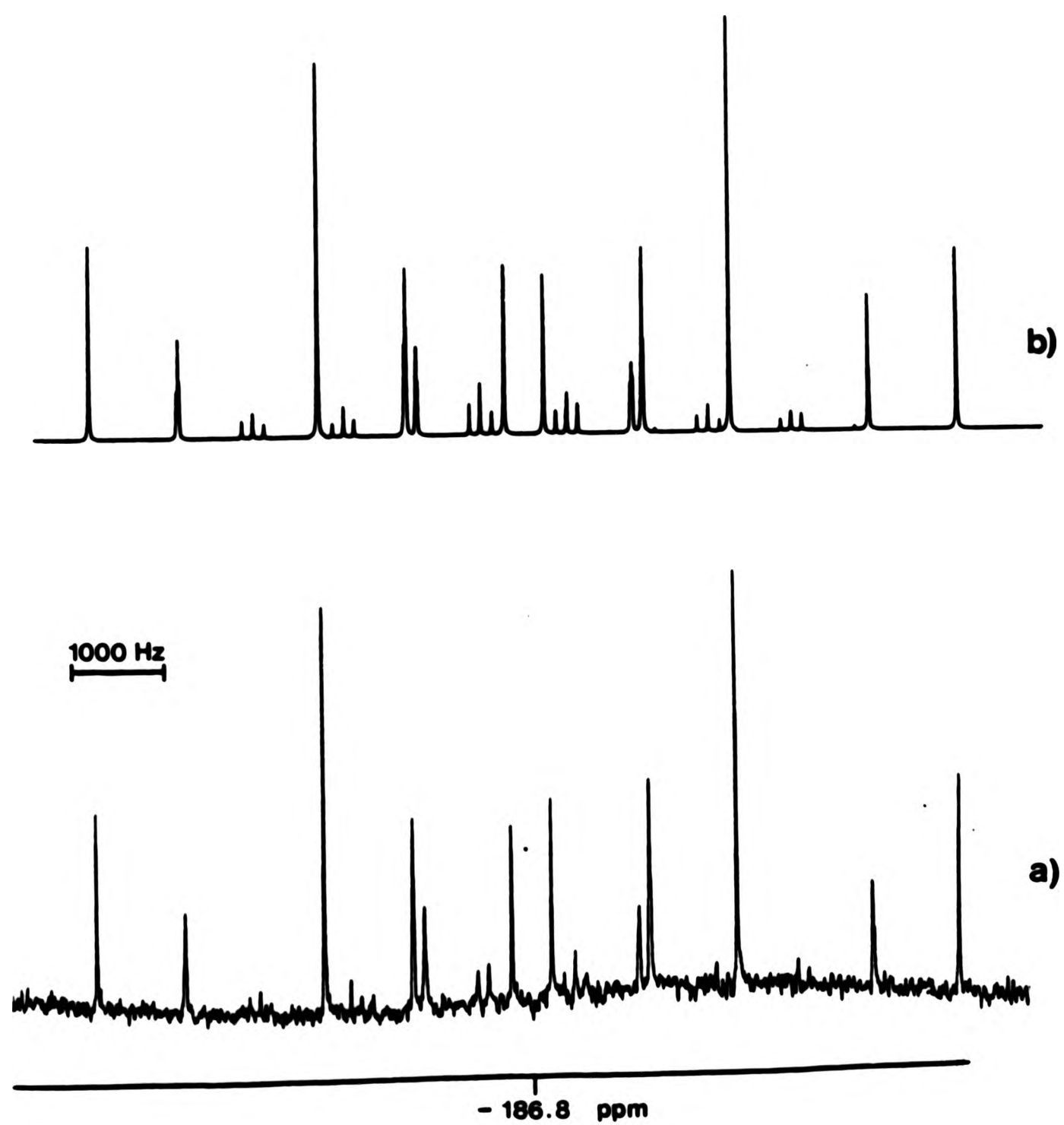


Fig. 5.17 a) Observed ^{195}Pt spectrum of $[\text{PdPt}(\text{I})_2\{\text{P}(\text{OMe})_3\}_2](\text{PF}_6)_2$

b) Simulated spectrum



CHAPTER 6

SULPHUR AND SELENIUM DERIVATIVES OF THE NEW POLYPHOSPHORUS LIGANDS

1. INTRODUCTION

There is a formal analogy between the coordination of a metal to a phosphorus atom and the oxidation of that atom by sulphur, selenium etc. In particular, for the polydentate ligands dealt with here, sulphurisation reactions have, in principle, the potential to yield a range of isomeric and diastereomeric products analogous to those produced by simple non-chelate metal-coordination. In addition, coordination of two or more metal centres to the same ligand tends to yield products of low solubility which are therefore difficult to analyse by n.m.r. spectroscopy. For these reasons a study was undertaken into the reactions of some of the large polyphosphorus ligands with elemental sulphur in order to (a) analyse any isomeric and diastereomeric preferences and (b) attempt the syntheses of polysulphide derivatives which are analogous to the insoluble polymetallic species.

The first tertiary phosphine sulphides were prepared by direct reaction of a trialkylphosphine with elemental sulphur^{100,101}, and today this is still the most general and straightforward synthetic method available. Rates for these reactions are generally fast for octatomic sulphur¹⁰² and therefore the use of the other forms of sulphur, which results in even faster reaction rates¹⁰³, is seldom required. In addition, reaction rates are strongly solvent-dependent, anion-solvating solvents generally inducing faster reactions¹⁰⁴. Sulphurisation reactions of diphosphine species have been less extensively studied, but reactions analogous to those of monophosphines have been reported¹⁰⁵⁻¹⁰⁷.

The addition of selenium to tertiary phosphines is less vigorous than the analogous addition of sulphur. In general, whereas the lower aliphatic-substituted tertiary phosphines react with elemental selenium at room-temperature^{108,109} the higher homologues may require reflux in high boiling solvents or other more forcing methods to undergo reaction¹¹⁰⁻¹¹². Recently, workers have studied the reaction between elemental selenium and the triphosphine ligand 1,1,2-tris(diphenylphosphino)ethane, (II)¹¹³. This reaction leads to a mixture of mono-, di- and triselenium derivatives, and by the use of homonuclear ^{31}P 2D J-resolved n.m.r. spectroscopy it was possible to identify all the individual species in the reaction mixture. This chapter extends this work by examining the analogous but somewhat more diverse reactions of the larger polyphosphorus ligands already reported. In particular, isomeric and diastereomeric preferences have been analysed from which it was found possible to estimate relative effective reactivity of individual phosphorus atoms.

2. RESULTS AND DISCUSSION

In principle there are nineteen chemically inequivalent sulphur derivatives of the pentaphosphine ligand bis-[2,2-bis(diphenylphosphino)-ethyl]phenylphosphine, (XII), which contain from one to five sulphur atoms (compounds b)-t) Fig. 6.1). Note that due to the presence of the two chiral centres marked * , compounds b) and c) are diastereomers and are therefore chemically distinct. Diastereomers also exist in the di-, tri- and tetrasulphide groups.

Treatment of the free ligand XII with one atomic equivalent of sulphur yielded a reaction mixture whose ^{31}P n.m.r. spectrum (Fig. 6.2) showed it to contain a number of different species. This spectrum

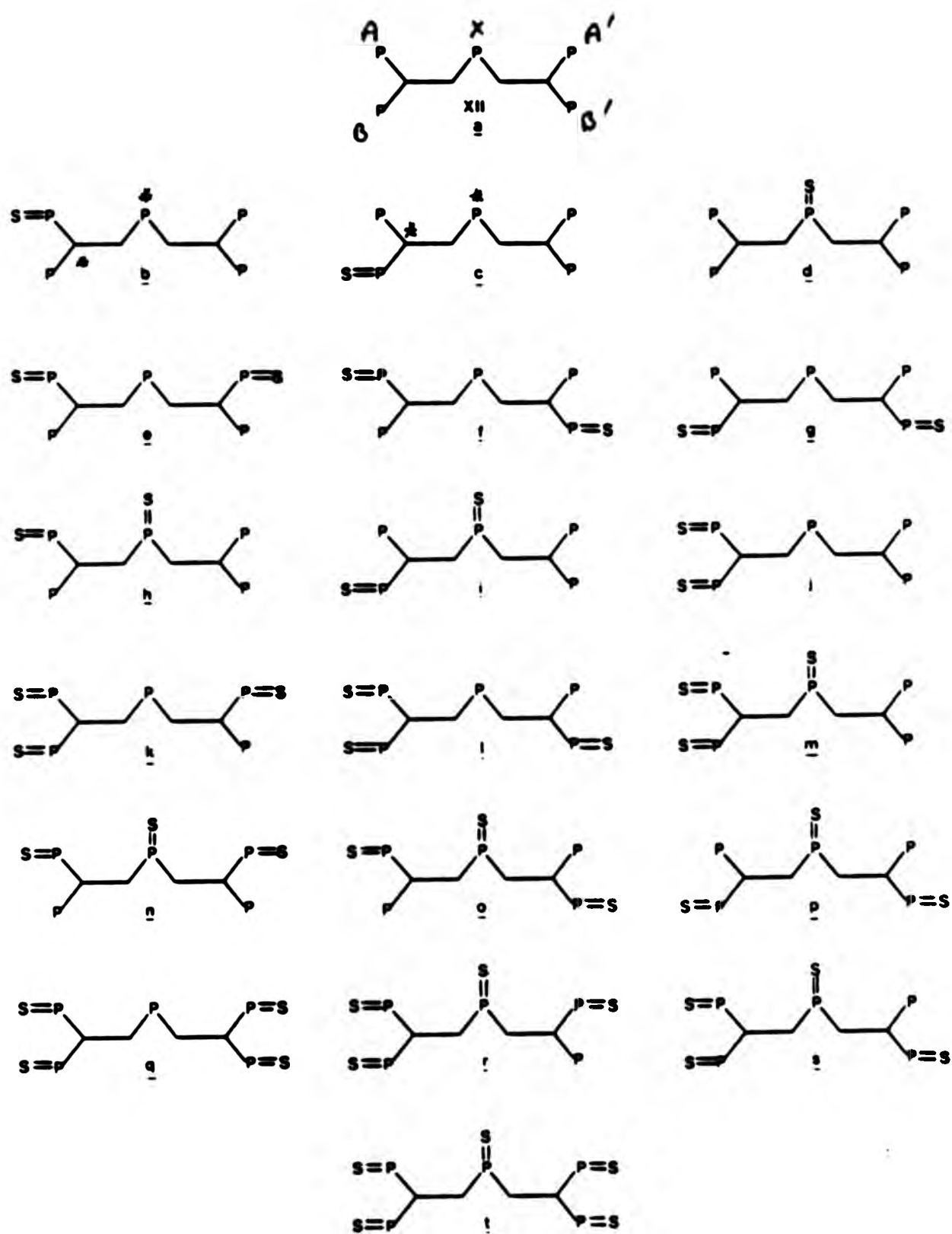


Fig. 6.1 Sulphide derivatives of bis-[2,2-bis(diphenylphosphino)ethyl]phenyl phosphine XII

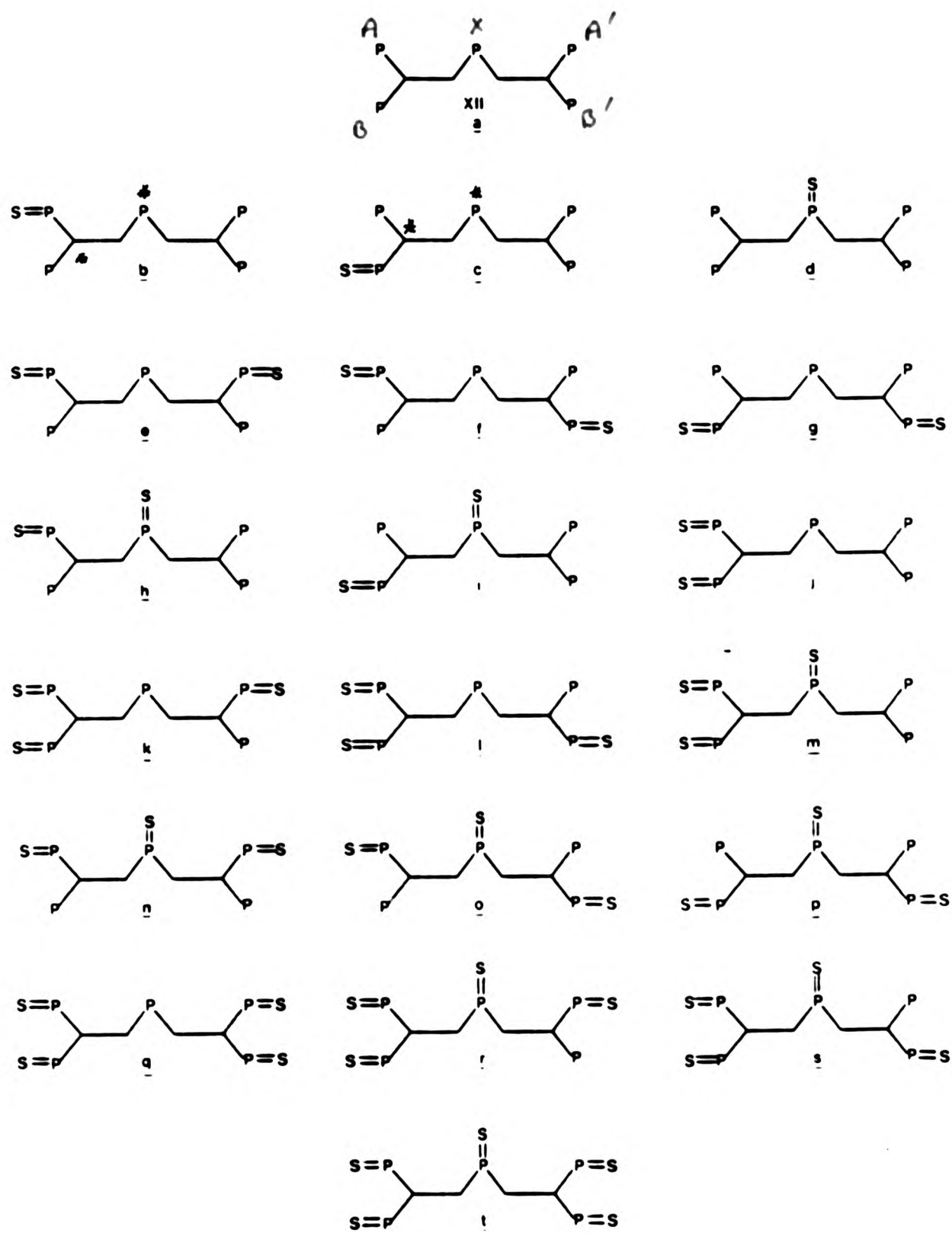
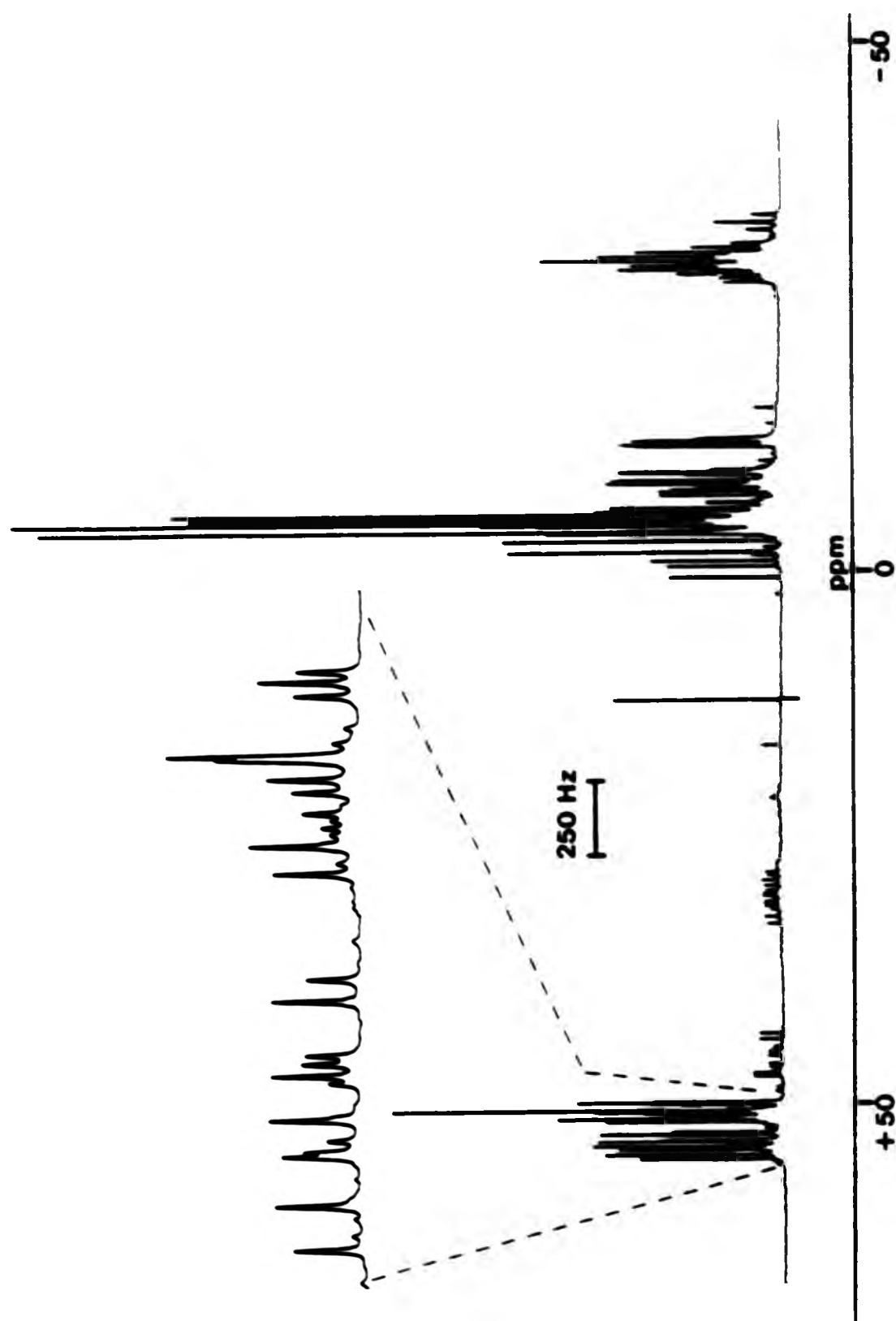


Fig. 6.1 Sulphide derivatives of bis-[2,2-bis(diphenylphosphino)ethyl]phenyl phosphine XII

Fig. 6.2 ^{31}P n.m.r. spectrum of the reaction mixture resulting from the addition of one equivalent of sulphur to the pentaphosphine compound XII



also shows the presence of some unreacted free ligand which suggests a non-proportional reaction giving a mixture of monosulphide, disulphide and possibly higher derivatives. The P^V region of the total spectrum is difficult to assign by inspection and although in principle an assignment could be obtained from a series of selective homonuclear decoupling experiments, these would be extremely tedious to perform. A better approach was found to be the use of homonuclear ^{31}P 2D J-resolved spectroscopy. 2D J-resolved spectroscopy is particularly useful in this context as it allows the separation of chemical shifts and coupling constants along two axes in a 2D plot thus reducing problems from overlapping resonances.

2D J-resolved n.m.r. spectroscopy^{114,115}

In describing J-resolved spectroscopy it is convenient to consider first a simple heteronuclear AX spin-system. The pulse-sequence and vector diagrams for this experiment are shown in Fig 6.3¹¹⁶. Initially a 90° pulse applied along the x-axis (90°_x) aligns the magnetization along the y-axis in the xy plane (a). The individual nuclear magnetic moments then precess at their Larmor frequencies and after a length of time $t_1/2$ are in position (b). A 180° pulse applied along the y-axis at the A frequency (180°_y (A)) then inverts the individual vectors about the y-axis whilst a simultaneous 180°_y (X) pulse changes the spin-states of the X nuclei, thus interchanging the precessional frequencies of the individual vectors (c). After a further time $t_1/2$ only the chemical shift position and effects due to magnetic field inhomogeneity are refocussed (d) and therefore the magnetization detected at time t_1 is t_1 -dependent. This sequence using a set of t_1 values followed by successive Fourier transformations with respect to t_2 (which achieves δ and J dispersion), and then t_1 (which achieves

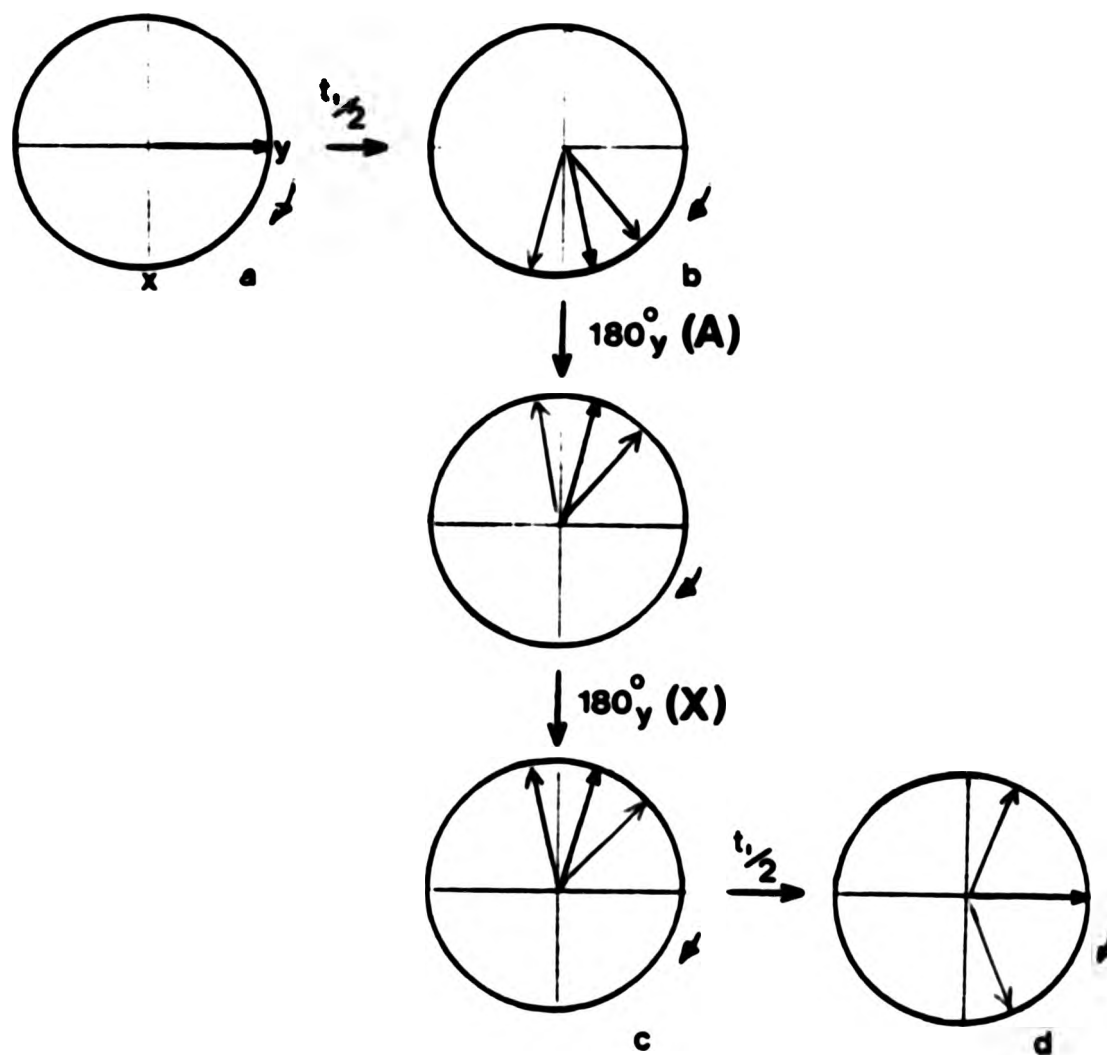
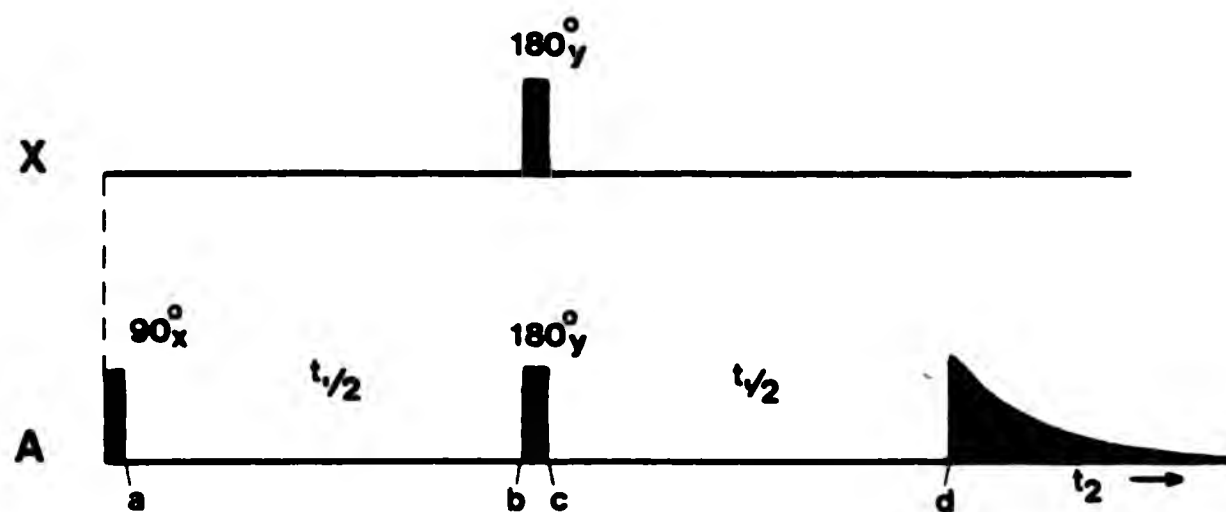


Fig. 6.3 Pulse-sequence and vector diagrams for heteronuclear J-resolved n.m.r. spectroscopy

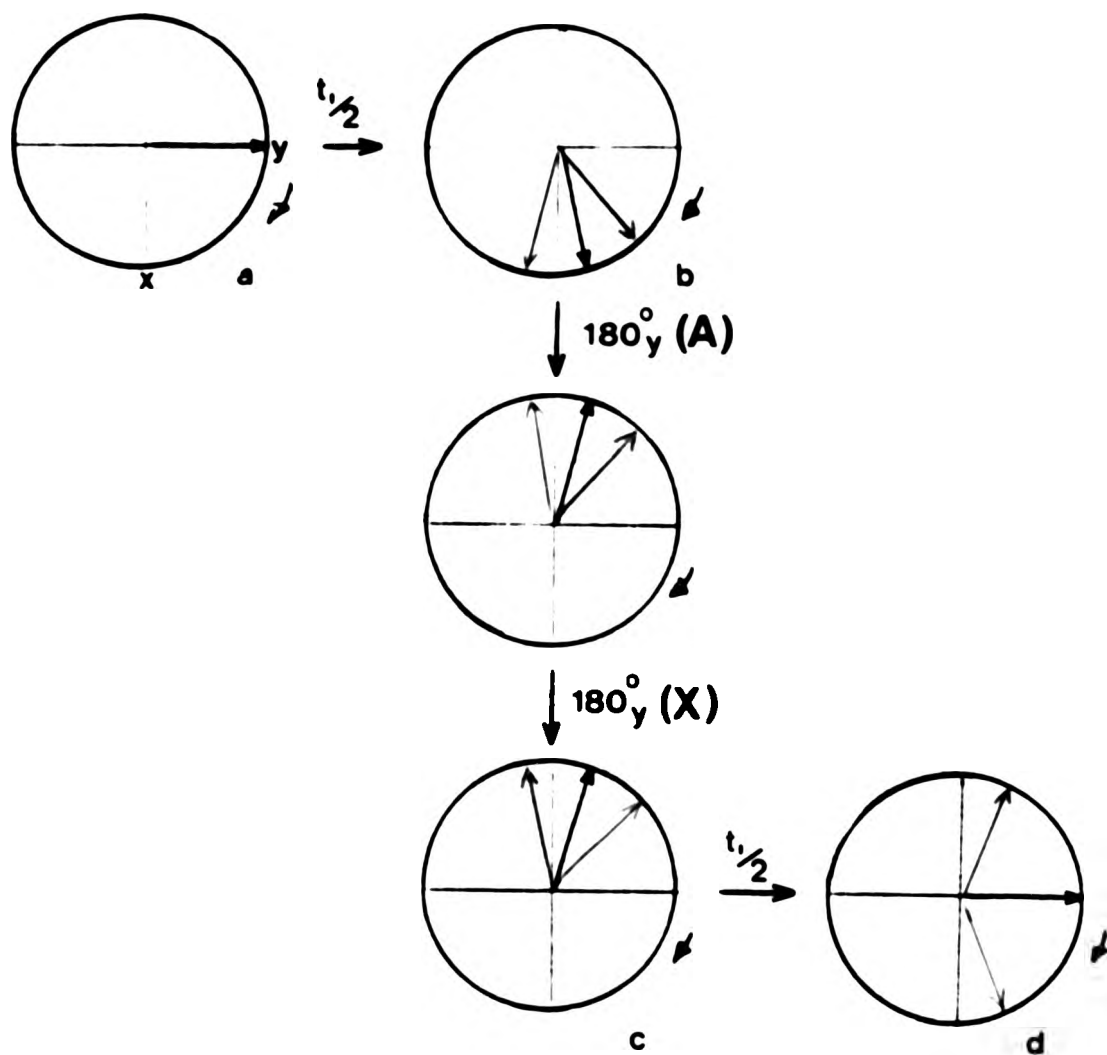
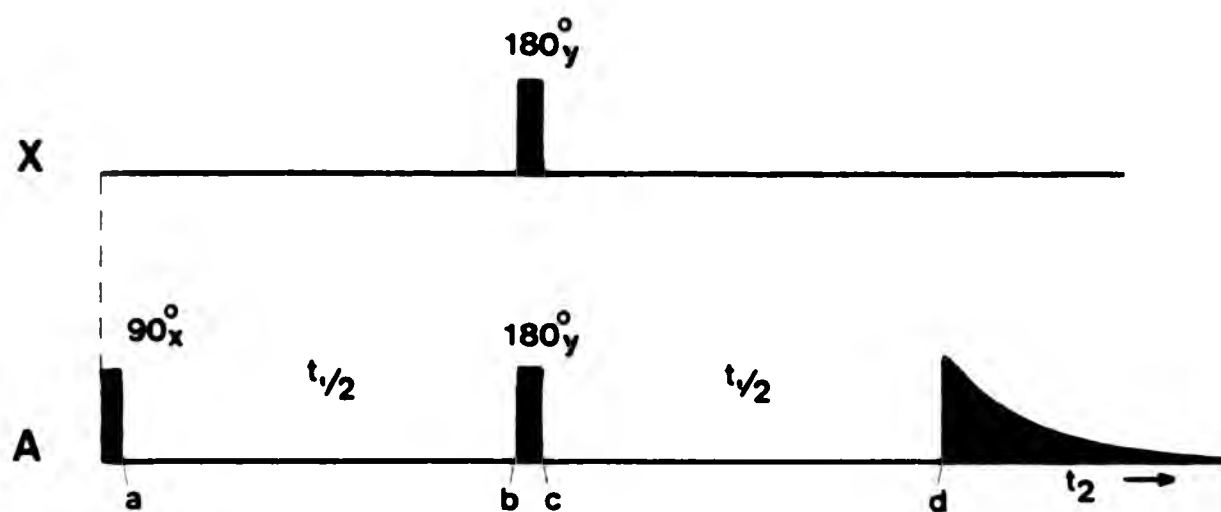


Fig. 6.3 Pulse-sequence and vector diagrams for heteronuclear J-resolved n.m.r. spectroscopy

J dispersion only) yields a 2D plot of the type shown in Fig 6.4.

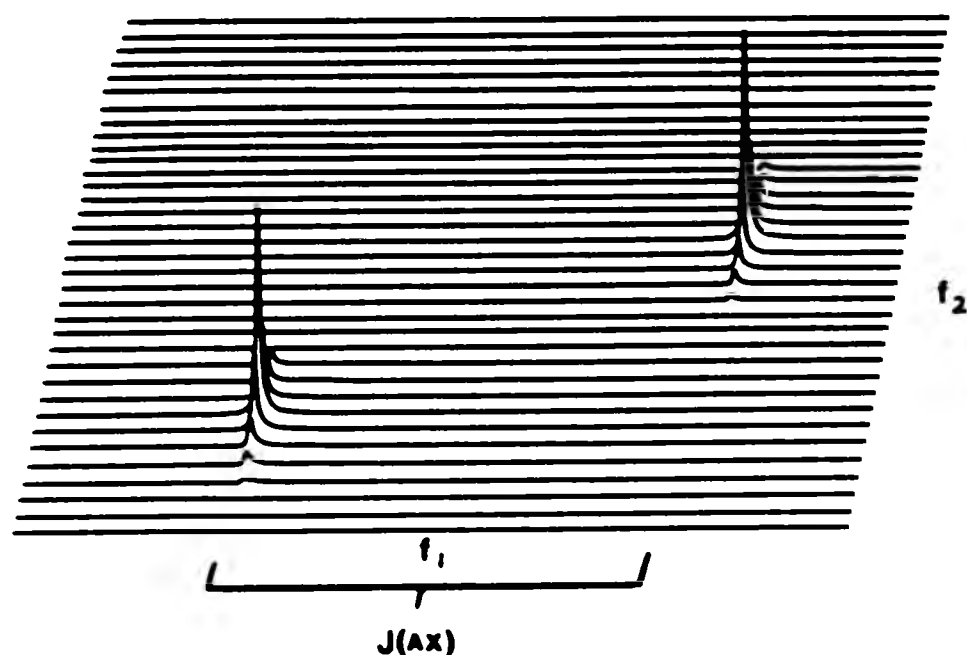


Fig 6.4

In this spectrum line separations parallel to the horizontal axis are all centred about the mid-point and arise solely from AX couplings. In addition a 45° projection yields an effectively fully decoupled A spectrum from which the chemical shift of A may be simply read off. Thus in a mixture of different AX spin-systems it is possible to assign individual resonances to specific A nuclei and thus obtain both chemical shifts and coupling constants relatively simply.

The analogous homonuclear 2D J-resolved n.m.r. experiment is closely related to the heteronuclear case and its pulse sequence is shown in Fig. 6.5¹¹⁷. In this system the 180°y(A) pulse has exactly



Fig 6.5

the same effect upon the individual vectors as do the simultaneous $180^\circ\gamma(X)$ and $180^\circ\gamma(A)$ pulses in the heteronuclear experiment (Fig. 6.3) since in homonuclear case a $180^\circ\gamma(A)$ pulse is by definition also a $180^\circ\gamma(X)$ pulse. Thus a simplified pulse sequence may be employed to produce analogous 2D plots to those in Fig. 6.4.

A homonuclear ^{31}P 2D J-resolved n.m.r. spectrum was obtained for the P^{V} region of the reaction mixture whose 1D ^{31}P n.m.r. spectrum is shown in Fig. 6.2 (i.e. from the reaction using one atomic equivalent of sulphur) and this yielded the 2D plot shown in Fig. 6.6. A 45° projection reveals six different P^{V} environments, and slices through this projection at the individual chemical shift positions then display the various P-P couplings in each system (Fig. 6.7). With these parameters it was found to be relatively simple to complete the analysis of the P^{III} region and thus from this reaction compounds b), c), e), f) and g) were identified (Table 6.1). Addition of one further atomic equivalent of sulphur was found to reduce the relative proportions of the two monosulphide derivatives b) and c) whilst increasing those of the three disulphide derivatives e) - g), thus confirming the original assignments. In addition, new resonances due to the trisulphide derivatives were produced in the n.m.r. spectrum thus making it possible to identify compounds k) and l). Further addition of sulphur reduced the relative proportions of e) - g), increased those of k) and l), and yielded new resonances due to the tetrasulphide q). Continued addition finally afforded the pentasulphide derivative t). Thus nine different derivatives out of the nineteen possible were identified at various stages in the reaction (Table 6.1), and from the distribution of these, two points clearly emerge:

- (i) The central phosphorus atom X is the last to be attacked.
- (ii) Species with geminally related P^{V} atoms are not favoured if

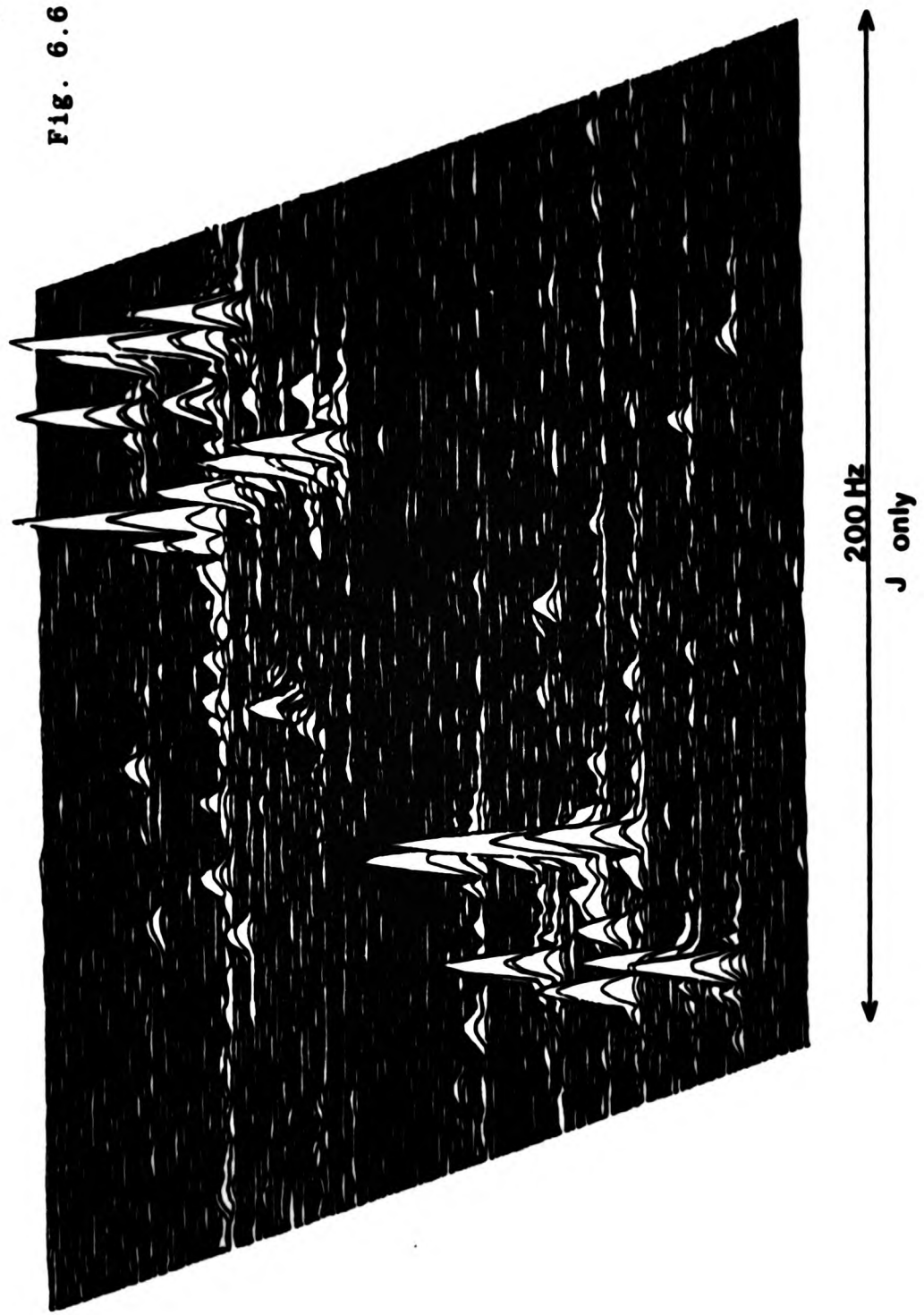


Fig. 6.6 ^{31}P 2D J-resolved n.m.r. spectrum of the PV region of Fig 6.2

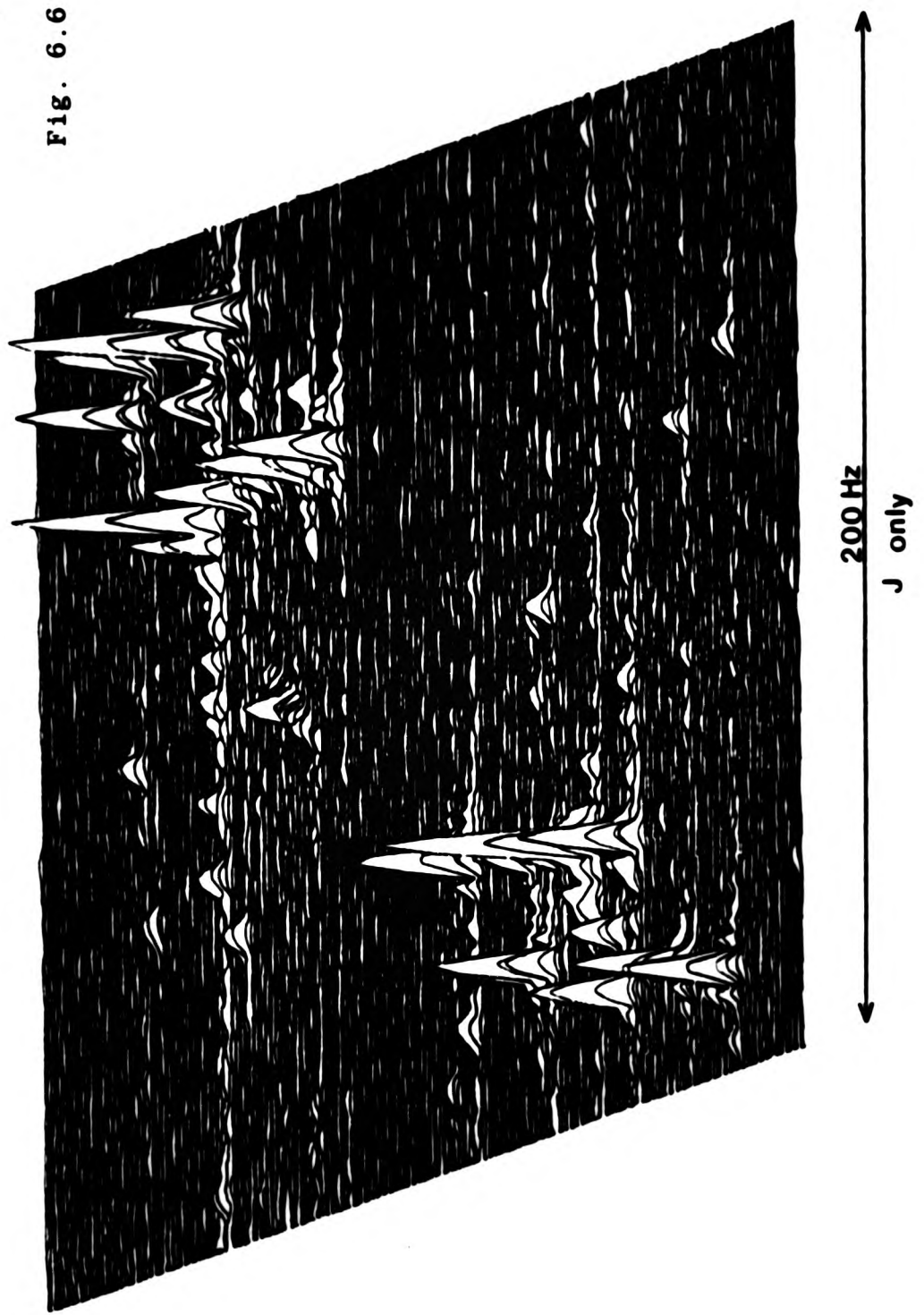


Fig. 6.6 ^{31}P 2D J-resolved n.m.r. spectrum of the P^{V} region of Fig 6.2

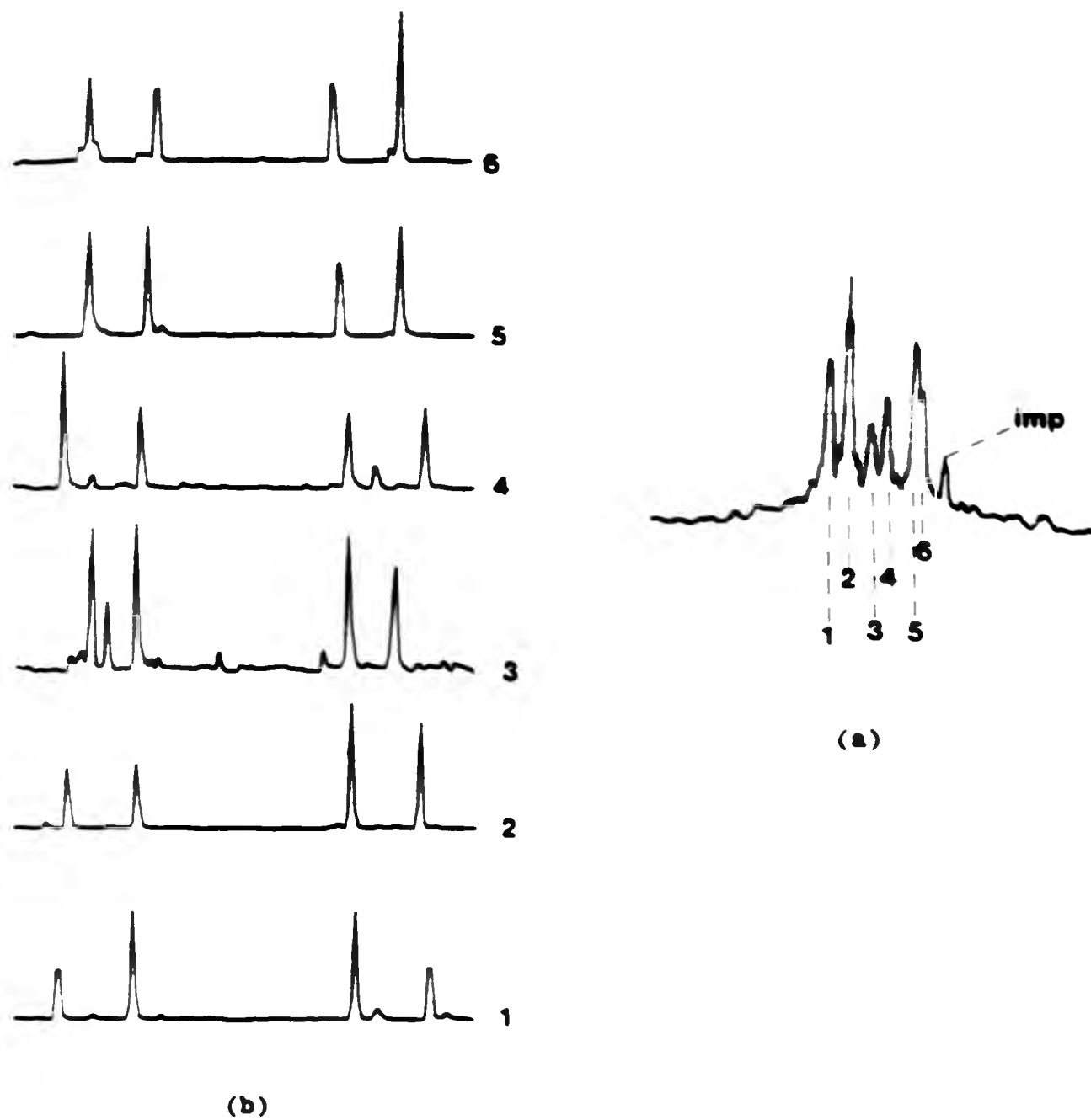


Fig. 6.7 a) 45° projection through the 2-D plot of Fig 6.6 showing effectively a decoupled ^{31}P n.m.r. spectrum

b) Slices through the 45° projection at the six chemical shift positions

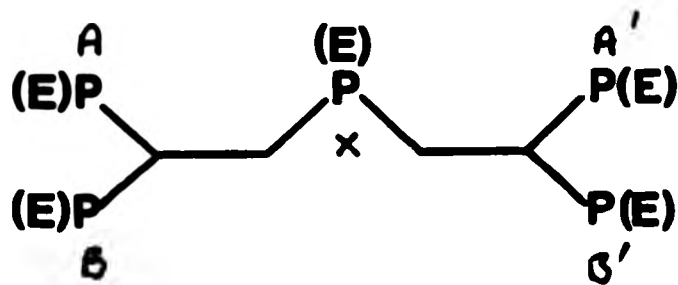


TABLE 6.1

Compound ^a	E ^{b,c}				
	A	A'	B	B'	X
a)	1.p.	1.p.	1.p.	1.p.	1.p.
b)	S	1.p.	1.p.	1.p.	1.p.
c)	1.p.	1.p.	S	1.p.	1.p.
e)	S	S	1.p.	1.p.	1.p.
f)	S	1.p.	1.p.	S	1.p.
g)	1.p.	1.p.	S	S	1.p.
k)	S	S	S	1.p.	1.p.
l)	S	1.p.	S	S	1.p.
q)	S	S	S	S	1.p.
t)	S	S	S	S	S

Notes a) See Fig. 6.1

b) 1.p. = electron lone pair.

c) See diagram above for labelling system.
 NB The labelling refers to the phosphorus spin-system in the free ligand XII and not to the spin-system of the derivatives.

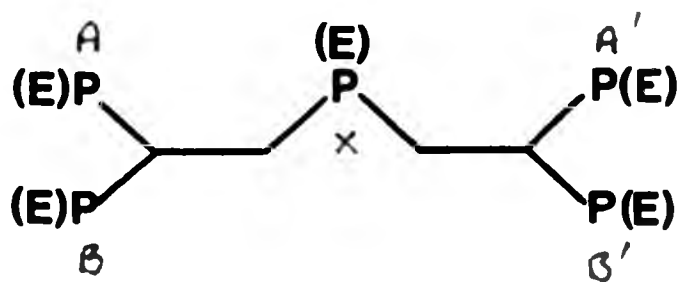


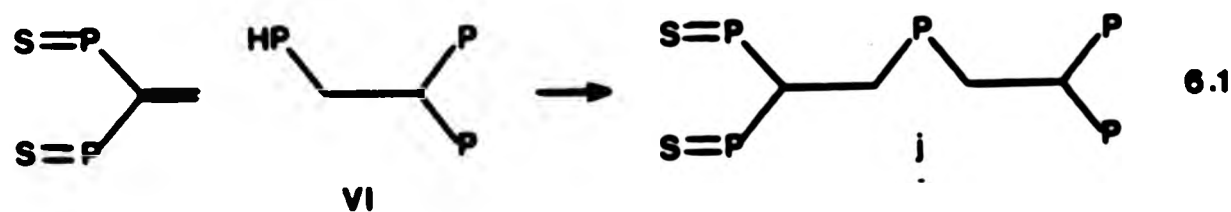
TABLE 6.1

Compound ^a	E ^{b,c}				
	A	A'	B	B'	X
a)	1.p.	1.p.	1.p.	1.p.	1.p.
b)	S	1.p.	1.p.	1.p.	1.p.
c)	1.p.	1.p.	S	1.p.	1.p.
e)	S	S	1.p.	1.p.	1.p.
f)	S	1.p.	1.p.	S	1.p.
g)	1.p.	1.p.	S	S	1.p.
k)	S	S	S	1.p.	1.p.
l)	S	1.p.	S	S	1.p.
q)	S	S	S	S	1.p.
t)	S	S	S	S	S

- Notes
- a) See Fig. 6.1
- b) 1.p. = electron lone pair.
- c) See diagram above for labelling system.
 NB The labelling refers to the phosphorus spin-system in the free ligand XII and not to the spin-system of the derivatives.

if another configuration is possible (this is subject to the previous condition).

The first of these apparent conditions precludes the formation of nine of the nineteen possible derivatives, namely d), h), i), m), n), o), p), r) and s) whilst the second precludes the formation of j). Thus these two conditions reduce the potential number of derivatives from nineteen to nine, and all of these nine have in fact been identified in the reaction mixture (Table 6.1). The origin of these conditions is difficult to examine since many different effects may play a significant role. Condition i) initially suggests that the central phosphorus atom X is relatively unreactive. However this is not necessarily the case since inter-phosphorus sulphur transfer is likely to occur. Intermolecular sulphur transfer has been well documented and indeed can be used as a synthetic route to many tertiary phosphine sulphides¹¹⁸. Reports of analogous intramolecular S-transfers are less common but Keat¹¹⁹ and others¹²⁰ have reported such processes in a number of diphosphine species. If S-transfer is a factor in the reactions studied in this chapter it may be that the outcome of the reactions is more dependent on configurational and conformational stability rather than the relative reactivity of the individual phosphorus atoms. In order to investigate this, the direct syntheses of a selection of the unfavoured derivatives, not formed in the reaction, and the examination of any subsequent rearrangements is required. Attempts to form compound j) in order to investigate condition ii) were undertaken utilizing the addition reaction of Eq. 6.1. However the outcome was



not straightforward and it is possible that addition across the P-S double-bonds may also occur.

The nine derivatives therefore formed by the reaction of XII with elemental sulphur are as follows:

- i) Two diastereomeric monosulphide derivatives b) and c).
- ii) Three diastereomeric disulphide derivatives e) - g).
- iii) Two diastereomeric trisulphide derivatives k) and l).
- iv) One tetrasulphide derivative q) with no diastereomers.
- v) One pentasulphide derivative t) with no diastereomers.

It was generally found that all members of a group of diastereomers were formed in approximately equal proportions but because of the nature of the reaction it was possible to isolate pure only the pentasulphide t).

NMR Characterisation

In this series of derivatives the ^{31}P chemical shifts (Table 6.2) of the P^{V} atoms lie within narrow ranges for each different environment. In discussing these it is therefore convenient to introduce a new parameter Δ_{s} (analogous with coordination chemical shift Δ) which is simply defined as the change in chemical shift upon sulphurisation (Eq. 6.2).

$$\Delta_{\text{s}} = \delta^{31}\text{P}^{\text{V}}_{(\text{s-derivative})} - \delta^{31}\text{P}^{\text{III}}_{(\text{free ligand})} \quad 6.2$$

For the species containing two geminally related P^{V} atoms (compounds k), l), q), t)) $\Delta_{\text{s}} = 51.4 \pm 2$ ppm, whilst for P^{V} atoms that are geminally related to P^{III} atoms (in compounds b), c), d) - g), k), l)) $\Delta_{\text{s}} = 57.3 \pm 1.2$ ppm. The two types of P^{V} atoms (Fig. 6.8) therefore

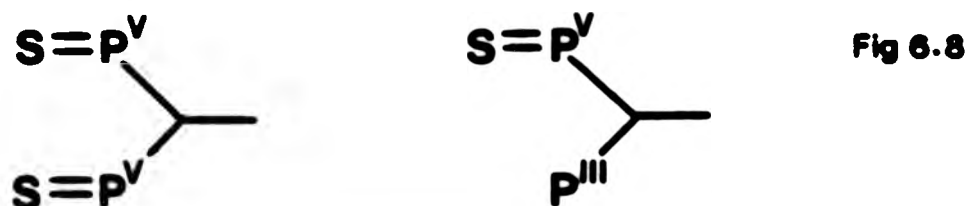


TABLE 6.2 ^{31}P chemical shift data for the sulphur derivatives of XII

Compound ^a	$\delta(^{31}\text{P}_\text{A})$ /ppm	$\Delta_\text{g}^{\text{A c}}$ /ppm	$\delta(^{31}\text{P}_\text{A},)$ /ppm	$\Delta_\text{g}^{\text{A' c}}$ /ppm	$\delta(^{31}\text{P}_\text{B})$ /ppm	$\Delta_\text{g}^{\text{B c}}$ /ppm	$\delta(^{31}\text{P}_\text{B},)$ /ppm	$\Delta_\text{g}^{\text{B' c}}$ /ppm	$\delta(^{31}\text{P}_\text{X})$ /ppm	$\Delta_\text{g}^{\text{X c}}$ /ppm
a) ^d	-2.9	-	-2.9	-	-4.8	-	-4.8	-	-29.7	-
b)	+54.1	+57.0	-0.6	-	-9.4	-	-6.6	-	-30.0	-
c)	-9.6	-	-2.7	-	+53.8	+58.6	-4.1	-	-28.6	-
e)	+53.5	+56.4	+53.5	+56.4	-7.4	-	-7.4	-	-29.0	-
f)	+53.3	+56.2	-5.2	-	-10.2	-	+52.8	+57.6	-29.1	-
g)	-10.2	-	-10.2	-	+52.9	+57.7	+52.9	+57.7	-32.1	-
k)	+48.4	+51.3	+54.0	+56.9	+44.6	+49.4	-13.1	-	-31.1	-
l)	+47.5	+50.4	-7.6	-	+46.3	+51.1	+53.4	+58.2	-26.9	-
q)	+49.7	+52.6	+49.7	+52.6	+46.2	+51.0	+46.2	+51.0	-27.6	-
t)	+48.9	+51.5	+48.9	+51.5	+48.7	+53.5	+48.7	+53.5	+51.6	+81.3

Notes a) See Table 6.1 for labelling system
b) Relative to external 85% H_3PO_4 = 0.0 ppm
c) See eq. 6.2
d) Free ligand XII

have characteristic and mutually exclusive Δ_{P} ranges. This ca 6 ppm difference is sufficient to separate resonances due to the two different types of P^{V} atoms in a mixture of derivatives and thus simplifies spectral analysis (Fig. 6.9). For the central phosphorus atom X, only one value of Δ_{P} can be obtained from this series of derivatives and the surprisingly large value observed (+81.3 ppm for compound t)) may reflect a large steric influence, which may also be the origin of the relative unreactivity of this type of phosphorus atom.

Rationalisation of the P-P couplings in these derivatives (Table 6.3) is somewhat more difficult, but some common features do emerge. The near zero values of $^2\text{J}(\text{}^{31}\text{P}^{\text{V}}-\text{C}-\text{}^{31}\text{P}^{\text{V}})$ in compounds k), l), q) and b) may be considered as normal since lone-pair interactions cannot occur and it is only when one or both phosphorus atoms bears a lone-pair that the magnitudes of $^2\text{J}(\text{}^{31}\text{P}^{\text{III}}-\text{}^{31}\text{P}^{\text{III}})$ are large. This observation is in conformity with the results of previous workers for a range of ditertiary phosphines and their selenium derivatives⁵⁴. Values of $^3\text{J}(\text{}^{31}\text{P}^{\text{V}}-\text{}^{31}\text{P}^{\text{III}})$ in these compounds are generally larger when one of the phosphorus atoms is pentavalent (compounds d) - h)). However, this cannot be attributed solely to greater s-character of the hybrid orbital used for the relevant bond, since it is clear both from the free ligand and from derivatives b) and c) (where different values of $^3\text{J}(\text{}^{31}\text{P}^{\text{III}}-\text{}^{31}\text{P}^{\text{III}})$ are observed within the molecule), that conformational effects play a significant role. Indeed it may be that the generally larger values of $^3\text{J}(\text{}^{31}\text{P}^{\text{V}}-\text{}^{31}\text{P}^{\text{III}})$ merely reflect conformational imbalances within the molecule arising from the increased bulk of the phosphorus moiety upon sulphurisation. This suggestion is supported by the two different values of $^3\text{J}(\text{}^{31}\text{P}-\text{}^{31}\text{P})$ (6.8 and 27.1 Hz) observed for the pentasulphide derivative t) where each phosphorus atom is pentavalent.

In a similar manner to the reaction previously described, the

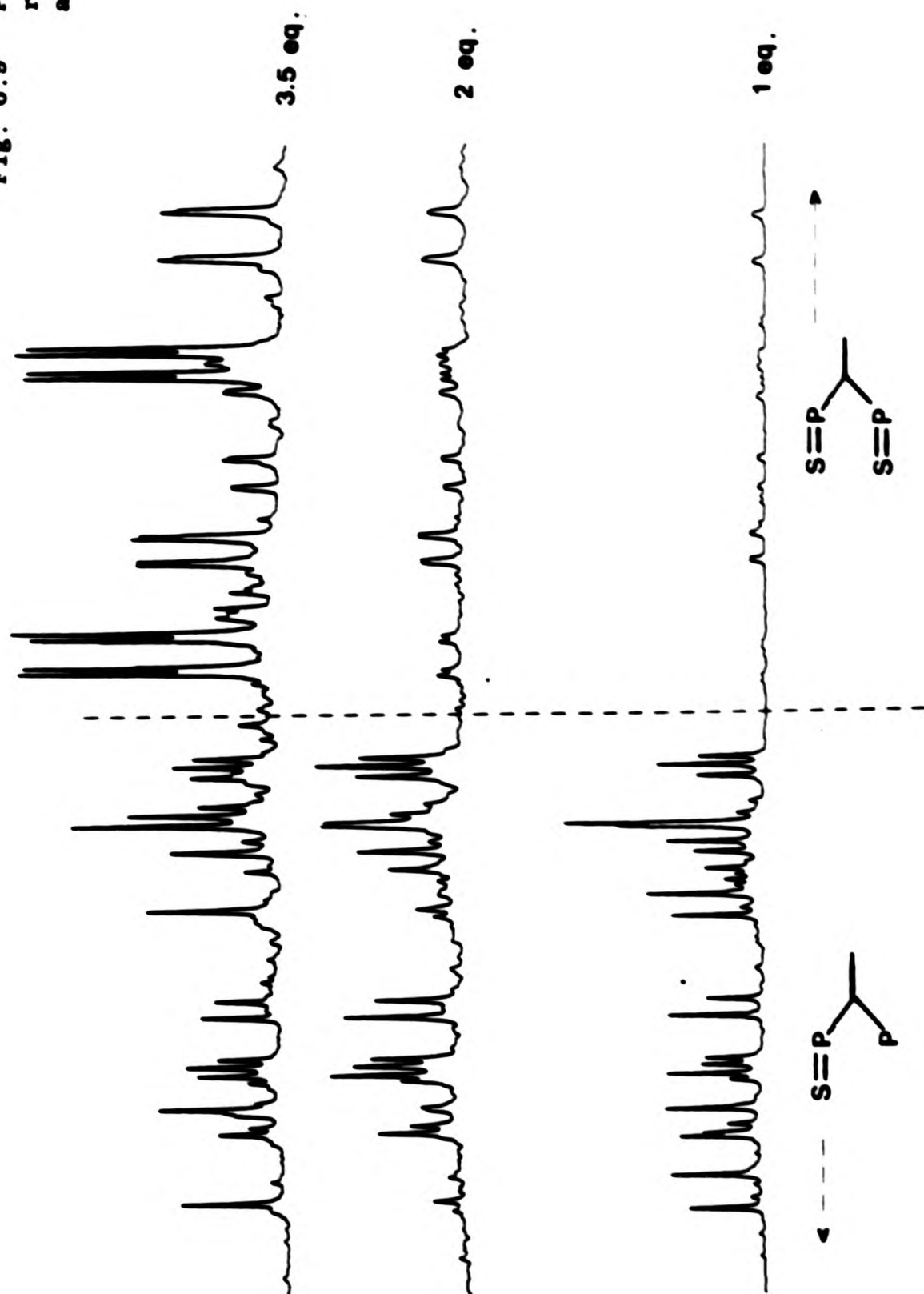
TABLE 6.3 ^{31}P coupling constants for the sulphur derivatives of XII

Compound ^a	$^3\text{J}(\text{AX})$ /Hz	$^3\text{J}(\text{A}'\text{X})$ /Hz	$^3\text{J}(\text{BX})$ /Hz	$^3\text{J}(\text{B}'\text{X})$ /Hz	$^2\text{J}(\text{AB})$ /Hz	$^2\text{J}(\text{A}'\text{B}')$ /Hz
a) b	28.6	28.6	17.0	17.0	100.7	100.7
b)	32.2	38.6	1.7	13.2	128.5	85.9
c)	2.4	35.0	29.8	8.5	122.8	75.0
e)	19.6	19.6	3.9	3.9	111.7	111.7
f)	32.9	12.7	2.0	28.7	122.6	105.3
g)	1.9	1.9	25.6	25.6	108.9	108.9
k)	11.2	41.3	20.5	0	1.4	127.7
l)	12.5	12.7	0.7	20.1	1.3	113.6
q)	14.9	14.9	10.5	10.5	2.7	2.7
t)	6.8	6.8	27.1	27.1	0	0

Notes a) See Table 6.1 for labelling system

b) Free Ligand XII

Fig. 6.9 ^VP regions of the ^{31}P spectra
resulting from the sequential
addition of sulphur to XII



tetratertiary phosphine, XI, reacted with four atomic equivalents of sulphur to give the corresponding tetrasulphide derivative quantitatively (Fig. 6.10). Similarly, the tetraphosphinoarsino ligand bis[2,2-bis-

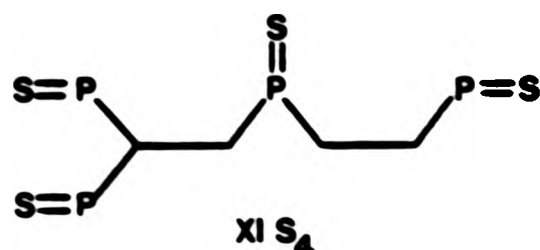


Fig 6.10

(diphenylphosphino)ethyl]phenylarsine, XVI, reacted with four atomic equivalents of sulphur to yield only the tetrasulphide derivative shown in Fig. 6.11. Further addition of sulphur produced no reaction and

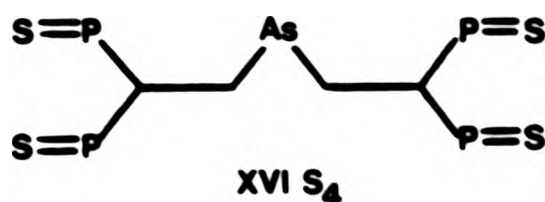
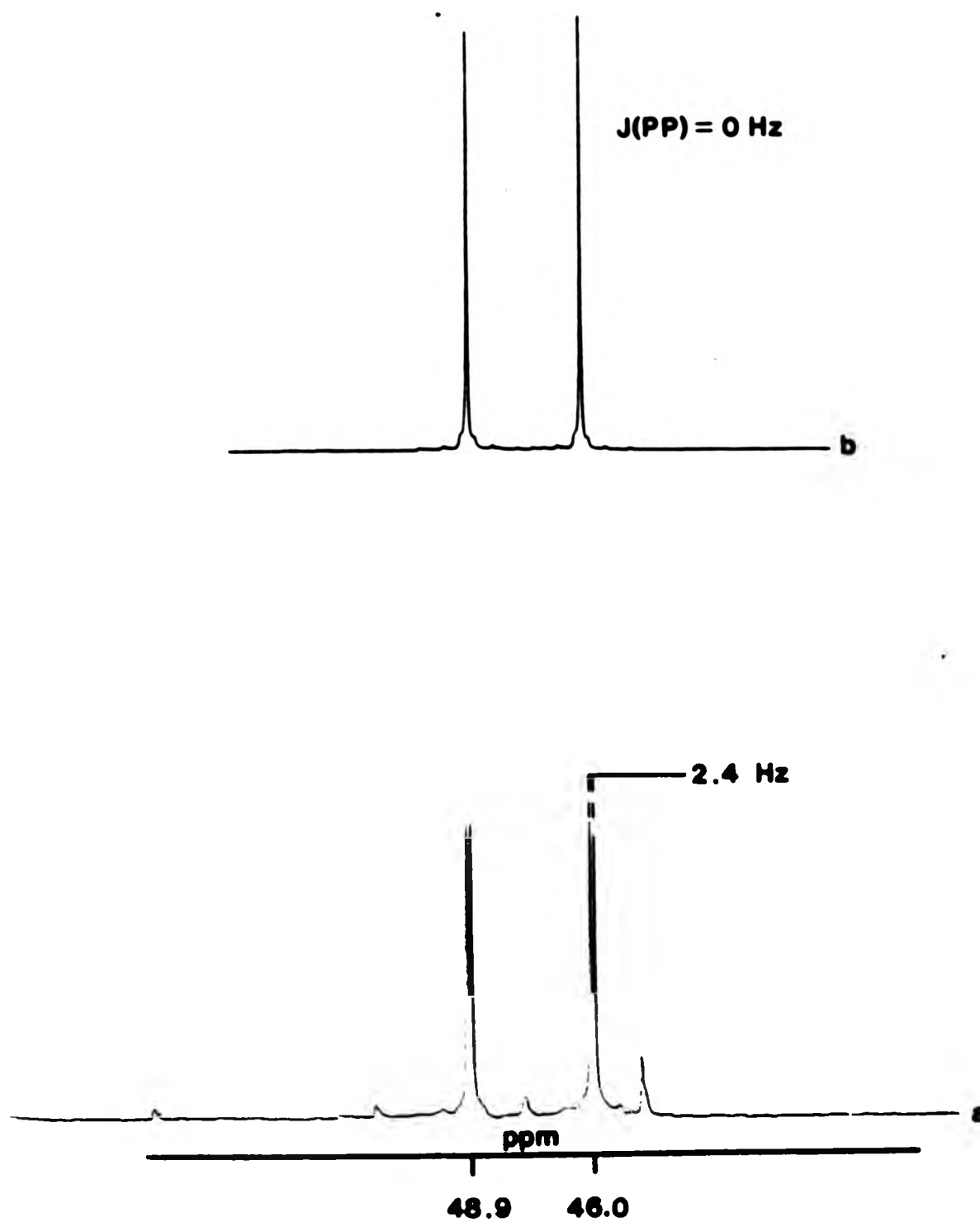


Fig 6.11

therefore no change in the ^{31}P n.m.r. spectrum of the reaction mixture (Fig. 6.12). This apparent low reactivity of the arsenic atom is perhaps surprising since in general trialkyl arsines are readily sulphurised¹²¹⁻¹²³, and therefore this is likely to be a result of a more binding form of condition i) as described for the pentaphosphine analogue. The ^{31}P n.m.r. parameters for each of these tetrasulphide derivatives (Tables 6.5, 6.6) are generally comparable with analogous parameters in the series of derivatives previously described.

Fig. 6.12 a) ^{31}P spectrum of an XVIS_4 reaction mixture in benzene showing residual trisulphide peaks

b) ^{31}P spectrum of XVIS_4 in CDCl_3



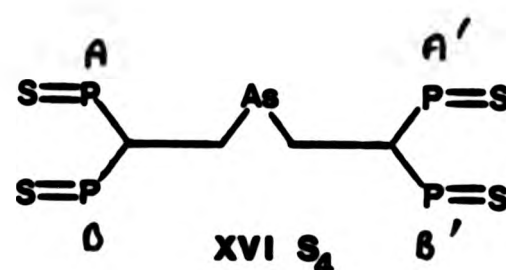
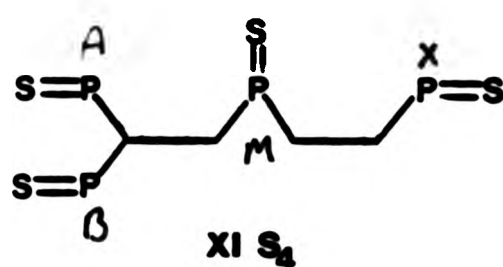


TABLE 6.4 ³¹P n.m.r. parameters for XI S₄

P _i ^a	δ(³¹ P _i) ^b /ppm	Δ _S ^c /ppm	J(P _A P _i) /Hz	J(P _B P _i) /Hz	J(P _M P _i) /Hz	J(P _X P _i) /Hz
P _A	+49.1	+53.1	-	0	20.5	0
P _B	+48.2	+52.2	0	-	13.2	0
P _M	+42.7	+53.9	20.5	13.2	-	60.5
P _X	+52.6	+76.4	0	0	60.5	-

TABLE 6.5 ³¹P n.m.r. parameters for XVI S₄

P _i ^a	δ(³¹ P _i) ^b /ppm	Δ _S ^c /ppm	J(P _A P _i) /Hz	J(P _B P _i) /Hz
P _A	+48.9	+52.1	-	2.4
P _B	+46.0	+50.6	2.4	-

Notes a) See diagrams above for labelling system
 b) Relative to external 85% H₃PO₄ = 0.0 ppm
 c) See eq. 6.2

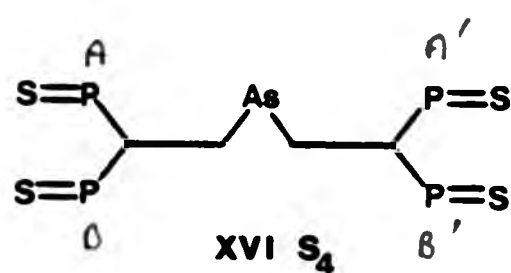
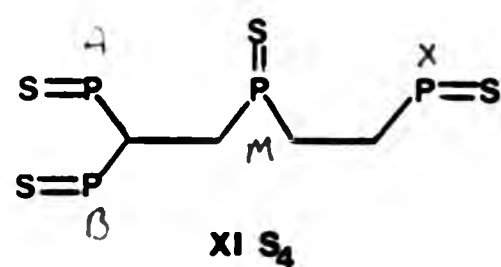


TABLE 6.4 ³¹P n.m.r. parameters for XI S₄

P _i ^a	δ(³¹ P _i) ^b /ppm	Δ _S ^c /ppm	J(P _A P _i) /Hz	J(P _B P _i) /Hz	J(P _M P _i) /Hz	J(P _X P _i) /Hz
P _A	+49.1	+53.1	-	0	20.5	0
P _B	+48.2	+52.2	0	-	13.2	0
P _M	+42.7	+53.9	20.5	13.2	-	60.5
P _X	+52.6	+76.4	0	0	60.5	-

TABLE 6.5 ³¹P n.m.r. parameters for XVI S₄

P _i ^a	δ(³¹ P _i) ^b /ppm	Δ _S ^c /ppm	J(P _A P _i) /Hz	J(P _B P _i) /Hz
P _A	+48.9	+52.1	-	2.4
P _B	+46.0	+50.6	2.4	-

Notes a) See diagrams above for labelling system
 b) Relative to external 85% H₃PO₄ = 0.0 ppm
 c) See eq. 6.2

CHAPTER 7

EXPERIMENTAL

1. PREPARATIONS

General

All reactions were carried out in an atmosphere of dry dinitrogen unless otherwise stated. Solvents were de-aerated immediately prior to use and in cases where dry solvents were required, these were dried by standard methods. Many reagents used in the following syntheses were prepared by standard literature methods as indicated in the text.

Chapter 2 - Ligands

1.1.2-tris(diphenylphosphino)ethane, II

1,1-bis(diphenylphosphino)ethene⁵⁴, I, (5 g, 12.6 mmol) and $\text{Ph}_2\text{PH}^{124-126}$ (2.35 g, 12.6 mmol) were refluxed in dry THF (50 cm³) for 5 mins in the presence of a catalytic amount of potassium tert-butoxide (KO^tBu). The solution was then cooled and the solvent was removed under vacuum to give an oily residue which on addition of EtOH (40 cm³) yielded a white solid. Recrystallisation of this solid from $\text{CH}_2\text{Cl}_2/\text{MeOH}$ yielded the product as a white powder. Yield 6.9 g (94%); mpt 107°C.

Analogous methods using $\text{Mes}_2\text{PH}^{127}$, $^t\text{Bu}_2\text{PH}^{128,129}$ or PhMePH^{130} in place of Ph_2PH afforded the related triphosphine species III, IV and V respectively (page 25), and these compounds were characterised by ^{31}P nmr spectroscopy.

[2,2-bis(diphenylphosphino)ethyl]phenylphosphine, VI

A solution of $\text{PhPH}_2^{131-133}$ (3 g, 27.3 mmol) in THF (25 cm³) was added in a dropwise manner to a stirred solution of 1,1-bis(diphenylphosphino)ethene, I, (10.8 g, 27.3 mmol) in dry THF (40 cm³) containing a catalytic amount of KO^tBu . When addition was complete the mixture was stirred for a further 15 mins and the solvent was then removed under vacuum. Addition of MeOH (40 cm³) to the resultant oily residue followed by 5 min reflux afforded a powdery white precipitate which was recrystallised from $\text{CH}_2\text{Cl}_2/\text{MeOH}$ to give the product as white crystals. Yield, 11.05 g (85%); m.pt. 110°C.

Analogous methods using $\text{CNCH}_2\text{CH}_2\text{PH}_2^{134}$ or $\text{nBuPH}_2^{135,136}$ in place of PhPH_2 afforded the related triphosphine species VII and IX respectively (see page 25) which were characterised in solution by ^{31}P nmr spectroscopy.

[2,2-bis(diphenylphosphino)ethyl][tritert-butylphenyl]phosphine, VII

A solution of (tritert-butylphenyl)phosphine¹³⁷ (2.06 g, 7.4 mmol), 1,1-bis(diphenylphosphino)ethene, I, (2.93 g 7.4 mmol) and a catalytic amount of KO^tBu in dry THF (40 cm³) was refluxed for 5 mins. The solvent was then removed under vacuum to leave an oily residue which on addition of MeOH (30 cm³) yielded a powdery white precipitate which was recrystallised from $\text{CH}_2\text{Cl}_2/\text{MeOH}$ to give the product as white crystals. Yield, 3.7 g (74%); m.pt. 150°C.

1,1,2-tris(diphenylphosphino)ethene, X

A solution of bis(diphenylphosphino)ethyne¹³⁸ (10 g, 25.4 mmol), Ph_2PH (4.7 g, 25.4 mmol) and a catalytic amount of KO^tBu in dry THF (150 cm³) was stirred at room temperature for 18 hrs. The solvent was then removed under vacuum to leave an oily red residue. Addition of

MeOH (200 cm³) followed by vigorous shaking gave a powdery white precipitate which was recrystallised twice from CH₂Cl₂/MeOH to give the product as white crystals. Yield, 7.5 g (51%); m.pt. 151°C.

[2,2-bis(diphenylphosphino)ethyl]-[2-(diphenylphosphino)ethyl]phenylphosphine, XI

A solution containing a mixture of [2,2-bis(diphenylphosphino)-ethyl]phenylphosphine, VI, (2.33 g, 4.6 mmol), vinylidiphenylphosphine 139-141 (0.97 g, 4.6 mmol) and a catalytic amount of KO^tBu in dry THF (30 cm³) was stirred at room temperature for 1 hr. The solvent was then removed under vacuum and MeOH (40 cm³) was added to the resultant residue. Upon cooling to ca -50°C a white solid precipitated which was filtered cold and stored at -10°C. Attempts to crystallise this compound at ambient temperatures generally yielded the product as a viscous oil and therefore this species was characterised in solution by ³¹P nmr spectroscopy. Yield, 2.6 g (66%).

Bis(2,2-bis(diphenylphosphino)ethyl)phenylphosphine, XII

A solution of PhPH₂ (1 g, 9.1 mmol), 1,1-bis(diphenylphosphino)ethene, I, (7.2 g, 18.2 mmol) and a catalytic amount of KO^tBu in dry THF (100 cm³) was refluxed for 15 mins. Removal of the solvent under vacuum yielded an oily residue which on addition of MeOH (50 cm³) afforded a powdery white precipitate. Recrystallisation (twice) of this solid from CH₂Cl₂/MeOH gave the product as white crystals. Yield 7.0 g (85%); m.pt. 154°C.

Analogous methods using CNCH₂CH₂PH₂ or n-BuPH₂ in place of PhPH₂ afforded the related pentaphosphine species XIII and XIV respectively (see page 47) which were characterised in solution by ³¹P nmr spectroscopy.

Bis(2,2-bis(diphenylphosphino)ethyl)phenylarsine, XVI

A solution of PhAsH_2 ^{142,143} (0.82 g, 5.3 mmol), 1,1-bis(diphenylphosphino)ethene, I, (4.2 g, 10.6 mmol) and a catalytic amount of KO^tBu in dry THF (40 cm³) was stirred at room temperature for 18 hrs and finally refluxed for 30 mins. The solvent was removed under vacuum and MeOH (40 cm³) was added to the residue to yield a white precipitate. Recrystallisation (twice) from $\text{CH}_2\text{Cl}_2/\text{MeOH}$ gave the product as white crystals. Yield, 3.37 g (67%); m.pt. 148°C.

P,P'-bis[2,2-bis(diphenylphosphino)ethyl]bis(phenylphosphino)ethane, XVII

Butyllithium (1.67 cm³ of a 2.6 M solution in hexane) was added in a dropwise manner to a solution of [2,2-bis(diphenylphosphino)ethyl]-phenylphosphine, VI, (2.2 g, 4.4 mmol) in THF (30 cm³) contained in a pressure equalising dropping funnel. Dinitrogen was then bubbled through this solution for 5 mins which was then added slowly to a stirred solution of CH_2Cl_2 (0.19 g, 2.17 mmol) in THF (20 cm³). The solvent was then removed under vacuum and the residue was recrystallised from $\text{CH}_2\text{Cl}_2/\text{MeOH}$ to give the crude product as a waxy white solid. Yield, 0.5 g (22%).

P,P'-bis[2,2-bis(diphenylphosphino)ethyl]-1,2-bis(phenylphosphino)ethane, XVIII

A solution of 1,2-bis(phenylphosphino)ethane¹⁴⁴ (0.56 g, 2.3 mmol), 1,1-bis(diphenylphosphino)ethene, I, (1.80 g, 4.6 mmol) and a catalytic amount of KO^tBu in THF (40 cm³) was stirred at room temperature for 5 mins. The solvent was then removed under vacuum and MeOH (20 cm³) was added to the residue. Subsequent cooling to ca -50°C yielded the product as a powdery white precipitate which was characterised by ³¹P nmr spectroscopy.

An analogous method using 1,3-bis(phenylphosphino)propane¹⁴⁵ in place of 1,2-bis(phenylphosphino)ethane yielded the related propane derivative XIX (see page 54).

The three hexaphosphine species XVII-XIX appear to be waxy materials at ambient temperatures, and attempts to isolate these ligands in pure crystalline form were not successful.

Tris(2,2-bis(diphenylphosphino)ethyl)phosphine, XXII

Phosphine gas was generated by the addition of dil. H_2SO_4 (50 cm³) to Zn_3P_2 (5 g, 19 mmol) and passed together with a continuous stream of dinitrogen through two successive traps at -78°C (dry ice/acetone) in order to remove any traces of P_2H_4 and then through a drying column containing KOH pellets^{146,147}. The dried PH_3 was then bubbled through a solution of 1,1-bis(diphenylphosphino)ethene, I, (1 g, 2.5 mmol) in dry THF (40 cm³) containing a catalytic amount of KO^tBu . Excess phosphine gas was allowed to pass into a 20% w/v solution of copper sulphate. When the generation of PH_3 had ceased dinitrogen was passed through the system and the reaction solution to remove any remaining PH_3 . A ^{31}P nmr spectrum of the reaction mixture was then obtained in order to assess the amount of PH_3 reacted, and from this an estimate was made of the additional amount of I required. Addition of this and any further amounts of I deemed appropriate yielded a reaction mixture whose ^{31}P nmr spectrum indicated virtually quantitative formation of the required product. (Total amount of I used; 2.40 g, 6.1 mmol). The solvent was then removed at the pump to give a residue which on addition of MeOH (25 cm³) yielded white crystals. Recrystallisation from $\text{CH}_2\text{Cl}_2/\text{MeOH}$ gave the product as white crystals. Yield, 1.5 g (61%); m.pt 183°C.

Chapter 3 - Complexes of Triphosphine Ligands

$W(CO)_5[Ia]$

This complex was prepared using the u.v. irradiation methods of Strohmeier¹⁴⁸⁻¹⁵² via the reactive intermediate, $W(CO)_5.THF^{66}$. A stirred solution of $W(CO)_6$, (6.5 g, 18.5 mmol) in dry THF (250 cm³) was irradiated for 18 hrs at room temperature. This solution was then transferred under dinitrogen to a dropping funnel and then added in a dropwise manner to a stirred solution of 1,1-bis(diphenylphosphino)ethene, I, (7.3 g, 18.5 mmol) in THF (50 cm³). The solvent was then removed under reduced pressure and the unreacted metal hexacarbonyl was removed by vacuum sublimation. The remaining residue was then recrystallised from $CH_2Cl_2/MeOH$ to give the product as pale yellow crystals. Yield, 6.3 g (47%); m.pt. 150°C.

$Mo(CO)_5[Ia]$

N.B. This complex could not be prepared by an adaptation of the previous method because of difficulties found in the generation of $Mo(CO)_5[THF]$.

A sample of $Et_4N^+[Mo(CO)_5.THF]$ (7 mmol) was prepared by the method of Abel et al^{153,154} and was left as a suspension in 40/60 petroleum ether (40 cm³). A solution of 1,1-bis(diphenylphosphino)ethene, I, (2.8 g, 7.0 mmol) in CH_2Cl_2 (50 cm³), and then $AlCl_3$ (2 g, 15 mmol) were added successively and the mixture was stirred for 18 hrs. The solvent was then removed under reduced pressure leaving a residue which was redissolved in CH_2Cl_2 (25 cm³) and filtered. Addition of MeOH to the filtrate and subsequent cooling yielded a crude yellow green product which was recrystallised from $CH_2Cl_2/MeOH$ to give the required complex as pale yellow crystals. Yield, 1.9 g (43%); m.pt. 135°C.

The related chromium complex $\text{Cr(CO)}_5[\text{Ia}]$ was prepared similarly using adaptations of each of the above methods which gave the product as pale-yellow crystals in yields comparable to those above, m.pt. 132°C .

$\text{Cr(CO)}_5[\text{IIa}]$

A solution containing $\text{Cr(CO)}_5[\text{Ia}]$ (0.94 g, 1.6 mmol), Ph_2PH (0.3 g, 1.6 mmol) and a catalytic amount of KO^tBu in dry THF (30 cm^3) was stirred at room temperature for 30 mins. The solvent was then removed under reduced pressure and the residue was dissolved in CH_2Cl_2 (10 cm^3) and filtered. Addition of MeOH yielded a pale green precipitate which was recrystallised from $\text{CH}_2\text{Cl}_2/\text{MeOH}$ to give the product as white crystals. Yield, 0.8 g (65%); m.pt. 166°C .

Analogous methods were used to prepare the corresponding molybdenum and tungsten complexes $\text{Mo(CO)}_5[\text{IIa}]$ - white crystals. Yield, 65%; m.pt. 230°C . $\text{W(CO)}_5[\text{IIa}]$ - white crystals. Yield, 56%; m.pt. 177°C .

$\text{Cr(CO)}_4[\text{IIc}]$

A solution containing $\text{Cr(CO)}_4[\text{Ib}]^{155}$ (1.5 g, 2.7 mmol), Ph_2PH (0.50 g, 2.7 mmol) and a catalytic amount of KO^tBu in dry THF (30 cm^3) was stirred at room temperature for 1 hr. Removal of the solvent under vacuum left a residue which was dissolved in CH_2Cl_2 (10 cm^3) and filtered. MeOH was then added to the filtrate and yielded a yellow precipitate which was recrystallised from $\text{CH}_2\text{Cl}_2/\text{MeOH}$ to give the product as bright yellow crystals. Yield, 1.25 g (63%); m.pt. 200°C .

The corresponding molybdenum and tungsten complexes were prepared in an analogous manner. $\text{Mo(CO)}_4[\text{IIc}]$ - yellow crystals. Yield, 58%; m.pt. 194°C . $\text{W(CO)}_4[\text{IIc}]$ - yellow crystals. Yield, 53%; m.pt. 212°C .

Cr(CO)₄[IIId]

A solution of 1,1-bis(diphenylphosphino)ethene, I, (0.79 g, 2 mmol) in dry THF (25 cm³) was added in a dropwise manner to a refluxing solution of Cr(CO)₅PPh₂H¹⁵⁶ (0.76 g, 2 mmol) in dry THF (30 cm³) containing a catalytic amount of KO^tBu. When cool the solvent was removed under vacuum to leave a residue which was dissolved in CH₂Cl₂ (10 cm³) and filtered. Addition of MeOH to the filtrate yielded yellow-green crystals which were recrystallised from CH₂Cl₂/MeOH to give the product as pale yellow crystals. Yield, 0.66 g (40%); m.pt. 209°C.

An analogous method was used to prepare the corresponding tungsten complex - W(CO)₄[IIId] as pale yellow crystals. Yield, 61%; m.pt. 190°C.

W(CO)₃[IIe]

A solution of W(CO)₆ (0.64 g, 1.8 mmol) in propionitrile (30 cm³) was refluxed for 72 hrs to give fac W(CO)₃(EtCN)₃ in solution as described by Kubas^{157,158}. A solution of 1,1,2-tris(diphenylphosphino)ethane, II, (1.06 g, 1.8 mmol) in CH₂Cl₂ (10 cm³) was then added and the mixture was refluxed for 1 hr. The solvent was removed under vacuum to leave a yellow brown solid which was recrystallised twice from CH₂Cl₂/MeOH to give the product as bright yellow crystals. Yield 0.82 g (53%); m.pt. 290°C (dec).

Analogous methods were used to prepare the corresponding molybdenum and chromium complexes. Mo(CO)₃[IIe] - yellow crystals. Yield, 30%; m.pt. 278°C. Cr(CO)₃[IIe] - yellow crystals. Yield, 26%; m.pt. 240°C.

Mo(CO)₄[Vic]/Mo(CO)₄[Vie]

A ca 1:1 mixture of these isomeric complexes was obtained by refluxing Mo(CO)₄[piperidine]₂¹⁵⁹ (0.77 g, 2 mmol) and VI (1.0 g, 2 mmol) in CH₂Cl₂ (40 cm³) for 10 mins. MeOH was added to the solution to yield yellow-green crystals which ³¹P n.m.r. spectroscopy showed to be a mixture of the two diastereomers of Mo(CO)₄[Vid] (see page 75) and the related complex Mo(CO)₄[Vic]. Attempts to isolate each of these three species from the mixture proved unsuccessful.

Mo(CO)₃[Vie]

This complex was prepared in an analogous manner to the similar complex Mo(CO)₃[Ile] (see page 173). The product was isolated as bright yellow crystals. Yield 46%; m.pt. 193°C.

Mo(CO)₄[Xc]/Mo(CO)₄[Xd]

A ca 1:1 mixture of these isomers was obtained by refluxing Mo(CO)₄(piperidine)₂ (0.38 g, 1 mmol) and 1,1,2-tris(diphenylphosphino)-ethene, X, (0.58 g, 1 mmol) in CH₂Cl₂ (30 cm³) for 10 mins. Continued reflux was found not to significantly alter the relative proportions of the two isomers. These species were characterised in solution by ³¹P nmr spectroscopy.

PtCl₂[IIId]

Method (i) A solution containing PtCl₂[COD]¹⁶⁰ (0.374 g, 1 mmol) and 1,1,2-tris(diphenylphosphino)ethane, II, (0.582 g, 1 mmol) in CH₂Cl₂ (20 cm³) was stirred at room temperature for 30 mins. Addition of 40/60 petroleum ether precipitated the product as fine pale-yellow crystals. Yield, 0.55 g (65%).

Method (ii) A solution containing $\text{PtCl}_2[\text{Ib}]^{161}$ (0.662 g, 1 mmol), Ph_2Ph (0.186 g, 1 mmol) and a catalytic amount of KO^tBu in dry THF (15 cm^3) was stirred at room temperature for 10 mins by which time the product had precipitated as fine pale yellow crystals. Yield, 0.52 g (61%). ^{31}P nmr spectroscopy revealed this product to be identical to that of the previous method.

Adaptions of method (i) were used to prepare a range of related species as follows:

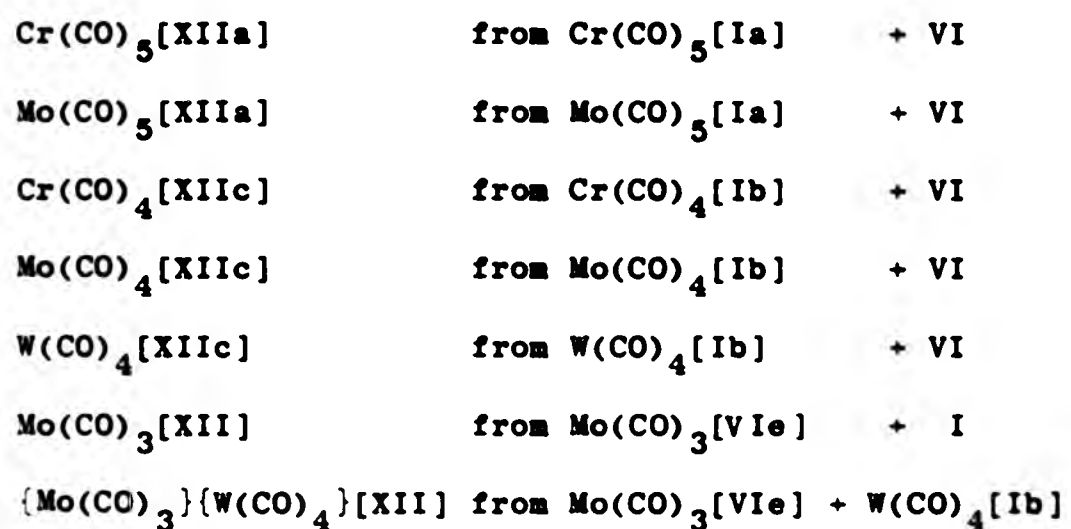
$\text{PtCl}_2[\text{Ib}]$	from $\text{PtCl}_2[\text{COD}]$	+ I
$\text{PdCl}_2[\text{Ib}]$	from $\text{PdCl}_2(\text{PhCN})_2^{162}$	+ I
$\text{PdCl}_2[\text{IIId}]$	from $\text{PdCl}_2(\text{PhCN})_2$	+ II
$\text{Pt}(\text{Me})\text{Cl}[\text{Ib}]$	from $\text{Pt}(\text{Me})\text{Cl}[\text{COD}]^{163}$	+ I
$\text{Pt}(\text{Me})_2[\text{Ib}]$	from $\text{Pt}(\text{Me})_2[\text{COD}]^{164}$	+ I
$\text{Pt}(\text{Me})_2[\text{IIId}]$	from $\text{Pt}(\text{Me})_2[\text{COD}]$	+ II
$\text{Pt}(\text{Me})\text{Cl}[\text{IIId}]$	isomers a) and b) from $\text{Pt}(\text{Me})\text{Cl}[\text{COD}]$	+ II
$\text{PtCl}_2[\text{Xd}]$	from $\text{PtCl}_2[\text{COD}]$	+ X
$\text{PdCl}_2[\text{Xd}]$	from $\text{PdCl}_2(\text{PhCN})_2$	+ X

$\text{Pt}(\text{Me})\text{Cl}[\text{IIId}]$ (isomer a) only)

A solution containing $\text{Pt}(\text{Me})\text{Cl}[\text{Ib}]$ (0.3 g, 0.44 mmol), Ph_2PH (0.08 g, 0.44 mmol) and a catalytic amount of KO^tBu in dry THF (5 cm^3) was stirred at room temperature for 5 mins. This solution was analysed by ^{31}P nmr spectroscopy which indicated the virtually quantitative formation of isomer a).

Chapter 4 - Complexes of Pentaphosphine Ligands

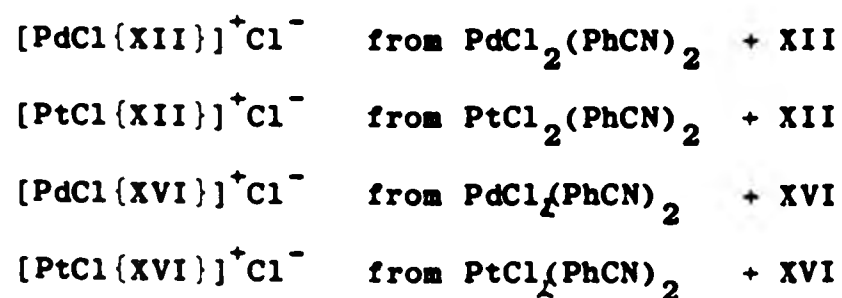
The octahedral complexes described in Chapter 4 were mostly prepared by addition reaction methods analogous to those described for Chapter 3. In general, equimolar amounts of the two starting reagents in dry THF were stirred at room temperature for 30 mins in the presence of KO^tBu . Species prepared in this manner are as follows:



$\{\text{Mo}(\text{CO})_4\}_2[\text{XIIc}]$

This complex was prepared by refluxing $\text{Mo}(\text{CO})_4[\text{piperidine}]_2$ (0.38 g, 1 mmol) and bis(2.2-bis(diphenylphosphino)ethyl)phenylphosphine, XII, (9.45 g, 0.5 mmol) in CH_2Cl_2 (25 cm^3) for 10 mins. The product was characterised by ^{31}P nmr spectroscopy

The four square-planar complexes described in Chapter 4 were each prepared in a similar manner. Reaction of $\text{MCl}_2(\text{PhCN})_2$ with an equimolar amount of the free ligand in CH_2Cl_2 at room temperature resulted in the virtually quantitative formation of the desired complexes as follows:



Attempts to achieve a quantitative displacement of the chloride anion by a more stabilising counterion such as PF_6^- were unsuccessful⁹⁶.

Chapter 5 - Complexes Involving 1,1-bis(diphenylphosphino)ethene, I
as a Bridging Ligand

$\text{Pd}_2[\text{I}]_2\text{Cl}_2$

$\text{Pd}_2(\text{dba})_3 \cdot \text{CHCl}_3$ ¹⁶⁵ (1.35 g, 1.3 mmol), $\text{Pd}(\text{PhCN})_2\text{Cl}_2$ (1.0 g, 2.6 mmol) and 1,1-bis(diphenylphosphino)ethene, I, (2.0 g, 5.2 mmol) were refluxed in dry CH_2Cl_2 (50 cm³) for 30 mins. The solution was then reduced in volume to ca 10 cm³ under reduced pressure and MeOH (40 cm³) was added. The orange-red precipitate formed was recrystallised from $\text{CH}_2\text{Cl}_2/\text{MeOH}$ to give the product as red crystals. Yield 2.10 g (75%).

An analogous method using $\text{Pt}(\text{PhCN})_2\text{Cl}_2$ ¹⁶² in place of $\text{Pd}(\text{PhCN})_2\text{Cl}_2$ afforded the corresponding mixed Pd/Pt complex $\text{PdPt}[\text{I}]_2\text{Cl}_2$ as orange-red crystals. Yield, 1.2 g (79%); m.pt 274°C (dec). This method also yields a small amount (<5%) of the dipalladium species as an impurity.

$\text{Pd}_2(\mu\text{-CH}_2)[\text{I}]_2\text{Cl}_2$

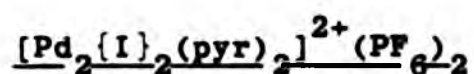
(i) Preparation of diazomethane/ether solution¹⁶⁶

1-methyl-3-nitro-1-nitrosoguanidine (220 mg) was added slowly to a cooled (0°C) mixture of aqueous KOH solution (40% w/v, 20 cm³) and ether (20 cm³). This mixture was stirred until the aqueous layer was colourless and the ether layer yellow. The ether layer was then carefully decanted into a flask containing KOH pellets and the solution was left to dry at 0°C for 1 hr.

(ii) Preparation of the complex

A solution of $\text{Pd}_2[\text{I}]_2\text{Cl}_2$ (0.5 g, 0.47 mmol) in CH_2Cl_2 (10 cm³) and diethylether (20 cm³) was cooled to 0°C and an ether solution of

diazomethane (4 mmol) was then added. The mixture was stirred at 0°C until the evolution of gas had ceased and was then allowed to warm to room temperature. Removal of the solvent under reduced pressure yielded a residue which was recrystallised from $\text{CH}_2\text{Cl}_2/\text{MeOH}$ to give the product as orange crystals. Yield, 0.35 g (69%). m.pt 255°C (dec.).



$\text{Pd}_2[\text{I}]_2\text{Cl}_2$ (0.46 g, 0.43 mmol) was suspended in MeOH (20 cm^3) and then pyridine (1 cm^3 , excess) was added with stirring. When the solution had cleared a solution of NH_4PF_6 (0.5 g, 3 mmol) in MeOH (5 cm^3) was added which immediately precipitated a bright yellow solid which was filtered and washed with water, MeOH and n-hexane. Recrystallisation of this solid from $\text{CH}_2\text{Cl}_2/\text{n-hexane}$ afforded the product as a bright yellow crystalline solid. Yield, 0.56 g (90%). m.pt 223°C (dec.).

Analogous methods were used to prepare the following related complexes: $[\text{Pd}_2\{\text{I}\}_2\{\text{P}(\text{OMe})_3\}]^{2+}(\text{PF}_6^-)_2$, $[\text{Pd}_2\{\text{I}\}_2(\text{Ph}_2\text{PH})_2]^{2+}(\text{PF}_6^-)_2$, $[\text{PdPt}\{\text{I}\}_2(\text{pyr})_2]^{2+}(\text{PF}_6^-)_2$, $[\text{PdPt}\{\text{I}\}_2(\text{Ph}_2\text{PH})_2]^{2+}(\text{PF}_6^-)_2$, $[\text{PdPt}\{\text{I}\}_2\{\text{P}(\text{OMe})_3\}]^{2+}(\text{PF}_6^-)_2$, $[\text{PdPt}(\mu\text{-CH}_2)\{\text{I}\}_2\{\text{P}(\text{OMe})_3\}]^{2+}(\text{PF}_6^-)_2$.

Chapter 6 - Sulphur Derivatives

The sulphurisation reactions described in Chapter 6 occur slowly merely by stirring a solution containing the free ligand and elemental sulphur in benzene at room temperature. However reaction rates were increased by warming the solution to ca 50°C. In cases where only one species was present in the reaction mixture this was precipitated by the addition of MeOH and then recrystallised from $\text{CH}_2\text{Cl}_2/\text{MeOH}$. Derivatives isolated in this manner were the pentasulphide derivative

of bis[2,2-bis(diphenylphosphino)ethyl]phenyl phosphine - XXI S₅ and the tetrasulphide derivative of bis[2,2-bis(diphenylphosphino)ethyl]-phenyl arsine - XVI S₄.

XII S₅ - white crystals. Yield 85%. m.pt 201°C

XVI S₄ - white crystals. Yield 78%. m.pt 165°C (dec.)

Microanalytical results for C, H, P and N are shown in Table 7.1. For species that contain arsenic, phosphorus determinations were precluded owing to arsenic interference. Mass spectroscopy figures are shown in Table 7.2 and these were found to be most informative for the free ligands and the metal carbonyl complexes. For the smaller ligands detection of the parent molecular ion M⁺ was possible but for the larger ligands only breakdown products were identified. The breakdown of these ligands follows a consistent pattern in that generally the most intense signal was found to be M/e = 185 corresponding to Ph₂P- fragments. In addition common features at M/e 397 ([Ph₂P]₂CHCH₂) confirm the proposed molecular structures. For VII signals at M/e 617 and M/e 429 correspond to cleavage of (C₄H₉) and (2,4,6-[^tC₄H₉]₃C₆H₂) groups respectively from the parent molecule. For X a signal at M/e 395 corresponding to a [Ph₂P]₂C:CH group confirms the presence of the double bond. In the case of the metal carbonyl complexes detection of the molecular ion was often possible and in addition breakdown products resulting from the sequential cleavage of carbonyl groups was observed. Characteristic isotope patterns for Cr, Mo and W also help confirm the proposed structures. In several groups of complexes mass spectroscopy

revealed the presence of CH_2Cl_2 as a molecule of crystallisation which could only be removed at temperatures approaching 200°C in a vacuum. Careful scrutiny of the proton n.m.r. spectra of these species followed by accurate integration of the signal from CH_2Cl_2 against the CH and CH_2 protons in the ligand chain revealed the amount of CH_2Cl_2 present as indicated in Table 7.1

TABLE 7.1 Microanalytical results

compound	FOUND %			CALCULATED %		
	C	H	P	C	H	P
II	78.4	5.7	15.7	78.3	5.7	15.9
VI	75.8	5.8	18.4	75.8	5.8	18.4
VII	78.5	7.9	13.7	78.5	7.9	13.8
X	78.4	5.4	15.5	78.6	5.4	16.0
XII	77.0	5.8	17.2	77.2	5.7	17.2
XVI	72.7	5.4	-	73.6	5.4	-
XXII	75.9	5.7	17.2	76.6	5.7	17.9
$\text{Cr}(\text{CO})_5[\text{Ia}]$	62.7	3.8	10.5	63.3	3.8	10.5
$\text{Mo}(\text{CO})_5[\text{Ia}]$	58.5	3.5	9.6	58.8	3.5	9.8
$\text{W}(\text{CO})_5[\text{Ia}]$	51.3	3.0	8.6	51.7	3.1	8.6
$\text{Cr}(\text{CO})_5[\text{IIa}]^a$	65.0	4.1	11.6	64.7	4.2	11.6
$\text{Mo}(\text{CO})_5[\text{IIa}]^a$	62.2	3.9	11.2	61.4	4.0	11.0
$\text{W}(\text{CO})_5[\text{IIa}]^a$	55.4	3.6	9.7	55.6	3.6	9.9

Notes a) Calculated to include 0.35 equivalents of CH_2Cl_2 as molecules of crystallisation as indicated by mass spectroscopy and ^1H n.m.r.

[contd]

TABLE 7.1 cont

COMPOUND	FOUND %			CALCULATED %		
	C	H	P	C	H	P
Cr(CO) ₄ [IIc]	66.9	4.4	12.1	67.6	4.4	12.4
Mo(CO) ₄ [IIc]	63.9	4.1	11.7	63.8	4.2	11.8
W(CO) ₄ [IIc]	57.2	3.7	10.7	57.4	3.8	10.6
Cr(CO) ₄ [IIId] ^b	64.4	4.3	12.0	64.7	4.3	11.8
W(CO) ₄ [IIId] ^b	55.0	3.7	9.8	55.4	3.7	10.1
Cr(CO) ₃ [IIe] ^a	65.4	4.5	12.3	66.3	4.5	12.4
Mo(CO) ₃ [IIe] ^a	63.3	4.4	11.9	62.7	4.3	11.7
PdCl ₂ [IIId]	58.6	4.4	12.1	58.8	4.3	12.0
[PtCl{XII}] ⁺ (PF ₆) ⁻	53.3	3.9	14.1	54.5	4.0	14.5
[PtCl{XVI}] ⁺ (PF ₆) ⁻	52.1	3.7	-	52.7	3.8	-
Mo(CO) ₃ [VIe]	61.0	4.2	13.4	61.2	4.3	13.5
Pd ₂ {I} ₂ Cl ₂	57.3	4.1	11.9	58.0	4.1	11.5
[Pd ₂ {I} ₂ (pyr) ₂](PF ₆) ₂ [*]	50.7	3.6	12.7	51.2	3.7	12.8
[Pd ₂ {I} ₂ (P(OMe) ₃) ₂](PF ₆) ₂	44.6	3.9	15.7	45.1	4.0	16.1
[PdPt{I} ₂ (Ph ₂ PH) ₂](PF ₆) ₂	50.9	3.7	14.1	51.9	3.8	14.1
[PdPt{I} ₂ (P(OMe) ₃) ₂](PF ₆) ₂	42.4	3.6	15.0	42.7	3.8	15.2
XII S ₅	65.5	4.7	14.2	65.5	4.8	14.6
XVI S ₄	65.5	4.9	-	64.8	4.8	

Notes b) Calculated to include 0.5 equivalents of CH₂Cl₂

* Found N 1.9% calc N 1.9%

TABLE 7.2 Mass spectroscopy results

COMPOUND	Molecular ion M/e	Major Ions Detected M/e
II	580	397, 185
VI	506	397, 185, 109
VII	674	617, 429, 277, 185
X	580	395, 185
XII	-	717, 505, 397, 185
XVI	-	370, 185
XVII	-	627, 519, 505, 397, 370, 185
XVIII	-	505, 397, 185
XXII	-	397, 370, 320, 185

TABLE 7.2 contd

COMPOUND	M ⁺	(M-CO) ⁺	(M-2CO) ⁺	(M-3CO) ⁺	(M-4CO) ⁺	(M-5CO) ⁺	CH ₂ Cl ₂
Cr(CO) ₅ [Ia]	588	560	-	504	476	448	
Mo(CO) ₅ [Ia]	-	604	-	548	520	492	
W(CO) ₅ [Ia]	720	692	-	636	608	580	
Cr(CO) ₅ [IIa]	-	746	718	-	662	634	✓
Mo(CO) ₅ [IIa]	-	-	762	-	706	678	✓
W(CO) ₅ [IIa]	-	878	850	-	794	766	✓
Cr(CO) ₄ [IIc]	746	718	-	662	634	-	
Mo(CO) ₄ [IIc]	-	762	-	706	678	-	
W(CO) ₄ [IIc]	878	850	-	794	766	-	
Cr(CO) ₄ [IIId]	746	718	-	662	634	-	✓
W(CO) ₄ [IIId]	878	850	-	794	766	-	✓
Cr(CO) ₄ [IIe]	718	-	662	634	-	-	✓
Mo(CO) ₄ [IIe]	762	-	706	678	-	-	✓
W(CO) ₄ [IIe]	850	-	794	-	-	-	✓

2. INSTRUMENTATION

^{31}P n.m.r. spectra were recorded on a JEOL FX60 Fourier transform n.m.r. spectrometer operating at 24.2 MHz and on a JEOL FX90Q Fourier transform n.m.r. spectrometer operating at 36.2 MHz. Spectra of other nuclei were recorded solely on the JEOL FX90Q spectrometer. For the spin-tickling and selective-decoupling experiments additional radio-frequencies were supplied by a Gen Rad model 1061 frequency synthesiser and applied via a tuned amplifier to an additional coil incorporated into the probe. Samples were examined as solutions in 10 mm o.d. spinning tubes at ambient temperature (21°C) unless otherwise stated. The field-frequency lock was provided by means of the ^2D signal from either a permanent external (D_2O) sample or in cases where higher resolution was required, from a suitable deuterated solvent added to the sample. ^{31}P spectra were recorded using appropriate spectral widths (typically 5000 Hz) and sufficient data points (typically 8K) to give a digital resolution of 1.25 Hz / point or better in the transformed spectrum.

Chemical shifts are expressed relative to the standard references as indicated in the text using the δ convention i.e. shifts to high frequency of the reference are positive.

2-Dimensional n.m.r. experiments were performed using typically 256 data points along the t_1/f_1 axis and 1024 points along the t_2/f_2 axis. Quadrature detection was employed to prevent problems from folded signals.

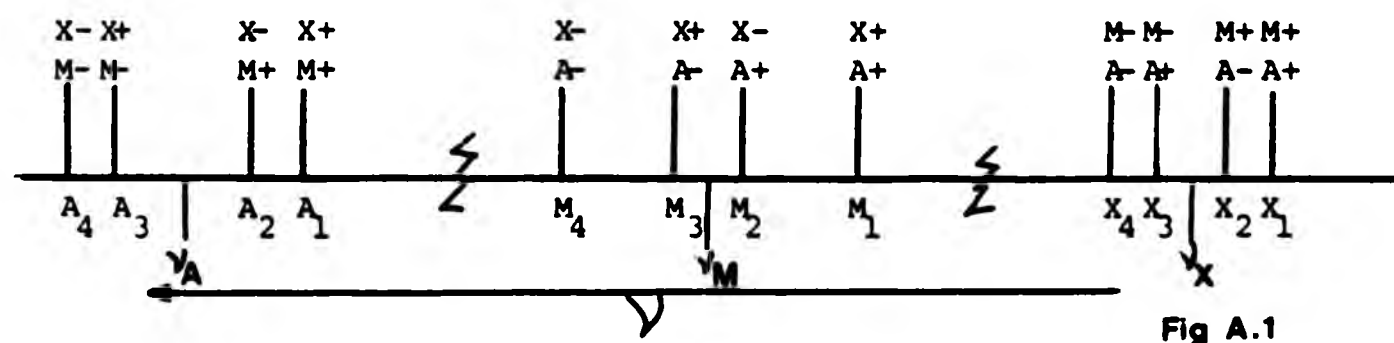
APPENDIX I

Spin Tickling and Selective Decoupling

Information regarding the relative signs of coupling constants may be obtained by analysis of second-order spectra but not from first-order spectra. Therefore, sign determinations on such systems have to be performed by other methods, the most widely-applied of which is multiple resonance¹⁶⁷.

Spin Tickling

Perhaps the simplest way of describing spin-tickling experiments is by reference to a theoretical homonuclear AMX spin system. An AMX spin system is characterised by three chemical shifts ν_A , ν_M and ν_X and three coupling constants JAM, JAX AND JMX. A schematic representation of a homonuclear AMX spectrum where $I_A = I_M = I_X = \frac{1}{2}$ and where $\gamma > 0$ and JAM, JAX, JMX > 0 is depicted in Fig A.1.



The four A transitions $A_1 - A_4$ have frequencies defined by the expression

$$\nu = \nu_A - JAM.M_M - JAX.M_X$$

where M_M = magnetic quantum number of nucleus M and can take values of $\pm \frac{1}{2}$.

Thus the four A transitions correspond to the four possible combinations of M_M and M_X as denoted above each A transition. Similarly the four M and four X transitions are defined as

$$\nu = \nu_M - JAM.M_A - JMX.M_X$$

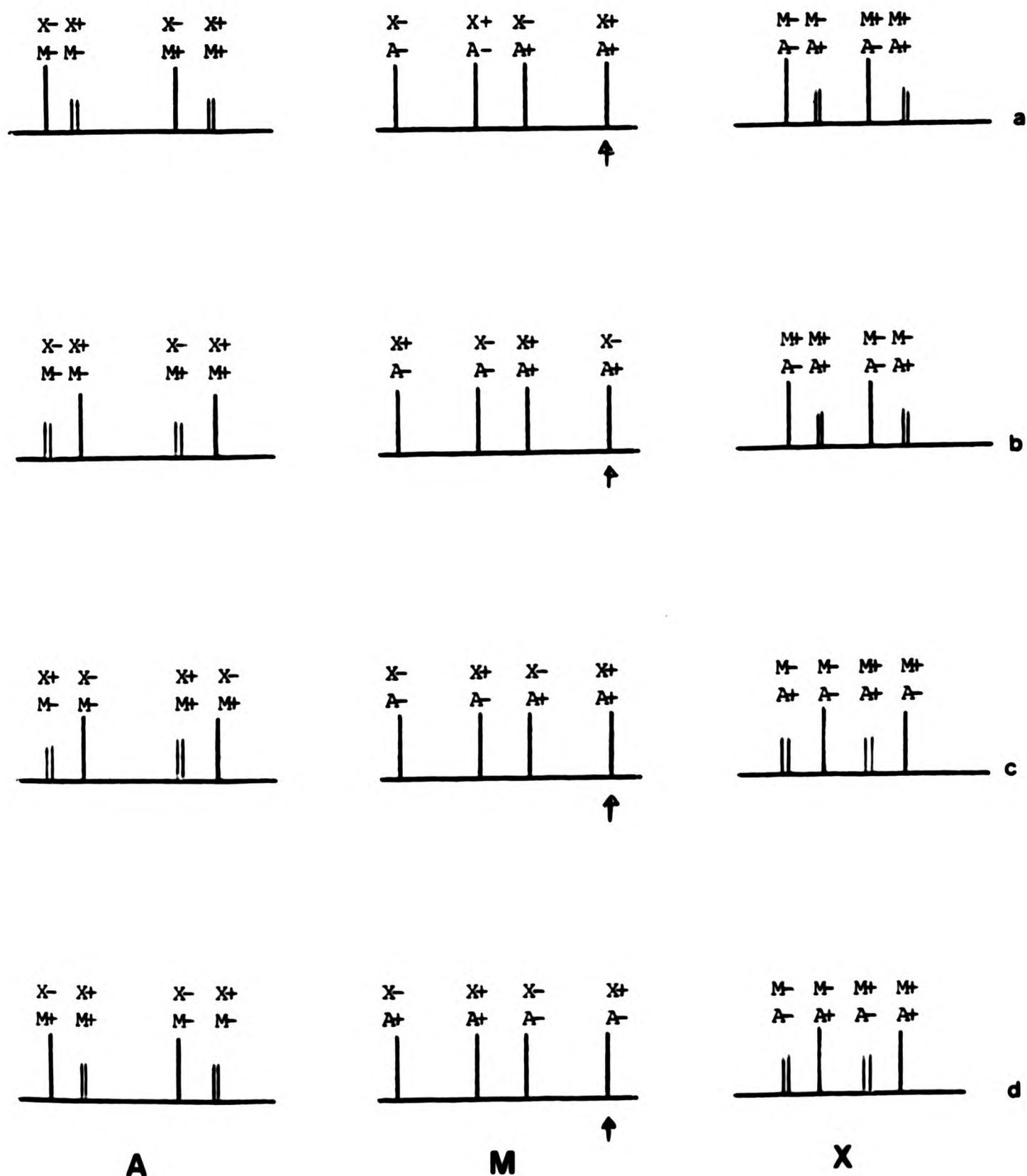
$$\nu = \nu_X - JAX.M_A - JMX.M_M$$

and can be similarly assigned to the various combinations of M_A , M_M and M_X . Such a description can be simply extended to cases where the three coupling constants do not have the same sign.

For the purpose of describing spin tickling experiments it is now necessary to consider the effects on the appearance of the spectrum whilst applying an irradiating frequency ν_2 corresponding to one transition in the total spectrum. For the spectrum shown it would be preferable to irradiate one of the outer M transitions M_1 or M_4 since these are most distinct from other transitions. Irradiation at M_1 will affect only other transitions that like M_1 , arise from molecules where $M_X = +\frac{1}{2}$ and $M_A = +\frac{1}{2}$ which by inspection of the diagram can be seen to be A_1 and A_3 where $M_X = +\frac{1}{2}$ and X_1 and X_3 where $M_A = +\frac{1}{2}$. The manifestation of this effect if ν_2 is set exactly on M_1 is to split the A_1 , A_3 , X_1 and X_3 transitions into symmetrical doublets, the magnitude of the splitting being a function of the amplitude of ν_2 . It is therefore possible to determine the relative signs of JAM, JAX and JMX by the consideration of the appearance of spectra under irradiation with regard to the possible combinations of M_A , M_M and M_X . Fig. A.2 shows the appearance of spectra under irradiation for the four possible sign relationships of JAM, JAX and JMX for a particular irradiation frequency and because each spectrum is unique it is possible for relative sign determinations to result from a single spin-tickling experiment.

Fig. A.2 - The appearance of AMX spectra under conditions of irradiation at one of the M transitions (arrowed) for the four possible sign relationships of JAM, JAX and JMX.

- a) JAM, JAX and JMX all positive (or all negative)
- b) JAM, JAX positive ; JMX negative.
- c) JAM, JMX positive ; JAX negative.
- d) JAM positive ; JAX, JMX negative.



Selective decoupling

Selective decoupling experiments differ from spin-tickling ones in that they generally involve irradiation of a group of coupled transitions. For instance, irradiation at a frequency centred between M_1 and M_2 (which corresponds to the JMX coupling) and at an amplitude large in comparison to JMX but small in comparison to JAM such that no significant irradiation at M_3 occurs, will lead to the collapse of JMX coupling for molecules in which the spin state of A is the same as for the irradiated transitions M_1 and M_2 i.e. $+\frac{1}{2}$. Thus in Fig. A.1 lines X_1 and X_3 will collapse to a single line centred between X_1 and X_3 and of double intensity while lines X_2 and X_4 should remain unperturbed. Again considerations of the possible combinations of M_A , M_M and M_X lead to sign information although this experiment alone reveals only the relative signs of JAM and JAX and therefore complete sign determination for this system by selective decoupling requires more than one experiment. Practically it is preferred to irradiate at the centre of two relatively closely coupled transitions since lower irradiating power levels are required. Thus for a case such as in Fig. A.1 it is likely that irradiation would be chosen to be centred between A_1 and A_2 rather than M_1 and M_2 . Where a choice between experiments exists selective decoupling is usually preferred to spin-tickling since the experiment is not so dependent on exact frequency ν_2 or power level and is therefore generally easier to perform. It must be remembered that such experiments only give relative signs of coupling constants. Absolute sign determinations must relate unknown couplings to those of known sign.

APPENDIX II

Analysis of AA'XX' spectra

In an AA'XX' spectrum the AA' and XX' resonances are identical in appearance and are symmetrical about the chemical shift positions ν_A and ν_X respectively. Unless the spectrum is deceptively simple each multiplet consists of 10 resolvable lines the relative positions of which depend upon the following parameters:

$$|K| = J_{AA'} + J_{XX'}$$

$$|L| = J_{AX} - J_{AX'}$$

$$|M| = J_{AA'} - J_{XX'}$$

$$|N| = J_{AX} + J_{AX'}$$

The two strongest lines in each multiplet are centred about the chemical shift position and are separated by $|N|$ and together they account for one half of the total intensity in the multiplet. The eight remaining lines consist of two 'ab' subspectra, each accounting for one half of the remaining intensity i.e. one quarter of the total and may be analysed by the standard procedure. The two apparent chemical shifts ν_a and ν_b should be identical for each subspectrum and their difference $|\nu_a - \nu_b|$ is equal to $|L|$ in magnitude. The two apparent spin coupling constants derived from the subspectra are equal to $|K|$ and $|M|$ in magnitude but it is not possible to distinguish between them.

Example - $\text{PdPt}(\text{I})_2\text{Cl}_2$

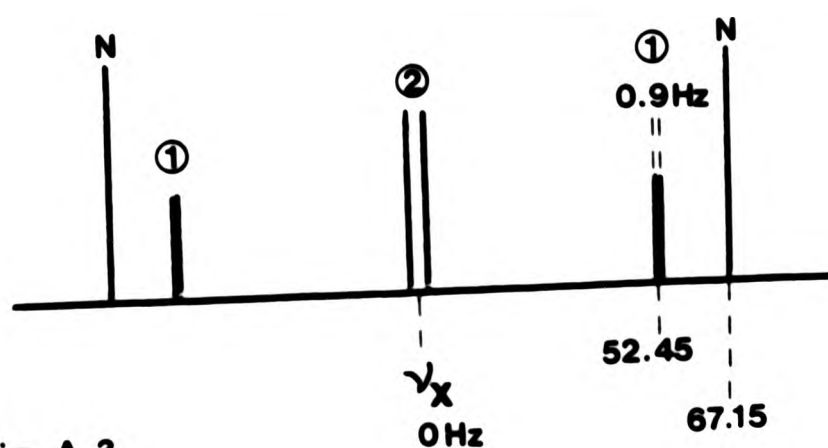
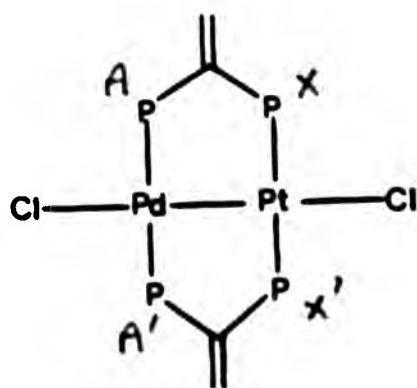


Fig A.3

APPENDIX II

Analysis of AA'XX' spectra

In an AA'XX' spectrum the AA' and XX' resonances are identical in appearance and are symmetrical about the chemical shift positions ν_A and ν_X respectively. Unless the spectrum is deceptively simple each multiplet consists of 10 resolvable lines the relative positions of which depend upon the following parameters:

$$|K| = J_{AA'} + J_{XX'}$$

$$|L| = J_{AX} - J_{AX'}$$

$$|M| = J_{AA'} - J_{XX'}$$

$$|N| = J_{AX} + J_{AX'}$$

The two strongest lines in each multiplet are centred about the chemical shift position and are separated by $|N|$ and together they account for one half of the total intensity in the multiplet. The eight remaining lines consist of two 'ab' subspectra, each accounting for one half of the remaining intensity i.e. one quarter of the total and may be analysed by the standard procedure. The two apparent chemical shifts ν_a and ν_b should be identical for each subspectrum and their difference $|\nu_a - \nu_b|$ is equal to $|L|$ in magnitude. The two apparent spin coupling constants derived from the subspectra are equal to $|K|$ and $|M|$ in magnitude but it is not possible to distinguish between them.

Example - $\text{PdPt}(\text{I})_2\text{Cl}_2$

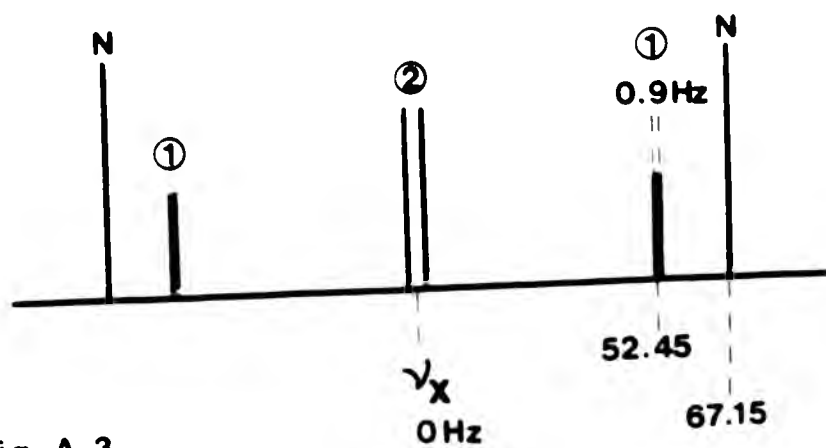
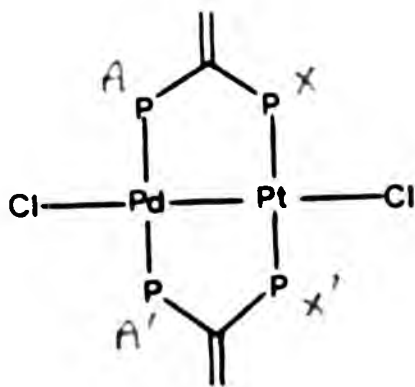


Fig A.3

The resonances due to XX' in molecules of $PdPt(I)_2Cl_2$ (Fig. A.3) which contain the isotope $^{195}Pt(I = \frac{1}{2})$ constitute one half of an $AA'XX'$ spectrum, well separated from the rest of the spectrum, and a schematic representation is shown above. In this the weak outer lines of the ab subspectrum labelled (2) are too weak for detection but this does not preclude a full analysis. The two strongest lines are the $|N|$ lines separated by 134.3 Hz, thus $|JAX + JAX'| = 134.3$ Hz. The ab subspectrum (1) has $J_{ab} = 0.9$ Hz and a chemical shift separation of (1) = 104.9 Hz. Combining $|N|$ and $|L|$ two possible results are obtained:

$$1) \quad JAX = 14.7 \text{ Hz and } JAX' = 119.6 \text{ Hz}$$

$$\text{or } 2) \quad JAX = 119.6 \text{ Hz and } JAX' = 14.7 \text{ Hz.}$$

Since it is likely that for this molecule $^2JAX > ^3JAX'$ it is possible to deduce $JAX = 119.6$ Hz and $JAX' = 14.7$ Hz.

The ab subspectrum labelled (2) has identical chemical shifts ν_a and ν_b to those of (1) and therefore the positions of the weak outer lines may be calculated to give $J_{ab} = \text{ca } 800$ Hz. Since phosphorus-phosphorus couplings through palladium and platinum are known to be large and of comparable magnitude, it is clear that this value represents the sum of the two couplings $JAA' + JXX'$ whilst the value of 0.9 Hz derived from subspectrum 1 represents the difference $JAA' - JXX'$

$$\text{i.e. } JAA' \approx JXX' \approx 400 \text{ Hz.}$$

This figure cannot be quoted with any great certainty however since the appearance of the multiplet in this case does not alter significantly even with quite large changes in JAA' and JXX' and a better value may be derived from computer simulation of the central $AA'BB'$ spectrum due to molecules containing non-magnetic isotopes of platinum using the values of JAX and JAX' obtained from the preceding analysis.

Deceptive simplicity

The ^{31}P spectra of the A_2 and B_2 diastereomers of $[\text{PdCl}\{\text{XVI}\}]\text{Cl}$ (Fig. A.4) show the AA' and XX' resonances as triplets and this demonstrates nicely a case of deceptive simplicity. By considering

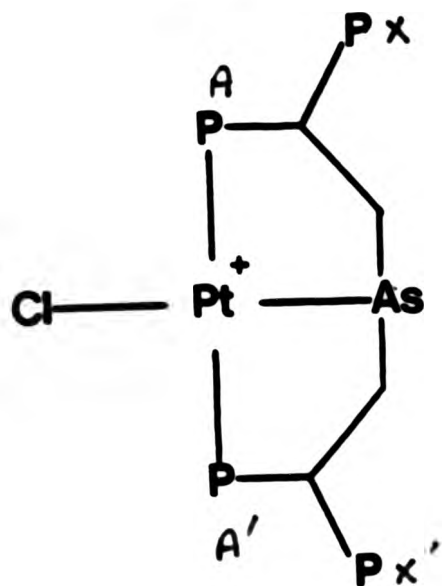


Fig A.4

the dependence of the appearance of $AA'XX'$ spectra on the four parameters $|K|$, $|L|$, $|M|$, and $|N|$ it is clear that if $|K|$ and $|M|$ are equal the ab subspectra of the multiplets will be superposed. In addition if these values are large in comparison to $|L|$ the ab subspectra will appear as a single line at the chemical shift position accounting for half the total intensity of the multiplet. Providing $|N| \neq 0$ the $|N|$ lines are then symmetrically displaced either side of these coincident resonances, each having one quarter of the total intensity and the multiplet therefore appears deceptively as a simple triplet. Clearly this is the case for the symmetric A_2 and B_2 diastereomers of $[\text{PdCl}\{\text{XVI}\}]\text{Cl}$ where $^6J_{XX'}$ is likely to be zero and where $^2J_{AA'}$ is of the order of 400 Hz (by analogy with the AB diastereomer).

Deceptive simplicity

The ^{31}P spectra of the A_2 and B_2 diastereomers of $[\text{PdCl}\{\text{XVI}\}]\text{Cl}$ (Fig. A.4) show the AA' and XX' resonances as triplets and this demonstrates nicely a case of deceptive simplicity. By considering

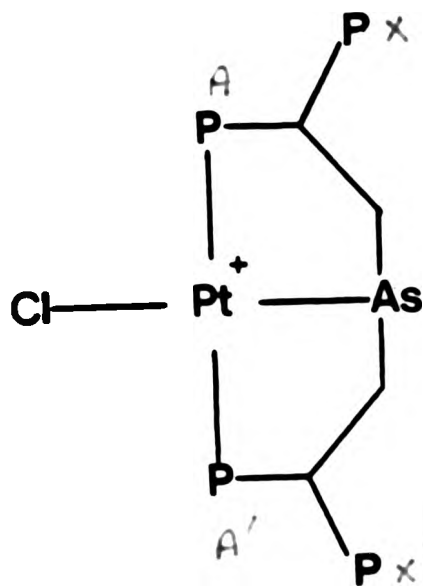


Fig A.4

the dependence of the appearance of $AA'XX'$ spectra on the four parameters K , L , M , and N it is clear that if K and M are equal the ab subspectra of the multiplets will be superposed. In addition if these values are large in comparison to L the ab subspectra will appear as a single line at the chemical shift position accounting for half the total intensity of the multiplet. Providing $N \neq 0$ the N lines are then symmetrically displaced either side of these coincident resonances, each having one quarter of the total intensity and the multiplet therefore appears deceptively as a simple triplet. Clearly this is the case for the symmetric A_2 and B_2 diastereomers of $[\text{PdCl}\{\text{XVI}\}]\text{Cl}$ where $^6J_{XX'}$ is likely to be zero and where $^2J_{AA'}$ is of the order of 400 Hz (by analogy with the AB diastereomer).

References

1. K. Issleib and D.W. Müller, Chem. Ber., 1959, 92, 3175.
2. A.M. Aguiar and J. Beisler, J. Org. Chem., 1964, 29, 1660.
3. K. Issleib and G. Döhl, Chem. Ber., 1961, 94, 2664.
4. R.A. Baldwin and R.M. Washburn, J. Org. Chem., 1965, 30, 3860.
5. A.M. Aguiar and D. Daigle, J. Am. Chem. Soc., 1964, 86, 2299.
6. H. Hartmann, C. Beermann, and H. Czempik, Z. Anorg. Allg. Chem., 1956, 287, 261.
7. R.B. King and P.N. Kapoor, J. Am. Chem. Soc., 1969, 91, 5191.
8. S.O. Grim, R.P. Molenda and R.L. Keiter, Chem. Ind. (London), 1970, 1378.
9. R.B. King and P.N. Kapoor, J. Am. Chem. Soc., 1971, 93, 4158.
10. S.O. Grim, J. Del Gaudio, R.P. Molena, C.A. Tolman and J.P. Jesson, J. Am. Chem. Soc., 1974, 96, 3416.
11. S.O. Grim and R.C. Barth, J. Organomet. Chem., 1975, 94, 327.
12. G. Kordosky, B.R. Cook, J.C. Cloyd and D.W. Meek, Inorg. Synth., 1973, 14, 14.
13. K.K. Chow, W. Levason and C.A. McAuliffe, J. Chem. Soc., Dalton Trans., 1976, 14, 1429.
14. W. Levason, C.A. McAuliffe, A.I. Plaza and S.O. Grim, Inorg. Synth., 1976, 16, 184.
15. R.B. King and J.C. Cloyd, J. Am. Chem. Soc., 1975, 97, 46.
16. R.B. King, J.C. Cloyd and P.N. Kapoor, J. Chem. Soc., Perkin I, 1973, 2226.
- 16a. R. Uriarte, T.J. Mazanec, K.D. Tau and D.W. Meek, Inorg. Chem., 1980, 19, 79.
17. Phosphine, Arsine and Stibine Complexes of the Transition Elements. C.A. McAuliffe and W. Levason. Elsevier Scientific Publishing Co., 1979.
- 17a. Transition Metal Complexes Containing Phosphorus, Arsenic and Antimony Ligands, ed C.A. McAuliffe, Macmillan Press, London, 1973.
18. R.J. Puddephatt, Chem. Soc. Rev., 1983, 12, 99.
19. A.R. Sanger, J. Chem. Soc., Chem. Commun., 1975, 893.

- 19a J.A. Connor, J.P. Day, E.M. Jones and G.K. McEwen, J. Chem. Soc., Dalton Trans., 1973, 347.
20. E.E. Isaacs and W.A.G. Graham, Inorg. Chem., 1975, 14, 2560.
21. J.A. Connor, G.K. McEwen and C.J. Rix, J. Chem. Soc., Dalton Trans., 1974, 589.
22. J. Chatt and F.A. Hart, J. Chem. Soc., 1960, 1378.
- 22a. D.L. Berglund and D.W. Meek, J. Am. Chem. Soc., 1968, 90, 518.
23. R.B. King, Accs. Chem. Res., 1972, 5, 177.
24. R.B. King and M.S. Saran, Inorg. Chem., 1971, 10, 1861.
25. R.B. King, R.N. Kapoor, M.S. Saran and P.N. Kapoor. Inorg. Chem., 1971, 10, 1851.
26. R.B. King, P.N. Kapoor and R.N. Kapoor, Inorg. Chem., 1971, 10, 1841.
27. R.B. King and J.C. Cloyd, Inorg. Chem., 1974, 14, 1550.
28. W.O. Siegl, S.J. Lapporte and J.P. Collman, Inorg. Chem., 1973, 12, 674.
29. J. Chatt, G.T. Leigh and N. Thankarajan, J. Organomet. Chem., 1971, 29, 105.
30. J.C. Cloyd and D.W. Meek, Inorg. Chem. Acta, 1972, 6, 607.
31. R.B. King, P. Zinich and J.C. Cloyd, Inorg. Chem., 1975, 14, 1554.
32. K.D. Tau, R. Uriarte, T.J. Mazanec and D.W. Meek, J. Am. Chem. Soc., 1979, 101, 6614.
33. L. Pauling, The Nature of the Chemical Bond, 1940, Cornell University Press, New York.
34. T. Kruck, H. Diederhagen, and A. Engelmann, Z. Anorg. Allg. Chem., 1973, 397, 31.
35. M.M. Taqui Khan and A.E. Martell, Inorg. Chem., 1974, 14, 676.
36. S.O. Grim, W. McFarlane and E.F. Davidoff, J. Org. Chem., 1967, 32, 781.
37. J. Lewis, R.S. Nyholm, A.G. Osborne, S.S. Sandhu and M.H.B. Stiddard, J. Chem. Soc., 1964, 2825.
38. L.S. Merriwether and J.R. Leto, J. Am. Chem. Soc., 1961, 83, 3182.
39. S.O. Grim, R.L. Keiter and W. McFarlane, Inorg. Chem., 1967, 6, 1113.
40. A.R. Sanger, J. Chem. Soc., Dalton Trans., 1977, 1971.
- 40a. P.E. Garrou, Inorg. Chem., 1975, 14, 1435.

- 40b. P.E. Garrou, Chem. Rev., 1981, 229.
41. R. Keat, L. Manojlovic-Muir, K.W. Muir and D.S. Rycroft, J. Chem. Soc., Dalton Trans., 1981, 2192.
42. W. McFarlane, Quart. Rev., 1969, 23, 187.
- 42a. S.O. Grim, D.A. Wheatland and P.R. McAllister, Inorg. Chem., 1968, 7, 161.
43. J.G. Verkade, Coord. Chem. Rev., 1972, 9, 1; R.L. Keiter and J.G. Verkade, Inorg. Chem., 1969, 8, 2115; E.O. Fischer, R.L. Keiter, L. Knauss and J.G. Verkade, J. Organomet. Chem., 1972, 37, C7; G.G. Mather and A. Pidcock, J. Chem. Soc. A, 1970, 1226.
44. A. Bright, B.E. Mann, C. Masters, B.L. Shaw, R.M. Slade and R.E. Stainbank, J. Chem. Soc. A, 1971, 1826.
45. F.H. Allen, A. Pidcock and C.R. Waterhouse, J. Chem. Soc. A, 1970, 2087.
46. S.O. Grim, R.C. Barth, J.D. Mitchell and J. Del Gaudio, Inorg. Chem., 1977, 16, 1776.
47. K. Moedritzer, L. Maier, and L.D.C. Groenweghe, J. Phys. Chem., 1962, 66, 901.
48. T.G. Appleton, H.C. Clark and L.E. Manzer, Coord. Chem. Rev., 1973, 10, 335.
- 48a. J.F. Nixon and A. Pidcock, Ann. Rev. Spectrosc., 1968, 2, 345.
49. F.H. Allen and S.N. Sze, J. Chem. Soc. A, 1968, 3047.
50. B.E. Mann and V.F. Taylor, ¹³C NMR Data for Organometallic Compounds, Academic Press, 1981.
51. P.S. Pregosin, Coord. Chem. Rev., 1982, 44, 247.
52. J.J. Dechter, Prog. Inorg. Chem., 1985, 33, 393.
53. High Resolution Nuclear Magnetic Resonance Spectroscopy, Vol.1, J.W. Emsley, J. Feeney and L.H. Sutcliffe, Pergamon Press, 1965; P. Diehl, E. Fluck and R. Kosfeld (eds.), NMR Basic Principles and Progress, 1971, Springer Berlin.
54. I.J. Colquhoun and W. McFarlane, J. Chem. Soc., Dalton Trans., 1982, 1915.
- 54a. R. Benn and H. Günther, Angew. Chem. Int. Ed. Engl., 1983, 22, 350.
55. M. Karplus, J. Am. Chem. Soc., 1962, 84, 2458.
56. A.A. Bothner-By, Adv. Magn. Reson., 1965, 1, 195.
57. G.W. Parshall and R.V. Lindsey, J. Am. Chem. Soc., 1959, 81, 6273.
58. K. Issleib and D. Jacob, Chem. Ber., 1961, 94, 107.

59. I.J. Colquhoun, personal communication.
60. Organic Phosphorus Compounds Vol.1, G.M. Kosolapoff and L. Maier, Wiley, 1972.
61. V.M. Potapov, Stereochemistry, 1979, MIR, Moscow.
63. D.G. Gorenstein, Progress in N.M.R. Spectroscopy (Eds. J.W. Emsley, J. Feeney and L.H. Sutcliffe) Vol.16, p.1, Pergamon Press, Oxford, 1983.
64. R. Colton, Coord. Chem. Rev., 1985, 62, 85-130, 145-265.
65. R.L. Keiter, Y.Y. Sun, J.W. Brodack and L.W. Cary, J. Am. Chem. Soc., 1979, 101, 2638.
66. W. Strohmeier and F. Müller, Chem. Ber., 1969, 102, 3608.
67. W. McFarlane and D.S. Rycroft, J. Chem. Soc., Dalton Trans., 1976, 1616.
68. N.F. Ramsey, Phys. Rev., 1952, 78, 689.
69. J. Mason, Adv. Inorg. Chem. Radiochem., 1979, 22, 199.
70. C.J. Jameson and H.S. Gutowsky, J. Chem. Phys., 1964, 40, 1714.
71. P.S. Braterman, G.W. Milne, E.W. Randall and E. Rosenberg, J. Chem. Soc., Dalton Trans., 1973, 1027.
72. J.A. Pople and D.A. Santry, Mol. Phys., 1964, 8, 1.
73. J.R. Morton and K.R. Preston, J. Mag. Res., 1978, 30, 577.
74. R.R. Vold and R.L. Vold. J. Magn. Reson., 1975, 19, 365.
75. R.C. Taylor, R.L. Keiter and L.W. Cary, Inorg. Chem., 1974, 13, 1928.
76. U. Belluco, Organometallic and Coordination Chemistry of Platinum, 1974, Academic Press, London.
77. W.L. Steffen and G.J. Palenik, Inorg. Chem., 1976, 15, 2432; D.W. Meek, P.E. Nicpon and V.I. Meek, J. Am. Chem. Soc., 1970, 92, 5351; R.J. Dickinson, W. Levason, C.A. McAuliffe and R.V. Parish, J. Chem. Soc., Dalton Trans., 1978, 177.
78. T.G. Appleton, M.A. Bennett and I.B. Tomkins, J. Chem. Soc., Dalton Trans., 1976, 439.
79. G.R. Cooper, F. Hassan, B.L. Shaw and M. Thornton-Pett, J. Chem. Soc., Chem. Commun., 1985, 614.
80. F. Basolo and R.G. Pearson, Progr. Inorg. Chem., 1962, 4, 381.
81. A.J. Carty, D.K. Johnson and S.E. Jacobson, J. Am. Chem. Soc., 1979, 101, 5612.

82. K.D. Tau, D.W. Meek, T. Sorrell and J.A. Ibers, Inorg. Chem., 1978, 17, 3454.
83. S. Hietkamp, D.J. Stuffken and K. Vrieze, J. Organomet. Chem., 1979, 169, 107; J.D. Kennedy, W. McFarlane, R.J. Puddephatt and P.H. Thompson, J. Chem. Soc., Dalton Trans., 1976, 874.
84. P.L. Goggin, R.J. Goodfellow, S.R. Haddock, B.F. Taylor and F.R.H. Marshall, J. Chem. Soc., Dalton Trans., 1976, 459.
- 84a. W. McFarlane, J. Chem. Soc. A, 1967, 1922.
85. P.S. Presogin and S.N. Sze, Helv. Chim. Acta, 1978, 61, 1848.
86. G. Balimann, PhD thesis, ETH Zürich, 1977
87. R.J. Puddephatt, M.A. Thompson, Lj. Manojlovic-Muir, K.W. Muir, A.A. Frew and M.P. Brown, J. Chem. Soc., Chem. Commun., 1981, 805; A.R. Sanger, J. Chem. Soc., Dalton Trans., 1981, 228; P.G. Pringle and B.L. Shaw, J. Chem. Soc., Chem. Commun., 1982, 581; M.P. Brown, R.J. Puddephatt, and M. Rashidi, J. Chem. Soc., Dalton Trans., 1978, 1540; M.C. Grossel, M.P. Brown, C.D. Nelson, A. Yavari, E. Kallas, R.P. Moulding and K.R. Seddon, J. Organomet. Chem., 1982, 232, C13; A.L. Balch, J. Am. Chem. Soc., 1976, 98, 8049.
88. M.P. Brown, R.J. Puddephatt, M. Rashidi and K.R. Seddon, J. Chem. Soc., Dalton Trans., 1977, 951.
89. R. Colton, M.J. McCormick and C.D. Pannan, Austr. J. Chem., 1978, 31, 1425.
90. L.S. Benner and A.L. Balch, J. Am. Chem. Soc., 1978, 100, 6099.
91. M.P. Brown, R.J. Puddephatt, M. Rashidi and K.R. Seddon, J. Chem. Soc., Dalton Trans., 1978, 516.
92. C. Lee, C.T. Hunt and A.L. Balch, Inorg. Chem., 1981, 20, 2498.
93. M.P. Brown, J.R. Fisher, R.J. Puddephatt and K.R. Seddon, Inorg. Chem., 1979, 18, 2808.
94. T.S. Cameron, P.A. Gardner and K.R. Grundy, J. Organomet. Chem., 1981, 212, C19.
95. P. Pringle and B.L. Shaw, J. Chem. Soc., Chem. Commun., 1982, 81.
96. M.P. Brown, S.J. Franklin, R.J. Puddephatt, M.A. Thomson and K.R. Seddon, J. Organomet. Chem., 1979, 178, 281.
97. M.M. Olmstead, H. Hope, L.S. Benner and A.L. Balch, J. Am. Chem. Soc., 1977, 99, 5502.
98. C.T. Hunt and A.L. Balch, Inorg. Chem., 1981, 20, 2267.
99. R.K. Harris and B.E. Mann, N.M.R. and the Periodic Table, 1978, Academic Press, London
100. A. Cahours and A.W. Hofman, Ann., 1857, 104, 1.

101. L. Maier, Topics in Phosphorus Chemistry, (Eds. M. Grayson and E.J. Griffiths), Interscience, New York 1965, Vol.2.
102. H. Goetz, G. Nerdel and E. Busch, Ann., 1963, 665, 14.
103. P.D. Bartlett, E.F. Cox and R.E. Davis, J. Am. Chem. Soc., 1961, 83, 103.
104. P.D. Bartlett and G. Meguerian, J. Am. Chem. Soc., 1956, 78, 3710.
105. K. Issleib and F. Krech, Chem. Ber., 1961, 94, 2656.
106. K. Issleib, F. Krech and K. Grüber, Chem. Ber., 1963, 96, 2186.
107. K. Issleib and D.W. Müller, Chem. Ber., 1959, 92, 3175.
108. R.R. Renshaw and F.K. Bell, J. Am. Chem. Soc., 1921, 43, 916.
109. P. Nicpon and D.W. Meek, Inorg. Synth., 1967, 10, 157.
110. W. Hewerton, R.A. Shaw and B.C. Smith, J. Chem. Soc., 1964, 1020.
111. C. Screttas and A.F. Isbell, J. Org. Chem., 1962, 27, 2573.
112. P. Nicpon and D.W. Meek, Inorg. Chem., 1966, 5, 1297.
113. I.J. Colquhoun and W. McFarlane, J. Chem. Soc., Chem. Commun., 1982, 484.
114. L. Müller, A. Kumar, and R.R. Ernst, J. Chem. Phys., 1975, 63, 5490.
115. A. Bax, Two-Dimensional Nuclear Magnetic Resonance in Liquids, 1982, Delft University Press.
116. G. Bodenhausen, R. Freeman, R. Niedermeyer and D.L. Turner, J. Magn. Reson., 1976, 24, 291.
117. W. P. Aue, J. Karhan and R.R. Ernst, J. Chem. Phys., 1976, 65, 839.
118. J. Ellermann and D. Schirmacher, Chem. Ber., 1967, 100, 2220.
119. R. Keat and D.G. Thompson, J. Organomet. Chem., 1977, 141, C13.
120. O.J. Scherer and G. Schnab, Angew. Chem. Int. Ed., 1977, 16, 486.
121. Y.F. Gatilov, L.B. Ionov and G. Kamai, Zh. Obshch. Khim., 1968, 38, 372.
122. M. Dub (ed) Organometallic compounds: Methods of Synthesis, Physical Constants and Chemical Reactions, 1968, Vol.3, Springer,
123. R.A. Zingaro, R.E. McGlothlin and R.M. Hedges, Trans. Faraday Soc., 1963, 59, 798.
124. K.B. Mallion and F.B. Mann, J. Chem. Soc., 1964, 6121.
125. C.E. Griffin and M.L. Kaufman, Tetrahedron Lett., 1965, 773.
126. W. Gee, R.A. Shaw and B.C. Smith, Inorg. Synth., 1967, 9, 19.

127. H. Fritzsche, U. Hasseroth and F. Korte, Chem. Ber., 1965, 98, 1681.
128. H. Hoffmann and P. Schellenbeck, Chem. Ber., 1966, 99, 1134.
129. S.O. Grim, A.W. Yankowsky, S.A. Bruno, W.J. Bailey, E.F. Davidoff and T.J. Marks, J. Chem. Eng. Data, 1970, 15, 497.
130. L. Horner, H. Hoffmann and P. Beck, Chem. Ber., 1958, 91, 1583.
131. J.E. Bissey and H. Goldwhite, Tetrahedron Lett., 1966, 3247.
132. W. Kuchen and H. Buchwald, Angew. Chem., 1956, 68, 791.
133. M. Sander, Chem. Ber., 1960, 93, 1220.
134. L. Maier, Helv. Chim. Acta, 1966, 49, 1718.
135. M.M. Rauhut and A.M. Sessel, J. Org. Chem., 1963, 28, 473.
136. L.V. Kaabak, M.I. Kabachnik, A.P. Tomilov and S.L. Varshavskii, Zh. Obshch. Khim., 1966, 36, 2060.
137. K. Issleib, H. Schmidt and C. Wirkner, Z. Anorg. Allg. Chem., 1982, 488, 75.
138. E.H. Brooks and F. Glockling, J. Chem. Soc., A, 1967, 1030.
139. D.J. Peterson, J. Org. Chem., 1966, 31, 950.
140. C. Wu and F.J. Welch, J. Org. Chem., 1965, 30, 1229.
141. K.D. Berlin and G.B. Butler, J. Org. Chem., 1961, 26, 2537.
142. R.C. Cookson et al., J. Chem. Soc., 1947, 618.
143. P.J. Busse, C.P. Hrung, K.J. Irgolic, D.H. O'Brien and F.L. Kolar, J. Organomet. Chem., 1980, 185, 1.
144. K. Issleib and H. Weichmann, Chem. Ber., 1968, 101, 2197.
145. K. Issleib and D. Jacob, Chem. Ber., 1961, 94, 107.
146. R.C. Marriot, J.D. Odom and C.T. Sears, Inorg. Synth., 1973, 14, 1.
147. W.E. White and A.H. Bushey, J. Am. Chem. Soc., 1944, 66, 1666.
148. W. Strohmeier and G. Schöner, Chem. Ber., 1961, 94, 1346.
149. W. Strohmeier, K. Gerlach and D.V. Hobe, Chem. Ber., 1961, 94, 164.
150. W. Strohmeier and D.V. Hobe, Chem. Ber., 1961, 94, 2031.
151. W. Strohmeier and D.V. Hobe, Chem. Ber., 1961, 94, 761.
152. W. Strohmeier and H. Hellmann, Chem. Ber., 1963, 96, 2859.
153. E.W. Abel, I.S. Butler and J.G. Reid, J. Chem. Soc., 1963, 2068.
154. J.A. Connor, E.M. Jones and G.K. McEwen, J. Organomet. Chem., 1972, 43, 357.

155. G.T. Andrews, I.J. Colquhoun, W. McFarlane and S.O. Grim, J. Chem. Soc., Dalton Trans., 1982, 2353.
156. J.G. Smith and D.T. Thompson, J. Chem. Soc., A, 1967, 1694.
157. G.J. Kubas, Inorg. Chem., 1983, 22, 693.
158. D.P. Tate, W.R. Knipple and J.M. Augl, Inorg. Chem., 1962, 1, 433.
159. D.J. Darensbourg and R.L. Kump, Inorg. Chem., 1978, 17, 2680.
160. J.X. McDermott, J.F. White and G.M. Whitesides, J. Am. Chem. Soc., 1976, 98, 6521.
161. X.L.R. Fontaine, F.S.M. Hassan, S.J. Higgins, G.B. Jacobsen, B.L. Shaw and M. Thorton-Pett, J. Chem. Soc., Chem. Commun., 1985, 1635.
162. M.S. Kharasch, R.C. Seyler and F.R. Mayor, J. Am. Chem. Soc., 1938, 60, 882.
163. H.C. Clark and L.E. Manzer, J. Organomet. Chem., 1973, 59, 411.
164. C.R. Kistner, J.H. Hutchinson, J.R. Doyle and J.C. Storlie, Inorg. Chem., 1963, 2, 1255.
165. T. Uka1, H. Kawazura, J. Bonnet and J.A. Ibers, J. Organomet. Chem., 1974, 65, 253.
166. F. Arnett, Org. Synth., 1943, Collect. Vol., II, 165.
167. W. McFarlane, Ann. Rev. N.M.R. Spectr., 1968, 1, 135.

New Polyphosphorus Ligands: Addition Reactions of 1,1-Bisdiphenylphosphinoethene

Jonathan L. Bookham,^a William McFarlane,^{a*} and Ian J. Colquhoun^b

^a *Department of Chemistry, City of London Polytechnic, Jewry Street, London EC3N 2EY, U.K.*

^b *School of Chemical Sciences, University of East Anglia, Norwich NR4 7TJ, U.K.*

The reactivity of the double bond adjacent to the geminal diphenylphosphino groups of $(\text{Ph}_2\text{P})_2\text{C}=\text{CH}_2$ facilitates the addition of species with one or more P-H bonds to provide a convenient high-yielding route to a range of new poly and ambi-dentate ligands which can form a wide variety of different types of transition metal complex.

**Reprinted from the Journal of The Chemical Society
Chemical Communications 1986**

New Polyphosphorus Ligands: Addition Reactions of 1,1-Bisdiphenylphosphinoethene

Jonathan L. Bookham,^a William McFarlane,^{a*} and Ian J. Colquhoun^b

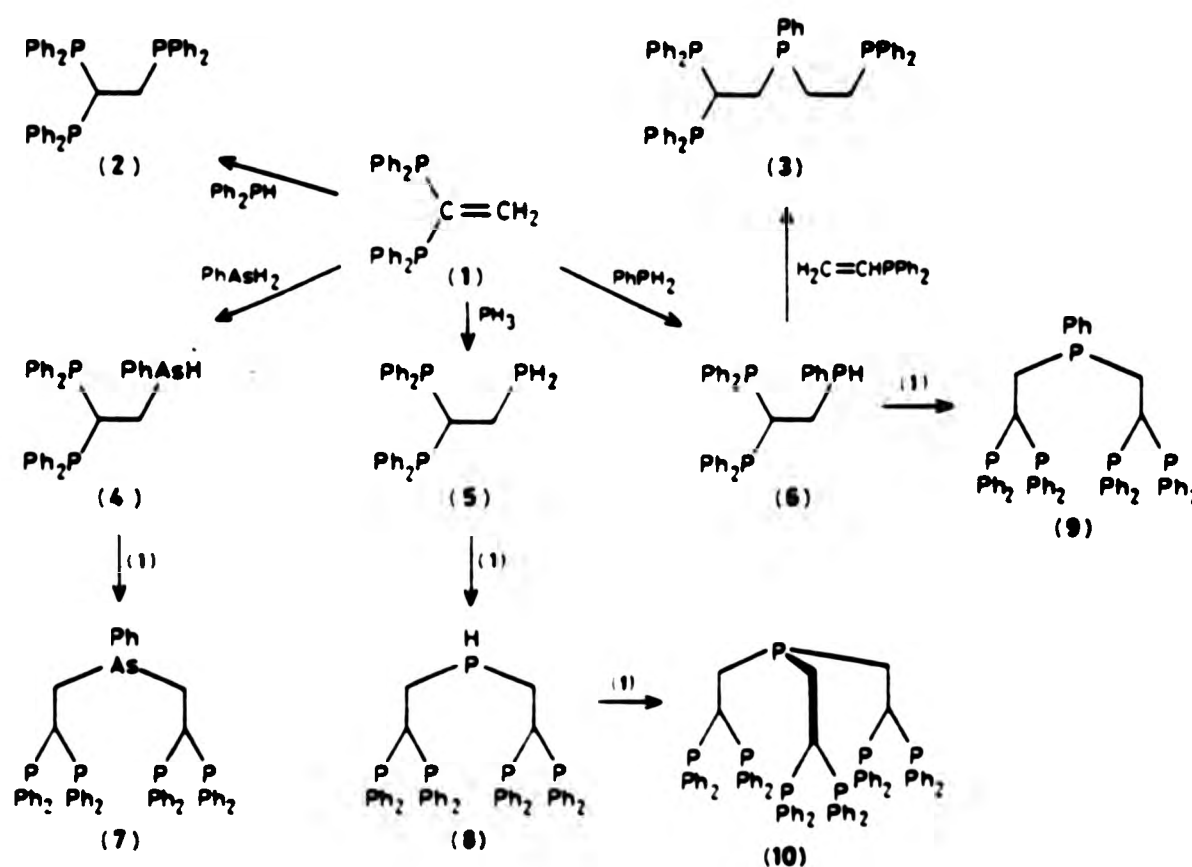
^a Department of Chemistry, City of London Polytechnic, Jewry Street, London EC3N 2EY, U.K.

^b School of Chemical Sciences, University of East Anglia, Norwich NR4 7TJ, U.K.

The reactivity of the double bond adjacent to the geminal diphenylphosphino groups of $(\text{Ph}_2\text{P})_2\text{C}=\text{CH}_2$ facilitates the addition of species with one or more P-H bonds to provide a convenient high-yielding route to a range of new poly- and ambi-dentate ligands which can form a wide variety of different types of transition metal complex.

We have previously described¹ the synthesis of 1,1-bisdiphenylphosphinoethene (1), a versatile chelating ligand with a somewhat larger bite than bisdiphenylphosphinoethane, dppm,² and some of its transition metal complexes.¹

The presence of the double bond in (1) and its complexes provides the opportunity for a range of addition reactions not available to dppm, and we have used this feature to prepare 1,1,2-trisdiphenylphosphinoethane (2) and some of its deriva-

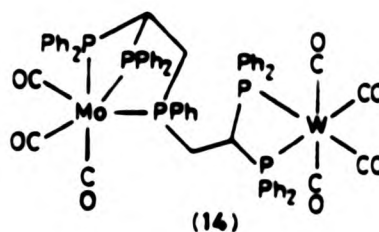
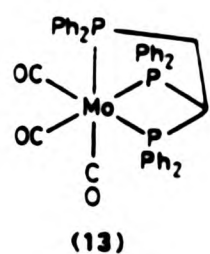
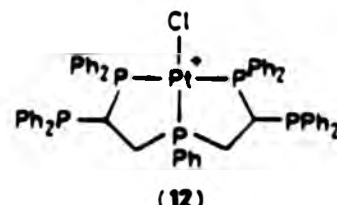
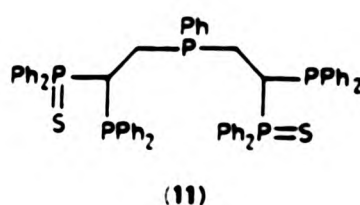


Scheme 1. Addition reactions of 1,1-bisdiphenylphosphinoethene (1) (Room temperature, in tetrahydrofuran, with Bu^tOK catalyst)

Table 1. ^{31}P n.m.r. data for the ligands.

Compound	Chemical shift, p.p.m. ^a			Coupling constant/Hz		
	P _A	P _B	P _C	$^2J(\text{P}_A\text{P}_B)$	$^2J(\text{P}_A\text{P}_C)$	$^2J(\text{P}_B\text{P}_C)$
(2)	-4.0	—	-19.6	b	24.4	—
(3) ^c	-4.0	-4.0	-23.8	b	20.1	20.1
(6)	-3.9	-5.8	-54.8	112.3	15.9	17.1
(7)	-3.2	-4.6	—	96.3	—	—
(9)	-2.9	-4.8	-29.7	100.7	28.6	17.0
(10)	-2.7	—	-27.3	b	25.3	—

^a To high frequency of 85% H_3PO_4 . P_A and P_B refer to geminal P atoms. ^b Not directly measurable from ^{31}P n.m.r. spectrum. ^c $\delta(\text{P}_B) = -11.2$ p.p.m., $^2J(\text{P}_C\text{P}_B) = 27.5$ Hz. ^d In CH_2Cl_2 , 10 mm tube.



tives.⁴ We now report that this reaction is of wide scope owing to the enhanced reactivity of the double bond arising from the presence of the geminal diphenylphosphino groups even without any effect due to metal co-ordination,^{4b} and that it provides a straightforward high-yielding route to a range of potentially ambi- and poly-dentate ligands.

Typically, species with P-H bonds add to (1) in the presence of potassium *t*-butoxide⁷ as shown in Scheme 1, which also illustrates corresponding reactions of some species with As-H bonds. The products were identified primarily from their characteristic ^{31}P n.m.r. spectra (multinuclear JEOL FX90Q operating at 36.2 MHz), and in addition compounds (2), (3), (6), (7), (9), and (10) have been obtained as air-stable white crystalline solids with sharp melting points and satisfactory elemental analyses.

In certain of these molecules the geminally related phosphorus atoms are rendered inequivalent by the presence of a chiral [(4) and (6)] or prochiral [(7)–(9)] centre at the other phosphorus or the arsenic atom, and this has important consequences for their n.m.r. spectra and their chemical behaviour. Thus different values of $\delta(^{31}\text{P})$ and $^2J(^{31}\text{P}-^{31}\text{P})$ occur (Table 1), and it is possible to measure $^2J(^{31}\text{P}-^{31}\text{P})$ directly, values between 97 and 113 Hz being found. These may be compared with 125 Hz in dppm as determined by $^{13}\text{C}\{^{31}\text{P}\}$ multiple resonance experiments.¹ To a large extent the different values of the vicinal $^{31}\text{P}-^{31}\text{P}$ couplings probably reflect substantial imbalances in the conformational populations, and this is confirmed by the significant temperature dependences that we have found for these couplings. These conformational imbalances also have differential effects upon the reactivity of the phosphorus atoms, so that in reactions

[e.g. with S_8 to give (11)] that can yield diastereoisomeric products these are not obtained in the proportions to be expected on a simple statistical basis. This observation has considerable bearing on the formation of metal complexes such as (12) by these ligands, and here too we find that the three isomers (arising from different relative orientations of the Ph_2P and Ph groups) are produced in apparently anomalous proportions.

As ligands, (2), (5), and (6) can co-ordinate in many different ways, and in particular resemble dppm and dppe in having the capability to form complexes with four- and five-membered chelate rings. In practice, direct reaction between the ligand and the metal-containing substrate tends to give complexes in which five-membered (presumably less strained) rings are favoured, but complexes with four-membered rings can be made indirectly although they tend to rearrange at elevated temperatures. It is also possible to make complexes such as (13) in which all three phosphorus atoms are co-ordinated to the same metal atom to give one four- and two five-membered chelate rings despite the considerable strain involved.

The possibilities for (7)–(10) are even more extensive, and we find that complexes such as (12) with two five-membered chelate rings and the remaining phosphorus atoms unco-ordinated are especially favoured. Further co-ordination to the same metal atom would involve very substantial strain, but we have made complexes in which the ligands have become pentadentate by bridging two metals as in (14).

We thank Dr. B. Wrackmeyer for gifts of phenylphosphine and phenylarsine, and the S.E.R.C. and the Sir John Cass's Foundation for support.

Received, 27th March 1986; Com. 403

References

- 1 I. J. Colquhoun and W. McFarlane, *J. Chem. Soc., Dalton Trans.*, 1982, 1915.
- 2 R. J. Puddephatt, *Chem. Soc. Rev.*, 1983, 12, 99.
- 3 G. T. Andrews, I. J. Colquhoun, W. McFarlane, and S. O. Grim, *J. Chem. Soc., Dalton Trans.*, 1981, 2353.
- 4 I. J. Colquhoun and W. McFarlane, *J. Chem. Soc., Chem. Commun.*, 1981, 484.
- 5 G. R. Cooper, F. Hassan, B. L. Shaw, and M. Thornton-Pett, *J. Chem. Soc., Chem. Commun.*, 1985, 614.
- 6 X. L. R. Fontaine, F. S. M. Hassan, S. J. Higgins, G. B. Jacobsen, B. L. Shaw, and M. Thornton-Pett, *J. Chem. Soc., Chem. Commun.*, 1985, 1635.
- 7 R. B. King and P. N. Kapoor, *J. Am. Chem. Soc.*, 1971, 93, 4158.

Attention is drawn to the fact that the copyright of this thesis rests with its author.

This copy of the thesis has been supplied on condition that anyone who consults it is understood to recognise that its copyright rests with its author and that no quotation from the thesis and no information derived from it may be published without the author's prior written consent.

VI

D74326'87

END